Quick Scan model municipal concrete slab bridges

With additional FEM research to the α reduction factor and force transmission in slab bridges

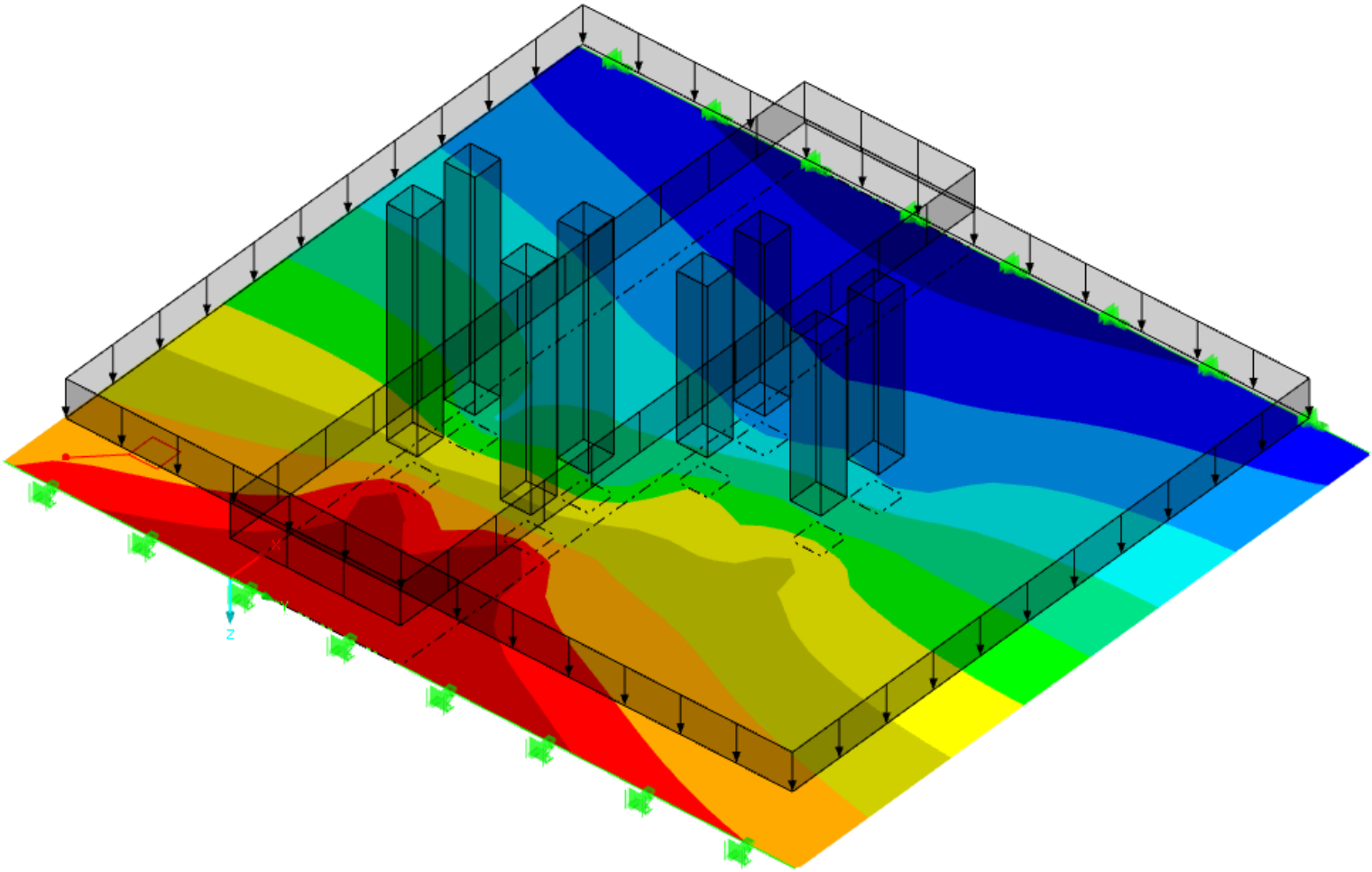

Master Thesis

Nick Montenij

August 2017

TU Delft SWECO

Nick Montenij, 2017

Graduation Committe

Chair: ***Prof. Ir. A.Q.C. Van der Horst***
TU Delft; Structural and Building Engineering

Members: ***Dr. Ir. C. Van der Veen***
TU Delft; Structural and Building Engineering

Ir. R.P.H. Vergoossen
TU Delft; Structural and Building Engineering

Ing. N.A. Broek
Sweco; Asset Management Civil Structures

Ir. F.H. Schotman
Sweco; Structural Engineer Civil Structures

Quick Scan model municipal concrete slab bridges

With additional FEM research to the α reduction factor and force transmission in slab bridges

Thesis

Submitted in partial fulfilment of the
requirements for the degree of

Master of Science

in

Civil Engineering

By Nick Montenij

Date : August 03, 2017

Authors : Nick Montenij

E-mail : Nick.Montenij@sweco.nl

Contact : Sweco Nederland B.V.
De Holle Bilt 22
3732 HM De Bilt
PO Box 203
3730 AE De Bilt

TU Delft SWECO

Preface

This thesis was written as part of the fulfillment for the Master of Science in Structural Engineering at the Delft University of Technology. The research was mainly carried out at the head office of Sweco Nederland.

In this research I faced a lot of uncertainties that existing bridges have, including uncertain loads and capacities. Hopefully this thesis contributes to the reduction of these uncertainties. It seems that the government and municipalities in the Netherlands are one step ahead of a huge problem that is about to be reality: a series of bridge collapses which leads to the demand of the renovation of a huge number of bridges. They seem increasingly aware of the danger of uncertainties of their bridges' structural safety. This has already led to standards for existing bridges, an increasing number of researches to relevant topics, and innovation programs like 'stroomversnelling bruggen', which brings together the government, municipalities, engineering companies and knowledge institutes and lets them cooperate. It seems that we act proactively instead of reactively.

I owe my gratitude to several people who gave me support on the way of completing this thesis. Firstly, I would like to thank all my colleagues from Sweco for the support they gave me. Especially Nico Broek and all structural engineers from the compartment Roads, Team Civil Structures. Among others Frank Schotman, who helped me with practical insights and his knowledge of existing bridges. I would like to thank Richard Mulder from 'Bouwend Nederland' for his time and insight in the non-structural facts of municipal bridges.

I would like to express my gratitude to my committee for their help and feedback. I would like to thank prof. A.Q.C. Van der Horst for being the chairman, for his feedback and his insights in the practical side of existing bridges. I would also like to thank dr. C. Van de Veen for sharing his knowledge about concrete structures and his insightful questions. Finally I would like to thank Ir. R. Vergoossen for his time, useful meetings and for sharing his knowledge about existing bridges and the Quick Scan Model.

Last but not least, I would like to thank my family and friends for their patience, love, support, and for cheering me up now and then.

Summary

In this thesis, existing concrete municipal slab bridges are regarded. Many of these bridges were designed and built in the 1960s and 1970s. These bridges are still in service, and subjected to higher and more frequent loads than at the time of design. This leads to uncertainties in the safety of these bridges. Many municipalities become increasingly aware of these uncertainties and want to verify their bridges according to current standards. Especially the shear assessment is critical, since some former codes do not contain shear checks.

Municipalities usually do not have sufficient financial resources to investigate and recalculate all of their bridges. A Quick Scan model is a cheap and fast tool to do structural checks, or to classify a number of bridges for structural safety. A literature study and Finite Element Modelling research was performed in order to make the Quick Scan more accurate. In general, existing municipal bridges are not exposed to the same heavy traffic as governmental highways. Nevertheless, municipal bridges were calculated with the same load models as governmental bridges. For the assessment of existing municipal bridges research was done to the possibility of reducing the design loads of Load Model 1 (LM1) from the Eurocode. This reduction can be done with the α-factor on variable loads. The possible reasons for this reduction is threefold.

Firstly, municipal roads are significantly less exposed to heavy traffic compared to governmental highways. Therefore the chance of occurrence of the governing vehicle according to LM1 is decreasing. This assumption was supported by Weight-in-Motion measurements on a municipal road in Rotterdam. With the reliability index (β) for existing bridges in Consequence Class 2, this lead to a governing axle load of 225 kN, instead of the 300kN from LM1. The second reason for the reduction of the design load is the fact that municipal bridges usually have relatively small spans (5-20m). LM1 is designed to simulate a fully loaded bridge with a span of at least 20m. For small spans it can be useful to calculate with real occurring traffic, since axle distance is more important than axle loads only. A third (small) reduction is the fact that an existing bridge has a shorter reference period than a new bridge. This leads to smaller chances of the occurrence of the governing vehicle. New load models for small span municipal bridges were designed taking into account these reductions. The governing vehicle for small span bridges is a 5-axle vehicle with axle loads of 137,5-165 kN and axle distances of 140-175mm. Occurring shear forces due to these loads are higher than due to a long vehicle with higher loads, mora axles and greater axle distances.

The new governing vehicle was used to determine the reduction factor α. This was determined by a comparative research in the Finite Element Modelling program RFEM. The resulting shear stresses and flexural stresses from the different load models were compared. For spans up to 11m the loads from LM1 can be reduced by an α factor 0,8. This factor increases linearly to a factor 1,0 for a 20m span.

Besides the differences in loads and dimensions, municipal bridges also differ from governmental bridges in lay-out. In general, the distance from the carriageway to the edge of the slab is larger for municipal bridges due to the presence of a footpath or bicycle lane separated by a kerb. Bridges in 10 different municipalities were examined on lay-out. Roughly 58% of the municipal bridges in the Netherlands have significant edge distance (>1,2m) This leads to a difference in the force transmission, since the high axle loads from LM1 cannot occur near the edge of the slab. The influence of this edge distance for different spans was investigated with RFEM. Also, the variable and permanent loads were investigated separately to give insight in the resulting shear stress due to different loads. Distinction was made between slabs in cracked and uncracked

state. Cracking has significant influence on the transverse force transmission of the axle loads. The transverse force transmission is influenced by the ratio between longitudinal and transverse stiffness, which was conservatively chosen as 1/3. Also, distinction was made between in-situ casted slabs and prefab slabs. The self-weight of in-situ casted slabs leads to a constant shear force on the support. A prefab slab was treated like a theoretical slab, where the self-weight leads to peak forces near the edge due to torsional moments near the edge.

The critical edge distance was determined for different spans. For a cracked in-situ casted slab with an edge distance >1,5m, the middle of the slab is always governing in shear. An edge distance <0,7 leads to the edge of the support being governing in shear.

Research by Eva Lantsoght to shear force in reinforced slabs under concentrated loads close to the supports was used for rules and assumptions based on experiments. These rules were used to get a better understanding of the results in RFEM, and to develop the Quick Scan Model.

The Quick Scan model uses findings from literature research combined with findings from finite element modelling. The output is a Unity Check which can function as real structural shear check if the concrete compressive strength and steel yield strength are known. When only dimensions are known, the Quick Scan model can function as classification for a series of bridges in a municipality. The Quick Scan model was tested by a series of case studies, which did not yet lead to the verification of the model.

Results from the Quick Scan model were compared to results from the FEM research. Occurring shear stresses in the Quick Scan model are conservative with a maximum error of 11%. With the possibility of lowering the reliability index β to 2,5 (‘disapproval’ level) and taking into account the possible error due to several uncertainties, the upper boundary of the Unity Check was found as 1,4. Bridges with a Unity Check: $1 < UC < 1,4$ according to the Quick Scan model need further assessment or material testing in order to fulfil the requirements.

Extensive research was done to loads according to the Eurocode (LM1) on slab bridges and the force transmission of these loads. The capacity of existing concrete slabs was investigated relatively brief. More research to the capacity side of existing concrete bridges is expected to be beneficial.

Table of contents

Preface 4

Summary 5

1 Introduction 12
1.1 Scope 12
1.2 Research 13
1.2.1 Reduction of the loads 13
1.2.2 Force transmission in concrete slabs 13
1.3 Thesis outline 14

SECTION 1 - Literature research and background

2 Municipal bridges 17
2.1 Differences government bridges and municipal bridges 17
2.1.1 Loads 17
2.1.2 Dimensions 17
2.1.3 Materials 17
2.1.4 Standards 18
2.2 Research 'Bouwend Nederland' to bridges in municipalities [1] 18
2.2.1 The survey 18
2.2.1.1 Overview bridges 19
2.2.1.2 Periodic inspection 20
2.2.1.3 Policy maintenance and replacement 20
2.2.1.4 Budget 20
2.3 Internal Research Sweco 21
2.4 Research edge distance municipal bridges 22
2.4.1 Introduction 22
2.4.2 General lay-out bridge deck 22
2.4.3 Results and conclusions 23

3 Assessing existing concrete bridges 26
3.1 Bridge asset management in general 26
3.2 Types of bridges 28
3.2.1 Slab bridge 28
3.2.1.1 Longitudinal cross-section 28
3.2.1.2 Transverse cross-section 29
3.2.2 Concrete bridges nowadays 29
3.2.2.1 ZIP bridges (rail beam bridges) 29
3.2.2.2 SJP bridges 29
3.3 Overview parameters of concrete slab bridges 30
3.3.1 Number of lanes 30
3.3.2 Edge distance 30
3.3.3 Angle of skew 30
3.3.4 Static system and number of spans 31
3.3.5 Dimensions 31

3.3.6 Execution type of the slab ... 31
3.3.7 Edge beam ... 31
3.3.8 Material characteristics ... 32
3.3.9 Stiffness ... 32
3.3.10 Loads ... 34
3.4 Former standards ... 34
3.4.1 Material properties in former standards ... 34
3.4.2 Shear capacity in former design codes ... 35
3.5 Current standards existing bridges ... 35
3.6 Safety assessment of existing bridges ... 36
3.6.1 Introduction ... 36
3.6.2 Reliability index (β) ... 36
3.6.3 Reliability levels for new structures ... 37
3.6.4 Reliability levels for existing structures ... 38
3.6.4.1 Cost aspect ... 38
3.6.4.2 Time aspect ... 39
3.6.4.3 Data aspect ... 40
3.6.4.4 Reliability levels ... 40
3.6.5 Traffic load modelling ... 42
3.6.5.1 Traffic load model Eurocode ... 42
3.6.6 Probabilistic traffic model ... 43
3.6.6.1 Weight-in-motion (WIM) data ... 43
3.6.6.2 Governing truck ... 45
3.6.7 Partial factors for existing bridges ... 47
3.7 Conclusion ... 48
3.8 Discussion ... 48

4 Shear assessment of concrete slab bridges ... 50
4.1 Failure of slab bridges ... 50
4.1.1 Proof loading ... 50
4.1.2 Effect of predamaging ... 51
4.2 Loads for shear assessment (Load Model 1) ... 51
4.3 Effective width ... 52
4.3.1 Transverse load distribution factor β ... 52
4.3.2 Asymmetric effective width ... 53
4.3.3 Effective width of an axle load ... 53
4.3.4 Skewed slabs ... 54
4.3.5 Results and recommendations experiments ... 55
4.4 Live load model ... 55
4.4.1 Superposition of loads ... 56
4.4.2 Static indeterminacy ... 58
4.5 Shear capacity ... 59
4.5.1 The minimum shear capacity v_{min} ... 59
4.5.1.1 Background v_{min} ... 59
4.5.1.2 v_{min} for plates ... 60
4.5.2 Concrete compressive strength ... 62
4.5.3 Reinforcement type ... 62
4.5.4 Transverse flexural reinforcement ... 63
4.5.5 Support type ... 63
4.6 Conclusions and recommendations ... 63

5 Finite Element Modelling ... 65
5.1 Introduction ... 65
5.2 Plates in finite element programs ... 65
5.2.1 Theory behind plates ... 65
5.2.2 Difference Mindlin and Kirchhoff ... 67
5.2.2.1 Tests Mindlin/Kirchhoff ... 69
5.2.3 Tests cracked/ uncracked concrete ... 70

5.3 Parameters Finite Element model ... 71
5.4 Load models ... 72
5.4.1 Load Model 1 ... 73
5.4.2 Load classes 60 and 45 ... 73
5.4.3 Fatigue load models ... 75
5.4.3.1 Dynamics in bridge assessment ... 76
5.4.3.2 Fatigue load models to strength load models ... 78
5.4.4 Existing heavy lorry (Asphalt lorry) ... 79
5.4.4.1 Location specific load models ... 80
5.5 Conclusion ... 80
5.5.1 Summary ... 81

SECTION 2 - FEM research existing concrete slab bridges

6 The adjustment factor α ... 83
6.1 Modelling ... 84
6.1.1 Flexural moment ... 84
6.1.2 Shear force ... 85
6.1.3 Action plan modelling ... 85
6.1.4 Governing load model ... 85
6.1.4.1 Conclusion ... 86
6.1.5 Results comparison LM1 ... 87
6.1.5.1 Results flexural moment ... 87
6.1.5.2 Conclusion flexural moment ... 89
6.1.5.3 Shear force ... 90
6.1.5.4 Conclusion shear force ... 91
6.2 Conclusion ... 93

7 Force transmission in concrete slabs ... 94
7.1 Introduction ... 94
7.2 Description of the research ... 94
7.3 Difference cracked and uncracked slabs ... 96
7.3.1 Comparison axle loads ... 96
7.3.2 Comparison self-weight ... 96
7.3.3 Comparison total loads ... 97
7.3.4 Conclusion ... 97
7.4 Shear force due to dead load and variable load separately ... 97
7.4.1 Shear force due to self-weight ... 97
7.4.1.1 Comparison middle / edge ... 98
7.4.1.2 Difference cast in-situ and prefab ... 98
7.4.2 Shear force due to axles loads of Load Model 1 ... 99
7.4.2.1 Comparison middle/ edge ... 101
7.5 Critical edge distance ... 101
7.5.1 Middle of the support governing ... 101
7.5.1.1 Governing distance of the axle loads to the support ... 101
7.5.1.2 Results ... 103
7.5.2 Edge support governing ... 104
7.5.2.1 a_v for different dimensions ... 104
7.5.2.2 Results ... 105
7.5.3 Comparing results ... 106
7.5.3.1 Results uncracked prefab slabs ... 106
7.5.3.2 Results cracked prefab slabs ... 107
7.5.3.3 Results uncracked in-situ slabs ... 107
7.5.3.4 Results cracked in-situ slabs ... 108
7.6 Conclusion ... 109

SECTION 3 - Quick Scan Model

8 Quick Scan model ... 111
8.1 Introduction ... 111
8.2 Scope ... 111
8.2.1 Background ... 111
8.3 How to use ... 111
8.3.1 Material properties tab ... 111
8.3.2 Axle loads tab ... 111
8.3.3 Calculation shear force tab ... 113
8.3.3.1 Peak force due to permanent loads ... 114
8.3.3.2 Calculation UDL loads ... 114
8.3.3.3 Correction factors cracked slabs ... 115
8.3.3.4 Shear force due to axle loads ... 115
8.3.4 Input and Output tab ... 116
8.3.4.1 Input ... 116
8.3.4.2 Output ... 118
8.3.5 Macro tab ... 118
8.4 Parametric analysis ... 118
8.4.1 Concrete class ... 118
8.4.2 Steel type ... 118
8.4.3 Thickness slabs ... 120
8.4.4 Comparison RFEM and the Quick Scan Model ... 121
8.4.5 Critical consideration reliability Quick Scan ... 123
8.4.5.1 General assumptions ... 123
8.4.5.2 Loads ... 124
8.4.5.3 Shear capacity ... 125
8.4.5.4 Conclusion ... 127
8.5 Reliability model ... 128
8.5.1 General parameters ... 129
8.5.2 Parameters used in researches and modelling ... 130
8.5.3 Critical unity check ... 131
8.6 Conclusion ... 132
8.7 Discussion ... 133
8.8 Limitations ... 133

9 Case Study ... 134
9.1 Underpass N23 Westfrisiaweg ... 134
9.2 Viaduct Bakkersloot ... 135
9.3 Conclusion ... 136
9.4 Discussion and recommendation ... 136

10 Conclusions and Recommendations ... 137
10.1 Conclusions ... 137
10.1.1 Difference municipal and governmental bridges ... 137
10.1.2 Difference existing and new bridges ... 137
10.1.3 Research questions ... 137
10.2 Quick Scan model ... 139
10.3 Discussion and recommendations ... 139
10.3.1 Further experimental research ... 139
10.3.2 α factor ... 139
10.3.3 Capacity ... 139
10.3.4 Slab cracking ... 140
10.3.5 The Finite Element Model ... 140
10.3.6 Quick Scan ... 140

11 Bibliografie ... 141

1 Appendix A – Investigated municipalities ... 144

2 Appendix B – Load reduction signs 145
2.1 Signs 145
2.1.1 Reduction total mass 145
2.1.2 Reduction total axle load 145

3 Appendix C – Other types of concrete bridges 146
3.1.1 T-beam bridge 146
3.1.2 Beam or girder bridge 146
3.1.3 Concrete rigid frames 146
3.1.4 Box girder bridges 147
3.1.5 Prestressing 147

4 Appendix D – Former codes 149
4.1 GBV 1950 149
4.2 GBV 1962 150
4.3 RVB 1962/1967 150
4.4 VB 74 and VB 74/84 150

5 Appendix E - Tests Mindlin/Kirchhoff 152

6 Appendix F – Tests cracked/uncracked slabs 154

7 Appendix G – Deflection due to self-weight 158

8 Appendix H - Comparative FEM test results for different fatigue load models 160
8.1 Flexural moment 160
8.2 Shear force 161

9 Appendix I – FEM results: calculation of the α factor 163
9.1 Flexural moment 163
9.1.1 A factor flexural moment 165
9.1.2 Summary α factors flexural moment 170
9.2 Shear force 171
9.2.1 A factor shear force 173
9.2.2 Summary α factors flexural moment 178

10 Appendix J – Comparing shear forces 179
10.1 Occurring shear forces 179
10.2 Total shear forces in-situ slabs 182
10.3 Comparison cracked/uncracked 184
10.4 Comparison shear force edge/middle support 188

11 Appendix K – Tests with axles at different distances from the support 193

12 Appendix L – values for a_v for the governing axle configuration 194

13 Appendix M – Determination critical edge width 196
13.1 Uncracked slab 196
13.2 Cracked slab 197

14 Appendix N – Comparison RFEM – Excel 199
14.1 Comparison axle loads 199
14.2 Comparison total loads 201

1 Introduction

In the Netherlands, many bridges and viaducts have been built in the 1960s and 1970s. These bridges are still in service, and subjected to the current traffic loads and volumes, which are significantly larger than those at the time of design. Current codes have become more strict and since the typical existing slab bridges were typically designed according to flexural moment check, the current requirements for shear are sometimes not met. This leads to the fact that many structures need to be re-calculated in order to verify their structural safety.

In 2009, the Dutch Department of Waterways and Public Works (Rijkswaterstaat) investigated if and how the structural safety of existing structures is guaranteed. Their conclusion was that the structural risks are often unknown. Also, the association of construction and infra companies, named 'Bouwend Nederland', has done research to the state of municipal bridges (Chapter 2.2). After these investigations, municipalities and counties want to verify the structural safety of their bridges more and more. For municipalities, a recalculation of all of their bridges is not an option, due to insufficient financial resources. There is an increasing demand for an easier and cheaper way to verify the structural safety of existing bridges.

The Netherlands has 403 municipalities with a total of around 23.000 bridges [1]. The total recalculation costs of all municipal bridges would be more than 100 million euro's. Most small municipalities do not have a high budget (or none at all) for bridge inspection, re-calculation and renovation. Therefore, there is an increasing demand for a Quick Scan model to calculate the structural safety of these structures. This tool allows the owners of the structures can see which structures are safe according to the current standards and which structures need further assessment.

The general goal of this research work is to receive more insight in the structural safety of existing municipal small span concrete slab bridges. Finite Element Modeling was used to investigate the shear force transmission in slabs. Also, Load Model 1 (LM1) from the Eurocode was compared to a new developed, more realistic load model. This leads to a reduction factor α that can be applied to LM1. A Quick Scan Model was developed to use the results from this thesis for a quick structural safety check of existing municipal concrete slab bridges.

1.1 Scope

In this thesis the term 'bridges' is used for every type of overpass that is meant for traffic. In general, governmental bridges are under good supervision and are maintained regularly. Therefore municipal bridges are regarded in this thesis. Research done in this thesis will also be applicable to governmental bridges to a certain extent. Municipal bridges differ from governmental bridges in a number of ways.

The most occurring material type for municipal bridges is concrete (Figure 2-1). For small span existing bridges, a solid slab is the common type. Different types of supports and static systems exist. The main focus will be on simply supported bridges, since this type occurs the most. The other static systems are discussed briefly. However, since only shear failure is checked extensively, the static system is not of major importance.

Most municipal bridges have a span of 5-20m. For larger spans, mostly another type of bridge was chosen in the design phase, such as a prestressed beam bridge or box girder bridge. Overpasses with a span smaller than 5m are mostly tunnels, underpasses or culverts. For spans

smaller than 5m the direct load transfer to the support becomes increasingly governing and the Quick Scan model becomes less accurate.

In principal, prestressed concrete bridges fall outside the scope of this thesis. Prestressed bridges are expected to be less critical than reinforced concrete bridges. Also, most small span municipal bridges are not prestressed.

The Quick Scan model was developed to cover the most occurring types of bridges. Bridges that fall outside the scope of the model, such static indeterminate structures, bridges with a load carrying edge beam and a varying thickness of the slab can be tested with the model with a certain uncertainty.

1.2 Research

Research was done in order to gain more insight in the real force transmission due to traffic in existing solid slab bridges. The is done by a comparative research in the Finite Element Program RFEM. This is divided in three main researches:

- Reduction of the loads according to the Eurocode (the α factor);
- Force transmission in concrete slabs;
- The critical edge distance.

Since there are three research objectives, three main research questions are formulated.

1.2.1 Reduction of the loads

The Eurocode (with the National Annex) provides the possibility to reduce the loads from Load Model 1 with an α factor. For new bridges the use of a certain α factor can be established. For existing bridges in municipalities a standard α factor is determined. The reason why a reduction on the loads can be applied is threefold:

- Reduction due to location of the bridge: LM1 stands for a high percentage of heavy lorries, as present on governmental highways. This is not the case for municipal bridges;
- Reduction due to span: Load Model 1 (LM1) is especially designed for bridges with a span larger than 20m. For smaller spans, the axle configuration (number of axles and axle distance) is more important. Also, the governing vehicle might not fit on the bridge entirely;
- Reduction due to lifetime: For existing bridges a reference period shorter than 100 years can be assumed since the bridge has a certain age. LM1 covers the whole lifetime of a bridge, which is not representative for existing bridges.

The research question for this part of the research is:

1. ***How much can the loads from Load Model 1 be reduced for existing municipal concrete slab bridges?***

This question will be answered by comparing the occurring stresses due to Load Model 1 with a new load model. This load model has to represent real occurring traffic on a municipal bridge more accurately. In order to create this model, certain issues need to be investigated.

1. Determination of the real occurring axle loads on municipal roads by WIM measurements;
2. Getting insight in the reliability index for existing municipal bridges;
3. Determining the governing lorry for small span bridges.

1.2.2 Force transmission in concrete slabs

In former codes, there is no or little attention to shear force capacity. For concrete slab bridges the force transmission from wheel loads is of interest. For governmental bridges the edge of the slab (near the support) can commonly assumed to be governing. Municipal bridges often have a separated sidewalk or bicycle lane. In this situation the governing wheel loads cannot occur near the edge of the slab and there is a certain edge distance from the drive lane to the edge of the slab. Research was done to the force transmission, critical edge distance and the difference

between a cracked and uncracked concrete slab. This was done for different spans and edge distances.

The research questions for this part of the research is:

2. ***How do the shear forces due to loads from Load Model 1 transmit through a solid concrete slab?***

In this FEM research, different issues are investigated:

1. The shear assessment in concrete slabs;
2. The force transmission of the permanent loads and variable loads of Load Model 1 separately;
3. The influence of cracking of the concrete.

The influence of the span and the edge distance on the governing place for shear assessment (edge or middle of the support) is also investigated in research question 3. With the results of these researches a more detailed Quick Scan can be made which provides less conservative results.

3. What is the critical edge distance of a concrete slab bridge?

The critical edge distance is the distance from the carriageway to the edge of the slab where the middle of the support is governing in shear instead of the edge of the support. This is investigated by comparing the maximum occurring shear forces near the edge end the middle of the support for different combinations of span and edge distance.

1.3 Thesis outline

This thesis is divided into a literature part and a research part. In the literature part, all relevant issues found in literature are described. These issues can be used for the research part. The literature part consist of chapter 2 to chapter 5. The research part consist of chapter 6 and chapter 7. The Quick Scan model with the case studies are described in chapter 8 and 9.

In chapter 2, municipal bridges in the Netherlands in general and the difference with governmental bridges is described. Chapter 3 contains a description of the assessment of existing concrete bridges according to standards and researches. Also, it focusses on the reliability index for existing municipal bridges, and on WIM measurements for the determination of the governing real occurring loads. In chapter 4, researches that have been done to the shear assessment of concrete slab bridges are described. In order to criticize the results found with FEM research, chapter 5 contains a description of relevant issues about Finite Element Modelling. Also, the different load models which represent loads on small span bridges are described and compared with Load Model 1. The research part starts with chapter 6. In this chapter the load models from the previous chapter are compared with the finite element model to determine the α factor that can be used for existing municipal bridges. In chapter 7, different researches to the force transmission in concrete slabs are described. The share of the axle loads and permanent loads to the occurring shear force are regarded separately. Also, the influence of cracking of the slab and the influence of a certain edge distance is investigated. In chapter 8 the Quick Scan model that has been created with results found in the previous chapters is described. Chapter 9 contains case studies to check the Quick Scan. Finally chapter 10 contains the conclusions and outlook.

A sketch of the thesis outline is presented in Figure 1-1.

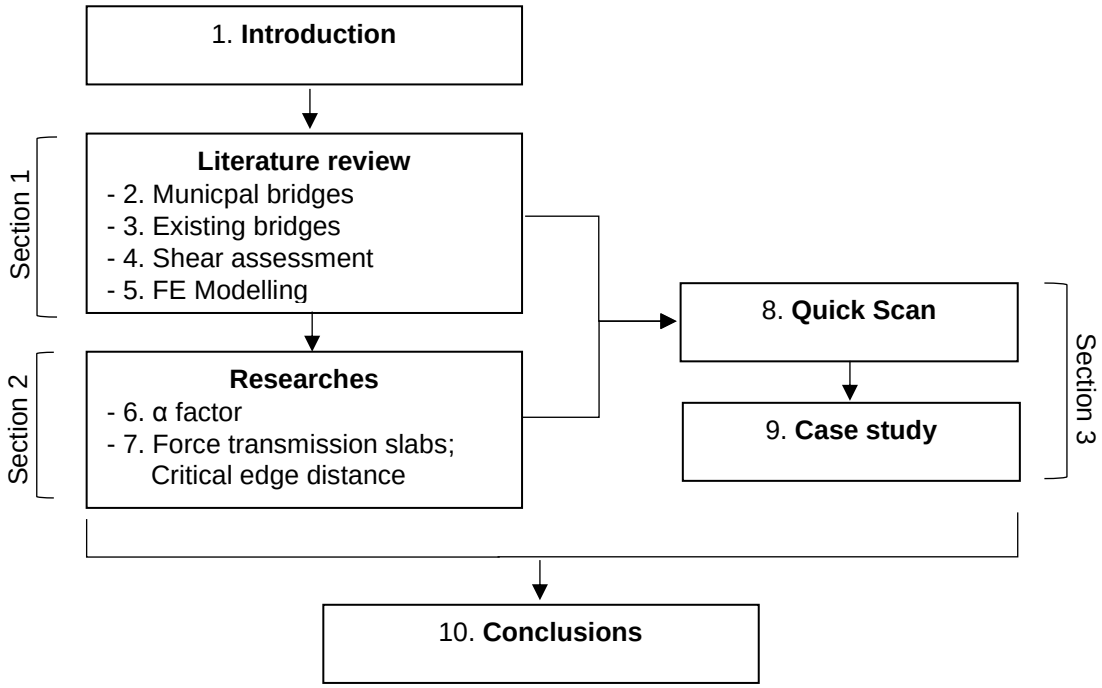

Figure 1-1 - Overview of the contents and structure

Section 1
Literature research and background

2 Municipal bridges

Bridges considered in this thesis are bridges owned by municipalities. These bridges mostly have relatively small spans (<20m). Many municipalities in the Netherlands have a small budget. A recalculation or repair of a bridge is relatively expensive. This leads to the fact that municipalities spent little or no budget to the maintenance or assessment of their bridges. This increases the risks for bridge collapse every year. The last years, people responsible for the municipal bridges became more and more aware of the potential risks of the lack of existing bridge assessment. The consequences of a bridge collapse can be enormous for a municipality. This leads to the demand for a quick and cheap way to reduce the risks.

Bridges owned by the the Dutch Department of Waterways and Public Works are generally better maintained and the risks are better known. Therefore it is useful to compare municipal bridges with these governmental bridges.

2.1 Differences government bridges and municipal bridges

General differences between governmental and municipal bridges are divided in the categories loads, dimensions, materials and standards.

2.1.1 Loads

In general, governmental bridges are larger and designed for heavier and more vehicles. This is especially the case for bridges in highways. Loads are also linked to number of lanes and therefore to dimensions. Most municipal bridges have only 2 lanes. This means that there are only two lanes with a tandem system according to the Eurocode (EN 1991-2 [2]).

The variable loads can be reduced by a factor α. Among other issues, this factor depends on the number of trucks per year per lane. For municipal bridges this number is in general lower than for governmental bridges. In practice for a new bridge, this factor can be chosen in consultation with the client. For existing municipal bridges, this factor is investigated in Chapter 6.

2.1.2 Dimensions

Since loads on governmental bridges are in general higher, also the dimensions are larger. The lay-out of the bridge can differ. Governmental bridge often have an emergency lane and municipal bridges mostly have separated cycling lanes or footpaths. This can lead to differences in the load transfer mechanism.

Spans up to 20 meter are considered. This is because bridges with larger spans are barely found in municipalities. Also, slab bridges in general have no spans higher than 20m. This is because the self-weight of the slab becomes very significant for large spans. In this thesis, especially for the researches, only 2 lanes are considered. This can be done because a third lane does not contribute to the maximum shear force or maximum flexural moment significantly for small spans. For the width of the separated sidewalk and/or bicycle lane a distance of 0,0m to 6,0m is considered. The edge widths that exists the most in municipal bridges are investigated in chapter 2.4. As a rule of thumb, the height of the concrete slab is considered to be 1/20 * L (where L is the span [m]). Other determinations for dimensions are described in chapter 5.3.

2.1.3 Materials

The Dutch Department of Waterways and Public Works has determined a lower boundary for the concrete class of their bridges. This is C30/35. It is questionable if this can also be assumed for municipal bridges. The execution of municipal bridges that were built around 1960 was not under

great supervision. Moreover, the concrete strength after completion and the recent concrete strength is often unknown. If the building year is known, the minimum applied concrete strength and steel strength at that time could be applied. However, this leads to a too conservative assessment. More about applied concrete classes according to former codes can be found in chapter 3.4.

A slab bridge can be prestressed or reinforced. The amount, type and quality of the steel is important for the capacity. However, for shear capacity there can be calculated with the lower boundary of a slab without shear reinforcement if there are no flexural cracks observed. This would imply that the bridge does not fail due to flexural moment. If the lower boundary check for shear fulfills, this means the bridge also not fails due to shear force. More about the application of the Quick Scan model is described in chapter 8.

2.1.4 Standards

Municipal and governmental bridges built nowadays have to fulfil the requirements of the Eurocode [3]. Municipal bridges may deviate from these standards if the principal (the municipality itself) demands this, by varying with the α factor. Also, municipalities can choose which consequence class they want to apply. Mostly CC2 is chosen. For governmental bridges, CC3 is mandatory.

The Dutch Department of Waterways and Public Works has made guidelines for the design of structures (ROK, Richtlijnen Ontwerpen Kunstwerken [4]). These are extensions of the current Eurocode. The Dutch Department of Waterways and Public Works also has the RBK [5] (Richtlijnen Beoordeling Kunstwerken). This contains guidelines about the asset management of existing structures. Also, this report contains information about former standards for the design of structures.

Also, there is an extra part of the Eurocode for Dutch existing bridges. This is NEN8700 [6] and NEN8701 [7], [2], which is for existing bridges in general and the loads on existing bridges, respectively. NEN8702 is currently being developed. This part is about the capacity of existing structures.

Some parts of the documents mentioned above can be used for the assessment of existing municipal bridges.

2.2 Research ‘Bouwend Nederland’ to bridges in municipalities [1]

The Netherlands consist of 403 municipalities. Each municipality owns structures in their region. Since they are the owners, they are responsible for the maintenance of the structures. If the maintenance is done badly, or not at all, this could lead to unsafety and eventually failure of the structure. This leads to great costs for the municipality. Nowadays, municipalities are increasingly aware of their lack of awareness of the structural safety of their structures.
In 2015, the association of construction and infra companies, named ‘Bouwend Nederland’, has done research to the knowledge of municipalities regarding asset management of their bridges. They have sent a survey to all municipalities in the Netherlands [1]. The results are discussed briefly.

2.2.1 The survey

The survey consisted of only 4 questions. This was done in order to make it easy end accessible to fill in the survey. Despite this, only 34% of the municipalities returned the survey. This seems a little, but taking an average of 138 municipalities still provides an acceptable estimation. Also, the distribution of size, population and number of structures of the cooperating municipalities are an acceptable representation of all municipalities in the Netherlands. The cooperating municipalities have a total of 7,1 million inhabitants and have a total of 8000 bridges.
The 4 questions were the following:

1. Do you have a recent overview of all your bridges and fly-overs, including building year and building material?

2. Do you perform periodic inspection of your bridges and viaducts regarding structural safety?
3. Which policy does your municipality apply regarding maintenance and replacement of the bridges and viaducts?
4. Do you have a budget specifically for maintenance and renovation of bridges and viaducts?

2.2.1.1 Overview bridges

69% of the municipalities stated that they have an overview of their bridges. It is not typically clear what kind of overview they mean. It could be only name and location of the bridges, more data like building year, material and dimensions, or even more detailed data like original drawings and calculations. Most municipalities indicate that they use a digital management system where they keep all available information of the bridges and viaducts. Municipal bridges consist primarily of concrete (Figure 2-1). The bridges made out of timber are mainly cyclist or pedestrian bridges.

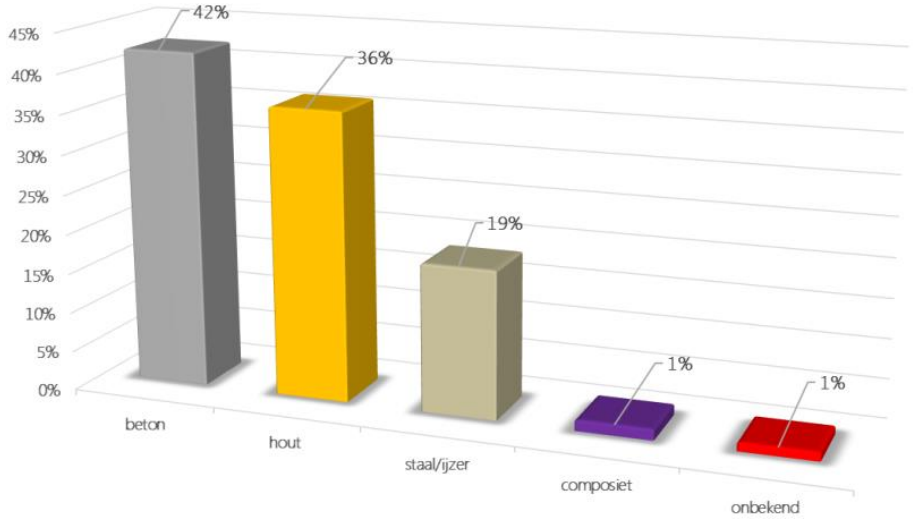

Figure 2-1 - Structural material bridges. (Translation from left to right: concrete, timber, steel, composite, unknown) [1]

The average design lifetime of concrete bridges is 50 to 80 years. Thereafter they require renovation or replacement in most cases. The increase of traffic and/or the increase of traffic weight can lead to the fact that bridges might not fulfill the safety requirements according to the standards anymore. Also, the building year provides insight in which design standards were applicable at that moment. The standards changed over time, so the bridge might not fulfill the requirements of the current standards. Figure 2-2 illustrates the building year of the concrete bridges in municipalities. A large part of the municipal concrete bridges (almost 40%)[1] is built before 1980. This means that these bridges have to be evaluated shortly. The main part of these concrete bridges are reinforced slab bridges, since this was the standard type of small span bridge.

[1] Probably more, since the building year of 15% of the concrete bridges is unknown. It is likely that especially the building year of old bridges is unknown. One could assume that 50% of the bridges was built before 1980.

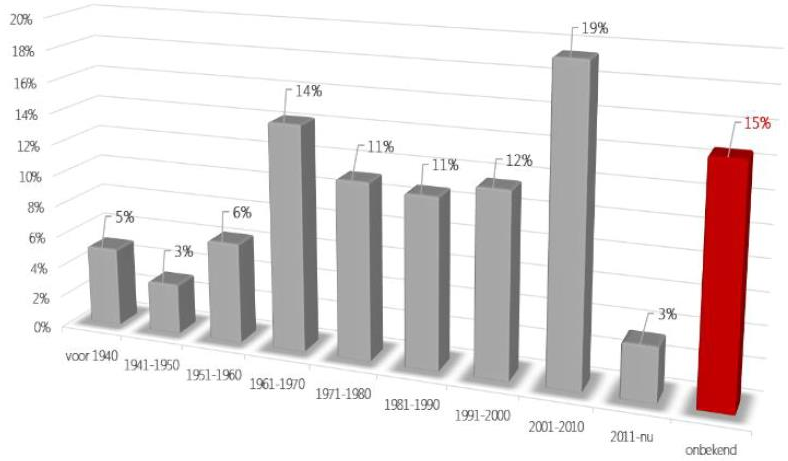

Figure 2-2 - Building year concrete bridges [1]

2.2.1.2 Periodic inspection

Over 47% of the municipalities stated that they do not perform periodic inspection to their bridges. This insists that hundreds of concrete bridges are not inspected at all and are therefore a serious threat to the safety of passers-by. 'Bouwend Nederland' also did research to the executed inspections. Only 41% of the concrete bridges were marked as good condition (Figure 2-3). Especially the condition of most bridges in smaller municipalities was marked as moderate or bad.

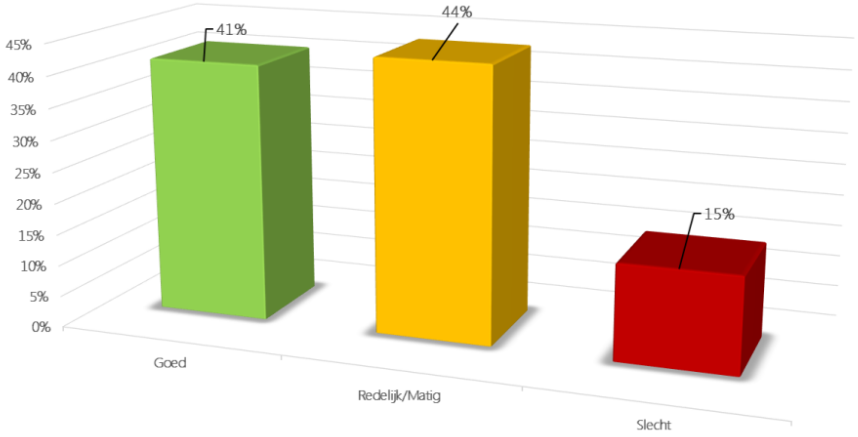

Figure 2-3 - State of the concrete bridges after inspection (green = good, yellow = moderate, red = bad) [1]

2.2.1.3 Policy maintenance and replacement

35% of the municipalities stated that they work with certain management plan or policy. The goal of such a policy is giving insight in the necessary maintenance or replacement, as well as giving insight of the associated costs.

2.2.1.4 Budget

Only 41% of the municipalities stated that they have a budget for maintenance of bridges. In some cases, also the inspection costs are paid from this budget. Problems are faced if a bridge needs sudden repair or replacement. Some municipalities may have significant problems if they keep on neglecting the necessity of inspection and maintenance. The chance of a bridge collapse increases with all its consequences.

The budget for maintenance of bridges in total is estimated to be €2 to €3 billion per year. The total replacement value is estimated to be €150 to €200 billion [1].

2.3 Internal Research Sweco

Sweco does inspections to structures in municipalities. Also, making an inventory of all structures is part of their task. Research to the inspections done by Sweco are used to indicate what the distribution of types of bridges in a municipality is. Also, these inspections indicate what type of bridges need maintenance the most. The outcome of this research should be roughly similar to the outcome of the research of 'Bouwend Nederland' as described in chapter 2.2.

The goal of this chapter is to verify the need of the Quick Scan model. This is done by making a substantiated estimation of the number of concrete slab bridges that are applicable to the Quick Scan model. Research to 10 different municipalities in the Netherlands has been done to the following issues: type of bridge (material), building year and number of bridges. The number of bridges per specific municipality and on average can be found in Figure 2-5. The average distribution of the structural building material per municipality can be found in Figure 2-4.

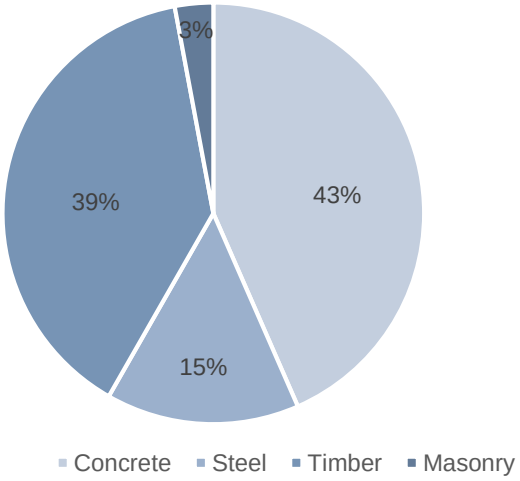

Figure 2-4 - Average distribution of the building material of bridges per municipality

The two researches are compared for the average distribution of bridge building materials in municipalities. An overview from Figure 2-1 and Figure 2-4 has been made in Table 2-1.

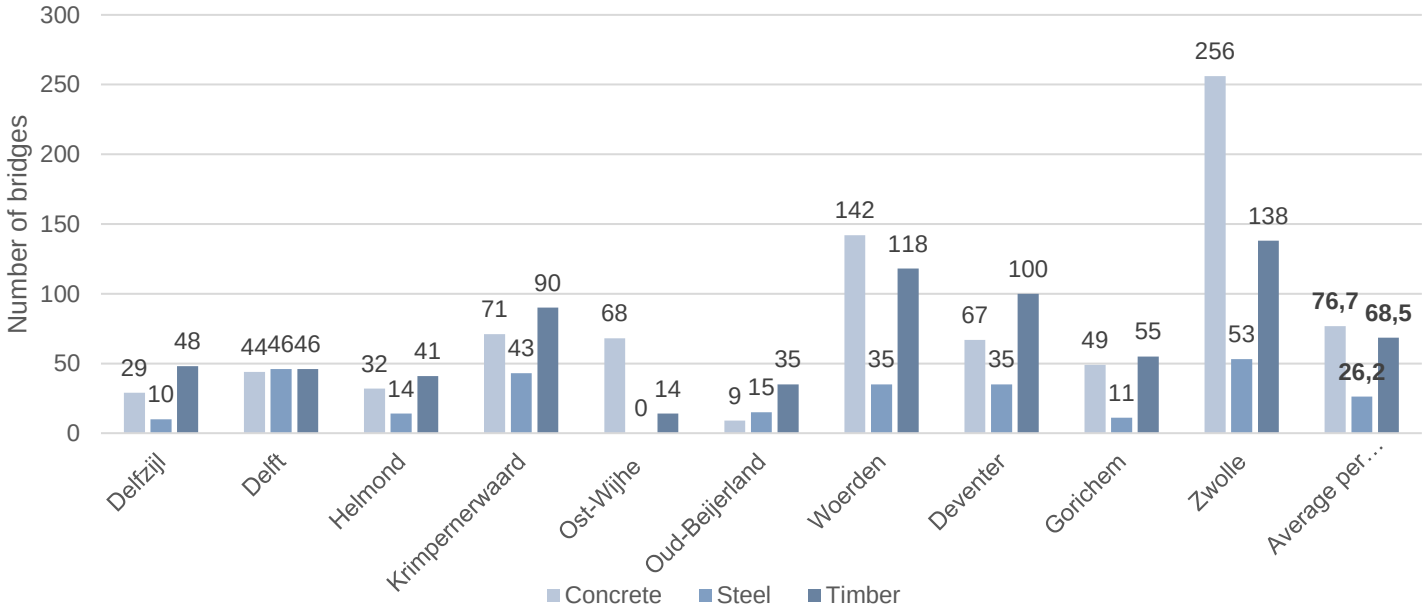

Figure 2-5 - Bar chart of the number of bridges per municipality [2]

Table 2-1 - Comparison research 'Bouwend Nederland' and Sweco intern

Material	Research 'Bouwend Nederland'	Research Sweco intern
Concrete	42 %	43 %
Timber	36 %	39 %
Steel	19 %	15%
Masonry	<1 %	3 %
Composite	1 %	< 1 %
Unknown	1 %	0 %

[2] Only concrete, steel and timber bridges have been counted

This table demonstrates that the outcome of the 2 researches is almost the same. Therefore, there can be assumed that this is a reliable average for the bridges in municipalities. The cooperating municipalities have a total of 8000 bridges. This means that Dutch municipalities have a total of around $\frac{8000}{0{,}34} \approx 23500$ bridges (since 34% of the municipalities participated in the research). The number of concrete bridges in a municipality is around 42% [1]. This is $23500 * 0{,}42 \approx 14500$ concrete bridges. According to the data from Sweco, 43% of the concrete bridges are traffic bridges. This makes the total municipal concrete bridge for traffic $14500 * 0{,}43 = 6235$. From these concrete bridges roughly 50% is a slab bridge. This makes a total of $6235 * 0{,}43 \approx 3120$ municipal concrete slab bridges in the Netherlands. For some concrete slab bridges the Quick Scan will not be applicable, or applicable with more uncertainty. For example due to an odd slab shape, large angle of skew or an unclear static system. There is assumed that 75% of the concrete slab bridges are applicable to the Quick Scan model. This makes the total bridge applicable to the Quick Scan model $3120 * 0{,}75 = 2340$ bridges in the Netherlands (municipal concrete slab bridges).

2.4 Research edge distance municipal bridges

2.4.1 Introduction

Dimensions and the built-up of municipal bridges are different compared to governmental bridges. Due to these differences, the assessment of both types of bridges can be different. General differences are stated in chapter 2.1. One of the differences is the presence of a separated sidewalk or bicycle lane. Most governmental bridges do not have sidewalks, because these are highways or provincial roads. Most municipal bridges contain sidewalks and/or bicycle lanes, since these bridges are often used by pedestrians and cyclists. According to recent standards (Eurocode), there can be assumed that the governing vehicle from Load Model 1 is not present on the sidewalk if the kerbs are higher than 100mm [8] , measured from the deck. This means that axle loads near the edge of the slab does not have to be taken into account if kerbs are present.

For the shear assessment of governmental concrete slab bridges there is assumed that the edge is governing (Figure 4-8). With the presence of sidewalks this might not be the case, since the distance to the edge is too great. Now the middle of the slab might be governing. For the Quick Scan model, it can be beneficial to know at what width of the adjacent sidewalk and/or bicycle lane the edge of the slab is still governing in shear.

2.4.2 General lay-out bridge deck

Research has been done to the general lay-out of bridge decks in municipalities. In this way municipal bridges can be divided in different categories regarding the lay-out. In total, concrete bridges in 10 different municipalities have been investigated. In total, 325 bridges have been examined. This has been done using inspection pictures from inspections done by Sweco and Google Maps. Sweco has a database with all inspections done in municipalities. The investigated Dutch municipalities are: Delft (Dl), Delfzijl (Dz), Deventer (Dv), Gorinchem (G), Helmond (H), Krimpernerwaard (K), Olst-Wijhe (O-W), Oud-Beijerland (O-B), Woerden (W) and Zwolle (Z) The locations of these municipalities are illustrated in Appendix Figure 11-1.

The following parameters from every investigated bridge have been noted.

- Code, name and location;
- Number of footpaths and bicycle lanes;
- Total width of the bridge;
- Total width of the footpaths and bicycle lanes;
- Distance from the side of the carriageway to the edge of the slab;
- Height of the kerb higher than 100mm?

From these parameters, most interesting parameter is the distance from the side of the carriageway to the edge of the slab.

2.4.3 Results and conclusions

The chosen municipalities differ in size, number of inhabitants, location (urban/rural) and number of bridges. In this way there has been tried to find an average for the lay-out of all concrete bridges in the Netherlands. The results for the edge distance of the investigated bridges are illustrated in Figure 2-6.

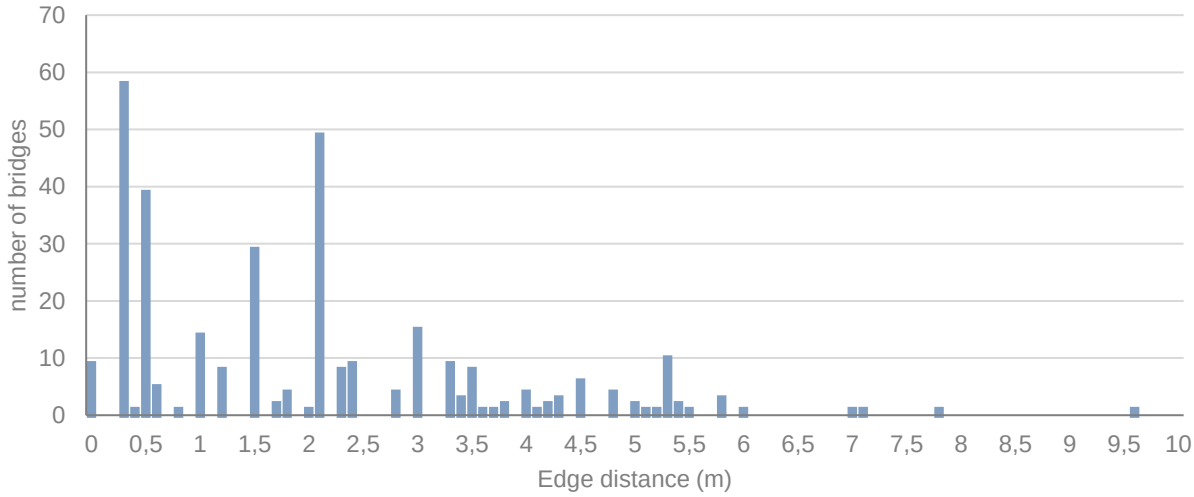

Figure 2-6 – Edge distance (b_{edge}) from the outer side of the carriageway to the edge of the deck (10 municipalities)

The first conclusion is that the lay-out of a bridge can differ. Looking at this figure two distances that occur several times can be distinguished. These are around 0,5 meter and around 2 meter width. These distances stand for no sidewalk and one sidewalk/ one bicycle lane respectively. Examining this figure the lay out of the bridges can be characterized. 4 categories can be distinguished.

1. No sidewalk or bicycle lane;
2. A sidewalk or bicycle lane;
3. A sidewalk and bicycle lane;
4. A sidewalk, and/or bicycle lane with additional space, for example a berm.

Standard dimensions for these parts of the bridge are the following.

- The standard dimensions for a footpath are 1,2 to 2,4 meters; [9]
- The standard dimensions for a bicycle lane are 2,0 to 3,0/3,5 meters; [9]
- Most bridges have an edge beam (Load-carrying or non load-carrying) with a hand rail. The width of this edge beam is mostly 0,3 to 0,5 meter.

With knowledge of these standard values the characterization in Table 2-2 has been made.

Table 2-2 - Categorization municipal bridges

	Distance from side carriageway to edge slab (m)	Number of bridges (looking at 'measured' distances)	Number of bridges (Google Maps and inspection pictures)
No bicycle lane or footpath	< 1,2	135	140
Bicycle lane or footpath	1,2 to 3,2	121	122
Bicycle lane and footpath	3,2 to 5,4	60	57
Bicycle lane, footpath and additional berm	>5,4	9	6
Total		325	325

This categorization is purely made to clarify the measured distances. It is not being used further because for the force transmission it does not matter in what category the bridge falls. The only

thing that matters is the edge distance. From some different edge distances a few examples are illustrated in Table 2-3.
For more than half of the municipal bridges the edge distance is significant (>1,2m). This means that it makes sense to investigate whether the edge of the support or the middle of the support is governing.

Description and location	Example 1	Example 2
No bicycle lane or footpath - N362, Delfzijl -Heemweg, Delfzijl		
Bicycle lane or footpath - Zuiderzeelaan, Zwolle - Maastrichterweg, Roermond		
Bicycle lane and footpath Leo Marjorlaan, Zwolle Gelreweg, Tilburg		
Bicycle lane, footpath and additional part - Wulverhorstbaan, Woerden - Burgemeester Geuljanslaan, Roermond		

Table 2-3 - Examples different categories (source: Google Maps)

For the shear assessment of governmental bridges, the edge of a slab is assumed to be governing. For municipal bridges, this might not be the case. In general, municipal bridges have another lay-out than governmental bridges as they may contain a footpath or bicycle lane. If this is the case, the governing loads from Load Model 1 have to be placed further from the edge of the slab (on the driving lane). In this case, the edge of the slab is not commonly likely to be governing anymore. Most municipal bridges have an edge distance of around 0,3m (18%), 0,5m (12%), 1,5m (9%) and 2,1m (15%). 190 of the 325 investigated bridges (58%) have significant edge distances (>1,2m). The edge distances of these bridges is different compared to governmental bridges, and the edge of the slab might not be governing. In chapter 7.5 is

calculated whether the edge or the middle of the support is governing in shear. This has been done for different combinations of span and edge width. In this way one can say if the edge or the middle of the support is governing for a certain combination of edge width and span.

3 Assessing existing concrete bridges

3.1 Bridge asset management in general

ISO 55000 defines Asset management as the "coordinated activity of an organization to realize value from assets". An asset is defined as ‘An item, thing or entity that has potential or actual value to an organization". So, asset management is a very broad term.

Asset management for bridges includes many aspects and is not commonly clear defined. In general, it includes the process of maintenance, upgrading and operating cost effectively. Bridge asset management is often an underrated phenomenon. But if managing of assets is not done, or done incorrectly, it can cost a substantial amount of money. In the end, the maintenance and reparation of a bridge is cheaper than rebuilding a bridge.

Nowadays, municipalities are more interested in asset management of their bridges. This is the result of some recent minor incidents with bridges in the Netherlands and other European counties (such a 2 recent bridge collapses in Italy). These incidents meanly forced closing of a bridge due to unsafe situations regarding the structural safety. Some examples are the incidental temporary closure of the bridges ‘Hollandse brug’ and ‘Merwedebrug’. Temporary closure of bridges of this size and importance cost between 100 and 200 thousand euros each day. Also a temporary closure of a municipal bridge can be expensive. For municipal bridges where the remaining capacity is doubted or not known, often a load reduction sign is placed (*Appendix B – Load reduction signs*)

These kind of closures, together with recent researches to the structural safety of existing bridges, raised questions at municipalities. They are becoming more aware of the danger of failing asset management, both financial and structural danger. The municipality itself is responsible of the guarantee of safety of their bridges.

There are several levels of bridge assessment. An often used distribution approach is the ‘step level’ approach [10]. This approach consist of 5 levels of assessment, each with different strength & load models, calculation models and assessment methodology. The different levels are stated below:

Level 1
This assessment provides a conservative estimation of the load capacity. Only simple analysis methods are necessary and partial safety factors are used.

Level 2
This assessment involves the use of more refined analysis and better structural idealisation. It also allows determination of characteristic strengths of materials based on available data.

Level 3
The level 3 assessment uses bridge-specific loading in the safety evaluation. It also allows material testing in order to determine characteristic material strength properties. Again, partial safety factors are recommended to apply.

Level 4
This level assessment specifies any additional safety characteristic. Any changes to the criteria used may be determined through reliability analysis, or by judgement changes to the partial safety factors.

Level 5
The level 5 assessment makes use of reliability theory in the process of load carrying capacity evaluation. This analysis requires statistical data for all the variables defined in the loading and resistance equation.

These levels of assessment are summed up in Table 3-1. The recommendation is to go forward to the next level only if the bridge fails to pass the previous assessment level.

Table 3-1 - General scheme of the 5 assessment levels [10]

<table>
<tr><th>Level</th><th>Strength & Load Models</th><th>Calculation Models</th><th>Assessment Methodology</th></tr>
<tr><td>1</td><td rowspan="2">Strength and load models as in design code. Material properties based on design documentation and standard</td><td>Simple, linear-elastic calculation</td><td rowspan="2">LRFD[3]-based analysis. Load combinations and partial factors as in design code</td></tr>
<tr><td>2</td><td rowspan="3">Refined, load redistribution is allowed, provided that the ductility requirement are fulfilled</td></tr>
<tr><td>3</td><td rowspan="2">Material properties and load models can be updated on the basis of in-situ testing and observations</td></tr>
<tr><td>4</td><td>LRFD-based analysis. Modified partial factors are allowed</td></tr>
<tr><td>5</td><td>Strength model including probability distribution for all variables</td><td>Probabilistic analysis</td></tr>
</table>

As can be seen in the table, most advanced assessment methods combines load distribution analysis (non-linear) with a probabilistic analysis This level can be applied as the last resort to save the bridge from unnecessary repair or strengthening. This level reflects more accurately the real structural behaviour of the bridge. Therefore, many bridges that are declared unsafe in the previous levels may have enough reserve strength to safely support the applied loads when analysed at this level. However, for the execution of assessment level 4 and 5, much information is needed. Gathering this information costs a much time and money. In principle, the Quick Scan model will be applicable for assessment level 1. If more detailed parameters are known, such as material strength due to testing, level 2 or 3 could be reached. This is also true because the Quick Scan is based on results from Finite Element Modelling.

When designing a bridge, this is mostly done for a lifetime of 50 or 100 years. It can be assumed that the bridge will fulfil the safety requirements during this lifetime if adequate maintenance is done. Nevertheless, during the assessment of existing bridges it sometimes turn out that the bridge does not fulfil the safety requirements anymore. This is considered to be caused by one or more of the following reasons:

- Increases in loading, so that the current loading is greater than the structure was originally designed for;
- Updates in the standards in response to research, so that the assessment capacity is less than the original design capacity according to the design code of the time (for example shear assessment);
- Lack of design information leading to conservative assumptions;
- Reduced capacity due to deterioration or damage;
- Poor original design or construction;
- Inappropriate or too conservative analysis for assessment;
- Misinterpretation or inappropriate application of the assessment code.

[3] Load and Resistance Factor Design

3.2 Types of bridges

Over the last 3000 years, engineers and architects have devised many ways of building bridges. Because of the variation in many parameters, such as materials, loads, span and costs, there are many different types of bridges possible.

The main focus in this thesis is slab bridges. This type is one of the most applied types of bridges in the Netherlands, especially before 1980/1975. Other types of bridges are discussed briefly in *Appendix C – Other types of concrete bridges*. These are:

- Beam or girder bridge;
  - T-beam;
  - I-beam;
  - M-beam;
- Rigid frame bridge;
- Box girder bridge.

3.2.1 Slab bridge

A slab bridge is the simplest design type. It consists of one or more slabs that provide strength and stability. The slab design is often chosen for small span bridges with the lower load classes. Slab bridges are generally cast in-situ, rather than prefab (especially decades ago). This is more cost-effective, because since the shape is simple, also the formwork is rather simple. Moreover, the reinforcement is relatively easy to apply. Prefab or precast slabs can be used for small spans in some cases. In order to reduce self-weight, the voided slab has been invented, This can be used as modern replacement for the cast-in-place slab.

Slab bridges can only be applied for small spans. Therefore, slab bridges are often used in series, with vertical supports between the bridge abutments to allow a longer total length. Such series of shorter slab spans are called “multiple span” slab bridges. If the bridge consists of one continues slab with multiple supports, it is called a “continues span” slab bridge. A continues span slab is statically undetermined. This is often achieved by casting a compression layer together with the joint between the prefab slabs.

If the span becomes larger, the slab has to be thicker in order to carry the loads. Now, self-weight becomes a problem. The maximum span of a reinforced slab bridge that is still economical is about 12 meters. A typical cross-section is illustrated in Figure 3-1. If prestressing steel has been used, the maximum span can be up to 22 meters (economically). Larger spans using prestressing steel are obviously possible. In that case, other types of bridges such as prestressed beam bridges or box girders are mostly chosen. [11] [12] [13]

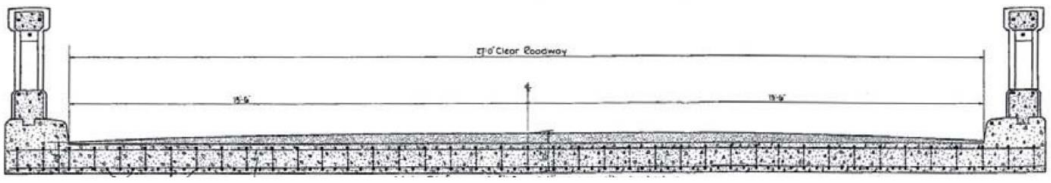

Figure 3-1 - Example of the cross-section of a reinforced slab bridge (with edge beams)

3.2.1.1 Longitudinal cross-section

Basically there are 3 different types of longitudinal cross-sections. These are the constant, arched and inflected cross-section. Obviously the constant cross-section is the easiest to fabricate. Also the reinforcement and the formwork. The other shapes can be chosen is an increased capacity near the support is needed.

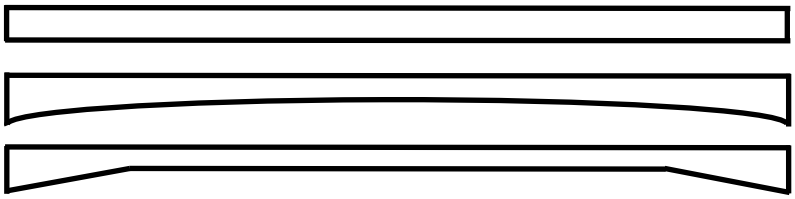

Figure 3-2 - longitudinal cross-section slab bridge (constant, arched and inflected)

3.2.1.2 Transverse cross-section

In general there are 3 different types of transverse cross-sections. A constant thickness is the most occurring type. The other 2 types may differ. The length of the constant or arched decreasing part can vary from a small part where the angle is 45 degrees, to a large part where angle is much less. This shape is sometimes chosen to decrease the amount of material that is being used. This is possible when the bridge has less loaded parts at the edges, such as footpaths or bicycle lanes.

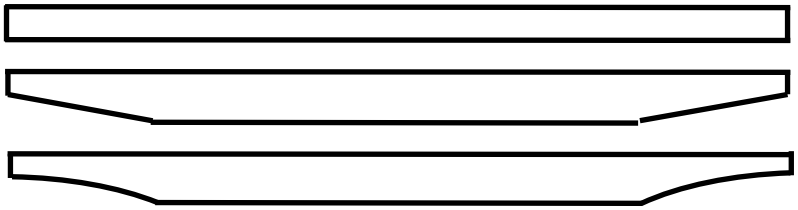

Figure 3-3 - Transverse cross-section of a slab bridge (constant, decreasing thickness constant, decreasing thickness arched)

3.2.2 Concrete bridges nowadays

Nowadays, often a combination of (prestressed) prefab and cast in-situ bridges is used in the Dutch municipalities and in Dutch highways. These are the so called ZIP and SJP bridges.

3.2.2.1 ZIP bridges (rail beam bridges)

ZIP bridges consist of reversed prestressed T-beams and a reinforced concrete compression layer on top (Figure 3-4). This compression layer is cast in-situ and is only a top layer. This means hollow spaces appear in the bridge. This is positive for the self-weight of the bridge. Sometimes holes near the edge are filled with concrete to resist impact forces. A special type of ZIP bridges uses prestressed I-beams as structural elements. In this case, the upper flange of the I section is also the formwork for the in-situ compression layer. This type of bridge can theoretically reach spans of 60m. The construction depth of the bridge is more than 2 meter in this case. Other types of bridges are mostly economically more attractive. ZIP bridges are also known as rail beam bridges. These type of bridges are not suited for the Quick Scan model.

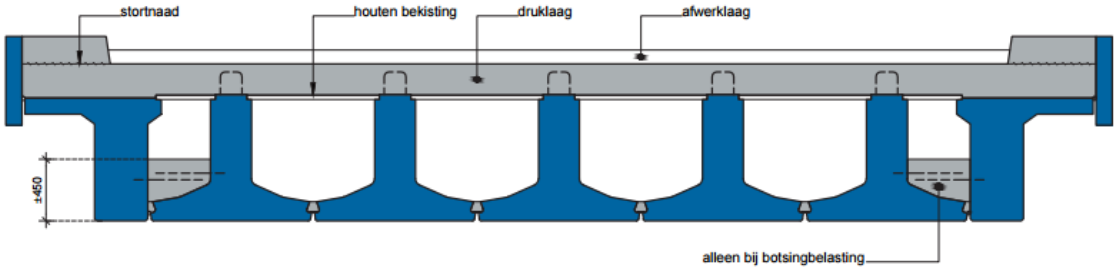

Figure 3-4 - cross-section ZIP bridge [14]

3.2.2.2 SJP bridges

SJP bridges also make use of reversed prefab prestressed T – beams. However, the web of these beams is thicker than in ZIP bridges. The in-situ concrete of SJP bridges fills the spaces between the beams (Figure 3-5). This makes the bridge, after curing, actually a prestressed slab bridge. The maximum span is about 20-25 meters. The construction depth of the bridge will then be around 0,8m.

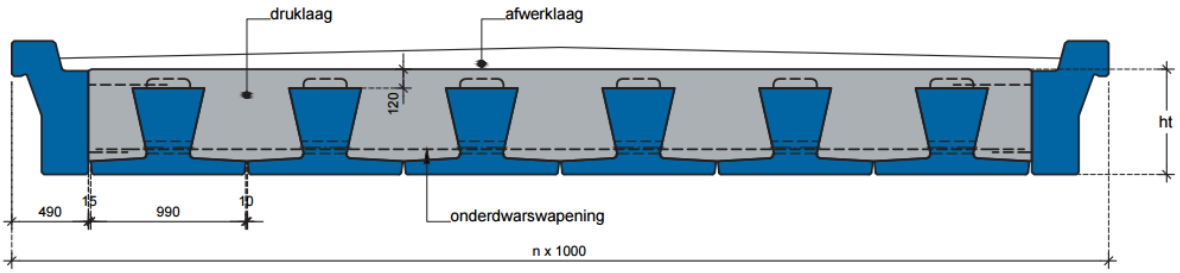

Figure 3-5 - cross-section SJP bridge [14]

3.3 Overview parameters of concrete slab bridges

In this section, an overview of different important parameters is provided. Every parameter is explained briefly.

3.3.1 Number of lanes

The difference between driving lanes and notional lanes is important. The number of lanes can be seen directly when looking at the bridge. The number of notional lanes might be different. Notional lanes indicate how many driving lanes there can be theoretically. The number of notional lanes is important since this might be higher than the number of practical lanes. If there is no separation (by a kerb) between the footpath or bicycle lane there might be an extra notional lane.

3.3.2 Edge distance

A difference between governmental bridges and municipal bridges is that municipal bridges might have a sidewalk or cycling lane. If this part is separated from the driving lanes by a kerb with a height of at least 100mm, the axle loads from Load Model 1 do not have tot be placed near the edge of the slab. This makes the model less conservative. Also, this makes the edge distance more important, since it might not be clear if the middle or the edge of the support is governing in shear.

3.3.3 Angle of skew

The angle of skew might be important for municipal bridges. Some papers about the influence of the angle of skew on the bending moment, torsional moment and shear distribution were found. Mostly the angle of skew is tested with a finite element program. The conclusions of the these papers however, are not typically the same. It is clear that more research to the influence of the angle of skew is needed. Some conclusions from [15], [16] and [17] are stated below.

- For skew angles 70˚ - 90˚ (77,8gon – 100gon), no skew at all can be assumed, since influences are negligible.
- The reaction forces on the obtuse skew angled end slab of the bridge are larger than the other end. The increase in reaction force ranging from 0 to 50% for skew angle of 70˚ to 40˚. (Figure 3-6)
- As skew angle increases, torsional moments gradually shift towards the obtuse angle

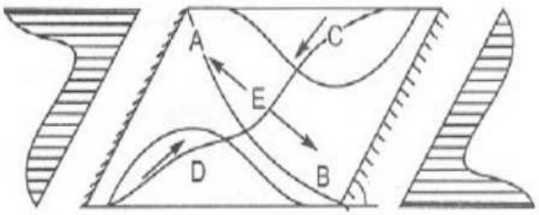

Figure 3-6 - Direction and magnitude of moment flow in skewed bridge decks [16]

Since no solid conclusions were drawn for a varying skew angle only bridges with skew angles of 90˚ are regarded. An decrease or increase in skew angle leads to an increase of the uncertainty of bridge assessment.

3.3.4 Static system and number of spans

The static system is an important parameter for the bending moment distribution. A short-span single slab bridge can be executed with fixed ends. In this case , there is a hogging bending moments at the supports. A continues slab is mostly simply supported. At the intermediate spans, a hogging bending moment originates. The rotation at intermediate spans is commonly zero. An intermediate support can therefore be considered as a fixed support. A multiple span bridge, such as a continues slab, can also consist of multiple single slab bridges. In this case, there is no hogging bending moments at the intermediate support, since this supports can be considered as a hinge. More about static indeterminacy can be found in chapter 4.4.2.

Reference projects [18] reveals that a spreadsheet program can calculate single and multiple spans. Quick Scans from the Dutch Department of Waterways and Public Works do not regard 2 span slabs, since this type of bridge does not exist in governmental reinforced slab bridges. Municipal 2 span bridges do exist, so this type of bridge is considered.

3.3.5 Dimensions

The dimensions are of course one of the most important parameters for bridge assessment. Dimensions are linked with other parameters such as number of lanes, static system or material characteristics. Since only slab bridges are considered, the dimensions are rather easy to measure. A slab only has a length (span), width and height. Sometimes, the height of the slab increases when the slab approaches a support. This is described in chapter 3.2.1. Dimensions of interest are: span, width, edge distance, height and other distances if the slab does not have a constant shape longitudinally or in transverse direction.

3.3.6 Execution type of the slab

A slab can either be cast in-situ or prefab (precast). Decades ago, (1960s and 1970s) concrete slabs were mostly cast in situ rather than prefab. In general, prefab concrete has a more constant quality since the production process is better controlled. The quality of in-situ concrete is less constant due to weather conditions and execution errors. Also, the force transmission due to self-weight may be different. In a prefab slab, torsional forces may occur near the edge of the slab, which leads to peak (shear) forces near the edge. This is explained in chapter 5.2. For slabs cast in-situ, these peak forces will generally not occur. Reason for this is that the concrete is cast in the formwork before hardening. The concrete can distribute its self-weight over the support entirely. The resulting shear force due to self-weight is constant. Therefore, these types of slabs has to be assessed differently. For example, cracking has no influence on the force transmission of the self-weight for slabs cast in-situ.

3.3.7 Edge beam

The edge beam is positioned longitudinally at the edge of the bridge deck. The main function of the edge beam is to work as support for the railing and to be a part of the drainage system. Alongside these attributions the edge beam is seen as a stiffening structure of the bridge deck and can also be of a load-carrying or non-load-carrying type [19]. Four different types of edge beams can be distinguished:

I. Integrated concrete edge beam;
II. Prefab concrete edge beam;
III. No real edge beam;
IV. Steel edge beam.

Examples these different types of edge beam are illustrated in Figure 3-7. An integrated edge beam (I) without dilatation joints can contribute to the shear capacity and stiffness of the bridge. For a prefab concrete edge beam (II) this depends on the type of connection between the edge beam and the slab. A steel edge beam and no (real) edge beam do not contribute to the shear capacity. In older concrete slab bridges (bridges form the 1960s -1970s) type I and III occurs the most. In general, edge beams in older bridges do not contain dilatation joints.

A load carrying edge beam leads to a higher capacity near the edge of the slab. In former codes, the additional capacity was calculated by replacing the edge beam by a strip of slab having equal

flexural stiffness. The structural calculation of an edge beam falls outside the scope of this thesis. The Quick Scan model will still be applicable to slab bridges with an edge beam. Then, the middle of the slab is assumed to be governing in shear.

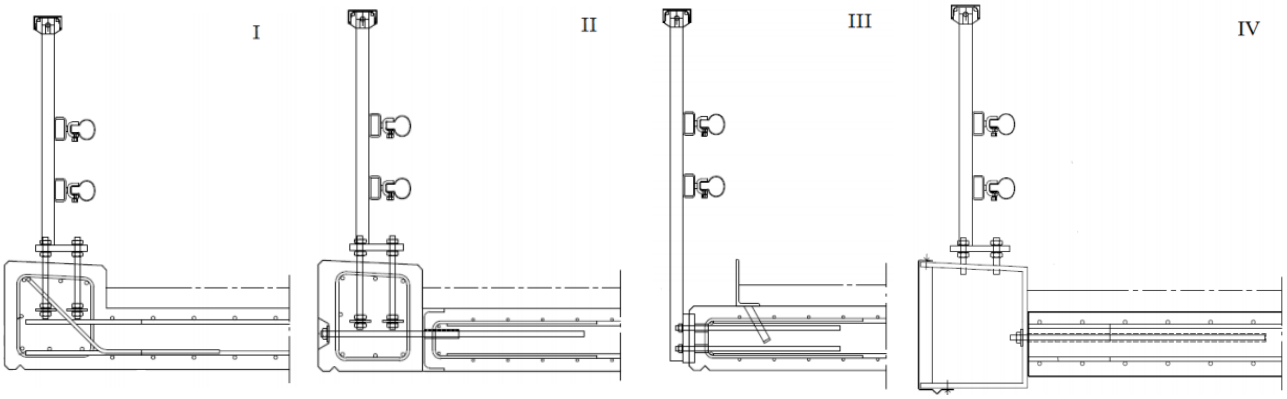

Figure 3-7 – Different types of edge beams

3.3.8 Material characteristics

Material characteristics are very important for determination of the strength of the bridge. A problem with existing bridges is that sometimes these parameters are unknown. Other parameters such as dimensions, number of spans and angle of skew can be measures quite easily. If the material characteristics, such as concrete type, steel type and reinforcement ratio are unknown, lower bound values could be applied. This however, would result in very conservative results. For more realistic results, the values from the Dutch Department of Waterways and Public Works for minimum concrete and steel strength can be assumed. This will be the choice of the user of the Quick Scan.

3.3.9 Stiffness

The stiffness of the concrete slab can be determining for the force transmission. Especially the transverse stiffness relating to the longitudinal stiffness is important for the transverse force distribution and therefore for the effective width. Cracking of the slab influences the longitudinal and transverse stiffness. Therefore it is important to differentiate between a slab that is fully cracked or uncracked. The ratio between the longitudinal and transverse stiffness is most important, since it has influence on the force transmission. As rule of thumb, the transverse stiffness of 1/3 of the uncracked stiffness if often used. In this chapter, this assumption is verified.

The stiffness of cracked concrete can be determined by the Moment – Curvature diagram (M – κ diagram). Two types of the M – κ diagram are illustrated in Figure 3-8.

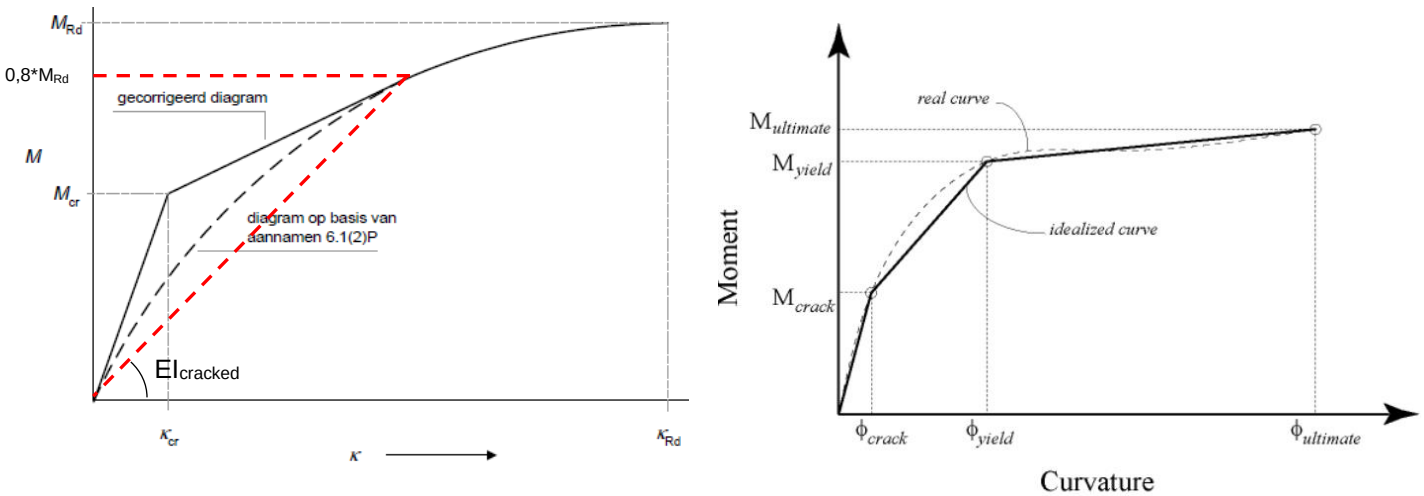

Figure 3-8 – M – κ diagram according to EC2 (left); M – κ diagram (simplified) for reinforced concrete (right) [20]

A trilinear moment-curvature relationship shown in Figure 3-8 is defined by three important states: crack, yield and ultimate. When the concrete stress in the far most tension fibre reaches the rapture modulus of concrete, the state of crack occurs. In the yield state, the far most tension rebars starts yielding. Finally, for ultimate state either the maximum compressive strain in concrete or the tensile strength in steel reaches their ultimate capacity. The ultimate strain capacity of concrete is about 0.004 and the ultimate tensile strength of rebar is its nominal ultimate tensile stress times its area [20].

The stiffness can be determined by using the maximum occurred flexural moment. For existing bridges, usually a value of 80% of the design moment is chosen ($0{,}8*M_{Rd}$). From this point a horizontal line can be drawn to the graph. From the intersection a straight line to the origin can be drawn. The slope of this line represents the stiffness times the moment of inertia according to equation 3.1.

$$M = EI*\kappa \qquad \textit{(3.1)}$$

Since the actual assumed stiffness is based on the maximum occurred flexural moment, no general rule for the stiffness of cracked slabs can be formulated. However, only the ratio between the longitudinal and transverse stiffness has significant influence on the force transmission. This ratio is determined by comparing the longitudinal and transverse fictional stiffness.

The stiffness from equation (3.1) can be replaced by the fictional stiffness. The described rule of thumb ($E_y=1/3*E_x$) is based on the difference between the longitudinal and transverse reinforcement ratio. The determination of the fictional stiffness E_f is demonstrated in Table NB-1 of NEN-EN 1992-1-1+C2/NB. Note that the fictional stiffness must not be compared to the concrete stiffness E_{Cm}, since this is the stiffness due to one axial pressure.

Some test were performed with different reinforcement ratios and concrete classes. For the transverse reinforcement a minimum of 20% of the longitudinal reinforcement can be assumed. Results are demonstrated in Table 3-2. Note that the minimum value for the fictional elastic modulus is determined by the minimum longitudinal reinforcement ratio, Therefore this minimum value only applies for the longitudinal reinforcement.

Table 3-2 - Fictional elastic modulus E_f (N/mm^2)

Concrete class	formula	Reinforcement ratio (%)									
		0,2	0,4	0,6	0,8	1,0	1,2	1,4	1,6	1,8	2,0
C16/20	$(2{,}35+520\rho)10^3 \geq 3250$	3390	4430	5470	6510	7550	8590	9630	10670	11710	12750
C30/37	$(2{,}50+550\rho)10^3 \geq 3600$	3600	4700	5800	6900	8000	9100	10200	11300	12400	13500
C40/50	$(3{,}10+670\rho)10^3 \geq 5350$	4440	5780	7120	8460	9800	11140	12480	13820	15160	16500

Some practical combinations of longitudinal and transverse reinforcement are demonstrated in Table 3-3.

Table 3-3 - Ratio between transverse and longitudinal fictional elastic modulus for different practical combination of reinforcement ratios

Longitudinal reinforcement ratio	Transverse reinforcement ratio	% ρ_t/ρ_l (min 20%)	$E_{f,T}/E_{f,L}$ C16/20	$E_{f,T}/E_{f,L}$ C30/27	$E_{f,T}/E_{f,L}$ C40/50
0,5	0,1	20%	0,58	0,58	0,58
1,0	0,2	20%	0,45	0,45	0,45
1,5	0,3	20%	0,39	0,39	0,39

0,6	0,2	30%	0,62	0,62	0,62
0,9	0,3	30%	0,56	0,56	0,56
1,2	0,4	30%	0,52	0,52	0,52
1,5	0,5	30%	0,49	0,49	0,49
0,5	0,2	40%	0,68	0,69	0,69
0,75	0,3	40%	0,63	0,63	0,63
1,0	0,4	40%	0,59	0,59	0,59
1,25	0,5	40%	0,56	0,56	0,56
1,5	0,6	40%	0,54	0,54	0,54

In this thesis is assumed that the transverse stiffness of cracked slabs is 1/3 of the longitudinal stiffness. As demonstrated in Table 3-3, the assumption is an underestimation for every practical reinforcement combination. Since the combination of reinforcement is often unknown it is desired to use this lower boundary. A lower transverse stiffness leads to smaller effective widths and therefore higher peak shear forces.

The maximum found ratio between the fictional longitudinal and transverse stiffness was 68%. The minimum found ratio was 39%. A general rule for the ratio between longitudinal and transverse stiffness can be applied for cracked slabs: The transverse stiffness is between 1/3 and 2/3 of the longitudinal stiffness, depending on the ratio and the magnitude of the longitudinal and transverse reinforcement ratio, and the concrete class.

3.3.10 Loads

Loads according to the Eurocode together with the National Annex are (and have to be) used. This thesis focusses on the adaption of the loads according to Load Model 1 for municipal bridges. Also the force transmission to the support was investigated. Due to these researches the used loads for the unity checks are less conservative. In the following chapters the loads are described in detail. In chapter 4.2 the loads according to the Eurocode are described.

3.4 Former standards

In Table 3-4, an overview of the former standards in the Netherlands is presented.
This table only illustrates the year that the standards were available. However, this does not mean that only from that year onward these standards were used. Possibly, structures were calculated with concept versions of these standards at an earlier stage.

Table 3-4 - Former standards concrete structures [21]

Dutch Standard	Year
GBV 1912	1912
GVB 1918	1918
GVB 1930	1930
GVB 1940	1940
GVB 1950	1950
GVB 1962	1962
RVB 1962	1962
RVB 1967	1967
VB 74	1974
VB 74/84	1984
VBC 1990	1990
NEN 6700 series	1991
VBC 1995	1995
Eurocode (current)	2012

3.4.1 Material properties in former standards

In the RBBK, values are provided for the material properties and factors of former standards. In the old GVB standards, safety factors for concrete structures were assumed as $\gamma = 1{,}8$ in the first versions and $\gamma = 1{,}7$ in later versions. The reason for the magnitude of the factors is that material factors were included in this safety factors. The decreasing safety factor after 1974 was obtained by a decreasing uncertainty in material quality. The RBBK also provides strength classes for the concrete and reinforcing steel of former standards. From the introduction of the GBV 1962 a differentiation in different concrete qualities was made.

In *Appendix D – Former codes* different former standard are discussed briefly. This appendix provides information from the RBBK [21] about the former standards. In Appendix Table 4-1 the concrete quality used before 1974 is translated to a characteristic compressive strength. In Appendix Table 4-2, the material properties of reinforcing and prestressing steel in former standards are presented.

3.4.2 Shear capacity in former design codes

Over the years the assessment of shear capacity in concrete structures has changed reasonably. In the GVB, for every concrete quality the allowable stresses for the concrete and reinforcing steel are defined. These allowable stresses were chosen in such a way that the occurring stresses are commonly lower (with an overall safety factor of 1,8). The shear capacity was assumed to depend on the diagonal tensile stresses. If the occurring tensile stresses are higher than the tensile capacity, the shear reinforcement has to take up the all tensile stresses. This leads to much reinforcement. In many cases the effective depth is chosen in such a way that the tensile stresses are just allowable.

In VB 74/78, the lower boundary for the allowable tensile stresses has changed from $1,2*f_b$ to $0,6*f_b$ (taking into account the change of overall safety factor from 1,8 to 1,7). For the shear reinforcement, one was allowed to calculate with the difference $\tau_d - \tau_1$. Calculation with a compressive strut with an angle of 45° was allowed. In later researches was con-cluded that the formula in VB 1974 was incorrect.

In the VBC the overall safety factor was changed into partial factors on loads and materials separately. For shear assessment two different failure mechanisms were considered: shear failure where cracking starts with flexural cracks and shear failure due to tensile forces. The lower boundary was lowered to $0,4*f_b$. This value is compared to values from calculations from the Eurocode 2 in chapter 4.5.1.

3.5 Current standards existing bridges

In 2009, NEN8700 was introduced for the assessment of existing structures in case of reconstruction and disapproval. In 2011, this standard was extended with information about the assessment of existing bridges. In this year, also NEN 8701 was introduced. This standard contains rules about the loads that have to be taken into account when assessing existing structures in the Netherlands.
NEN8702 is currently being created. This standard contains rules for the assessment of existing concrete structures specifically. This standard is actually an extension of NEN-EN 1992-1-1 and NEN-EN 1992-2. NEN 8702 is therefore meant to be used together with the rules for new structures. Not all parts of NEN-EN1992-series can be extended by NEN8702 yet. For example, there is little information available about:

- The influence of damage to the structural behavior and structural safety;
- The remaining lifetime, potentially affected by degradation mechanisms;
- Fire safety aspects.

With the standards for the assessment of existing structures different structures can be criticized. This involves the minimum safety level when a structure has to be placed in the rejection state. Also, this involves the safety demands and usability for expansions, repair or replacement. [7]
From economical point of view, it is allowed to use certain reduction for the safety margins. For these economical adaptions the human safety has to be the lower boundary in every case.

The safety margins for existing structures are determined by probabilistic methods. This probabilistic method uses a reliability index (β) which is in direct relation with the probability of failure for a structure. In order to make the probabilistic method practical, the safety level is determined by the right choice of the following parameters [22]:

- The consequence class (CC) of the structure;
- The prescribed characteristic loads;
- The prescribed load factors (γ_f) and combination factors (ψ);
- The calculation rules and material properties from the standards;
- The prescribed material factors (γ_m)

The factors mentioned above are chosen in a way that the desired safety level is reached. The safety assessment of existing bridges is further explained in chapter 3.6.

3.6 Safety assessment of existing bridges

The goal of this chapter is to find the governing axle loads on municipal bridges eventually. These axle loads can be used for the creation of a new load model to compare with Load Model 1. This has been done by regarding results from Weight In Motion (WIM) measurements on a municipal road. In order to use results from the WIM measurements legitimately, more information is needed about:

- The reliability index β (Chapter 3.6.2);
- Reliability levels (Chapter 3.6.3 and 3.6.4);
- Probabilistic traffic load modelling (Chapter 3.6.5 and 3.6.6);
- WIM data (Chapter 3.6.6.2)
- Partial factors existing structures (Chapter 3.6.7)

When details of these aspects are known the governing truck (governing axle loads) for small span municipal bridges can be chosen (Chapter 3.6.6.2). These axle loads are used to create a new load model in chapter 5.4.

3.6.1 Introduction

The assessment of the structural safety of existing bridges becomes increasingly important in many countries due to the age of the structures and an increase in traffic loads. The reliability of existing bridges differs from new built bridges in a number of aspects [20] [21]:

- Increased safety levels usually involves more costs for existing bridges than for new bridges, which are in the design phase. Adapting an existing structure is more expensive than adapting a drawing of a bridge;
- The remaining design life of existing bridges is often different than for new built bridges (which is usually 50-100 years). This reduction of the reference period may lead to reductions in the values for representative loads;
- For existing bridges the actual structural conditions are visible or measurable. This may reduce the uncertainly compared to new bridges.

At present, the assessment of existing structures often leads to conservative results. These existing structures are mostly verified using simplified procedures based on the partial safety factor method (which is commonly applied in the design of new structures). This may result in expensive and unnecessary upgrades, or even in unnecessary demolition of existing bridges. [23] and [24] state that it would be uneconomical to use the same reliability levels existing structures and new structures. A probabilistic method or model describes the uncertainty of certain parameters, such as load and resistance. In general, this leads to a more realistic verification of the actual performance of an existing bridge. The safety level of a structure is expressed by the probability of failure. In practice, the reliability index β is being used, which has a direct relation to the probability of failure.

3.6.2 Reliability index (β)

Most problems in civil engineering consist of determining the capacity (R) and the load (S). In principal, a structure is safe when the capacity is higher than the loads. However, both parameters have their uncertainties. Due to this uncertainty, absolute safety is not applicable in practice. Therefore, safety can be expressed as the probability of non-failure P_{nf}. Typical measures of reliability in civil engineering are the probability of failure P_f (where $P_{nf} + P_f = 1$) and the reliability index β. The reliability index in general is defined as:

$$\beta = -\phi^{-1}(p_f)$$

Where:

ϕ = is the cumulative distribution function of standardised Normal distribution;
p_f = the probability of failure.

This correlation can be read from the standard normal distribution tables as illustrated in Figure 3-9.

P_f	10^{-1}	10^{-2}	10^{-3}	10^{-4}	10^{-5}	10^{-6}	10^{-7}
β	1,28	2,32	3,09	3,72	4,27	4,75	5,20

Figure 3-9 - Relation between β and P_f [3]

The parameter β reveals how often the standard deviation a random variable can be placed between zero and the mean value of M. For the value of M, the following equation holds: M = R – S. If the variables R and S are assumed normally distributed, the reliability index becomes:

$$\beta = \frac{\mu_M}{\sigma_M}$$

Where:

μ_M = the mean value of a parameter
σ_M = the standard deviation of a parameter

Figure 3-10 illustrates a visualization of M = R – S for the situation where R and S are normally distributed.

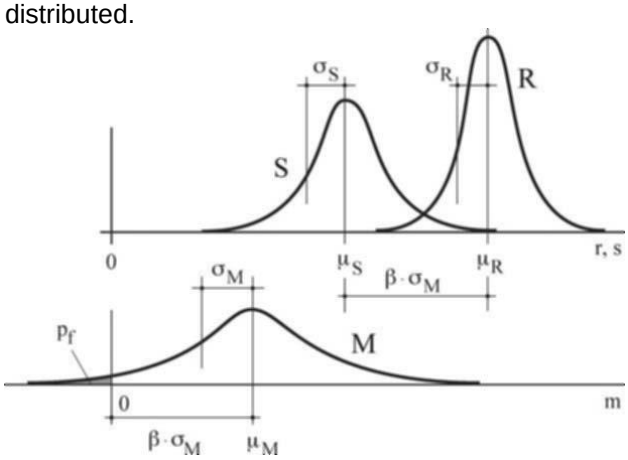

Figure 3-10 – Visualisation of the equation M = R – S [25]

The reliability index β is used to compare the different load models. From this reliability index the probability of failure can be calculated. This can be done by calculating the area under the normal distribution graph.

When looking at the design values of the loads an additional factor needs to be used to lower the reliability index β. This is according to NEN-EN 1990 [3]. The chance of the occurrence of a more unfavorable value than the design value of the load effect E_d is:

$$P(E > E_d) = \phi(+\alpha_E \beta) \qquad \textbf{(3.2)}$$

Where:

α_E = a FORM – sensitivity factor, which is -0,7 according to NEN-EN 1990

3.6.3 Reliability levels for new structures

The Eurocode EN 1990 [3] provides 3 consequence classes CC1, CC2 and CC3 for new structures. Each consequence class has different β-values (reliability index) and may be associated with 3 reliability classes (RC1, RC2 and RC3). Figure 3-11 illustrates the values for β for a reference period of 1 and 50 years in different reliability classes as stated in Eurocode EN 1990.

Reliability Class	Minimum values for β	
	1 year reference period	50 years reference period
RC3	5,2	4,3
RC2	4,7	3,8
RC1	4,2	3,3

Figure 3-11 - Values for β for different reliability classes [3]

The desired safety level, which is expressed by β, can be established by proper choice of the following parameters [23]:

- Consequence Class (CC);
- Characteristic loads;
- Load factors (γ_f), material factors (γ_m) and combination factors (ψ);
- Design rules and material properties.

3.6.4 Reliability levels for existing structures

As described in 3.6.1 the safety assessment of existing structures is different from new structures:

- The increase of the safety level of existing structures costs more than for new structures, relatively.
- The real reference period for an existing structure is different than the standard design reference period of 50 or 100 years
- With the use of measurements or tests, more about the current state of an existing structure can be known.

These 3 point are elaborated more in detail.

3.6.4.1 Cost aspect

If a reliability index for an existing structure has to be determined, 2 principles can be taken into account. These are economical principles and (human) safety principles. The first principle leads to economic optimization of the building costs. And the product of damage and probability of failure. This principle has been illustrated in Figure 3-12.

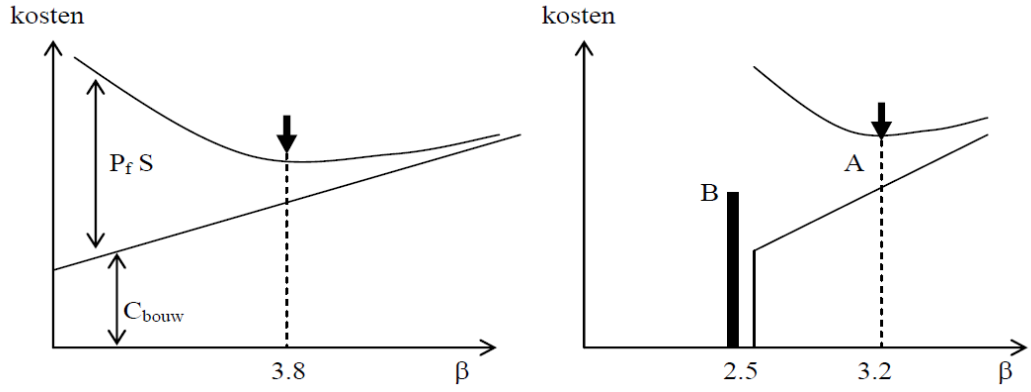

Figure 3-12 - Optimization of building and repair costs (right: new structures, left: existing structures) [22]

In the left part of Figure 3-12 a minimalization of the building costs C_{bouw} and the expected damage P_f S leads to certain beta factor. For structures in CC3, beta is around 3,8. This value is not the result of a optimization process, but has been formed in the course of time. Due to this process, there can be assumed that the economical optimum is being approached. The right part of Figure 3-12 is the schematized situation for existing structures. Improvement of reparation of existing structures in order to reach a higher safety level is in general more expensive than for new structures (which are in the design phase). Therefore the optimum safety level has a lower beta value. For CC3 this value is assumed to be around 3,2. One typically has to consider if it is more

economical to leave a structure in its current state and accept the greater risk. The optimum of repairing or adapting a structure (point A, β = 3,2) has to be lower risk B of the existing structure. In this case β = 2,5 is assumed (rejection level). In the situation of the right hand side of Figure 3-12 it is more beneficial to leave the structure in its current state. The second principle reduces the risk for human life loss. As illustrated in Figure 3-13 the economic principle may be overruled by the principle for human life loss. [22]

3.6.4.2 Time aspect

The shortening of the reference period (and thus the design lifetime) can be observed from the representative value and the partial factors. For the variable loads on a bridge, a shorter reference period leads to a decrease of the representative values. For partial factors a shorter reference period does not automatically lead to a decrease. For these partial factors (or safety factors) both economic arguments and human safety plays a role. If only economic optimization is considered the probability of failure increases linear in time. For human safety this is not the case. Limits for human safety play an important role because of the maximum allowable annual probability of failure. This annual probability may not exceed the limits for human safety. For short reference periods the limits for human safety becomes governing. One could raise the partial factors for short reference period. Instead, for CC2 and CC3 a minimum design lifetime of 15 years is required in structural design. In this case the probability of failure, and therefore the factor β are constant. This can be seen in Figure 3-13.

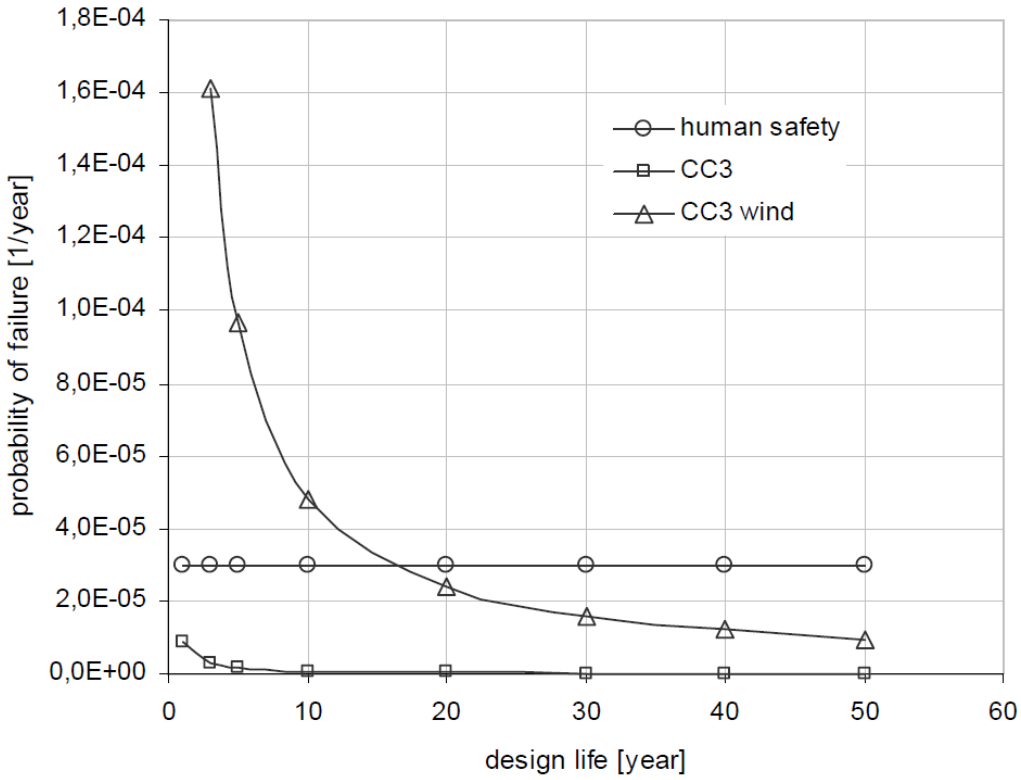

Figure 3-13 - Annual failure probability as a function of the design working life for new structures (CC3) [23]

Specifications in the Netherlands (National Annex of EN-1992-2 and NEN 8701) allow for taking into account a shorter reference period as well as the lower influence of traffic trends for a shorter remaining working life. In total 3 reduction factors can be applied:

1. Shorter time (NEN8701) (ψ_t)
2. Factor to account for no trend (α_{trend})
3. Factor for lower number of trucks (ψ)

The first load reduction factor stands for the fact that the actual reference period of an existing structure is not the same as for a new built structure. NEN8701 recommends a reference period of 15 years. For short span bridges (<20m) this factor is $\psi_t = 0,98$.

The second factor takes into account the consideration that load models were calibrated considering an increasing rate of heavy traffic in time, up to 2060. This means that if the service life ends before 2060, a reduction is allowed for the compared to the calibrated load value. This factor depends on the influence length and on remaining working life. For small span bridges (10m) this ranges from 0,95 in 2015 to 1,0 in 2060. For a reference period of 15 years (from 2017) this would be a factor of $\alpha_{trend} = 0,969$. Factors for other lengths an reference periods can be found in NEN 8701 [7].

The third factor has nothing to do with a shorter lifetime, but with the fact that municipal bridges are considered. The National Annex of NEN-EN 1991-2 presents a reduction factor for less than 2 000 000 trucks per lane per year. If 200 000 trucks are assumed the reduction is 0,97 for a span of 20m. The WIM measurements in Rotterdam as described in chapter 3.6.6.1 measured less than 25.000 trucks per month. This is 300.000 trucks per year. This municipality is assumed to be an upper boundary as far as the number of trucks (as explained in chapter 3.6.4.4). Therefore the factor of 0,97 is a reasonable factor.

If the magnitude of the factor is assumed as described above, the total factor is $0,98*0,969*0,97 = 0,92$. This could be the theoretical α factor for existing municipal bridges. An issue that has not been taken into account is the fact that axle distance and total number of axles is important for small span bridges. For small span bridges the α factor is assumed to be lower than the theoretical α factor. This is verified for different spans and edge distanced using FEM research. This has been done in chapter 6.

For the influence of time also the ageing of a structure is of influence. For example degradation processes, fatigue or damage. For a shorter reference period there is less chance of the occurrence of these phenomena. [22]

3.6.4.3 Data aspect

Regarding the available data for existing structures there are two possibilities:

- The specifications for a structure still exist and there is no reason to doubt about these specifications. In this case the same design values as for new structures can be applied. For existing structures these design values can be determined more precise by doing measurements. New measured values often lead to an increase in the design value. This is because a lower boundary value was assumed during the design phase of the structure.
- The specifications for a structure do not exist, or they do exist but there is a reason to have some doubt the quality of the execution for example. This leads to uncertainty of the design values of the structure. In practice, this can be solved by assuming the lowest possible value, or by taking measurements.

From both situations mentioned above it turns out that the reliability of a structure is no solid property, but has to do with the knowledge of a structure and the occurring loads. Lack of safety can be caused by lack of knowledge. This can be solved by measuring or by calculating more in detail. [22]

3.6.4.4 Reliability levels

For a structure in Consequence Class 2, the value of β is 3,8 according to the national annex B of NEN-EN 1990. The Dutch Department of Waterways and Public Works has done some research to the safety levels of existing bridges. For existing structures two safety levels are introduced [23]. β_u is the level below which the structure is unfit for use. β_r is the level for repair of existing structures. These values were established based on both economical arguments and limits for human safety. These values are demonstrated in Table 3-5.

Table 3-5 - β values for existing structures

CC	minimum reference-period	new β_n		repair β_r		unfit for use β_u	
		wn	wd	wn	wd	wn	wd
1A	1 year	3.3	2.3	2.8	1.8	1.8	0.8
1B	15 year	3.3	2.3	2.8	1.8	1.8	1.1*
2	15 year	3.8	2.8	3.3	2.5*	2.5*	2.5*
3	15 year	4.3	3.3	3.8	3.3*	3.3*	3.3*

wn = wind not dominant
wd = wind dominant
(*) = in this case the minimum limit for human safety is decisive

In former codes (NEN 6702) the highest reliability index was β = 3,6. However, The Dutch Department of Waterways and Public Works claimed that they used a higher β for their bridges. The magnitude of the used safety index was however not calculated. The higher safety index was a result of using a relatively high load factor for self-weight. The self-weight is a large part of the total load and often well known. Multiplying this value with a high load factor leads to a high safety margin.

For municipal bridges (or city bridges) less research was done to safety levels. Some probabilistic research has been done to city bridges in Rotterdam [26]. This research can be used to determine the reliability index for municipal bridges in general. Rotterdam is one of the largest municipalities in the Netherlands. Also, the largest harbour of Europe is located near Rotterdam. So, relatively many container lorries will cross Rotterdam. Therefore one can assume that bridges in the municipality of Rotterdam can represent bridges in any municipality of the Netherlands.

In the Netherlands, specific standards are being created for existing structures: NEN 8700. This standard uses different reliability requirements for existing structures than for new built structures. The norm differentiates between two levels:

- Rejection: if an existing structure does not comply with the required reliability index, it should be rejected, in practice meaning refurbished / renovated;
- Reconstruction / repair: the level to which an existing structure should be renovated.

Also, NEN 8700 states that in case wind is dominant, different reliability requirements are set. The reason for this is on the one hand the high cost of safety measures for resistance to wind loading, on the other hand the high variance of wind loading which further increases the costs to reduce the failure probability. A typical municipal bridge belongs to consequence class 2. As explained before, the reference period has a minimum of 15 years. Table 3-6 and Table 3-7 demonstrate the minimum reliability index for different consequence classes. For municipal bridges in the Netherlands values from NEN8700 are considered.

Table 3-6 - Minimum reliability indices for reconstruction level [26]

Minimum reliability indices for reconstruction			
Consequence class	Minimum reference period	β	
		Wind not dominant	Wind dominant
CC3	15 years[b]	3.8 (3.6)	3.3[a] (2.6)
CC2	15 years[b]	3.3 (3.1)	2.5[a]
CC1	15 years	2.8	1.8

[a] The limit for personal safety is dominant

[b] Generally a reference period of 30 years is recommended

The values in brackets may only be used for structures which obtained an environmental permit under the Building law of 2003 or before.

Table 3-7 - Minimum reliability indices for rejection level [26]

Minimum reliability indices for rejection			
Consequence class	Minimum reference period	β	
		Wind not dominant	Wind dominant
CC3	15 years[b]	3.3 [a]	3.3[a]
CC2	15 years[b]	2.5 [a]	2.5[a]
CC1b[b]	15 years	1.8	1.1
CC1a[b]	1 year	1.8	0.8

[a] The limit for personal safety is dominant

[b] Distinction is made between cases where human life is at risk (b) and where danger to human life is excluded (a)

This beta value (2,5) has been calculated by the following formula:

$$\beta_n = 3{,}4 - 0{,}75 \log t$$

Where:

t = time (years)

As stated before in 3.6.2, the probability of failure can be calculated from the beta factors. This can be done by calculating the area under the normal distribution graph. This has been done for the beta factor which occurs the most in existing structures according to NEN8700 (Table 3-8).

Table 3-8 - Probability of failure for some beta values

Beta	P.o.F.
1,8	$3{,}6*10^{-2}$
2,5	$6{,}2*10^{-3}$
3,1	$1{,}0*10^{-3}$
3,3	$5{,}0*10^{-4}$

For municipal bridges (and the Quick Scan model) the beta factors 3,1 (for repair level) and 2,5 (for rejection level) are used. These are the grey values as demonstrated in Table 3-6 and Table 3-7. In principle, the beta factor for repair/reconstruction are used. This choice has been made because if a the unity check for the recalculation turns out to be (just) over 1,0, this does not directly mean that the bridge has to be demolished or closed. So, by making this choice there is some additional capacity for the bridge to fulfil the requirements.

3.6.5 Traffic load modelling

The process of creating a traffic load model can lead to two different types of output: design values (deterministic or semi-probabilistic) or a probabilistic load model. In practice, it is typical to use semi-probabilistic models which are the result of code calibration procedures. NEN 8700 and NEN 8701 use factors accounting for statistical load effects. In literature it can be observed that axle loads and Gross Vehicle Weight (GVW) is often the basis for creating load models. One of the main challenges in creating a traffic load model is that knowing the distributions and / or design values of axle loads and GVW-s does not provide direct information about the global load effects. Information about axle- and vehicle distances has to be used and / or assumed, resulting in a complex task [26].

Until the 70's, static measurement systems were used. Heavily loaded vehicles were measured at weighing stations. The statistical relevance of such data is questionable. Since the 70's the weigh-in-motion systems were used more frequently, which gave results about the real occurring traffic on bridges.

3.6.5.1 Traffic load model Eurocode

For the development and calibration of the Eurocode, several measurements campaigns have been carried out on several locations in Europe. In the Netherlands continuous measurements are being carried out on highways to re-evaluate the load effects provided by the codes. Frequency distributions are approximated by bi-modal Rayleigh distributions, explained by the presence of loaded and unloaded vehicles. An example is illustrated in Figure 3-14.

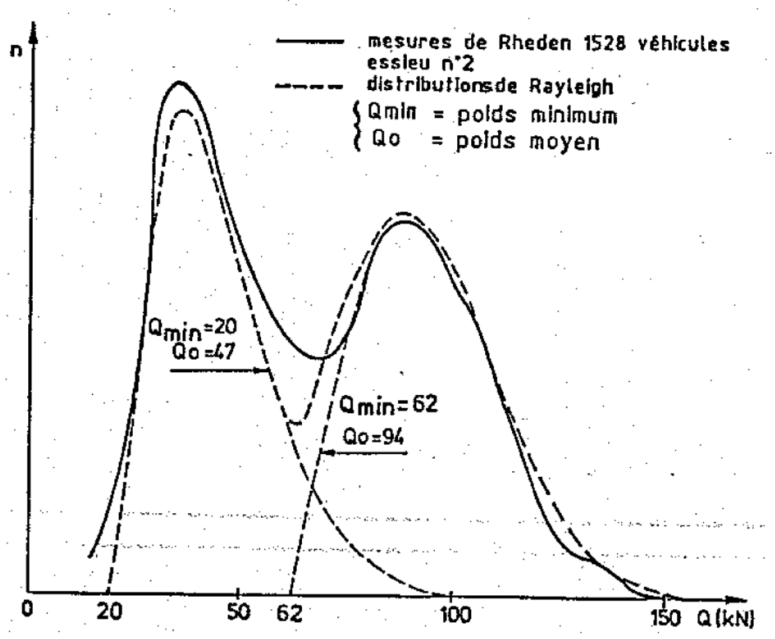

Figure 3-14 - Axle load distributions for Eurocode calibration [26]

With these measurements the daily extreme, annual extreme and 1000 years extreme is determined. Based on these measurements the axle load of 300kN from LM1 was determined. The values also include a dynamic amplification factor (DAF) which is a result from the unevenness of the road surface [26].

In 2013 a measurement program for municipal bridges (city bridges) started. Data were analyzed by TNO [27]. If the measurement program leads to reducing the design loads on city bridges, new bridges can be designed in a more economical way. The main gain however is expected for existing structures. Expensive renovation may turn out unnecessary if the expected loads for the remaining lifetime of the structure could be lowered in comparison to values indicated in the building codes. The exceedance-frequency diagrams from the WIM measurements can be found in chapter 3.6.6.1.

3.6.6 Probabilistic traffic model

Since partial factors are part of a semi-probabilistic approach, it makes sense to asses existing bridges in a probabilistic way. This chapter provides more insight in the probabilistic assessment of existing short-span city bridges. Various researches have been done to this subject [28] [26] [29]. In most cases, a probabilistic approach has been chosen if data from weight-in-motion measurement are available. As stated before, probabilistic research has been done to short span bridges in the municipality of Rotterdam [29] [26]. In this chapter the measurements, assumptions, results and conclusions are described. This can be used to determine a governing load model for municipal bridges.

3.6.6.1 Weight-in-motion (WIM) data

For the probabilistic traffic model for municipal bridges in Rotterdam, two heavily loaded locations within the city were chosen. The first location was on a descending road directly before traffic lights. It turned out that the decelerating and accelerating forces distorted the measurements greatly. The measurement system seemed to be too sensitive for horizontal forces. The second location suffered less from braking and accelerating forces. For this reason, only the WIM data from the second location were taken into account. However, also in this location the accuracy of the measurement were questionable, but were assumed to be conservative. As described in 3.6.4 the data from traffic in the municipality of Rotterdam can be assumed to be a standard for any municipality in the Netherlands. For the relevant data, only the heavy vehicles (with a GVW of 3.5 tons or more) were measured. After two months of measuring 48 586 heavy vehicles were measured.

Figure 3-16 and Figure 3-15 present the distribution functions of axle and vehicle weights. In these figures also the values from the Dutch highway RW16-L in 2008 are plotted since these were used for the calibration of the National Annex of EN-1991-1-4. Note that this calibration was not done for short spans, but only for 20m, 50m, 100m and 200m. Since small span bridges are examined, only one truck per lane is assumed. A sequence of trucks is not relevant and therefore neglectable. Also, gross vehicle weight is not that interesting for small span bridges. This is because the longest vehicles are likely to have the highest total vehicle weights. For small span bridges, these long vehicles may not fit on the bridge entirely. High axle loads close to each other generate higher stresses than axles which are more distributed. Therefore axle loads and axle distances are more of interest.

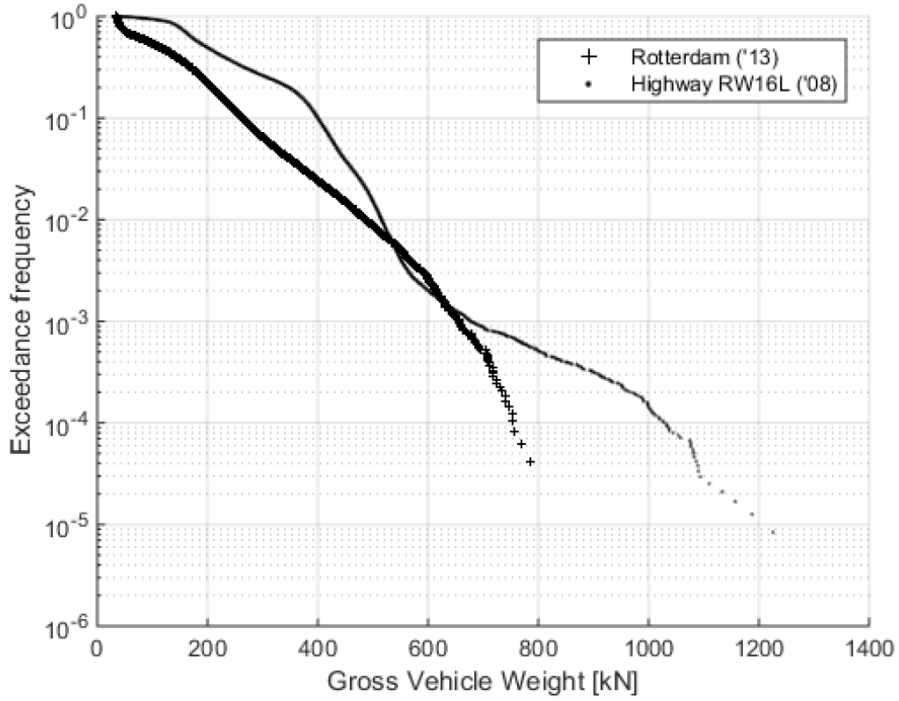

Figure 3-15 - Vehicle load distributions in Rotterdam and RW16-L [27]

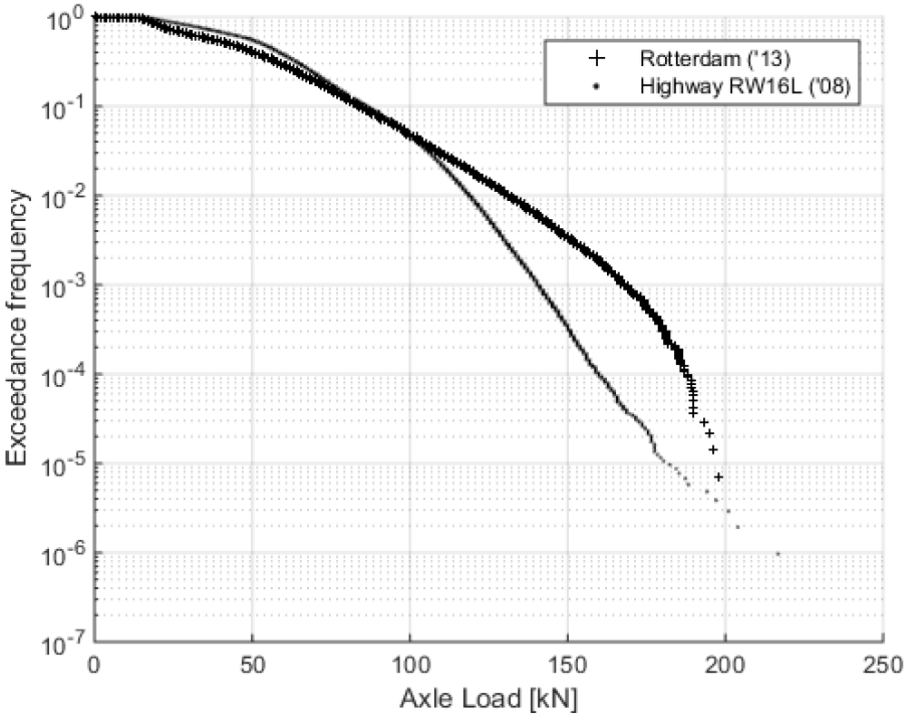

Figure 3-16 - Axle load distributions in Rotterdam and RW16-L [27]

Now the question rises which exceedance probability is relevant for an existing municipal bridge. The desired exceedance probability can be determined by the reliability index, reference period and the measurement results. In this section a calculation for the desired exceedance frequency has been made. This has been done according to the calculation method as described in chapter 2.2.3 of the TNO traffic load report [28]. The calculation was made for what is assumed to be the largest part of the existing concrete slab bridges. For slab bridges that fall outside this scope adaptions can be made which lead to slightly other values. Bridges can fall outside the scope for example due to location specific vehicles as described in chapter 5.4.4.1 (no access for trucks, provable more or heavier trucks than normal).

First some assumed parameters are described. For the determination of the reliability index the assumptions are: CC2, a reference period of 15 years and bridges built before 2003 (as described in 3.6.4.4), which leads to β = 3,1. α_E is -0,7 as described in 3.6.2.
These assumptions lead to the following probability of failure $(\mathrm{P}\ (\mathrm{S}>\mathrm{S_d})\ )$:

$$\phi(\alpha_E\beta) = \phi(-0{,}7*3{,}1) = \phi\ (2{,}17) = 1/67$$

Since the reference period is 15 years the return period which is being searched for is $67*15 \approx 1000\ \mathrm{years}$. This corresponds to a probability of failure of 1/365.000 per day.
For the number of days per year with sufficient heavy traffic (no holidays and weekends) 250 days is assumed. As described before, for the relevant data, only the heavy vehicles (with a GVW of 3.5 tons or more) were measured. After two months of measuring 48 586 heavy vehicles were measured. The exceedance frequency for 2 months of measuring becomes:

$$\frac{1}{48586*1000*\left(\frac{250}{365}\right)*6} = 5*10^{-9}$$

From Figure 3-17 the axle load can be determined. The measured data are extrapolated (red dotted line). For a exceedance frequency of $5*10^{-9}$ the maximum axle load is 205 kN.

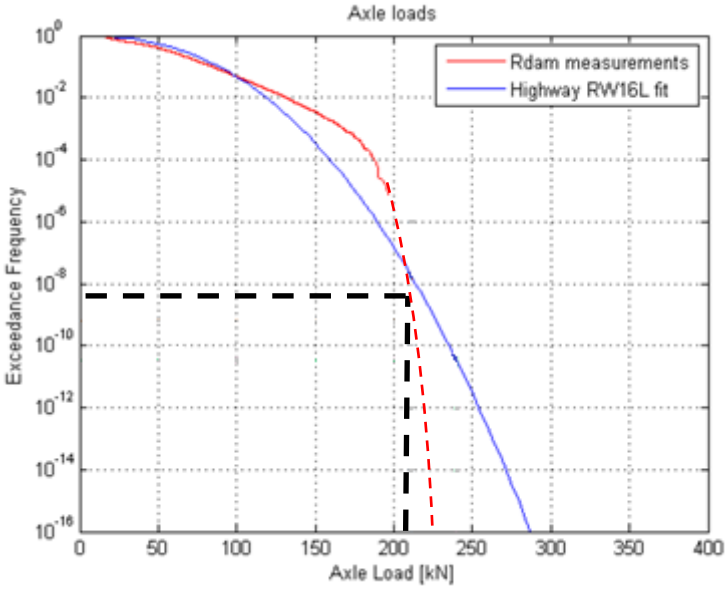

Figure 3-17 - Comparison of axle load distributions: Dutch highways (fit), Rotterdam (empirical), existing bridges (as calculated: $5*10^{-9}$) [26]

3.6.6.2 Governing truck

The results from the WIM measurements in Rotterdam did take into account axle distances. However, these axle distances were not provided in relation to the axle loads. Vehicles with the a high axle load do not directly lead to the highest occurring stresses in a bridge. This is because axle distances are important as well. In order to receive the highest shear stresses and flexural stresses a vehicle with many heavy weight axles close to each other may be governing. With

help of the measured data the relevant truck properties can be described. The measured data provide values for the gross vehicle weight and the axle load. Axle distances were only provided for the heaviest vehicles, which mostly need permission to drive on a highway. These vehicles will not be present on municipal bridges. No general overview for all measured axle distances were provided. This is because axle distances do not matter that much for highway roads. For bridges, the axles distance is more of interest. From the reported axles distances some examples of the governing (smallest) axle distances are illustrated in Table 3-9. These axles distances are used as comparing material to determine the governing truck for municipal bridges. This has been done in chapter 5.4.4. With a FE model there is determined if these vehicles with a small axle distance are governing compared to vehicle with greater axle loads, but also greater axle distances.

Table 3-9 - Examples of vehicles with small axle distances [27]

Vehicle 1: Axle distance (m): 0 – 1,91 – 1,95 – 1,82 – 1,36 	**Vehicle 2:** Axle distance (m): 0 – 1,91 – 1,95 – 1,82 – 1,36 
Vehicle 3: Axle distance (m): 0 – 1,99 – 1,88 – 1,68 	**Vehicle 4:** Axle distance (m): 0 – 1,76 – 2,66 –1,32 

For the governing axle weight the axle- and vehicle load distributions from the measurements have been used (Figure 3-15 and Figure 3-16). This has been described in chapter 3.6.6.1. It turned out that the governing axle load is 205 kN. However, it is likely that these kind of axle loads only occur for a long, heavily loaded vehicle with great axle distances. For example an axle configuration as described in lorry 7 of Table 5-4. Another real occurring examples is the lorry illustrated in Figure 3-18. This vehicle has a total weight of 1283 kN and a total length of 29m. This example demonstrates that for bridges with a small span the total weight does not matter, since not all axles can fit on a small span bridge. Moreover, this vehicle is very unlikely to appear on a municipal bridge. Also, this example demonstrates that very heavy axle weights are likely to be part of a long, heavy vehicle.

FEM calculation verifies if these kind of vehicles (although they will barely or not appear on a municipal bridge) are governing above the vehicles with 4 or 5 axles very close to each other.

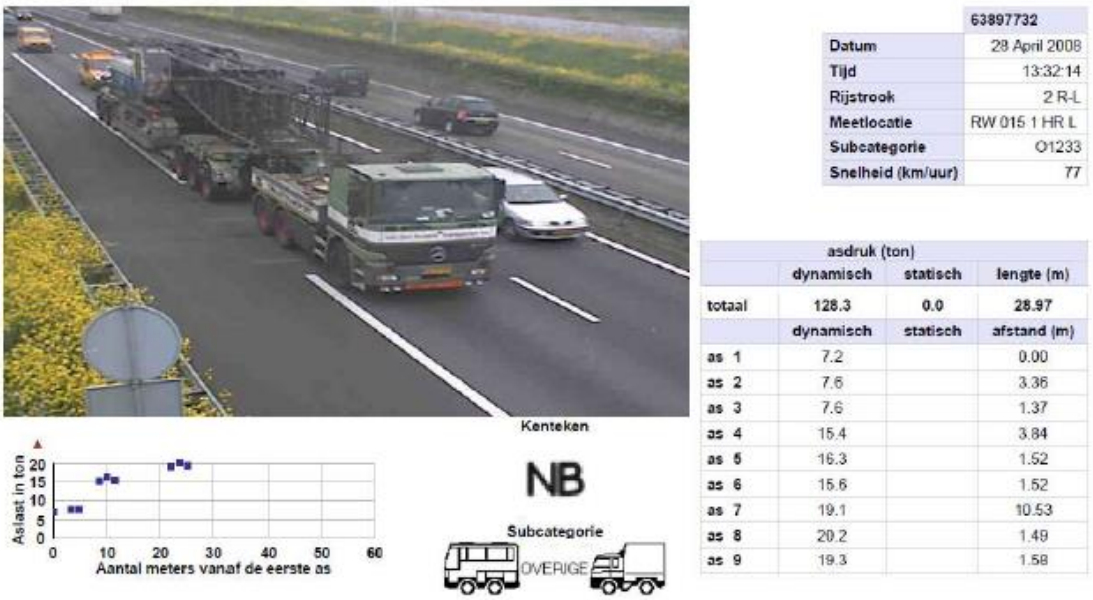

Figure 3-18 - Example of a long, heavy, special vehicle [27]

3.6.7 Partial factors for existing bridges

In order to obtain the required reliability for existing bridges, partial factors need to be established. This has been done by TNO [28] with a probabilistic calculation. In this calculation the traffic load T is used which passes the bridge in a period of 15 years. This assumption can be made in the case of a relatively small span. For small spans, a single truck determines to a large extend the design load on the bridge [24]. The statical distribution of the weight T of a single truck has been derived from weigh in motion (WIM) measurements in April 2008 on a Dutch highway (Figure 3-19). Since these measurements are for governmental roads, these values are too conservative for municipal roads.

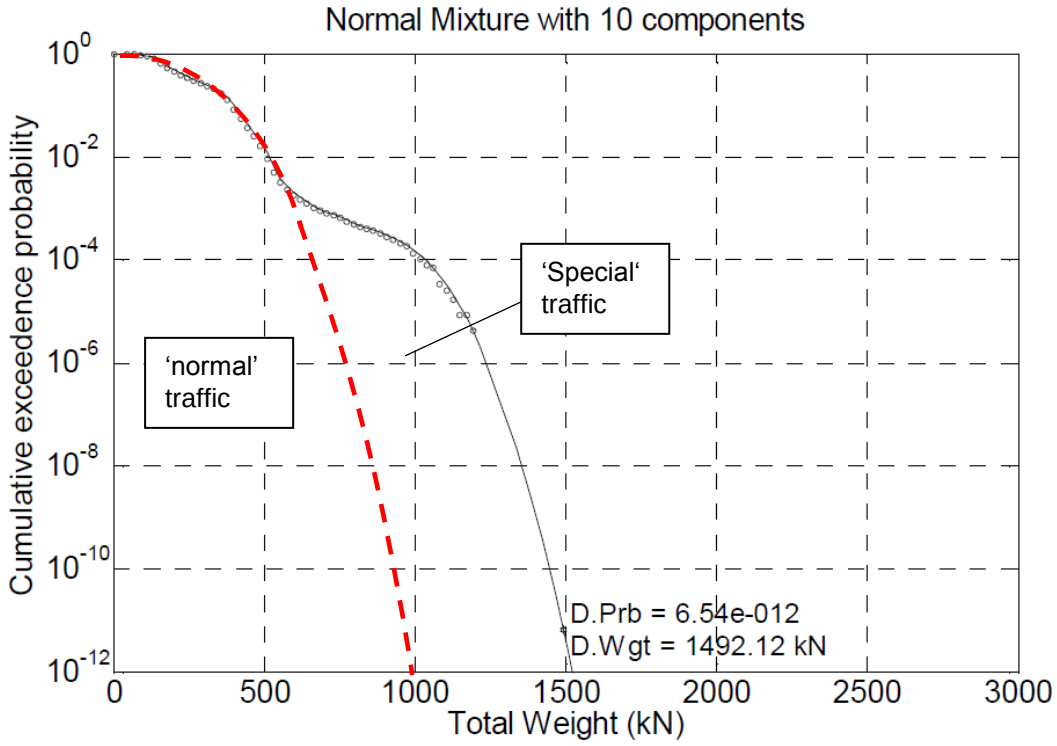

Figure 3-19 –Fitted analytical distribution of the vehicle weight (adapted from [24] and [28])

From Figure 3-19 2 different types of traffic can be distinguished which are represented by 2 different 'arches' in the graph. The left section in the graph stands for vehicles with a maximum weight of legitimate 60 tons. The right section stands for vehicles (lorries) with a legal permission for a maximum weight up to 100 tons. This distinction has also been made in the original TNO report [28].

The partial factors according to NEN8700 are used as illustrated in Table 3-10.

Table 3-10 - Partial factors for traffic bridges according to NEN8700 [22]

	γ_{Ga}	γ_{Gb}	γ_{Q}	Target β
CC1 repair	1,10	1,10	1,10	2,8
CC2 repair	1,25	1,15 (1,10)	1,25 (1,20)	3,3 (3,1)
CC3 repair	1,30	1,20 (1,15)	1,35 (1,30)	3,8 (3,6)
CC1 rejection	1,00	1,00	1,00	1,8
CC2 rejection	1,10	1,10	1,10	2,7
CC3 rejection	1,25	1,10	1,25	3,3

3.7 Conclusion

Regarding the researches as described above some assumptions can be made:

- Consequence Class 2 (CC2)
- The minimum reference period is 15 years
- The obtained reliability index is β = 3,3 for structures that have been built after the 'Bouwbesluit 2003' and β = 3,1 for structures that have been built before the 'Bouwbesluit 2003', which is the 'repair' level.
- The partial factor for self-weight is assumed to be 1,15 (1,1). The partial factor for variable loads is assumed to be 1,25 (1,2).
- Reduction factor for reference time of 15 years (ψ_t) = 0,98
- Factor to account for no trend (α_{trend}) = 0,969
- Factor for lower number of trucks (ψ) = 0,97
- The maximum axle weight is 205 kN (dynamic factor not included)

The chosen reliability index is rather high. In theory, a reliability index 2,5 could have been chosen as threshold value. However, If the existing structure seems to be just below this value, or if the reference period seems to be higher than 15 years there would be a need of immediate closure and repair or replacement. This is not desired, so a rather conservative reliability index has been chosen.

If an assessed bridge is certain to be in Consequence Class 1B, a lower value for the reliability index β can be assumed. In that case lower partial factor can be assumed. This is 1,1 according to Table 3-10.

3.8 Discussion

The governing vehicle for all municipal bridges is determined by considering WIM measurements from one (relative heavily loaded) road in Rotterdam. As can be seen in Figure 3-15 and Figure 3-16 higher axle loads occur more often in the Rotterdam measurements than in measurements on a highway roads. Also, the empirical fit for highway roads provides higher axle loads for the Rotterdam measurements. This may raise questions since this is not an expected result. Only for real high axle loads (>200kN) the trend predicts that these axle loads occur more often in highway roads.

It is remarkable that the results of measurements in the city suggest a higher ratio of very heavy axles than the values determined for the highway. The fact that the results of the city measurements suggest a higher ratio of very heavy axles than the values for highways is analyzed within the project carried out by TNO for Rotterdam [27] .This thesis does not focus on

investigating possible reasons. It is noted however, that if the measurement results of the city would turn out to be distorted or unreliable, the traffic load model developed in the further steps may be conservative [26].

In the following chapters load models for governing real occurring vehicles for the comparison with Load Model 1 were created (chapter 5). The loads from these load models are partly based on the WIM measurements in Rotterdam. Since the measured axle loads are considered to be conservative, creating a load model based on conservative measurements is permitted.

4 Shear assessment of concrete slab bridges

Nowadays, several existing slab bridges are found not to satisfy the criteria when assessed for shear according to the current codes. This is caused by the increased traffic loads since the completion of a certain bridge, and the fact that the rules for shear capacity as prescribed by the current standards are more strict than former standards, which leads to smaller allowed shear capacities. However, several inspected structures reveal no signs of deterioration or significant damage. This is verified by tests on a decommissioned slab bridge. This indicates that slab bridges are stronger than found by the current rating procedures [30].

After these conclusions, the Department of Waterways and Public Works (Rijkswaterstaat) started a project to improve the (shear) assessment of existing bridges under increased live loads. For this purpose, a fast, simple and conservative tool was created for their bridges: the Quick Scan model. The output of these spreadsheets is a Unity Check (UC) value. This is a ratio between the design value of the applied shear force and the shear resistance [30].

4.1 Failure of slab bridges

Slab bridges are robust structures, designed to fail in flexure. Shear was not considered in Dutch building codes from the post-war decades. Nowadays, researchers are more interested in the shear force transmission in slab bridges due to larger live loads and smaller allowed shear stresses. Existing bridges need to be verified according to the recent codes. Existing code provisions aim at limiting the shear stress so that flexural failures occur before brittle shear failures. Also, the shear provisions are suitable to determine the shear capacity of beams and do not take into account the beneficial geometric properties of a one-way slab. These approaches lead to a safe design, but are not suitable for assessing the real shear capacity of an existing slab bridge.

To assess the existing concrete bridges, it is interesting to take load transfer mechanisms into account that are typically neglected for design. A slab under a concentrated load for example fails in a failure mode that is not purely one-way (beam) shear or two-way (punching) shear. Most of our knowledge on shear is the result of experiments on small, heavily reinforced slender beams tested in four-point bending. Due to the difference in force transmission, this approach is not applicable to a slab under a concentrated load in shear.

For slabs under a concentrated load, a certain effective width, that ‘carries’ the load in shear, should be defined. TU Delft did much research on concentrated loads on slabs [31]. These researches quantified the effective width in shear experimentally for the first time. In this chapter some of the conclusions which can be used are described. These experiments were meant for slab bridges in general and not especially for existing bridges.

4.1.1 Proof loading

Proof loading is important to understand the bridges’ behavior and refining assessment methods. A study to multiple full scale tests all over the world [32] was performed. Generally, the tests indicated that theoretical calculations of the load-carrying capacity based on methods traditionally used for design and assessment provide conservative estimates. It can also be concluded that almost a third of the experiments resulted in unexpected types of failures, mainly shear instead of flexure. In addition, differences between theoretical and tested capacities are often apparently due to inaccurate representation of geometry, boundary conditions and materials.

4.1.2 Effect of predamaging

The transverse stiffness has a large influence on the transverse force transmission and therefore on the effective width. Cracks in a slab affect the stiffness of a slab. Several tests have been done to differentiate between a cracked and an uncracked slab by analysing the effect of predamaging [33]. Conclusions were that the influence of predamaging until failure is a lower bound, as the case in which a local failure has occurred does not occur in practice. The overall average is a residual capacity of 81% of the undamaged shear strength. This is surprisingly high and indicates an alternative load carrying path if local failure occurs. The experimental results indicate large residual capacity for severely damaged slabs.

4.2 Loads for shear assessment (Load Model 1)

Verifying an existing bridge for shear needs to be done using the Eurocode. Load model 1 from the Eurocode is assumed to be governing for the shear assessment. The prescribed live loads are larger than used by the previous national codes. The heavier prescribed live loads include significantly heavier and more closely spaced wheel loads that result in increased sectional shear forces at the support. In order to find the normative load combination for occurring shear stress, the most unfavorable combination for live loads needs to be found. The live loads are determined according to load model 1 from EN 1991-2 [2]. In this load model, wheel loads are combined with an increases lane load on lane 1. The axle loads have a contact area of 400mm x 400mm. The axle loads are demonstrated in Table 4-1. The application load model 1 is illustrated in Figure 4-1. The axle system can be moved over the lane in order to find the most unfavorable combination.

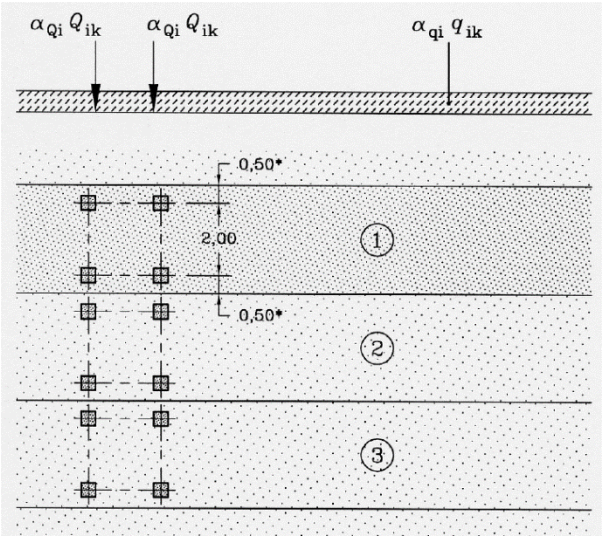

Figure 4-1 - Application of Load Model 1 [2]

Table 4-1 - LM1 - characteristic values [2]

Location	Tandem system (TS) Axle load Q_{ik} (kN)	UDL system q_{ik} (or q_{rk}) (kN/m^2)
Lane 1	300	9
Lane 2	200	2,5
Lane 3	100	2,5
Other lanes	0	2,5
Remaining area (q_{rk})	0	2,5

The values of α_{Qi} are provided in the National Annex and are equal to 1 for governmental bridges the Netherlands. Reduced values for $\alpha_{q1}$and α_{Qi} are presented in Table 4-2 and Figure 4-2. Correction factors for other spans can be found by interpolation. These reductions can be applied if less than 2.000.000 trucks can be assumed. A factors higher than 1 have to be used if a certain driving lane is meant for trucks.

Table 4-2 - Correction factors α_{Q1}, α_{q1} and α_{qr} [2]

Number of trucks per year per lane for heavy traffic N_{obs}	α_{Q1} and α_{q1} Max. span (L)				α_{qr}
	20 m	50m	100m	>200m	
≥ 2 000 000	1,00	1,00	1,00	1,00	
200 000	0,97	0,97	0,95	0,95	0,90
20 000	0,95	0,94	0,89	0,88	0,80
2 000	0,91	0,91	0,82	0,81	0,70
200	0,88	0,87	0,75	0,74	0,60

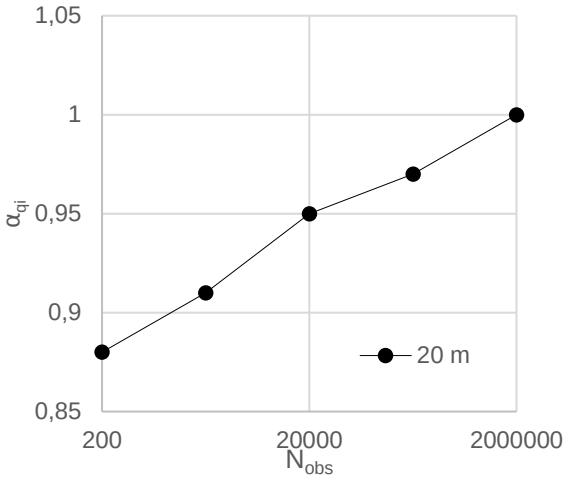

Figure 4-2 - Correction factors α_{Q1} and α_{q1} for different spans

For existing municipal bridges more reduction factors can be applied. This has been described in 3.6.4.2.

In the National Annex the expected number of heavy vehicles for different kinds of roads is described. For roads with an average number of trucks (such as the Dutch N-ways) the number of trucks per year per carriageway can be assumed as $0{,}5*10^6$. For roads with few trucks this number is $0{,}125*10^6$. This number of trucks can be assumed for remote municipalities.

4.3 Effective width

In the following chapters (4.3, 4.4 and 4.5) some results and assumptions are described which are based on research that has been done at the TU Delft (Lantsoght et al.).
Vertical loads on a slab spread horizontally to the support. Theoretically, the effective width b_{eff} is determined in such a way that the total shear stress over the support equals the maximum shear stress over de effective width. In practice, in order to calculate the load spreading, one can assume that the loads spread under a certain angle. This is called the concept of the effective width. In Dutch practice, this angle is assumed to be 45˚. See also Figure 4-3.

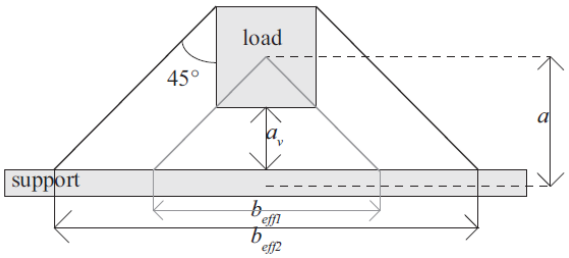

Figure 4-3 - Horizontal load spreading (2 approaches) [34]

The 2 approaches for determination of the effective width are illustrated in this figure. These are the the Dutch model, leading to b_{eff1}, and the French model, leading to b_{eff2}. Experiments [33] reveal that both approaches load to a rather conservative result. The comparison indicates that the French model, leading to b_{eff2}, provides the best results. [30]

The assumptions are the result of tests in the laberatory of TU Delft. The effective width in combination with the French spreading model seemed to fit the calculations with the point load at failure according to the Eurocode. In order to fit the test results entirely, an additional plate factor of k_p (or k_{cap}) was added.

4.3.1 Transverse load distribution factor β

The transverse load distribution factor β can be used to reduce the contribution of the concentrated loads to the total acting shear force. This reduction should be made in order to take into account the higher shear capacities of slabs compared to beams, because of the transverse load distribution. EN 1992-1-1:2005 prescribes the use of the reduction factor β as $\beta = a_v/2d_l$.

This is for direct load transfer of loads to the support. Experiments demonstrate that the reduction factor can be used as $\beta_{new} = a_v/2{,}5d_l$ for the case of concentrated loads on slabs with $0{,}5d_l \leq a_v \leq 2{,}5d_l$. [30]

4.3.2 Asymmetric effective width

An asymmetric effective width can be used if the concentrated loads are near the free edge of the slab. The effective width is limited by the edge distance on one side and by the load spreading model (French model) on the other side. This approximation leads to an unbalance between the location of the reaction forces of the load and of the shear distribution at the support (Figure 4-4). However, such a distribution statistically leads to better results. [31]

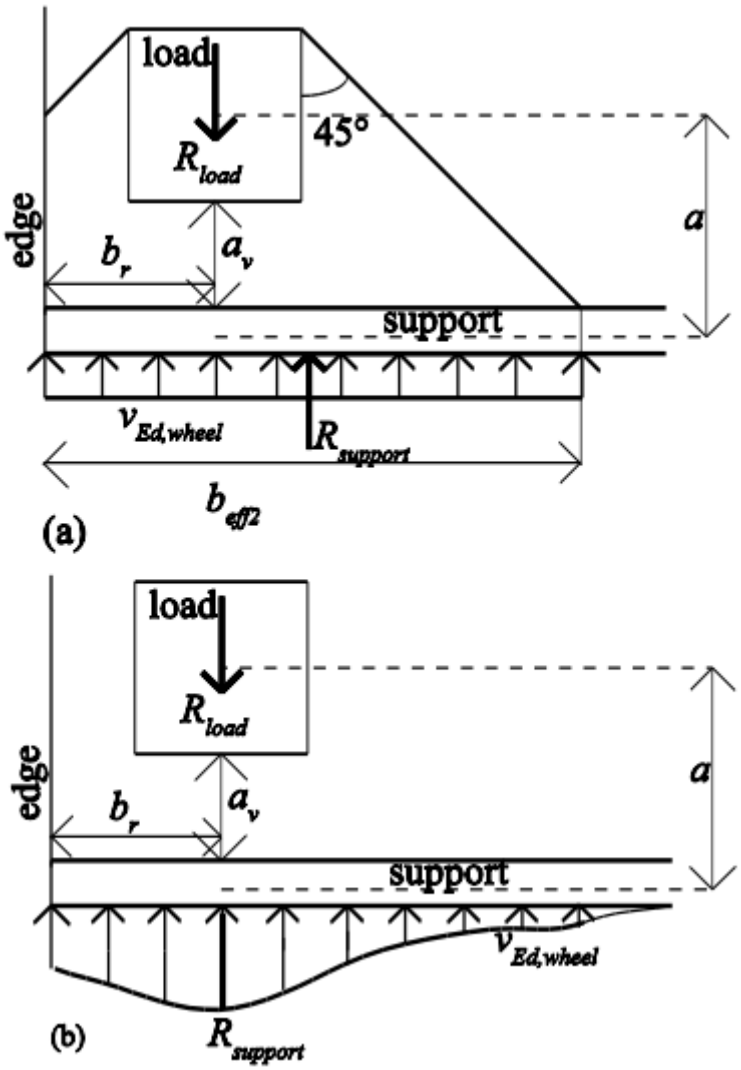

Figure 4-4 - Shear force for wheel loads close to the edge: (a) Different location of resultant of shear force over support $R_{support}$ and applied wheel load R_{load}; (b) Real stress distribution at the support, in which the moment imbalance is not occurring anymore. [31]

4.3.3 Effective width of an axle load

The French load spreading method results in overlapping effective widths when considering each wheel load of the axle separately. It is conservative to use the effective width of the entire axle (two wheel loads combined), as illustrated in Figure 4-5 a. It is recommended to place the first axle at a maximum distance $a_v = 2{,}5d_l$, so that the effective width of the axle is smaller than the sum of the effective widths of the two wheels separately. If the axle loads are placed closer to the support the reduction factor β applies. For the slab bridges under study in the Netherlands, this requirement is commonly fulfilled. There are, however, no experimental results available for slabs subjected to two or four concentrated loads (two axles at 1,2 m) [34].

If two lanes are examined, there has to be calculated with 4 axles next to each other. In this case it can be assumed that the 4 axles can be regarded together to determine the effective width. This principle is illustrated in Figure 4-6.

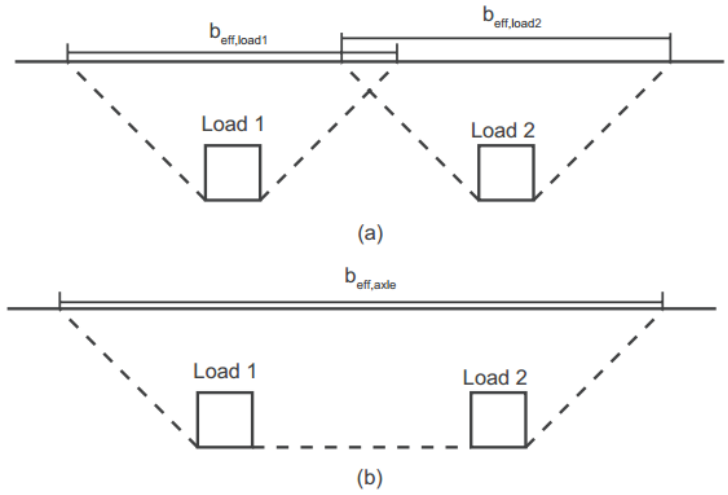

Figure 4-5 - a) effective width determined per wheel print. b) effective width determined per axle [34]

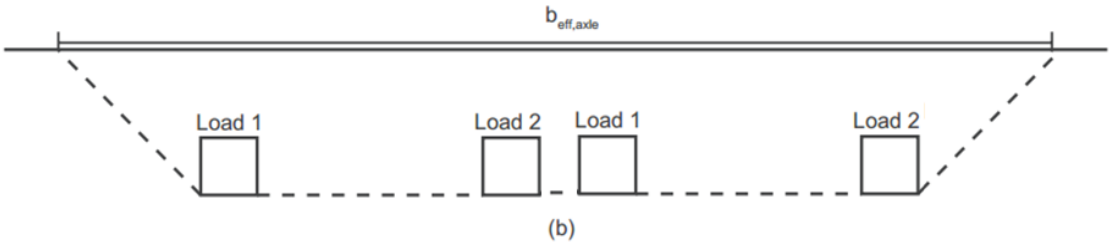

Figure 4-6 - Effective width of 2 axles together

4.3.4 Skewed slabs

In literature, some test with skewed slabs were done. These tests were analyzed to consider the effect of skewed slabs. The experimental results from literature cannot be used as a basis for a recommendation as none of the series demonstrate the influence of the skew angle on the shear capacity. For shear capacity, more experiments need to be done to take into account a certain skew in the right way. [31]

In general, it is not totally clear how the effective width of skewed slabs must be determined. In [35] three options for the load spreading of a single axle have been studied. These are:

a) b_{str}, the effective width of a straight slab;
b) b_{skew}, with horizontal load spreading under 45˚ from the far side of the wheel print to the face of the support
c) b_{para}, based on a parallel load spreading to the straight case

These options are illustrated in Figure 4-7.

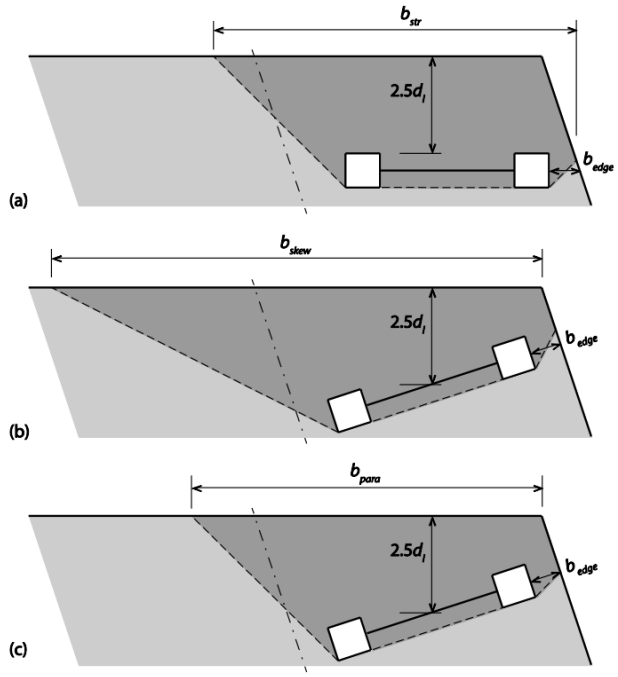

Figure 4-7 - Possible ways to determine the effective width of a single axle in shear for a skewed slab [35]

It turns out that option b is not realistic. The other 2 options are approaching the reality in a better way. It is still not totally clear how effective width method can be applied on skewed bridges. In chapter 3.3.3 there was found that for skew angles smaller than 20˚ no adaption of the effective width should be performed since the differences with a straight slab are neglectable. However, research to the influence of a skew angle is desired. In this thesis, skew angle lower or higher than 90˚ leads to less reliability of the outcome of the Quick Scan model.

4.3.5 Results and recommendations experiments

More experiments [30], [36] have been done on the load spreading. For a slab strip with a small width an increase of the specimen would lead to an increase of the shear capacity. For larger widths, a threshold value should apply above which no further increase in shear capacity is observed with an increase of specimen width. In this way the experiments have lead to the following conclusions and recommendations:

- Use the effective width resulting from load spreading under 45˚ from the far side of the loading plate to the face of the support (French model);
- Use a minimum effective width of $4d_l$;
- For concentrated loads close to the support on slabs, the reduction factor β from EN 1992-1-1:2005 can used and replaced by $\beta_{new} = a_v/2{,}5d_l$.

These recommendations can be applied to determine the most unfavorable position of the wheel loads. This results in the maximum shear force at the support.

4.4 Live load model

In order to obtain the most unfavorable positions of the loads, the conclusions and recommendations mentioned above can be used. The maximum shear stress at the edge of the support is obtained in the following way. The first axle (edge of the tyre) is placed at a distance of $a_v = 2{,}5\ d_l$ from the support. This load configuration is governing since the set of recommendations takes the influence of direct load transfer and transverse load redistribution into account up to $2{,}5\ d_l$. In the second and third lane, the design vehicle is placed in such a way what the front axle generates the largest shear force at the edge of the bridge. [30] This procedure is illustrated in Figure 4-8. Note that this is only valid for bridges with a small edge distance.

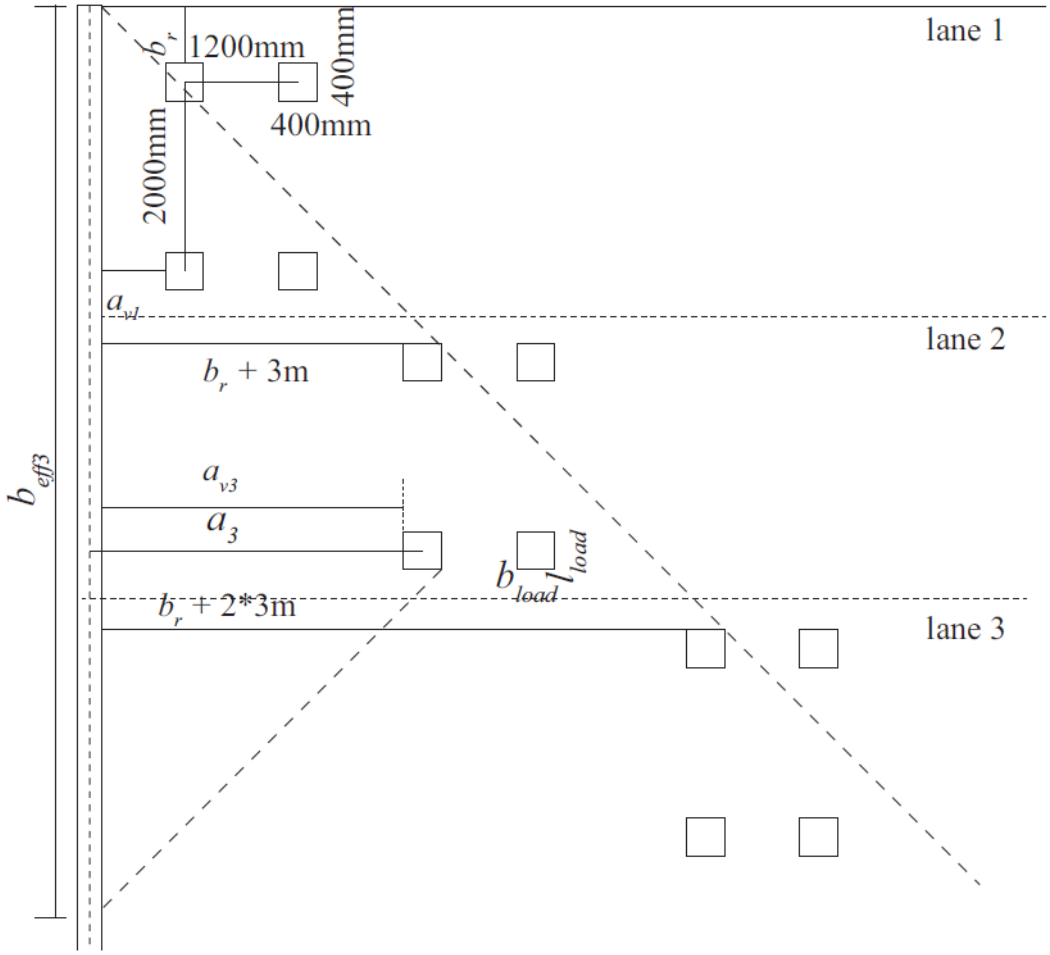

Figure 4-8 - Most unfavorable position of the design trucks [30]

The concentrated loads caused by vehicles spread horizontally, but also vertically into the concrete. Due to the asphalt layer, a vertical stress redistribution occurs. The wheel loads (400m x 400mm) redistribute through the asphalt layer ($d_{asphalt}$ in Figure 4-9) with an angle of 45˚. If the asphalt layer is assumed to 70mm (which is usual for municipal bridges), this results in a fictitious wheel print on the concrete surface of 540mm x 540mm.

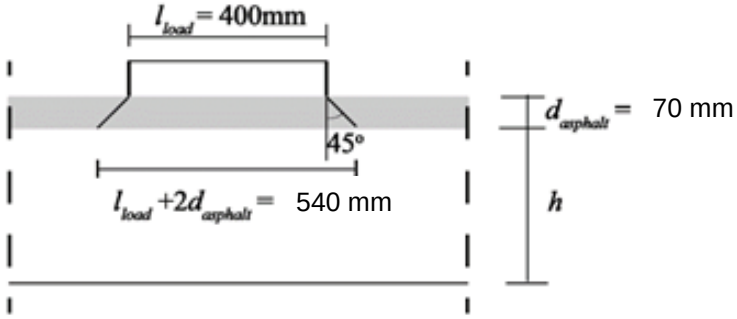

Figure 4-9 - Vertical load distribution of the wheel load through the wearing surface, adapted from [31]

4.4.1 Superposition of loads

Concentrated loads commonly occur simultaneously with other loads, such as dead load of the structure and asphalt layer. In order to take all loads into account for the determination of the shear stress, a superposition of loads is assumed. This hypothesis assumes that concentrated loads are transferred to the effective width of the support and distributed loads are transferred over the full length of the support. This is illustrated in Figure 4-10. Several tests have been done to confirm this hypothesis. [37] It was found that the hypothesis of superposition is valid and conservative. Typically, larger shear capacities were found for the case of combined loading.

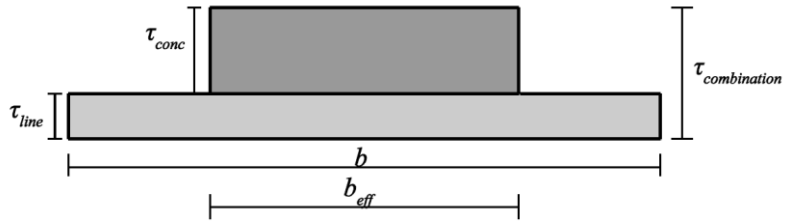

Figure 4-10 - Hypothesis of superposition [31]

As for the axle loads, also the uniform distributed loads spread to the support. The force distribution to the support can be approximated and schematized as a triangular distribution on the support as illustrated in Figure 4-11.

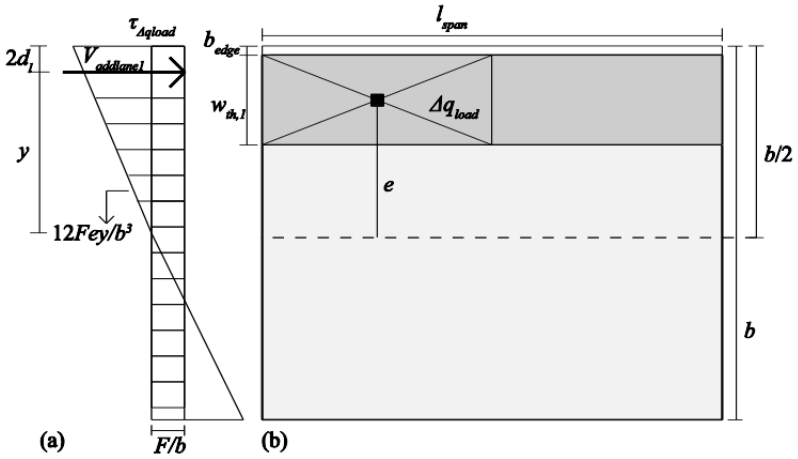

Figure 4-11 - Model for contribution of increased loading in the first heavily loaded lane as compared to other lanes assuming a triangular stress distribution over the support

According to this schematization, the highest stresses occur on the edge of the slab. This is correct according to tests that have been done [33] and the test in RFEM. However, this schematization is only applicable for small edge distances (b_{edge}).
The resulting shear force $V_{addlane1}$ is equal to:

$$V_{addlane1} = \frac{F}{b} + \frac{F*e*y}{\frac{1}{12}*b^3}$$

Where:

F = the reaction force of the additional load on lane 1 (kN)

The other parameters can be found in Figure 4-11. In this model, it is assumed that the slab is infinitely stiff in transverse direction but weak in torsion. A slab bridge however, typically has a torsional stiffness, which can be estimated with the approach of Guyon-Massonnet. Requirement for the method mentioned above is that is should provide a more conservative shear force than the analysis based on the method of Guyon-Massonet. In order to obtain this result, the maximum width over which the triangular distribution is used, is limited to a value of $0{,}75 * l_{span}$ as described in [30]. A model factor of 1,1 should be used in combination with this approach. The lower bound value of this approach is determined by vertical load distribution under an angle of 45° to half of the slab depth $d_l/2$. This approach is illustrated in Figure 4-13. Note that the width of the resulting shear force is slightly larger than the lane width due to vertical stress distribution to half of the slab depth. For the additional lane load on lane 1 Δq_{load}, a redistribution of forces is allowed. Vertical force

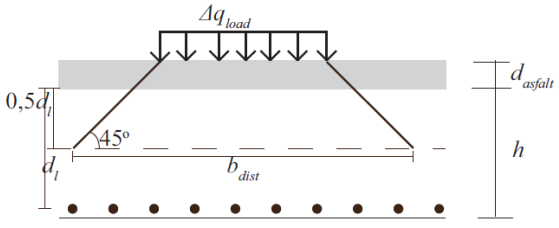

Figure 4-12 - Load spreading and contribution for the increased load on the first lane [31]

redistribution to the mid-depth position of the cross-section $(d_l/2)$ can be used as illustrated in Figure 4-12.

The resulting value for the minimum shear force becomes:

$$F_{min} = (\alpha_{q1} * 9 - \alpha_{q2} * 2,5) * \left(min\left(b_{edge}, \frac{d_l}{2} + d_{asphalt}\right) + w_{th,1} + \frac{d_l}{2} + d_{asphalt}\right) \quad (4.1)$$

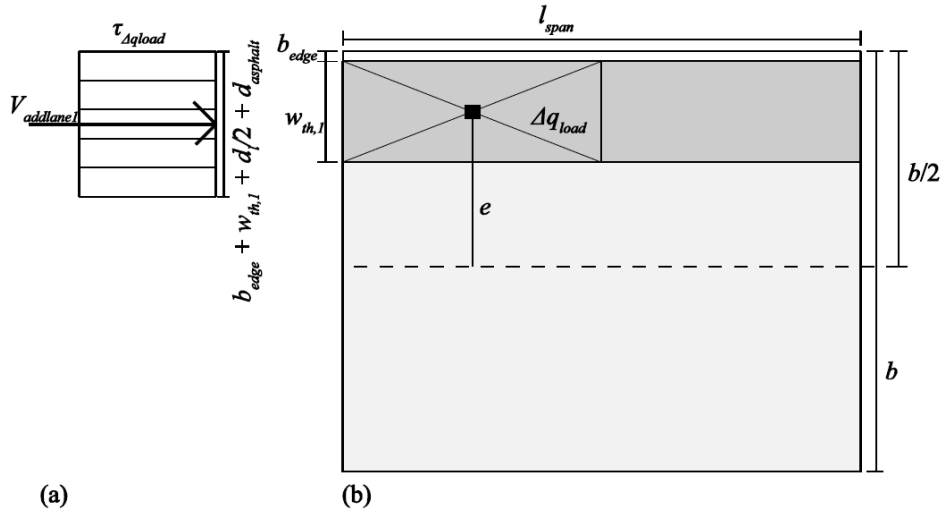

Figure 4-13 – model for the contribution of increased loading in the first heavily loaded lane. a) assumed stress distribution b) sketch of the top view with location of the first heavily loaded lane

The models described above are only valid for small edge distances.

4.4.2 Static indeterminacy

In the previous chapters only statically determinate structures were considered. Also static determinate structures are regarded. To expand the method to statically indeterminate structures, correction factors for the increased contributions of the loads to the shear force are the mid support are defined. These factors result from a series of case studies [38]. These factors are applicable for end spans between 0,7*l_{span} and 0,8*l_{span} where l_{span} is the length of the mid span, for cross-sectional depths between 600m and 1000mm and for edge distances between 300mm and 1400mm. Different factors for different loads are defined. The following symbols are used:

α_{TS1} correction factor on the shear stress for the statical indeterminacy for the 1st design truck;
α_{TS2} correction factor on the shear stress for the statical indeterminacy for the 2nd design truck;
α_{TS3} correction factor on the shear stress for the statical indeterminacy for the 3rd design truck;
α_{UDL} correction factor on the shear stress for the statical indeterminacy on the uniformly distributed lane load;
α_{DL} correction factor on the shear stress for the statical indeterminacy on the dead load.

The correction factors for different sections are presented in Table 4-3. The location of these sections is illustrated in Figure 4-14.

Table 4-3 – correction factors for statical indeterminate structures for three or more spans [31]

Section	α_{TS1}	α_{TS2}	α_{TS3}	α_{UDL}	α_{DL}
Support 1-2	0,95	0,90	0,78	0,94	0,75
Support 2-1	1,11	1,16	1,21	1,34	1,31
Support 2-3	1,06	1,05	1,04	1,10	1,00
Support 3-2	1,05	1,04	1,01	1,12	1,04

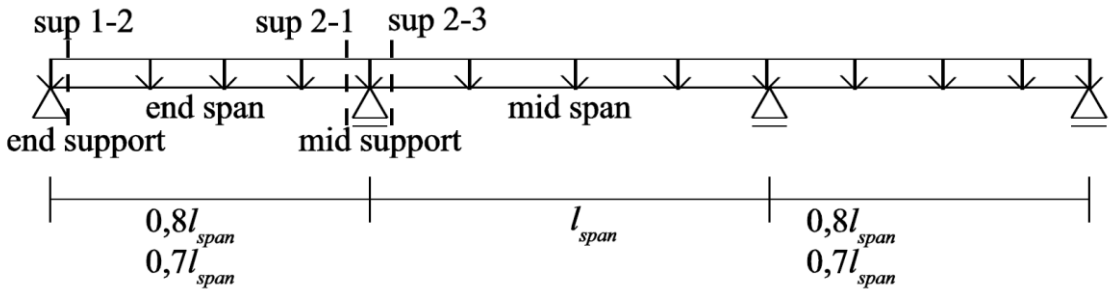

Figure 4-14 – Considered sections for a typical three span bridge [31]

These factors were meant for typical governmental bridge. It is questionable if existing municipal bridges with multiple spans have the same typical dimensions. Since the amount of research to correction factors for statically indeterminate structures is limited and the scope for these factors is limited, more research is needed to verify these factors. Also, a greater scope of bridge dimensions needs to be examined to make the use of these factors independent of the bridge dimensions. Therefore the correction factor can be used, but then the output of the Quick Scan model becomes more uncertain.

4.5 Shear capacity

This thesis mainly focuses on the loads on existing municipal slab bridges. Conclusions from previous researches [31], [35] and [39] are provided to calculate the shear capacity. Conclusions from the experiments carried out are summed up briefly in the following chapters.

The most critical slab bridges are the existing bridges that were built a decades ago (<1980). Especially slab bridges without prestressing steel are considered to be critical. When no excessive flexural cracks are visible, the bridge is assumed to be same for flexural moment. Most of these slab bridges do not have shear reinforcement. Therefore, the formula for unreinforced slabs from the Eurocode 2 (EC2) must be applied for these bridges:

$$V_{Rd,c} = \left[C_{Rd,c} k_{cap} k (100 \rho_l f_{ck})^{\frac{1}{3}} + k_1 \sigma_{cp}\right] b_w d \qquad \textit{(4.2)}$$

For reinforced slabs, the last part between brackets becomes zero (no prestressing). This formula contains a reinforcement ratio which is often unknown for old bridges. Therefore the minimum value for shear capacity v_{min} is used. This is explained in the following chapter

4.5.1 The minimum shear capacity v_{min}

With the introduction of the Eurocode (EC2) the expression for minimum shear force capacity from the former code VBC ($\tau_d \leq 0{,}4\, f_b$) has changed in:

$$v_{min} = 0{,}035 k^{\frac{3}{2}} * f_{ck}^{\frac{1}{2}} \qquad \textit{(4.3)}$$

Where f_{ck} is the characteristic cylinder compressive strength and k is a scale factor with:

$k = 1 + \sqrt{\frac{200}{d}} \leq 2{,}0$ where d is in mm.

The lower boundary according to EC2 more conservative than the formula from the VBC. This is especially the case for plates with a low reinforcement ratio and a large effective thickness. This leads to a problem in many concrete slab bridges.

4.5.1.1 Background v_{min}

The expression for the shear capacity for element without shear reinforcement is the result of a statical evaluation of 176 selected tests [40]. For the statical analysis the formula for shear capacity was assumed as:

$$V_{u,calc} = C_m * k(100\rho_l f_{cm})^{\frac{1}{3}} \quad (4.4)$$

Regarding the results the average value was described with $C_m = 0{,}163$. The design value was calculated with the sensitivity factor $\alpha_R = 0{,}8$, the coefficient of variation $\delta_R = 0{,}13$ and the reliability index β = 3,8. The following formula was used:

$$V_{Rd,c} = V_{um,calc}/(+\alpha_R * \beta * \delta_R - 0{,}5\ \delta_R^2) \quad (4.5)$$

The factor C_m now becomes 0,111. When f_{cm} is replaced by $1{,}15f_{ck}$ the factor becomes 0,116. For existing bridges the β factor may be lower. Therefore, the factor can increase up to 0,134 for β = 2,5. As 5% lower boundary a factor of 0,15 is used [39].

Low reinforcement ratios (<0,4%) cause failure due to flexural moment. Therefore a lower boundary of v_{min} is introduced in EC2 as described in equation (4.3) The factor 0,035 from V_{min} is based on some considerations. The most unfavourable situation for shear force is a point load at a distance of a = 2,5d from the support. This position corresponds with the smallest ratio between the shear capacity and the flexural moment capacity as described by Kani [41].

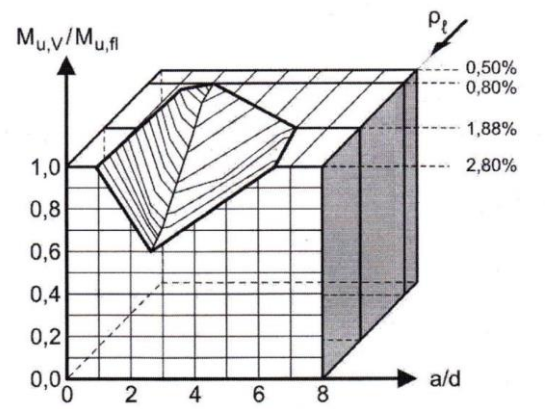

Appendix Figure 4-1 - Kani's shear valley [41]

When the characteristic shear capacity is reached, the flexural moment due to the point load (with the factor $C_m = 0{,}15$) can be described as:

$$M_{uv} = V_{uk} * 2{,}5d = 0{,}375k(100\rho f_{ck})^{\frac{1}{3}}bd^2 \quad (4.6)$$

An approximation of the characteristic yield moment is:

$$M_{uk} = 0{,}9d(\rho_l bd)f_{yk} \quad (4.7)$$

Equation 4.6 and 4.7 combined give an expression for the reinforcement ratio:

$$\rho_l = \frac{2{,}68 * k^{\frac{3}{2}} * f_{ck}^{\frac{1}{2}}}{f_{yk}^{\frac{1}{2}}} \quad (4.8)$$

This equation can be substituted into equation 4.4 and gives a new expression for v_{min}:

$$v_{u,min} = \frac{0{,}78 * k^{\frac{3}{2}} * f_{ck}^{\frac{1}{2}}}{f_{yk}^{\frac{1}{2}}} \quad (4.9)$$

4.5.1.2 v_{min} for plates

A plate can redistribute forces in a better way than a beam. A weak spot in a slab does therefore not directly lead to failure. Research was done to the shear capacity of slabs [39]. The results are a factor 1,6 above the prediction of EC2 (equation 4.3) and a factor of 1,3 above the prediction of

the average value for plates (equation 4.5), with a factor $C_m = 0{,}12$. A possible reason for the higher shear capacity for plates compared to beams is that a shear crack show vaulting, which leads to extra aggregate interlocking. This research show that a plate factor of 1,2 can be used. Regarding existing bridges, the following (minor) adaptions for the shear capacity are made [39]:

1. As explained in chapter 4.5.1.1, for the derivation of v_{min} the lower bound value of the shear- and flexural moment capacity was compared. This was related to the reliability index β. The shear capacity can be variable for different values of β. The differences however, are small.
2. In EC2, the derivation of v_{min} used a factor a/(2,5d). [42] shows that a factor of a_v/(2,5d) is more realistic, where a_v is the distance between the edge of the load and the edge of the support. In practical cases, this factor corresponds with 3d/a.
3. Problems with shear force capacity commonly occur for relatively low reinforcement ratios. The internal lever arm can be increased to 0,95d.

These adaptions together with the plate factor of k_p = 1,2 (also called k_{cap}) lead to a new expression for v_{min}.

$$v_{min} = \frac{1{,}08 * k_2^{\frac{3}{2}} * f_{ck}^{\frac{1}{2}}}{f_{yk}^{\frac{1}{2}}} \qquad \textit{(4.10)}$$

Note that the plate factor k_p can only be used for reinforced massive plates. Also, the plate has to be supported with a line support. A support is considered as line support if:

- The distance between the contact points of the support is less than 5d;
- The longitudinal reinforcement is positioned above the transverse reinforcement, or above the longitudinal reinforcing in the transverse beam at the support.

When comparing this expression with the expression for v_{min} in EC2 (equation 4.3) the differences are: 38,5% for f_{yk} = 500 N/mm², 55% for f_{yk} = 400 N/mm², 100% for f_{yk} = 240 N/mm². The fact that steel with f_{yk} = 240 N/mm² is commonly plain was not taken into account. In general, plain steel has a positive effect on the shear capacity. Figure 4-15 shows the different formula's for the minimum shear capacity according to the Eurocode (left) and the RBK (right). As comparison, the shear capacity according to the VBC is illustrated in both graphs.

When the β factor is variable, the factor 1,08 from equation 4.10 becomes variable. Taking into account the three points mentioned above, equation 4.8 becomes:

$$\boldsymbol{\rho_l = \frac{\left(3{,}92 * k^{\frac{3}{2}} * f_{ck}^{\frac{1}{2}}\right)}{f_{yk}^{\frac{3}{2}}}} \qquad \textit{(4.11)}$$

Substituting this into equation 4.4 with f_{cm} is replaced by $1{,}15f_{ck}$ gives

$$\boldsymbol{v_{min} = \frac{\left(C_{Rd,c} * k^{\frac{3}{2}} * f_{ck}^{\frac{1}{2}}\right)}{f_{yk}^{\frac{1}{2}}}} \qquad \textit{(4.12)}$$

Where:

$C_{Rd,c} = (100 * 3{,}92)^{\frac{1}{3}} * k_{cap} * \frac{C_m}{\exp(+\alpha_R * \beta * \delta_R - 0{,}5 * \delta_R^2)})$

$C_m = 0{,}163$

The variation of β gives a small variation of the (minimum) shear capacity. In the Eurocode and the RBK is reflected by different partial factors. These factors are illustrated in Table 3-10.

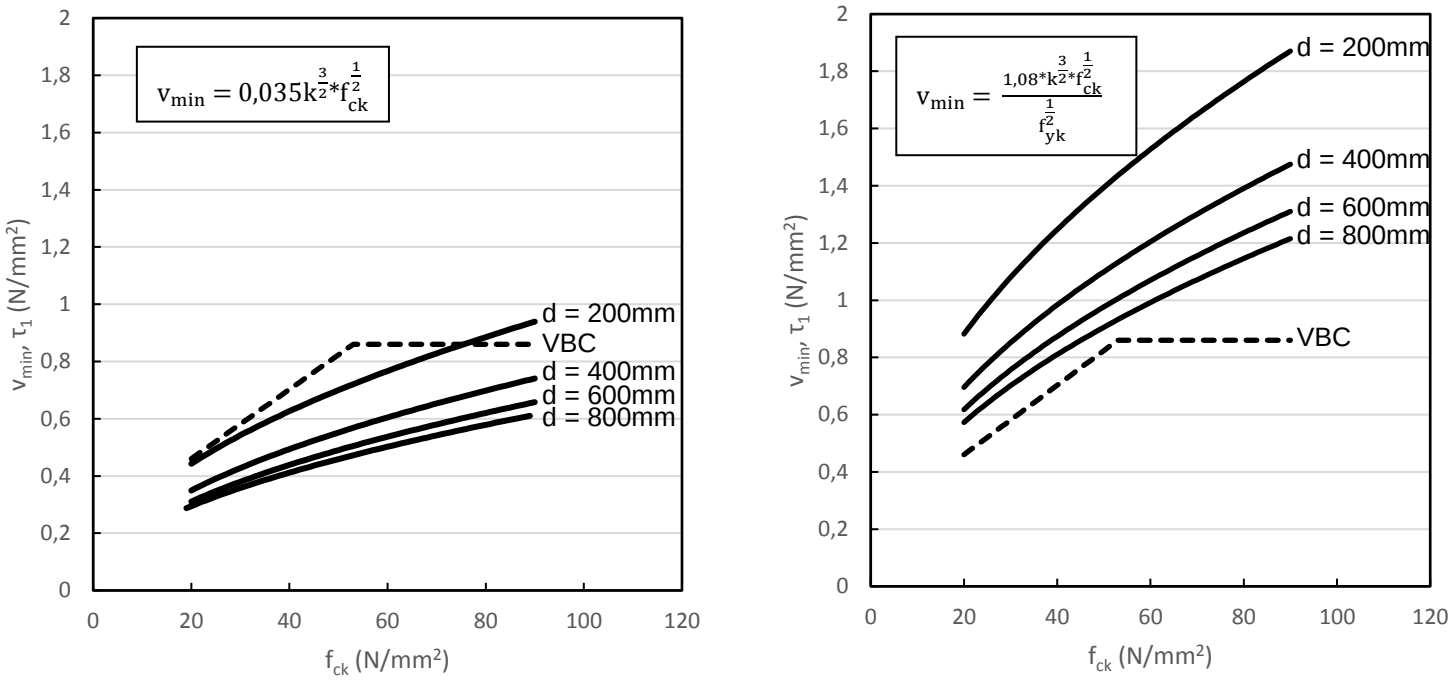

Figure 4-15 - v_{min} according to EC2 and VBC (left) and according to equation 6.8 (RBK) and VBC (right) for a yield strength of f_{yk} = 240 N/mm² [39]

4.5.2 Concrete compressive strength

The concrete compressive strength influences the shear capacity of beams, because it directly influences the concrete tensile strength, the dowel capacity limited by the tensile strength of the concrete cover supporting the dowel, the aggregate interlocking capacity and the strength of the compression zone. Therefore, in theory the concrete compressive strength should influence the shear capacity. However, no influence of the concrete compressive strength was experimentally observed in large, lightly reinforces beams [43]. It was stated that: The influence of concrete strength on the shear resistance of rectangular reinforced concrete beams without web reinforcement is negligible and can be omitted in strength analyses. Also, in [33] no increase in shear capacity with increasing compressive strength was observed. A possible explanation is the reduced aggregate interlocking capacity of higher strength concrete.

The RBK [5] states that a minimum concrete class C35/45 can be assumed for governmental bridges. For municipal bridges it is not sure if this assumptions is safe. The building year can be used to find the minimal concrete strength according to the standards applicable in the building year of the bridge. However, this may give very conservative results. For more certainty material test have to be done to determine the lower boundary of the compressive strength. In general it is recommended to perform more research to the concrete compressive strength in municipal bridges. Concrete is known to increase its strength over time, so it is possible that the strength is higher than expected. However, this has to be investigated. A possible method is to cooperate with several material testing companies such as NEBEST. It is likely that the knowledge is available at different companies, but has to be gathered and processed.

4.5.3 Reinforcement type

Shear tests on beams with plain bars typically reveal a larger shear capacity as compared to beams with deformed bars. However, for beams with loads close to the support and smaller reinforcement ratios, lower shear capacities with plain bars than with deformed bars have been reported. For this loading case, the action of direct load transfer is dominant. For this action, the use of plain or deformed bars makes no difference.

As described in chapter 4.5.1 a low yield strength leads to higher shear capacities. This is in favor of old bridges. In structures before approximately 1964, reinforcement steel with a yield strength of f_{yk} = 240 N/mm^2 is used. As for concrete compressive strength, more research is needed to the used steel in municipal bridges. Recommendations for the use of the concrete compressive strength and steel type in the Quick Scan model is described in chapter 8. A parametric study to the compressive strength and steel yield strength is described in chapter 8.4.

4.5.4 Transverse flexural reinforcement

Transverse reinforcement is activated due to the transverse moments, and shear is carried to a certain extent over the width of the slab. This means that a one-way slab does not behave like a beam. Research has been done to the influence of transverse flexural reinforcement ratio on the shear capacity. Although a difference in cracking pattern is observed, no increase in shear capacity is observed for an increased transverse reinforcement ratio. Observations however indicate that the transverse flexural reinforcement helps at distributing the cracks in transverse direction.

4.5.5 Support type

Concrete slabs on elastomeric and rigid steel bearings were compared [33]. This resulted in similar capacities for slabs with steel bearings as compared to slabs with elastomeric bearings. However, the effective widths based on the measurements of the reaction forces are clearly larger for slabs on steel bearings. Moreover, it was observed that slabs on elastomeric supports reveal a failure mode with more warning behavior. For the FE modeling, elastomeric line supports are used. The support type is important for the use of the plate factor k_p as described in chapter 4.5.1.2.

4.6 Conclusions and recommendations

The experiments demonstrate that the slabs can carry loads that are significantly larger than their design loads. Different codes (Dutch Code NEN 6720:1995, NEN-EN 1992-1-1, ACI 318 and Model Code 2010) all recommend very different approaches that result in different design shear capacities and take the parameters affecting the shear capacity into account in a different way.
The experimental results indicate a large residual capacity for severely damaged slabs. Also, slabs under concentrated loads close to the support fail in a more ductile mechanism than observed in typical beam shear experiments. Inclined cracks indicating shear failure were observed at 70% of the failure load. This indicates the ability of slabs to indicate warning behavior before brittle shear failure.

Based on the experimental research as described above, recommendations are summed up.

- Since cracking has influence on the force distribution in a slab, differentiation between both cracked and uncracked slabs can be made;
- The concentrated loads are distributed according to the effective width method as described in chapter 4.3 (French Model). Distributed loads are distributed over the full width;
- For concentrated loads close to the support on slabs, the reduction factor β from EN 1992-1-1:2005 can used and replaced by $\beta_{new} = a_v/2{,}5d_l$;
- For loads near the edge an asymmetric effective width can be assumes as described in chapter 4.3.2;
- A fictitious wheel print can be used on the concrete surface, assuming vertical load spreading under 45° through the asphalt layer;
- Only slabs with a skew angle higher than 70° can be considered. the influence on the shear force for a skew angle between 70° and 89° is yet unknown, which leads to more uncertainty in the model output. Therefore this thesis especially focusses on straight slabs (skew angle = 90°);
- For small edge distances, the increased lane loading on the first lane can be distributed assuming a triangular stress distribution over the support. A lower bound of vertical loading under 45° to the mid-depth of the slab depth is prescribed;
- Correction factors for statical indeterminacy can be applied. These factors lead more uncertainty in the output, since the factors have a limited applicability;

- The new formulation for v_{min} as described in chapter 4.5.1.2 is used as minimum shear capacity.

These recommendations can be used for the FEM calculations for existing municipal bridges. The goal of the FEM research is to gain insight in the force transmission in solid slabs, especially for municipal bridge. This means that larger edge distances are regarded. Since the scope is existing bridges, also the difference between cracked and uncracked slabs is investigated. This research is described in chapter 7. Additional research has been done to a reduction factor α to lower the live loads on existing municipal (small span) bridges (Chapter 6). In the next chapter the finite element modelling process is elaborated.

5 Finite Element Modelling

To gain a better understanding of force transmission, Finite Element Modeling (FE modelling or FEM) can be used. In this chapter, first the theory behind plates and FEM is explained. In this way, the output from the FE model can be better understood and explained. In the following chapters 2 different researches are done.

In chapter 6, Load model 1 from the Eurocode is critsized for existing municipal concrete slab bridges. This is done by comparing the resulting shear force and flexural moment due to Load Model 1 with load models which represent a real occurring lorry in a better way. By this comparison an α factor was found which may decrease the loads from Load Model 1. This may make a re-calculation for an existing bridge less conservative.

In chapter 7 the force transmission by load model 1 is investigated. There has been varied with different parameters such as span, edge width and transverse stiffness. Also, the loads from Load Model 1 (dead load and variable loads) are examined separately to gain a better understanding of the resulting maximum shear force at the support.

5.1 Introduction

Finite element modelling is best understood from its practical application, known as finite element analysis (FEA). FEA as applied in engineering is a computational tool for performing engineering analysis. It includes the use of mesh generation techniques for dividing a complex structure into small elements, as well as the use of software program coded with FEM algorithm. With FEM in civil engineering, the force and stress distribution in a structure can be determined in a relatively easy way. Many parameters, such a material properties, support properties or connections are standardized and do not have to be calculated. For plastic calculations, much knowledge and calculation time is needed. With the upcoming popularity of FEM calculations, plastic hand calculations of plates are replaced by FEM calculations more and more.

5.2 Plates in finite element programs

Before the Finite Element Modelling process can start it is useful to have insight in the calculation process of a finite element program in general. In this way, the output can be qualified in a better way. Special attention is provided to the behaviour of plates in finite element programs. In finite element modelling, a structure is divided in small elements. In this way the structure has a mesh grid of connected elements of the same size. For each element the stresses and strains are determined by the program. Since each element is in equilibrium the stresses and strains of the whole structure are determined by the program.

5.2.1 Theory behind plates

[44] and [45] describe the theory behind plates in detail. In this chapter the theory which is relevant for FE modelling of a simply supported bridge is described.

A plate is considered to be thin if the height is smaller than 1/5 of the width. In the case of a concrete slab bridge this is commonly the case. This assumption leads to some simplifications [46]:

1. The cross section of a segment stays straight and not curved;
2. There are no membrane forces, which is the consequence of the assumption that the deflection is small compared to the height of the slab;
3. Strains of the slab in z-direction (ε_{zz}) are neglected;

4. The stress in z-direction (σ_{zz}) is negligible compared to the stresses in x- and y-direction;
5. The deformation due to shear force is considered to be negligibly small, which allows us to state that $\gamma_x = 0$ and $\gamma_y = 0$

Due to the latter statement, the kinematic relations become:

$$\kappa_{xx} = -\frac{\partial^2 w}{\partial x^2} \qquad (5.1)$$

$$\kappa_{yy} = -\frac{\partial^2 w}{\partial y^2} \qquad (5.2)$$

$$\rho_{yy} = -2\frac{\partial^2 w}{\partial x \partial y} \qquad (5.3)$$

The constitutive relations now become:

$$m_{xx} = D(\kappa_{xx} + \upsilon\kappa_{yy}) \qquad (5.4)$$

$$m_{yy} = D(\upsilon\kappa_{xx} + \kappa_{yy}) \qquad (5.5)$$

$$m_{xy} = \frac{1}{2}D(1-\upsilon)\rho_{xy} \qquad (5.6)$$

Here, D represents the plate stiffness. Which was derived by integrating the bending moments per unit length.

$$D = \frac{Et^3}{12(1-\upsilon^2)} \qquad (5.7)$$

In this case (thin plates) the rotations are not independent degrees of freedom anymore. They are related to the displacements w. Substitution of the equations for shear force into the equilibrium equations leads to the following equilibrium equation:

$$-\left(\frac{\partial^2 m_{xx}}{\partial x^2} + 2\frac{\partial^2 m_{xy}}{\partial x \partial y} + \frac{\partial^2 m_{yy}}{\partial y^2}\right) = p \qquad (5.8)$$

In Figure 5-1 and Figure 5-2 the equilibrium in the directions w, φ_x and φ_y and the displacements and deformations of an element are considered.

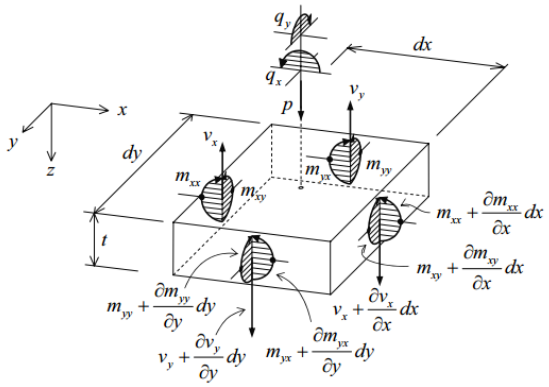

Figure 5-2 - positive loads and stress resultants [44]

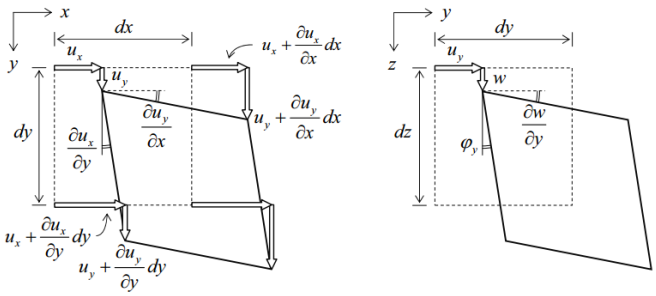

Figure 5-1 - Displacements and deformations of an elementary plate part [44]

For concrete plate elements a positive moment in x direction leads to a positive curvature in x-direction, but also to a negative curvature in y-direction and vice versa. This is the result of transverse contraction. A visualisation is presented in Figure 5-3.

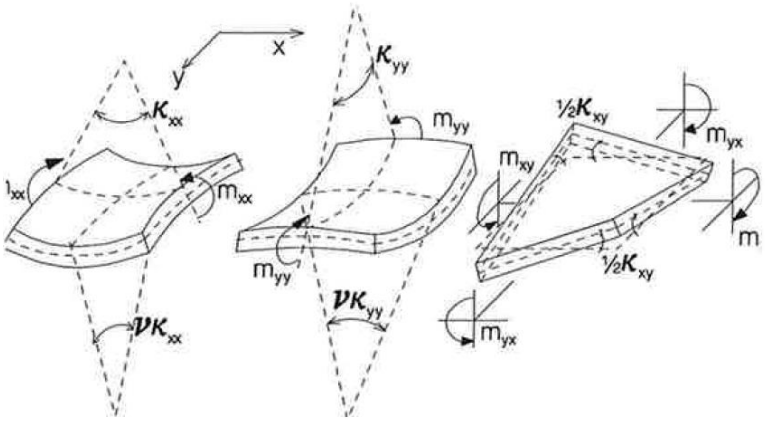

Figure 5-3 - Due to transverse contraction a flexural moment leads to curvature in the transverse direction [44]

In order to specify a certain slab, boundary conditions need to be specified. For a hinged support the earlier stated relations lead to: $w_{xx}+\nu w_{yy}=0$. This kinematic boundary condition leads to the fact that a support reaction occurs. Also, a torsional moment occurs. This has been visualised in Figure 5-4. The shear force due to the torsional moment results in a vertical shear force near the support.

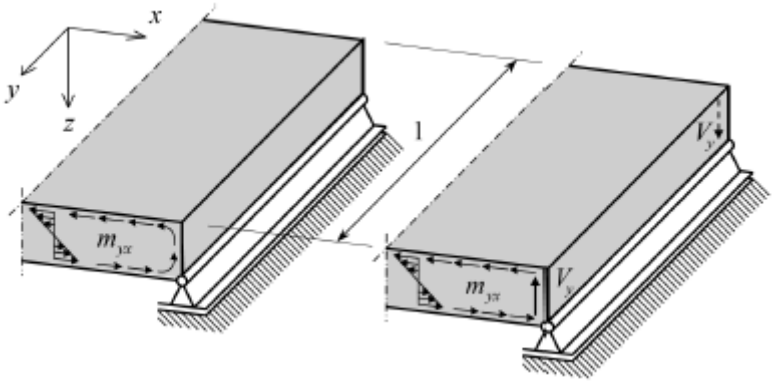

Figure 5-4 - Constant twisting moment at the edge [45]

Due to this phenomena, the resulting shear force due to self-weight near the support is not constant. There is a (small) peak shear forces near the edge of the support. This is only the case for prefab slabs. Slabs cast in-situ distribute their self-weight over the support during casting. This is explained in chapter 3.3.6. Finite element programs are known to have some trouble calculating these torsional moments. Therefore the residual shear forces might be not taken into account correctly. FEM programs can calculate according to 2 different theories: Mindlin and Kirchhoff. In order to know which theory is ideal for this modelling problem, the differences are investigated.

5.2.2 Difference Mindlin and Kirchhoff

In finite element modelling, a plate can be considered as being slender or thick. According to the theory of slender structures, deformation only takes place due to flexural moment. Deformation due to shear force is negligible. Nowadays, a (way more difficult) theory for thick plates is being used in some cases. Here, also deformation due to shear force is taken into account. In practice, FE modelling can be done according to the 'Mindlin' or 'Kirchhoff' theory. The difference is explained with an example provided by [47].

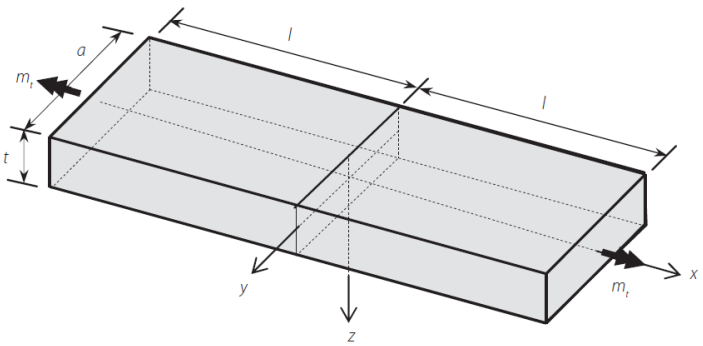

Figure 5-5 - Concrete strip as example [47]

As example a concrete strip is illustrated Figure 5-5. This strip is loaded by a torsional moment in x-direction. According to the theory of elasticity a circulating shear stress occurs. At the edge of the strip, the shear forces are directed vertically. In the middle of the strip, the shear forces are directed horizontally. If the strip is assumed to be a thick plate the horizontal shear stresses can be integrated to torsional moments m_{xy} per unit width and the vertical shear stresses can be integrated to shear forces v_x per unit width. The torsional moments have a constant value in the largest area of the strip. Only near the edge the torsional moment become zero. Vice versa, the shear force is zero at a large part of the strip. Only near the edge it increases to a maximum value. This is visualized in Figure 5-6. With this example the difference between 'Mindlin' and 'Kirchhoff' is explained.

Figure 5-6 - Visualisation of the torsional moment and shear force in a thick strip [47]

In principal, 'Mindlin' can be used for thick plates and 'Kirchhoff' for slender plates. In most FEM programs 'Mindlin' is the default setting. The idea behind this is that if a plate is thick indeed, the shear force deformation is taken into account correctly. If the plate appears to be slender, the calculations are more complicated than necessary, but the result would be more or less the same. But is this true?

'Mindlin' can provide the exact distribution of the torsional moment and shear force. The moment goes to zero at the edge and the shear force increases near the edge. This has been visualized in Figure 5-7. 'Kirchhoff' has a constant torsional moment till the edge. The resulting force V_x over a distance λ is shifted to the edge.

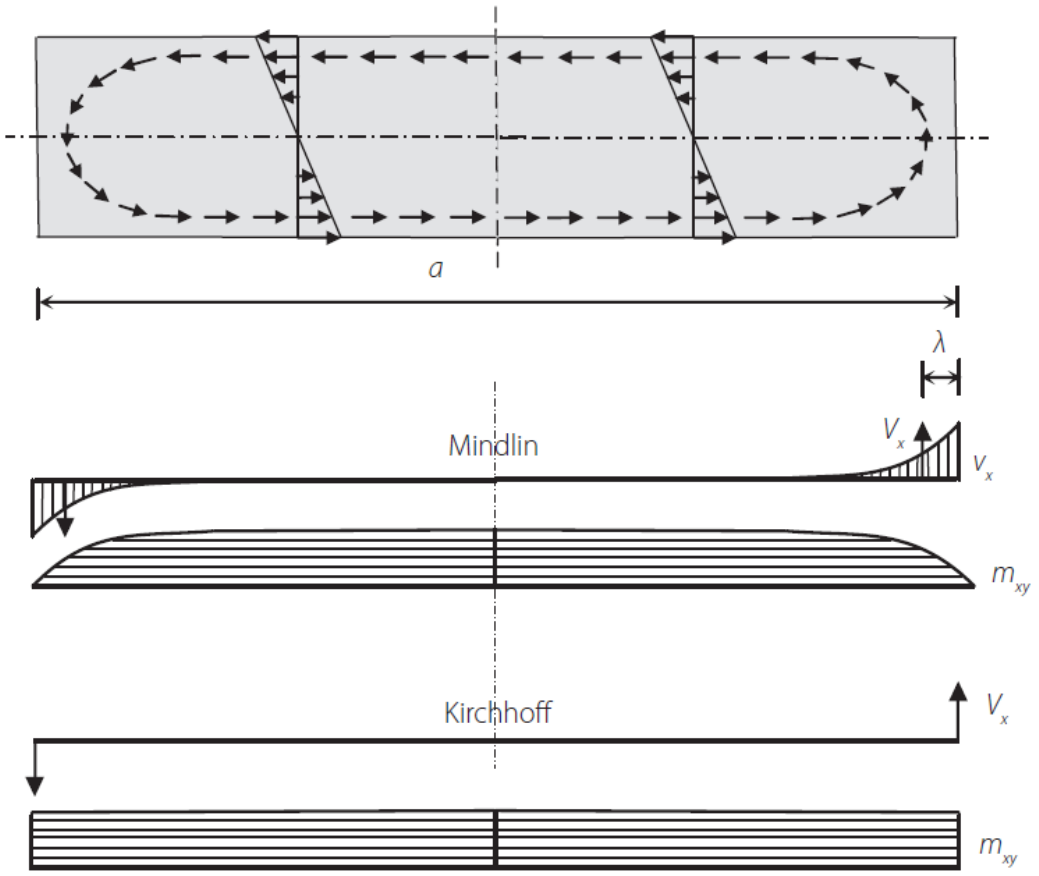

Figure 5-7 - Shear force and torsional moment according to Mindlin and Kirchhoff [47]

If 'Kirchhoff' has been chosen to do the calculations, there is no equilibrium because of the concentrated shear force which has not been taken into account. 'Mindlin' does take into account

the distributed shear force. If only this phenomenon is taken into account the preference would go to 'Mindlin'. However, with 'Mindlin' a problem occurs. 'Mindlin' has trouble describing the force distribution near the edge for a normal mesh size due to the exponential increasing stresses with a high gradient. This means an unpractical small mesh refinement would be necessary near the edge.

Tests have been done with a practical mesh of 10 elements [47]. The results for shear force were disappointing, with a resulting shear force of 73% compared to the exact value. This means a mesh refinement is indeed necessary for 'Mindlin'. [47] provides the advice to commonly use 'Kirchhoff'. This could raise questions, because 'Kirchhoff' is not suitable for thick plates. Now, the definition of 'thick' becomes of interest. As rule of thumb, a plate is considered to be slender if the thickness is smaller than 5 times the width. If a plate has a width which is 8 times the thickness (which seems like a thick plate) the concentrated shear force V_x has a distance λ which is 4% of the total thickness. One could say that in practice a plate is typically slender and shear force deformation can be neglected.

5.2.2.1 Tests Mindlin/Kirchhoff

In order to confirm the differences a comparing case study has been done by SCIA Engineer® [48]. A simply supported slab with dimensions of 8x8m has been subjected to a uniform distributed load. A thin (200mm) and a relatively thick (2250mm) plate are investigated. The mesh is 0,5m, but on the edges a denser mesh has been inserted. The results for the maximum shear forces on the edge can be found in Figure 5-8 and Figure 5-9.

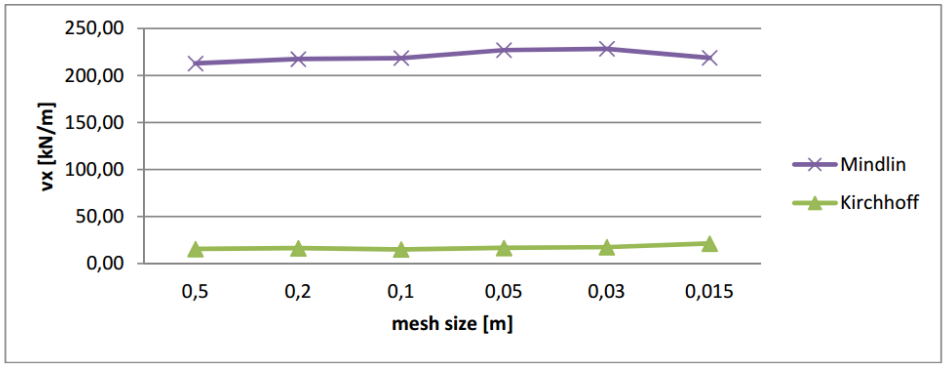

Figure 5-8 – Maximum shear force on the edge of a thin (200mm) plate for 'Mindlin' and 'Kirchhoff' [48]

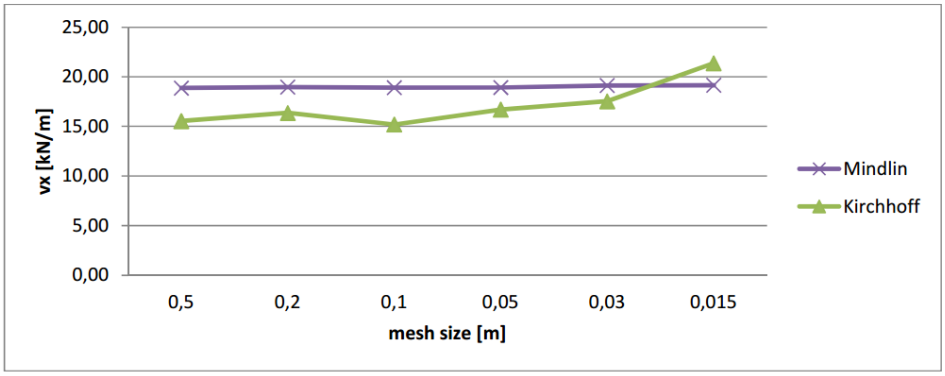

Figure 5-9 - Maximum shear force on the edge of a thick (2250mm) plate for 'Mindlin' and 'Kirchhoff' [48]

When looking at V_x for the thin plate, the small values for V_x at Kirchhoff's calculation can clearly be seen, even with a small number of elements. The Mindlin theory provides too high values for shear force near the edge. The conclusion is that 'Kirchhoff' is a better option for thin plates. When investigating the thick plate, it is clear that V_x remains very small for 'Kirchhoff', and also 'Mindlin' provides acceptable results for V_x. For each mesh size. So, for thick plates, calculating with

'Mindlin' results the best output [48]. Most finite element programs use 'Mindlin' as standard for finite element calculations [49].

One has to be aware of the thickness that has been chosen for the 'thick' plate. 2250mm as thickness for a slab bridge is not realistic and do not exist. In order to confirm the theory assuming that 'Kirchhoff' can be used in every case can be confirmed by some tests with the finite element program RFEM. For these tests different parameters are varied. The span and width are constant parameters, namely 20, and 12 m respectively. The thickness and support stiffness are variable parameters. A mesh size of 500mm has been chosen, and the mesh refinement for 'Mindlin' calculations is chosen as 1mm. The results can be found in Appendix Table 5-1. According to these results, the expectations are confirmed. For slender plates, the peak forces become unrealistically high. For the Kirchhoff calculation the peak force at the edge is missing. This is because Kirchhoff does not take into account the shear force due to torsion.

In this thesis 'Kirchhoff' is used. 'Mindlin' generates peak shear forces which are unrealistic. Also, Mindlin need a fine mesh, which leads to long calculation times. The additional shear force near the edge of the support which is not taken into account by Kirchhoff an additional calculation is made. However, the exact value does not matter that much because an average over 4*d is used. The total shear force near at the edge of the support according to [45] and [44] becomes:

$$V_{tot} = V_x + m_{xy} \qquad (5.9)$$

If the whole support is considered with a distance y, the vertical equilibrium of the considered plate part yields:

$$f = v_x + \frac{\partial m_{xy}}{\partial y} \qquad (5.10)$$

5.2.3 Tests cracked/ uncracked concrete

Over the past decades, a multitude of analytical methods have been developed. In most of these methods an average stresses and strains are used. The use of average stress-strain relations is a major simplification, as reality cracked concrete transmits stresses in a complex manner of opening and closing of existing cracks, forming new cracks, aggregate interlocking and variation of the bond stresses [33].

In existing concrete bridges, mostly cracks are present. Concrete cracks if too much tensional force or flexural moment is applied for the concrete to take up. When reinforced concrete is cracked, the reinforcement is 'activated' and takes up the tension or flexural forces. In general, an existing concrete bridge can only be assumed to be cracked if actual cracks are established. Due to cracks, the stiffness (longitudinal and/or transverse) of the slab changes. As rule of thumb for cracked slabs, a transverse stiffness of 1/3 times the longitudinal stiffness can be assumed. This comes from the amount of practical transverse reinforced that has been applied (around 20% compared to the longitudinal reinforcement). Experiments demonstrate that the existence of a crack in the shear plane reduces the ultimate shear strength [33]. The effect of predamaging was investigated. Results are demonstrated in Table 5-1. Loading near the edge (E) and near the middle (M) was investigated. Results show that a reduction of 26% can be reached for cracked slabs compared to uncracked slabs. One has to be aware that these tests were done with locally failed slabs, which indicates huge cracks. In practice, locally failed bridged will be closed down. Cracked slabs should be considered carefully, but do not have to be regarded as failed locally. The calculation with a reduced transverse stiffness is sufficient. This is described in chapter 5.2.3 and 7.3.

Table 5-1 - Comparison of shear capacity between un-damaged specimen (V_{uncr}) and locally failed specimen (V_c) [33]

Slab	ρ_t (%)	M/E	V_c/V_{uncr}
S3	0,182	M	80%
S4	0,258	E	
S5	0,258	M	95%
S6	0,258	E	
S7	0,258	E	77%
S8	0,258	M	
S9	0,258	M	81%
S10	0,258	E	
S11	0,258	M	80%
S12	0,258	E	
S13	0,258	M	90%
S14	0,258	E	
S15	0,258	M	75%
S16	0,258	E	
S17	0,258	M	74%
S18	0,258	E	

Prestressed slabs are generally not cracks due to the prestressing forces. The transverse stiffness of prestressed slabs is not commonly clear and

depends on the type of prestressing and the prestressing stress. As rule of thumb sometimes a transverse stiffness of ½ times the longitudinal stiffness is assumed for cracked slabs. Prestressed slab are however not used in these tests.

The transverse stiffness relative to the longitudinal stiffness plays a significant role in the force transfer to the support. Therefore some FEM tests have been done of slabs with different transverse stiffness's to indicate the force transmission. The tests have been done for a relatively large span (19m) and large edge widths (4m and 6m). The stiffness for uncracked concrete is assumed to be 33 GPa in both longitudinal and transverse direction. For cracked concrete the transverse stiffness is assumed to be 11 GPa, which corresponds to a transverse poisson's ratio of v_{yx} = 0,067. The tests have been done for axles loads of LM1 only (no self-weight).

The results can be found in *Appendix F – Tests cracked/uncracked slabs.* The results illustrate the shear force in x direction (V_x). Also the shear force at the support is illustrated below the figure. A different angle of force transfer can clearly be distinguished (red dotted line). Also, the shear force is higher near the middle of the support for a reduced transverse stiffness. This makes sense since forces are transferred to a smaller part of the support, so the shear force per m' is higher. Since the differences due to a variation is transverse stiffness is significant, it is desired to differentiate between cracked and uncracked slabs. This affects the results of the critical edge width calculations. The results for the shear force of cracked and uncracked slabs can be found in chapter 7.3.

Parameters that influence the force transmission to the support are:

- Execution type (prefab or in-situ)
- Size of the wheel print
- Thickness and thickness variation of the slab
- (Spring) stiffness of the support
- The presence of cracks in the concrete, which affects the transverse or longitudinal stiffness
- Width of the slab
- The stiffness of the slab
- Transverse force distribution (Poisson ratio)
- Type of concrete (aggregate interlocking)

5.3 Parameters Finite Element model

As finite element program Dlubal RFEM was used. RFEM has several options which are useful for making many different bridge configurations. Parametric modelling is one of the options. Different variables, such as length and width can easily be adapted by creating them as variable parameters. Also, node locations and load magnitudes can be variable parameters. In this way, testing different configurations costs relatively little time.

RFEM has different modules for specific cases. One of these modules is RF-MOVE-surface. This module generates moving loads on surfaces. In this way, RFEM searches the governing load case. All different load models from the Eurocode are programmed in RFEM. So, the different load models do not have to be created seperately. Load models which are not in the Eurocode, such as Load Class 45, Load Class 60 or the asphalt lorry (Chapter 5.4.4) have to be programmed.

Different parameters in the FE model should be chosen consequently for every load model. The variables are:

- The span (L);
- The edge distance (b_{edge}), which determines the total width;
- The thickness (h);
- The type of load model;
- The place of the load model on the bridge (edge or middle support governing);
- The spring stiffness of the support (C);

- The transverse stiffness (E).

For the span values from 5 to 19m with an interval of 2m is chosen. For the edge distance values from 0m to 6m with an interval of 1m is chosen. In every case 2 driving lanes are considered. The total width becomes the width of 2 lanes plus two times the edge distance.

The thickness is determined as a function of the span. The rule of thumb is:

$$h = L/20 \qquad \textbf{(5.11)}$$

Where:

h = thickness of the slab (m)
L = the span (m)

The rule of thumb provides the values for the height as demonstrated in Table 5-2. As lower bound value a thickness of 400mm has been chosen because traffic bridges with less thickness barely exist.

Table 5-2 - Height of the concrete slab for different spans

Span (m)	5	6	7	8	9	10	11	12	13	14	15	16	17	18	19	20
Height (m)	0,40	0,40	0,40	0,40	0,45	0,50	0,55	0,60	0,65	0,70	0,75	0,80	0,85	0,90	0,95	1,00

The spring stiffness of the support is also determined as a function of the span. In order to simulate a support stiffness that is representative for a real support, a rule of thumb is used: Due to the permanent loads on the bridge (self-weight and asphalt layer), the support displaces 1mm vertically. With this rule of thumb, the spring stiffness can be determined.

$$C = \left((\rho_c * h) + (\rho_a * t)\right) \frac{L}{2} \qquad \textbf{(5.12)}$$

Where:

ρ_c = Density of the concrete (25 kN/m^3)
ρ_a = Density of the asphalt (20 kN/m^3)
t = thickness of the asphalt layer (m)
C = the support stiffness (kN/m^2)

Table 5-3 - Support stiffness for different spans

Span (m)	5	6	7	8	9	10	11	12	13	14	15	16	17	18	19	20
Support stiffness (N/mm^2)	18	25	34	45	57	70	85	101	118	137	158	179	202	227	253	280

The support stiffness is depending on the thickness and the slab. Since the thickness is also depending on the span, the support stiffness increases quadratically with an increasing span. To make sure the support stiffness has been chosen in the right way, the deflection under self-weight only has been determined by RFEM. *Appendix G – Deflection due to self-weight* illustrates the deflection for different spans.

Different load models are compared. The governing place for maximum shear force and flexural moment of the load models are investigated. The different load models are elaborated in the following chapter.

5.4 Load models

Load Model 1 from the Eurocode are compared with various other load models to determine the adjustment factor α (Chapter 6). This is done because Load Model 1 with an α factor of 1,0 might be too conservative for existing municipal bridges. The maximum shear force and flexural moment due to Load Model 1 are compared with other models. If the occurring flexural moment or shear force due to Load Model 1 is higher than a load model that approaches reality in a better way, a certain α factor can be used. The α factor is chosen in such a way that the effects of load model

1 are the same as the effects of another load model. This leads to less conservative recalculations of existing bridges.

Load models that are investigated are:
- Load classes 60 and 45 from NEN 6723, annex A (Dutch standard before the Eurocode);
- The fatigue load models from NEN 1991-2 [2], table 4.6 and the National Annex, adapted to ULS load models;
- Heavy real lorry with small axle distances (which is an extended version of the second fatigue lorry as described in Table 5-4).

Comparing these different load models is not as easy as it seems, because there has to be dealt with different load factors, impact factors, dynamic factors and other reduction- or safety factors. These factors have to be chosen carefully in order to compare the different load models in a right and legitimate way. The load models are compared by using the reliability index β. First, the different load models are described, then the assumptions for the right comparison of the load models are described.

5.4.1 Load Model 1

Load Model 1 does not represent a real vehicle. The Load Model is intended to produce global as well as local effects caused by different types of vehicles. For bridges with a large span, this simplification is representative for the real occurring loads due to traffic. For smaller spans, smaller than 20m, it is questionable if this Load Model is representative.

As described in chapter 4.2, Load model 1 consist of:
- Double-axle concentrated loads (tandem system);
  - No more than one tandem system should be taken into account per notional lane;
  - Each axle of the tandem system be taken into account with two identical wheels, the load per wheel is equal to $0{,}5 * \alpha_Q * Q_k$;
  - The contact area of the wheels on the asphalt layer is 400mm x 400m.
- Uniformly distributed loads (UDL system), with higher loads on lane 1.

Load model 1 should be applied on each notional lane and on the remaining areas. On notional lane Number *i*, the load magnitudes are referred as $\alpha_{Qi}Q_{qi}$ and $\alpha_{qi}q_{ik}$. On the remaining areas, the load magnitude is referred to as $\alpha_{gr}q_{rk}$. Characteristic loads have a 1000 years return period [8].

A handbook for is design of bridges has been made in which the basis of bridge design related to the Eurocodes is described [8]. This handbook presents more insight in the used load models from the Eurocode. The static load models of EN 1991-2 have been developed so that the static load models satisfy the following criteria:

- Should be easy to use;
- Should be applicable independently in the static scheme and on the span length of the bridge;
- Should be able to reproduce the target values, covering all possible traffic scenarios;
- Should be able to easily combine local and global effects of actions;

The first phase of developing the Eurocode was a study of the European traffic data. Generally, the analysis of the European traffic data reveals that the mean values of axle-loads and total weight of heavy vehicles are strongly dependent on the traffic typology. They are generally very scattered. The loads from Load Model 1 include a certain dynamic amplification factor. Measurements from flowing traffic already contain some dynamic effects. For the ultimate limit states, the inherent amplification factor is 1,1 [50].

5.4.2 Load classes 60 and 45

Load class 60 was used for the Dutch highways, and load class 45 (or sometimes 30) was used for most municipal bridges. This is described in NEN 6723 [51]. After 2012 these load classes

were no longer used for the design of bridges. Since then, the Eurocode is being used. However, most existing municipal bridges are designed with these load classes. A re-calculation of these bridges with these load classes would not be desired, since the traffic loads nowadays are higher than during the building period and then the standards have been changed. Nevertheless, it is interesting to compare Load Model 1 with the load models the bridge were designed to originally.

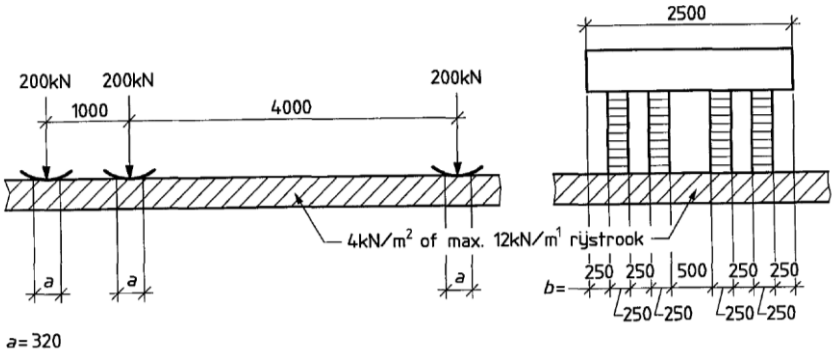

Figure 5-10 - Axle configuration of load class 60 [51]

The axle configuration and loads of load class 60 is illustrated in Figure 5-10. These loads are the characteristic values. The design values of the loads have to be compared. This means that the characteristic values have to be multiplied by an impact factor (S), load reduction factor (B) and load factors (γ_i).

$$S = 1 + \frac{40}{100+L}; \qquad \textit{(5.13)}$$

$$B = 0{,}6 + \frac{40}{100+L} \qquad \textit{(5.14)}$$

Where :

L = the span (m)

In former codes only an impact factor has to be applied. According to the GBV 1962 this factor is:

$$S = 1 + \frac{3}{10*L} \qquad \textit{(5.15)}$$

The load factor for permanent and variable load is harder to determine because there are different factors in different former codes. Load factors presented in NEN 6723:1995 [51] are assumed. This standard refers to the load factors from NEN 6702:1991 [52]. Safety class 2 is assumed, and the corresponding load factors are γ_G = 1,5 and γ_Q = 1,5.

The combination of these load factors provides rather high loads. NEN 6723:1995 [51] demonstrates an additional rule for 2 or more loaded lanes. It states: 'If more than one lane can be loaded by traffic, only 2 traffic lanes have to loaded by the governing vehicle together with the uniform distributed load. In this case, the total load combination can be reduced by a factor of 0,8 [51]. This means that 2 different load cases have to be considered: one fully loaded lane and two fully loaded lanes with a reduction of 0,8. It turned out that for shear force, one fully loaded lane was governing in most cases. For flexural moment, 2 lanes loaded with a factor of 0,8 was governing in most cases.

In former codes, only standards for new built bridges exist. There are no additional rules for the assessment of existing bridges. This means that LC60 and LC45 can only be compared to the recent Eurocode loads of new bridges. The comparison with LC45 and LC60 with LM1 for existing bridges (with reduced partial factors) has no meaning. Therefore only the comparison with LM1 for new bridges is made. Load Model 1 from the Eurocode is made by calibrating on loads on highways. These highways are typically made with Consequence Class 3. Therefore it is interesting to compare these loads with LC60 and try to explain the differences. Since municipal bridges were mostly designed with LC45, it is interesting to compare LC45 with Consequence

Class 2 from the Eurocode. Municipal bridges nowadays are mostly designed with Consequence Class 2.

5.4.3 Fatigue load models

In order to take into account the spans smaller than 20m, a model which represents a real lorry in a better way is required. The fatigue load models as described in the National Annex of the Eurocode [2] are axle configurations of real occurring lorries. These lorries are illustrated in Table 5-4.

Table 5-4 - Fatigue load model 4b: "frequent" lorries [2]

Type voertuig			Verkeerstype			
Afbeelding van de vrachtwagen	Afstand tussen de assen m	Gelijkwaardige aslast kN	Lange afstand (%) [a]	Middellange afstand (%) [a]	Lokaal verkeer (%) [a]	Wiel-type
	4,5	70 130	20,0	50,0	80,0	A B
	1,50 2,40 1,30	70 120 120 120	7,0	4,0	4,0	A C B B
	3,20 5,20 1,30 1,30	70 130 100 100 90	37,0	20,0	5,0	A B C C C
	3,40 6,00 1,80	70 140 90 90	20,0	12,0	4,0	A B C C
	4,80 3,60 4,40 1,30	70 150 80 80 70	10,0	10,0	5,0	A B C C C
	3,20 1,30 4,40 1,80 1,80	80 160 100 100 100 100	4,5	3,0	1,5	A B C C C C
	3,20 1,40 4,40 1,30 1,30 1,30	70 180 170 80 80 80 90	1,5	1,0	0,5	A B B C C C C

[a] Percentage vrachtwagens.

Although the bridge are not checked on fatigue resistance, these load models can be adapted and used for ULS checks. Axle loads and axle distances are realistic compared to real heavy traffic.

Some insight in the calibration methods of these fatigue lorries is presented. The calibration method of these models has been set-up according to the following scheme [8]:

- Choice of the most significant European traffic data;
- Selection of appropriate S-N curves;
- Evaluation of the stress histories in reference bridges;
- Cycle counting and stress spectra computation;
- First identification of fatigue models;

- Definition of standardised lorry geometries;
- Calibration of frequent load models, best fitting the maximum stress range $\Delta\sigma_{max}$ and the fatigue damage D induced by the real traffic.

The fatigue load model 4b has been created by looking at the comparison with reference traffic results. Essentially, the comparison concerns influence surfaces for a simply supported slab(M_0) for bending moment. Also, bending moments M_1 and M_2 at mid-span and on the support, respectively, of two span continuous slabs and bending moment M_3 of three span continuous slabs have been compared. This has led to the graph in Figure 5-11, where $\Delta M_{eq,LM4}$ is the equivalent stress range due to fatigue load model 4 and $\Delta M_{eq,real}$ is the equivalent stress range due to Auxerre traffic (which was chosen to be a representative for all traffic in Europe).

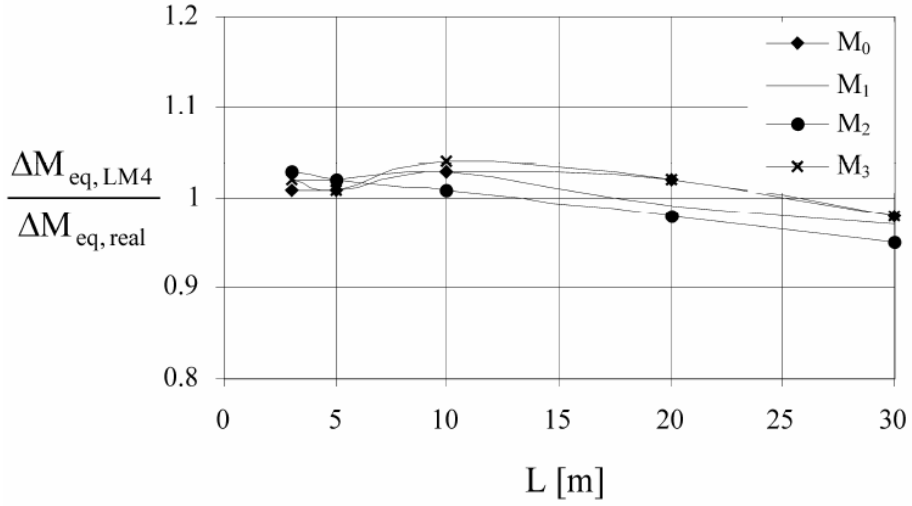

Figure 5-11 - Accuracy of fatigue load model 4 [8]

This figure illustrates that the fatigue load model is rather accurate. This is as expected because this load model is calibrated on real traffic. Other (more simplified) fatigue load models from the Eurocode are less accurate. Fatigue load model 1 for example is too conservative for small spans, with a factor up to 1,5 [8].

To compare these fatigue load models to Load Model 1 certain uniform distributed loads have to applied. The choice has been made to use the same uniform distributed load as used in load class 60. This is 4 kN/m^2 for the entire surface of the bridge. Load model 1 has 9 kN/m^2 for lane 1 and 2,5 kN/m^2 for the remaining area. For a small edge distance load model 1 provides higher stresses and for larger edge distances the other load models provide higher stresses. These differences are not decisive.

5.4.3.1 Dynamics in bridge assessment

First of all dynamic effects are not taken into account in the fatigue load models. NEN-EN-1991-2 presents a factor for dynamic effects. This factor depends on the distance from the expansion joint and can be determined from Figure 5-12.

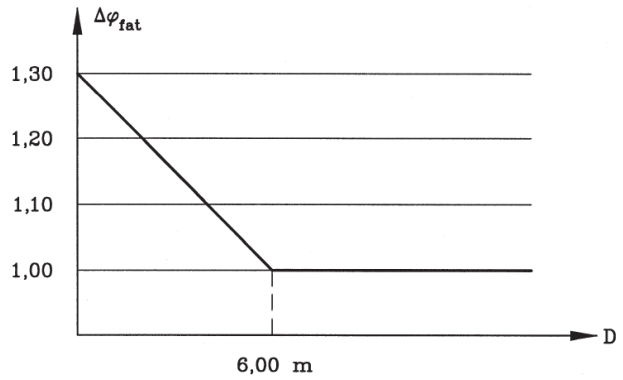

Figure 5-12 - The dynamic factor for the distance D from the expansion joint [2]

For the determination of the shear stresses the axles are not placed very close to the support, because not all forces would be transferred via shear force in that case. If the first axle has a minimum distance of 2,5*d there can be assumed that the forces are transferred via shear force only. The minimum span of a considered bridge is 5m. For this span a minimum thickness of 0,4m is assumed. This leads to a distance of 1m from the expansion joint. Looking at Figure 5-12 this distance D leads to a dynamic factor of $\Delta\varphi_{fat} = 1{,}25$ (also called impact factor). Although this factor is meant for fatigue checks, it can be used to transfer the fatigue lorry model into models for strength (ULS). For the sake of completeness and ease, this factor can be assumed for the whole length of the bridge, independent to the distance from the expansion joint. This is also stated in the National Annex of NEN-EN 1991-2 [2]. If the asphalt quality is assumed to be acceptable, a factor of 1,15 can be assumed. This is not applicable for this comparison, because the asphalt quality is unknown. The National Annex also provides a reduction factor (α_{fat}) if the bridge complies with certain requirements. Also this is not applicable for the comparison of the load models since some requirements are not certain to be met (for example a maximum speed of 50 km/h).

In addition to the Eurocode, the TNO report about traffic loads on highways [28] provides some recommendations about factors to take into account dynamic effects. To take in to account the effects of dynamics, a distinction has to be made between dynamics of the bridge and dynamics of the loads (the vehicles on the bridge). The dynamic movements of the vehicles are cause by roughness of the road and interruptions of the road by for example expansion joints. In TNO report 98-CON-R1813 a dynamic factor of 1,2 has been used. This value was determined by simulations. In [28] this factor has been criticized and looked if this factor is too conservative. Important parameters for the determination of this factor are:

- The model of the bridge
- The model of the vehicle
- The roughness of the road

TNO has done measurements to determine the dynamic factor. Most important conclusions were [28]:

- Most important parameter is the roughness of the road;
- The higher the static loads, the lower the dynamic factor;
- In the European project ARCHES a factor of 1,05 has been found with a return period of 1000 years;
- With a simulation of random traffic and random road roughness a factor of 1,1 has been found;
- All researches about this subject state that the standards are too conservative.

Based on literature a dynamic amplification factor (DAF) of 1,1 seems reasonable to take into account global resonance effects of the bridge. Background files of the Eurocode state that this factor for dynamics already has been integrated in the load models. In WIM measurements,

vehicle dynamics are already included in the measured values. For global dynamics of the bridge a factor of 1,1 was recommended. Table 5-5 provides an overview for values for the model uncertainties of the TNO work compared with the current work.

Table 5-5 - Model uncertainties

	Mean	CoV	Source	remark
DAF vehicle	1	0	[26]	
DAF bridge	1,1	0,05	[26]	
Statistical uncertainty	1	0,05	assumption	
Spatial spread (typical location in NL less loaded than the location of the measurement	0,86	0,07	[28]	Not necessary, because location-specific loading is taken
Load effect	1	0,1	[26]	

Spatial spread does not have to be taken into account since location specific loading is taken. Also, the location of the measurements (Rotterdam) is assumed to be governing for every municipality as described in 3.6.4.4. Therefore the obtained data can be assumed the be the upper boundary values.

5.4.3.2 Fatigue load models to strength load models

Using the axle loads and configurations as described in Table 5-4 for strength assessment needs sufficient substantiation. Therefore the goal of extra load models needs to be established again. For small span bridges (<20m) Load Model 1 may be too conservative. The two axles of 300kN at a distance of 1,2m represent a fully loaded bridge, and therefore very long and heavy lorries. For small spans bridges it can be beneficial to model a more realistic lorry. This is because the axle configuration does matter substantially more for smaller spans. Loads from Load Model 1 typically do not occur in a lifetime of a municipal bridge. With the use of new load models a more realistic situation can be modelled, which leads to less conservative calculations. In this way unnecessary improvements or repair can be prevented, which saves much money.

The load models from the fatigue lorries have been chosen because they represent the lorries which occur the most in a real situation. However, the loads are designed for fatigue calculations. This would imply that these are not the maximum loads. With making use of the measurements in Rotterdam [26] the loads from the fatigue models are calibrated.

In 3.6.6.1 a calculation for the maximum occurring axle load has been made. This is 205 kN with a return period of 1000 years. This chapter also states that there are not enough data available to draw conclusions about the correlation between axle loads and axle distances. It is likely to assume that high axle loads come from long lorries with a large gross vehicle weight. This is also the case for the fatigue lorry load models. The longest load model has the greatest axle loads (170kN and 180kN respectively), with a distance of 12,9m from the first to the last axle.

The axle loads as measured in the WIM measurement are real occurring loads. These maximum loads already include a dynamic effect. This principle is explained by Figure 5-13. The measured maximum axle values are likely to be caused by a dynamic peak and therefore already include a dynamic factor. Only the dynamic factor for dynamics of the bridge has to be taken into account additionally. This is 1,1 according to Table 5-5. The maximum axle load according to the WIM measurements is therefore 205*1,1 = 225 kN.

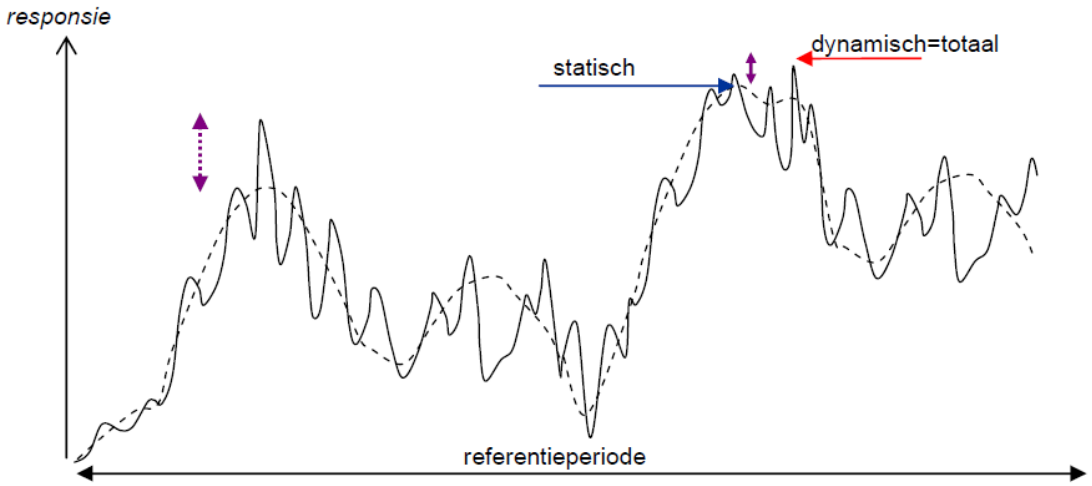

Figure 5-13 - Definition dynamic amplification factor. Dashed line: static response. solid line: dynamic response [28]

The following proposition has been made. The fatigue lorry models can be compared to the governing axle loads from WIM measurements if the dynamic factor of $\Delta\varphi_{fat} = 1{,}25$ (Also called impact factor) has been taken into account for every axle load. This would mean that the maximum occurring loads from the fatigue load models become $180{*}1{,}25 = 225\text{kN}$ and $170{*}1{,}25 = 212{,}5\text{kN}$. This is the same as the assumed maximum axle load according to the WIM measurements (with the dynamic bridge factor included).

The gross vehicle weight of the largest fatigue lorry of Table 5-4 (lorry 7) becomes $(70{+}180{+}170{+}80{+}80{+}90){*}1{,}25 = 937{,}5\text{kN}$. According to the measurements, the maximum gross vehicle weight (measured in 2 months of measuring) was 780 kN according to Figure 3-15. The exceedance frequency was $4{*}10^{-5}$. If the trend would be expanded to $5{*}10^{-9}$ (which is assumed to be the exceedance frequency for a reference period of 15 years) a value of 937,5 kN seems reasonable.

The fatigue lorries (with a dynamic factor of 1,25) are used to compare with Load Model 1.

5.4.4 Existing heavy lorry (Asphalt lorry)

Next to the fatigue load models, also a search for the most governing vehicle for small span bridges has been performed. This would be a lorry with high axle loads and small axle distances. This tuned out to be the GINAF X6 5249 CE. A lorry normally used for asphalt transport. Due to the combination of high axle loads and a relatively small length, it provides a high flexural moment and shear stress. This governing lorry has 5 axles with axle distances of 2,05m, 1,85m, 1,80m and 1,40m and characteristic axle loads of 2 times 100kN and 3 times 120 kN respectively. With the dynamic factor included the maximum axle load is 120 * 1,25 = 150kN. A picture together with the simplified schematization is illustrated in Figure 5-14.

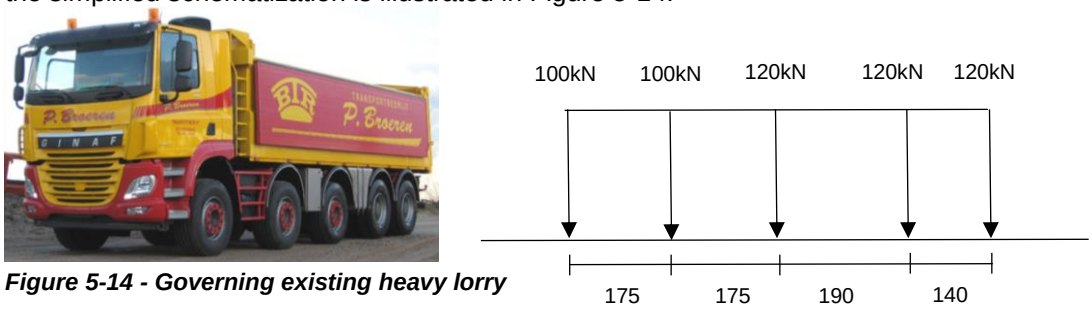

Figure 5-14 - Governing existing heavy lorry

As illustrated in Table 5-4, this lorry is similar to the 2nd fatigue lorry. The following proposition has been made: Adapt the 2nd lorry from Table 5-4 to a slightly larger vehicle with 5 axles as illustrated in Figure 5-14. This was done because this 5-axle vehicle generates higher shear forces and flexural moments than the 2nd Fatigue Lorry and is therefore governing. A uniform distributed load

is applied to take into account additional load from other vehicles or additional loads on the bridge. Since no rules are provided for the magnitude of this load, a rather conservative value is chosen. This value is the same as for Load Class 60 (4 kN/m^2), as for the other fatigue lorries.

In order to take into account dynamic loads, a factor of 1,25 is applied as demonstrated in 5.4.3.2. Now, an assumption is made for the second lane. It would be way too conservative to assume the same governing asphalt lorry on lane 1 and lane 2. As for the fatigue load models, there is assumed that fatigue load model 1 (normal lorry) occurs simultaneously with the asphalt lorry.

5.4.4.1 Location specific load models

There can be some exceptions for certain locations of a municipal bridge. If the location of the bridge indicates more chance of heavier traffic, 2 fully loaded lanes can be assumed. The probability of occurrence of the governing load model becomes significantly higher. Some examples of locations where heavier loading is likely are bridges near:

- A concrete or asphalt factory;
- A building site, where heavy cranes can occur on the bridge;
- A loading wharf of a harbour.

In these cases the axles loads of two asphalt lorries on two lanes can be assumed. The occurring flexural moment and shear force can be found in *Appendix I – FEM results: calculation of the α factor.*

5.5 Conclusion

In this chapter different issues for the FE model and the applicable load models were described. These load models are compared to provide more insight in the differences, and to conclude if Load Model 1 is too conservative for small span existing municipal bridges. This comparison is described in chapter 6 after which the α factor can be chosen for different bridge dimensions. A legitimate and valid comparison between the different load models is challenging (especially for the comparison of maximum shear force). The regarded load models differ for example in partial factors, axle configuration, axle loads and dynamics. Table 5-6 presents an overview of the different load models with associated parameters and factors. These factors and parameters are used in the FE model to compare the different load models in the right way.

Table 5-6 - Parameters and factors for different load models

Load model	LM1 new bridges	LM1 existing bridges	Load class 45	Load class 60	Fatigue lorries (and asphalt lorry)
Associated standard	Eurocode	Eurocode	NEN 6723-1995	NEN 6723-1995	Eurocode
Axles per lane	2	2	3	3	2-7
Load per axle (kN)	300	300	150	200	80-180
UDL lane 1 (kN/m^2)	9	9	3	4	4
UDL other (kN/m^2)	2,5	2,5	3	4	4
Impact coefficient (S)	1	1	1,33-1,38	1,33-1,38	1
Load coefficient (B)	1	1	0,93-0,98	0,93-0,98	1
Reduction if 2 lanes are fully loaded	no	no	0,8	0,8	no
Lane 2	2/3 of lane 1	2/3 of lane 1	As lane 1	As lane 1	Frequently occurring ‘normal’ lorry
Dynamic factor	1	1	1	1	1,25
Load factor permanent load (γ_G)	1,2 (CC2) 1,25 (CC3)	1,1	1,5	1,5	1,1
Load factor variable load (γ_Q)	1,35 (CC2) 1,5 (CC3)	1,2	1,5	1,5	1,2
Abbreviation	LM1	LM1	LC45	LC60	FL & AL

5.5.1 Summary

A summary of the assumptions, parameters and factors for the FE model is made:

- Consequence Class 2 (CC2) (chapter 3.6.4.4);
- The minimum reference period is 15 years (chapter 3.6)
- The obtained reliability index is β = 3,3 for structures that have been built after the 'Bouwbesluit 2003' and β = 3,1 for structures that have been built before the 'Bouwbesluit 2003', which is the 'repair' level. For the FEM research β = 3,1 is assumed (chapter 3.6.4.4);
- Taking into account these assumptions and according to the WIM measurements in Rotterdam, the exceedance probability is $5 * 10^{-9}$ (chapter 3.6.6.1);
- If this is compared to the measurements in Rotterdam the maximum axle load is 225 kN and the maximum gross vehicle weight is about 900 kN. The maximum axle load is assumed to be an axle from a large lorry with many axles (chapter 3.6.6.1);
- The partial factor for self-weight for β = 3,1 is 1,1. The partial factor for variable loads is 1,2 (chapter 3.6.7);
- According to literature, the α factor for existing municipal bridges is $\psi_t * \alpha_{trend} * \psi = 0,98 * 0,969 * 0,97 = 0,92$ (chapter 3.6.4.2)
- Fatigue lorries second lane: A normal lorry is used (As Fatigue Lorry 1) (Chapter 5.4.4)
- The comparison from LM 1 with Load class 45 and 60 is meant for comparing the results of current and former codes. The comparison from LM1 with the fatigue lorries and asphalt lorry as meant for comparing the results of the current code and real existing traffic.
- For the comparison with LC45 and LC60 partial factors for new bridges are used (CC2 and CC3) and for the comparison with the fatigue lorries the partial factors for existing bridges are used (3.6.7)
- The governing load model in order to determine the alpha factor is described in chapter 6.

Section 2 –
FEM research existing concrete slab bridges

6 The adjustment factor α

Load Model 1 is intended to cover flowing, congested or traffic jam situations with a high percentage of heavy lorries. In general, when used with the basic values, it covers the effects of a special vehicle of 600kN as defined in annex A [2]. For municipal bridges this might be too conservative since these kinds of vehicles might not appear on most of these municipal bridges. The values used in Load Model 1 are mainly based on real traffic loads measured in a number of different countries. It was found that the traffic parameters from the different countries were not very different, especially when comparing the maximum daily values of axle and vehicle weights. However, rather than base a traffic load model on a mix of all the traffic data, it was decided to use one set of data recorded on the A6 motorway in France, a 2-lane dual carriageway near the city of Auxerre. Because of the number of international vehicles using the A6, it was felt that the traffic data would provide an adequate representation of European traffic as a whole [53].

Further studies on loaded lengths less than 5m led to the discovery of the need to increase the intensity of the associated distributed load. It is stated that: “The basic values of the concentrated and distributed loads may be modified by adjustment factors which allow loading to be adopted in specific situations. These could be applied, for instance, for a particular class of road where the volume and mix of traffic is significantly different from that used in deriving the load models” [53]. Municipal bridges mostly have significantly less heavy weight traffic. This means that adjustment factors can be applied.

In practice, the governing loads for new bridges are discussed with the client. For existing bridges there is no standard adjustment factor available. Eurocode 1 states: “The values of adjustment factors α_{Qi}, α_{qi}, and α_{qr} should be selected depending on the expected traffic and possibly on different classes of routes. In the absence of specification these factors be taken to unity” [2]. The following minimum values are recommended:

$\alpha_{Q1} \geq 0{,}8$ and

For: $i \geq 2$, $\alpha_{q1} \geq 1$

Eurocode 1 states: “ Values of α factors may correspond to classes of traffic. When they are taken equal to 1, they correspond to a traffic for which a heavy industrial international traffic is expected, representing a large part of the total traffic of heavy vehicles. For more common traffic compositions, such as highways or motorways, a moderate reduction of α factors applied to tandems systems and the uniformly distributed loads on Lane 1 may be applied (10 to 20%)” [2]. As stated before, municipal bridges in general are not exposed much to very heavy traffic loads. Since LM1 with a α factor of 1 stand for a high percentage of heavy lorries, there can be assumed that a reduction of the loads can be applied for municipal bridges. The question is what the exact value of α is. There are some papers and articles available that say something about the magnitude of this value [53], [54]. This varies between 0,51 and 0,87 for spans from 6 to 18m. However, various studies come with very different results. Based on these studies, no solid conclusions can be made.

A study to the traffic loads on highway bridges reveals that the actual traffic load is up to 50% less than those in standards. It is found that the adjustment factor α is largely dependent on both the bridge span and width of the roadway and the road category. For short span bridges it was found that vehicles used today, compared to those historically used, are longer, with a higher number

of axles and the larger distance between them, so their effect on the load bearing construction of the bridge in many cases is smaller as all axles cannot fit onto a small-span bridge at the same time [54].

There are 3 reasons why using Load Model 1 with a α factor of 1 results in conservative values:

1. LM1 stands for a high percentage of heavy lorries, which is not the case for municipal bridges;
2. LM1 is especially designed for bridges with a larger span than 20m. For smaller spans, the axle configuration (number of axles and axle distance) is more important. Also, the governing vehicle might not fit on the bridge entirely;
3. For existing bridges a reference period shorter than 100 years can be assumed, since the bridge has a certain age. LM1 covers the whole lifetime of a bridge, which is not representative for existing bridges.

In order to cover the first reason, the Eurocode provides correction factors for bridges which are exposed to less heavy traffic. These values can be found in Table 4-2. For small span bridges (<20m), the factor for bridges with a span of 20m can be assumed. The factors are almost equal to 1, so it is not expected that this phenomenon has much influence on the loads and therefore on the reduction of the Eurocode loads.

For the second reason it was chosen that a more realistic load model is used. This has been done because the axle distance (which correlates to the distribution of the loads on the bridge) has a great influence for small span bridges. Load model 1 has 2 axles of 300kN at a distance of 1,2m from each other on the first lane. This is almost equal to one axle of 600 kN. Also, a distributed load of 9 kN/m^2 is present on the first lane. This is too much and unrealistic for a small span bridge. Research has been done to a governing existing lorry which applies loads more distributed, just as in a real situation in chapter 5.4.

The Eurocode provides a ψ factor for the third reason. Existing bridges have a reference period shorter than 100 years since the bridge has a certain age. This means that the chance of the occurrence of the normative load combination becomes smaller than when the bridge was built. According to the National Annex of the Eurocode one is allowed to reduce the loads with a ψ factor. The magnitude of this ψ factor can be found in Table 6-1. As for the first reason, regarding the magnitude of the factor, this phenomenon is expected to have little influence on the reduction of the loads.

Table 6-1 - ψ factor for short reference periods [2]

Referentieperiode	**ψ-factor** [a]			
	Lengte van de overspanning of invloedslengte *L*			
	20 m	**50 m**	**100 m**	**≥ 200 m**
100 jaar	1,00	1,00	1,00	1,00
50 jaar	0,99	0,99	0,99	0,99
30 jaar	0,99	0,99	0,98	0,97
15 jaar	0,98	0,98	0.96	0,96
1 jaar	0,95 [b]	0,94 [b]	0,89	0,88
1 maand	0,91 [b]	0,91 [b]	0,81	0,81

6.1 Modelling

6.1.1 Flexural moment

To achieve the maximum flexural moment the maximum axle load need to be placed as close as possible to the middle of the slab. For some load models it is clear where the loads have to be placed in order to achieve the maximum flexural moment. For some load models, such as some fatigue load models, this is not the case. RFEM determines the governing configuration in these situations. In every case, only the maximum occurring flexural moment has been reported. The mesh is chosen to be 0,5m. This is around 1 times the depth of the slab, which is recommended as maximum size of the mesh.

6.1.2 Shear force

Determining the right places of the axle load configuration for the maximum shear stress is not as clear as for flexural moment. Especially when using load models with many axles and a large edge width. The maximum shear stress can occur at the edge or near the middle of the support. In order to know which of these two places is governing, different load configurations need to be investigated. Also, the configuration of the axles on the two lanes can be different from each other in order to achieve the maximum shear stress. This is often the case when the maximum shear stress is near the edge of the slab. So, RFEM determines the governing configuration for shear force near the middle of the slab (this is commonly a result of the axles load configurations on the two lanes close to the support), and the configuration for the maximum shear force near the edge of the slab is determined by trial and error.

Both for the shear and flexural assessment the FE model calculates with the Kirchhoff method as explained in 5.2.2. The mesh is chosen to be 0,5m. This has been chosen because Kirchhoff works well with a relatively coarse mesh. Also it reduces the calculation time for RFEM. Regarding the number of calculations that have to be made (due to different spans, edge widths, load models etc.) reducing the calculation time per calculation a significant advantage. Also, since average values are used, exact values for shear force are not relevant. Therefore a very fine mesh is not necessary.

The RBK, a standard for existing civil works form The Dutch Ministry of Infrastructure and Environment, states that for FE modelling the shear force near the edge of a slab has to be averaged over 4*d [5].

6.1.3 Action plan modelling

For the modeling process in RFEM it is useful to make an action plan to make sure no mistakes are being made.

Modelling process (for shear force):

- Adapt span, edge width and thickness of the slab;
- Adapt support stiffness and transverse concrete stiffness if necessary;
- Adapt partial factors (the impact factor which depends on the span);
- Choose load model and determine minimum distance to support (2,5*d);
- Choose the governing locations for the load models (as close to the support as possible or under an edge of 45° for maximum shear force near the edge of the support);
- Note the maximum shear force and where it occurs: near the edge of the support or near the middle of the support.

6.1.4 Governing load model

It was explained in 5.4 that the fatigue lorries from the National Annex of the Eurocode (with some adaptions) are used as load models for real existing lorries. Since many calculations have to be made it is beneficial to determine the governing fatigue vehicle. Therefore different simplified tests are done with RFEM. These tests determine the shear force and flexural moment generated by the different load models. This comparison is made for a combination of a span of 5, 10, 15 and 20m and an edge distance of 0, 3 and 6m. From this comparison, the governing lorry can be chosen. In the end, this saves much time in the modelling process.

In Figure 6-1 the different used fatigue lorries can be found. Fatigue Lorry 6 has not been taken into account for this tests, since it is used as overload vehicle for the determination of the α factor. The Asphalt Lorry (AL) as illustrated in this figure is slightly adapted to a lorry with one more axle. This has been explained in 5.4.4.

The results can be found in *Appendix H - Comparative FEM test results for different fatigue load models*. From these figures the governing load model can be determine which is compared to Load Model 1.

Figure of lorry	Distance between axles m	Axle loads kN	Number
	4,5	70 130	1
	1,50 2,40 1,30	70 120 120 120	AL
	3,20 5,20 1,30 1,30	70 130 100 100 90	2
	3,40 6,00 1,80	70 140 90 90	3
	4,80 3,60 4,40 1,30	70 150 80 80 70	4
	3,20 1,30 4,40 1,80 1,80	80 160 100 100 100 100	5
	3,20 1,40 4,40 1,30 1,30 1,30	70 180 170 80 80 80 90	6

Figure 6-1 – Fatigue lorries as used in the modelling process (adapted from [2])

6.1.4.1 Conclusion

As can be seen in *Appendix H - Comparative FEM test results for different fatigue load models* for flexural moment as for shear force the asphalt lorry is governing for almost every bridge configuration. Only for very small spans (5m) this might not be the case. Here, the asphalt lorry does not fit on the bridge entirely, which results in the fact that a lorry with one high axle load is governing (for example lorry 5 with an axle load of 150 kN). From the other fatigue load models, load model 5 is mostly governing. When looking at the axle loads and axle distance this makes sense, since lorry 5 has high axle loads relatively close to each other (150kN and 100 kN at a distance of 1,3m). From these conclusions the following proposition has been made. Results from load model 1 is compared to the asphalt lorry and fatigue lorry 5 as real occurring vehicles on a bridge. Also, fatigue lorry 6 is used as comparison. This load model is seen as extreme overloading, since such high axles load are very unlikely to occur. However, it can be interesting to have some insight in the case of overloading. The used load models are marked with the red dashed square.

Now that the governing load models are chosen, the load model configuration of the whole bridge can be assumed. The axle loads of the governing load models are supported by results from the WIM measurements in Rotterdam (3.6.6.1). The load models are based on axle loads which occur once per 1000 years. Only one lane has been regarded in the whole process. For the determination of the α factor, two lanes are regarded. Assuming one governing vehicle on each lane would be too conservative, since the chance that two governing vehicles are present on the bridge next to each other at exactly the same time is nil. For the second lane the assumption is

made that lorry 1 occurs simultaneously with the other governing load model. This has been chosen because The National Annex of the Eurocode states that 80% of the heavy vehicles for local traffic can be assumed to be lorry 1 (Table 5-4). As example, the load configuration for the asphalt lorry is illustrated in Figure 6-2, with the asphalt lorry on lane 1 and lorry 1 (normal, frequently occurring truck) on lane 2.

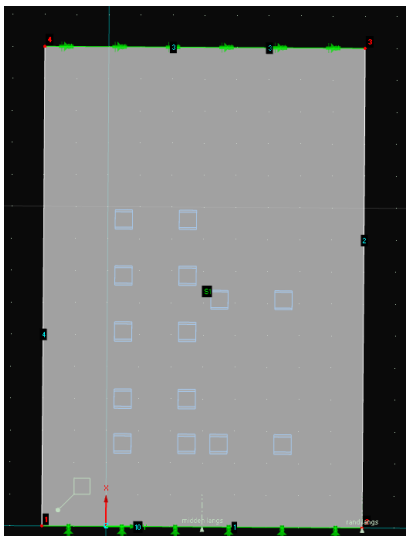

Figure 6-2 - Load model: asphalt lorry (with a normal truck on lane 2)

6.1.5 Results comparison LM1

Load Model 1 from the Eurocode has been compared with Load Class 60 & 45 from NEN 6723-1995 and the fatigue load models (FL5, FL6 and AL). The result is a graph which illustrates the α factor for different spans and edge widths. The α factor is determined by dividing the resulting shear force or flexural moment from a load model by the resulting shear force or flexural moment from Load Model 1. The α factor only influences the variable loads in load model 1, so the results of the self-weight of the slab has to be extracted before the results (shear force and flexural moment) can be compared.

Load Class 60 and 45 need to be compared with LM1 for new-built bridges (chapter 5.4.2) and the fatigue lorries can be compared with LM1 for existing bridges. The partial factors are different for these cases as described in chapter 3.6.7. The formulas which has been used for shear force are the following:

$$V_{tot,1} = V_{tot,LM1} \qquad \textit{(6.1)}$$

Where:

$V_{tot,1}$ = The resulting shear force by LC45, LC60, FL5, FL6 or AL (kN/m)
$V_{tot,LM1}$ = The resulting shear force by Load Model 1 (kN/m)

The shear force can be separated in shear force due to self-weight and shear force due to variable loads. The variable loads from Load Model 1 are multiplied by the α factor. This is the only unknown variable in the equation.

$$V_{SW1} + V_1 = V_{SW,LM1} + V_{LM1} * \alpha \qquad \textit{(6.2)}$$

Where:

V_{SW1} = The shear force due to self-weight by LC45, LC60 or AL (kN/m)
V_1 = The shear force due to variable loads LC45, LC60 or AL (kN/m)
$V_{SW,LM1}$ = The shear force due to self-weight by a Load Model 1 (kN/m)
V_{LM1} = The shear force due to variable loads by Load Model 1 (kN/m)

The formula for α then becomes:

$$\alpha = \frac{(V_{SW1} + V_1 - V_{SW,LM1})}{V_{LM1}} \qquad \textit{(6.3)}$$

Since FL5, FL6 and AL use the same self-weight as LM1, this formula can be simplified to division of the variable loads for these load models.

For the assessment of flexural moment the same formula's apply. In the following chapters the results for the α factor for flexural moment- and shear force assessment are demonstrated.

6.1.5.1 Results flexural moment

The results for the α factor for the flexural moment assessment are illustrated in *Appendix I – FEM results: calculation of the α factor*, chapter 9.1. Also the values for the flexural moment for every combination of bridge dimension can be found in this appendix. In Figure 6-3 and Figure 6-4 the graphs for the governing vehicles are provided.

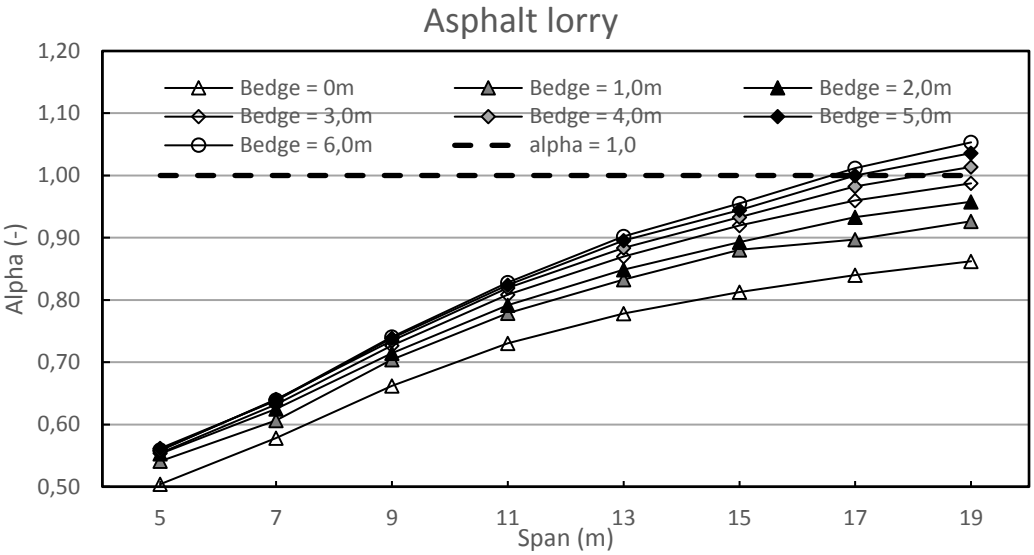

Figure 6-3 - α factor (flexural moment) for the comparison of Load Model 1 and the asphalt lorry for different spans and edge widths

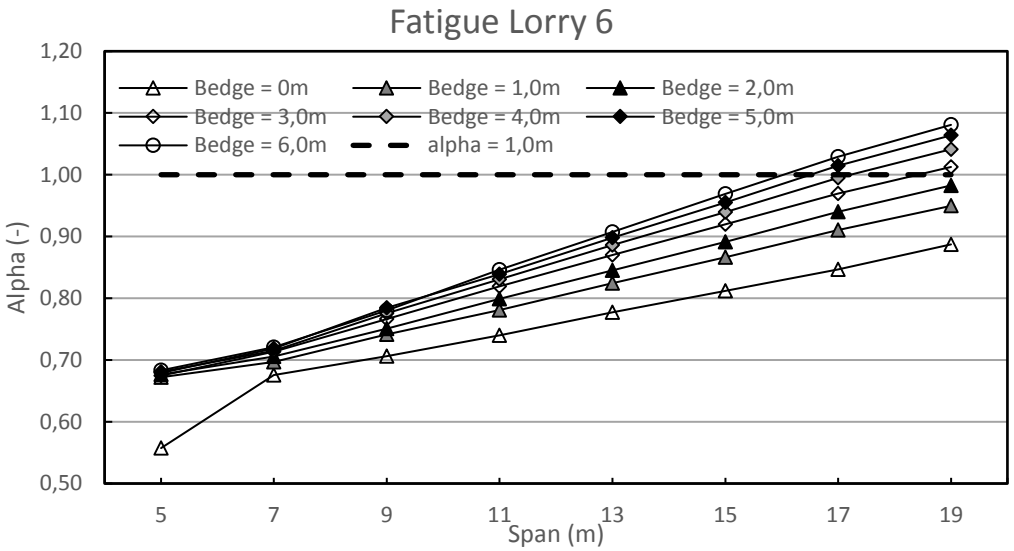

Figure 6-4 - α factor (flexural moment) for the comparison of Load Model 1 and fatigue load model 6 for different spans and edge widths

For the comparison with LC45 and LC60 two different graphs are displayed in the appendix. As explained in chapter 5.4.2, the comparison had been made for new built bridges in CC2 and CC3. In Figure 6-5 the comparison of LC60 and LM1 with CC3 from the Eurocode is displayed.

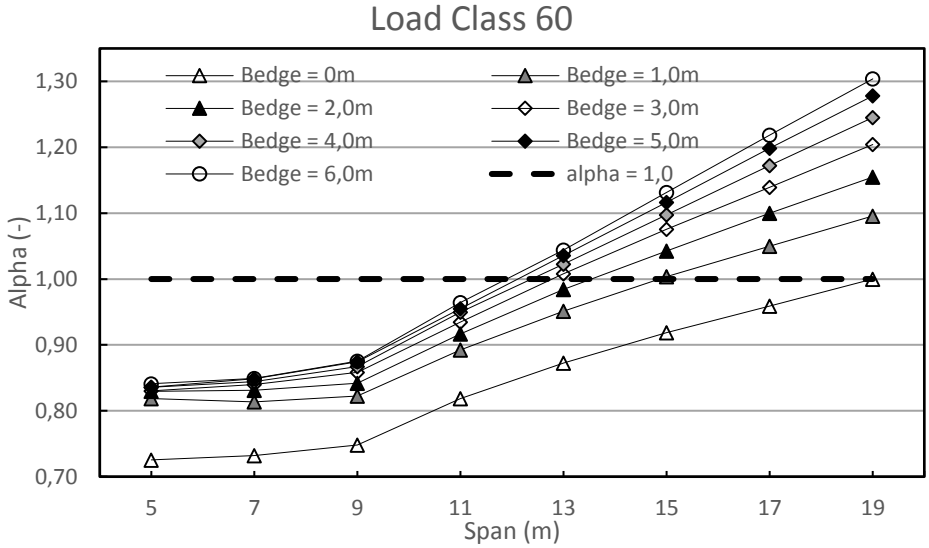

Figure 6-5 - α factor (flexural moment) for the comparison of Load Model 1 and Load Class 69 for different spans and edge widths

6.1.5.2 Conclusion flexural moment

Load Class 60
Load Class 60 has been compared to LM1, CC3. When an edge distance of 0m is not taken into account (which can be done, because highways normally have a certain edge distance due to a guardrail and an edge beam) the graphs for the different edge distances have rather the same shape. The graph start more or less horizontally because of the 3rd axle of LC60 that does not fit on the bridge for small spans. The reason for the different α factor for different edge distances has to do with the difference in the permanent load factor. For increasing edge widths the increase in maximum flexural moment comes due to the self-weight. This increase is larger for the flexural moment of LC60 than for LM1. The reason for the divergent shape of the graphs also has to do with the difference in permanent load factor. For an increasing span, the permanent loads have an increasing share of the total flexural moment compared to the axle loads. So, the total flexural moment due to LC60 increases more than the total flexural moment due to LM1 for an increasing span. Reasons for an α factor lower than 1,0 for small spans and higher than 1,0 for large spans is the same as for the shear assessment. This is described in chapter 6.1.5.4.

Load Class 45
The shapes of the comparison with Load Class 45 and Load Class 60 are very similar. This makes sense since the same load configuration was used. Small differences are found in the tyre dimensions, but this is negligible. Only load magnitude of the loads differ.

Fatigue Lorries
The shapes of the α graphs for the fatigue lorries are rather similar. The fact that the graphs are increasing towards an α factor of 1,0 has to do with the difference in axle distance compared to LM1. The axles of the fatigue lorries lie further away from each other than the axles of LM1. A higher flexural moment is provided by axles that lie in the middle of the slab. If the span increases more force from the axles is transferred by flexural moment, so the difference between LM1 and the fatigue lorries becomes less for an increasing span.

In Figure 6-6 The different fatigue lorries are compared for a slab with an edge width of 2,0m. FL6 has slightly higher α values for every span. This was as expected because this load model represents overloading. For 11m – 15m the α factor for the asphalt lorry is more or less the same. The asphalt lorry seems to be governing above FL5. Only for small spans the α factor for the asphalt lorry is lower. This is because the 5 axles do not fit on the bridges entirely. The other load models have 1 or 2 high axle loads which provide higher flexural moments for small spans.

In general there can be concluded that for spans smaller than 10m an α factor of 0,8 can be applied for every edge distance. For larger spans it makes sense to distinguish between different edge distances. For an edge distance of 1,0m the α factor increases from 0,8 at 12m to 0,95 at 20m. For an edge distance of 6,0m the α factor increases from 0,8 at 10m to 1,1 at 20m.

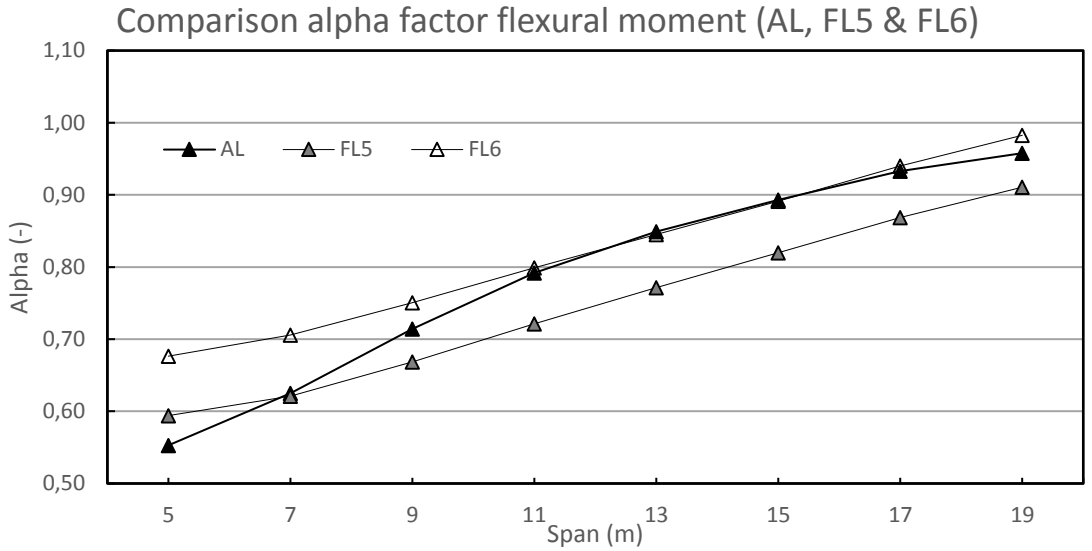

Figure 6-6 - α factors (flexural moment) for the comparison of Load Model 1 and AL, FL5 and FL 6 different spans. Edge width = 2m

6.1.5.3 Shear force

Determining the maximum shear force is harder than determining flexural moment. For some configurations the edge of the slab is governing, and for some other the middle is. Also, since different load models are being compared, for some bridge dimensions the middle is governing for one load model and the edge is governing for the other. This results in graphs for the α factor which are less smooth than graph for flexural moment. The results for the α factor for the shear force assessment are illustrated in *Appendix I – FEM results: calculation of the α factor*, chapter 9.2. Also the values for the shear force for every combination of bridge dimension can be found in this appendix. In Figure 6-7 and Figure 6-8 the comparison of LM1 with the Asphalt Lorry and Fatigue Lorry 6 has been displayed.

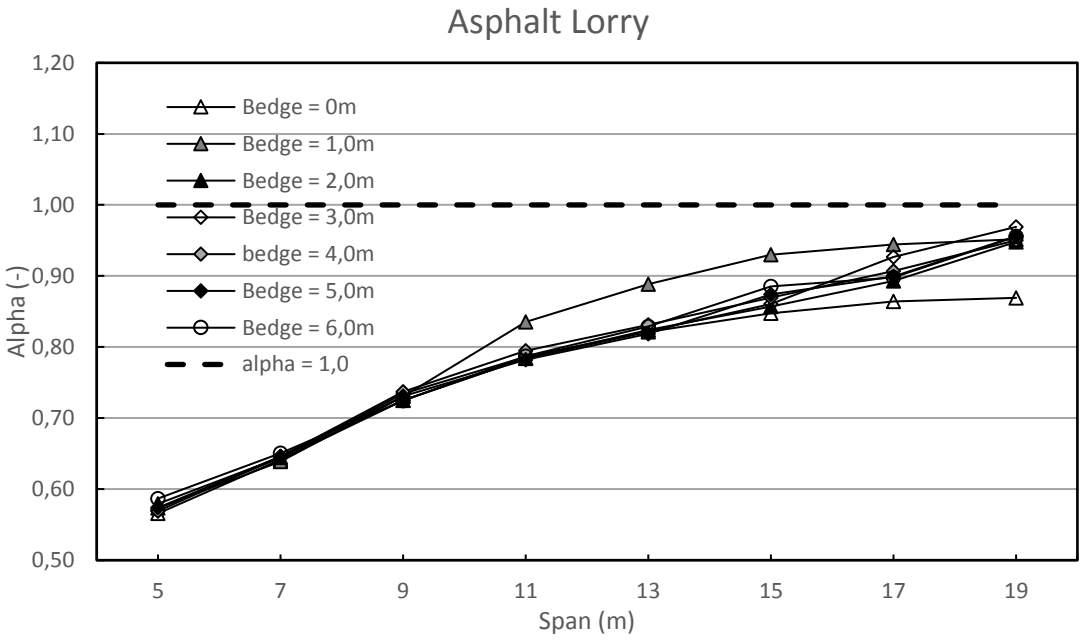

Figure 6-7 - α factor (Shear force) for the comparison of Load Model 1 and the Asphalt Lorry for different spans and edge widths

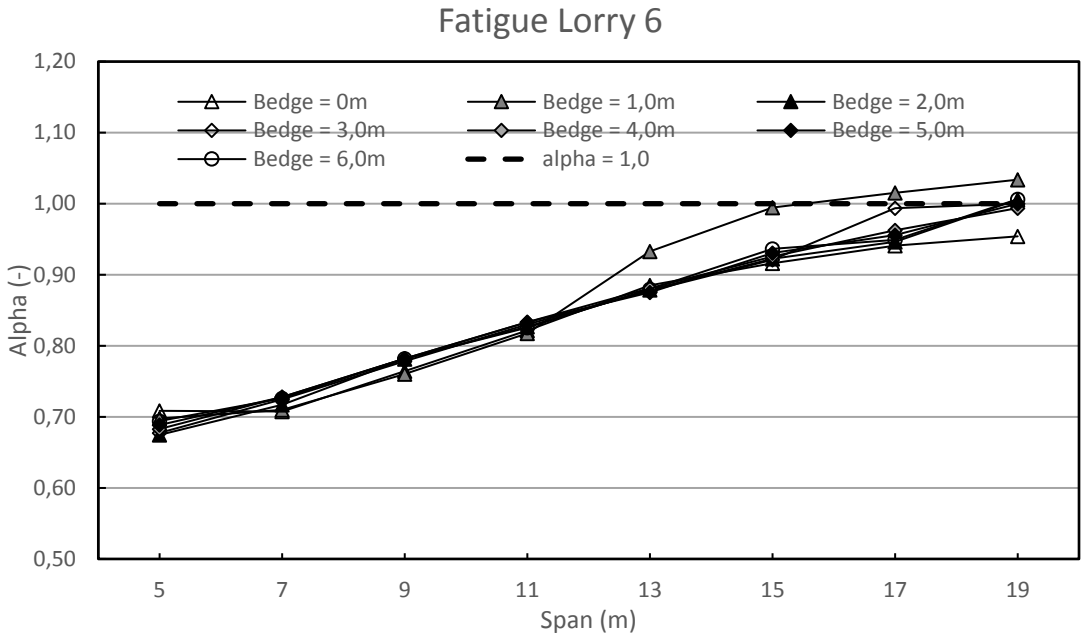

Figure 6-8 - α factor (Shear force) for the comparison of Load Model 1 and the Fatigue Lorry 6 for different spans and edge widths

As for flexural moment, the comparison had been made for new built bridges in CC2 and CC3. In Figure 6-9 the comparison of LC60 and LM1 with CC3 from the Eurocode is displayed.

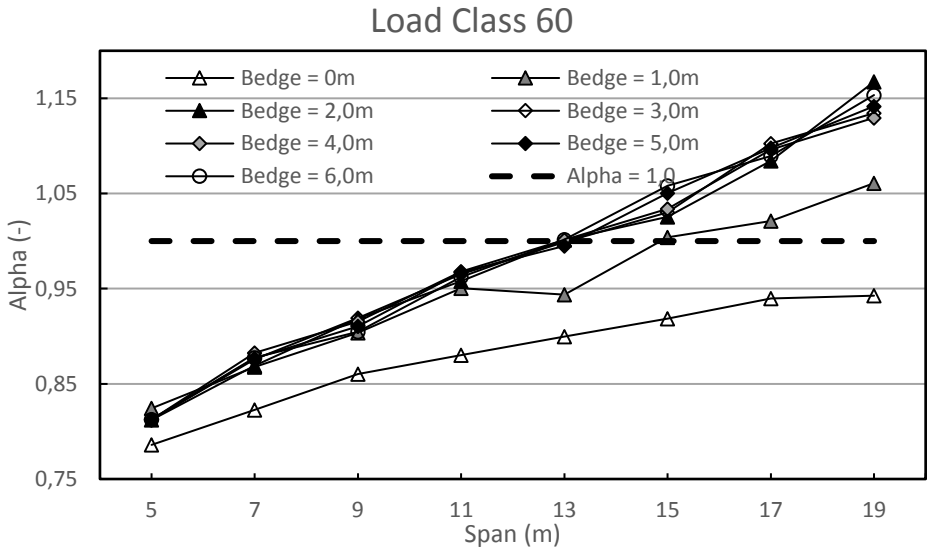

Figure 6-9 - α factor (Shear force) for the comparison of Load Model 1 and Load Class 60 for different spans and edge widths

6.1.5.4 Conclusion shear force

Load Class 60
Load Class 60 has been compared to LM1, CC3. When an edge distance of 0m is not taken into account (which can be done, because highways commonly have a certain edge distance due to a guardrail and an edge beam) the graphs for the different edge distances are rather the same. The α factor increases linearly with increasing span from an α value of 0,82 at a span of 5m to 1,17 at a span of 20m. This can be explained as follows.

The difference in permanent load factor (1,25 for LM1 and 1,5 for LC60) leads to an increasing α factor for an increasing span. For (governmental) highways typically more than 2 million heavy

lorries are assumed. This leads to an increase of the α factor of 1,15 for lane 1 and 1,4 for the UDL of the other lanes in the current standard. For this reason, the α factor is higher than 1,0 for a span of 20m, as illustrated in Figure 6-9. 10 years before the introduction of the Eurocode, the rules from the Eurocode were already used for highways.

Load Class 45
The shapes graphs for the comparison of LM1 with Load Class 45, and LM 1 with Load Class 60 are very similar. This makes sense since The same load configuration has been used. The tyre dimensions differ a little, but this is negligible. Only load magnitude of the loads differ.

Fatigue lorries
The α graphs for the fatigue lorries (AL, FL5 & FL6) have a rather similar shape. The reason for the increase of the α factor for increasing span is the fact that the fatigue lorries has to do with the number of axles and axles distances. If the span increases more force of axles further away from the support distribute to the critical support, while the amount of force distributed by LM1 stays more or less the same. The increase in span has barely influence on the force distribution of the axles of LM1.

For every graph applies that the α factor for edges distances of 2 meter or higher is more or less the same. This has to do with the fact that the middle of the support is commonly governing for high edges distances. If the fatigue lorries are compared with each other (as done in Figure 6-10 for an edge distance of 2,0m) there can be concluded that Fatigue Lorry 6 is governing for every span. This makes sense since the vehicle represents overloading.

The Asphalt Lorry is assumed to be a good comparison with LM1 for municipal bridges. The α graph increases more or less linearly from 0,6 at a span of 5m to 1,0 at a span of 20m. The Eurocode seems to be a good representation of real occurring loads for a span of 20m. For smaller spans the Eurocode is (way) too conservative. For a span of 5m a reduction of 40% on the occurring loads can be reached if real occurring maximum loads are assumed. If overloading is assumed (which is represented by FL6) a reduction of more than 30% can be reached.

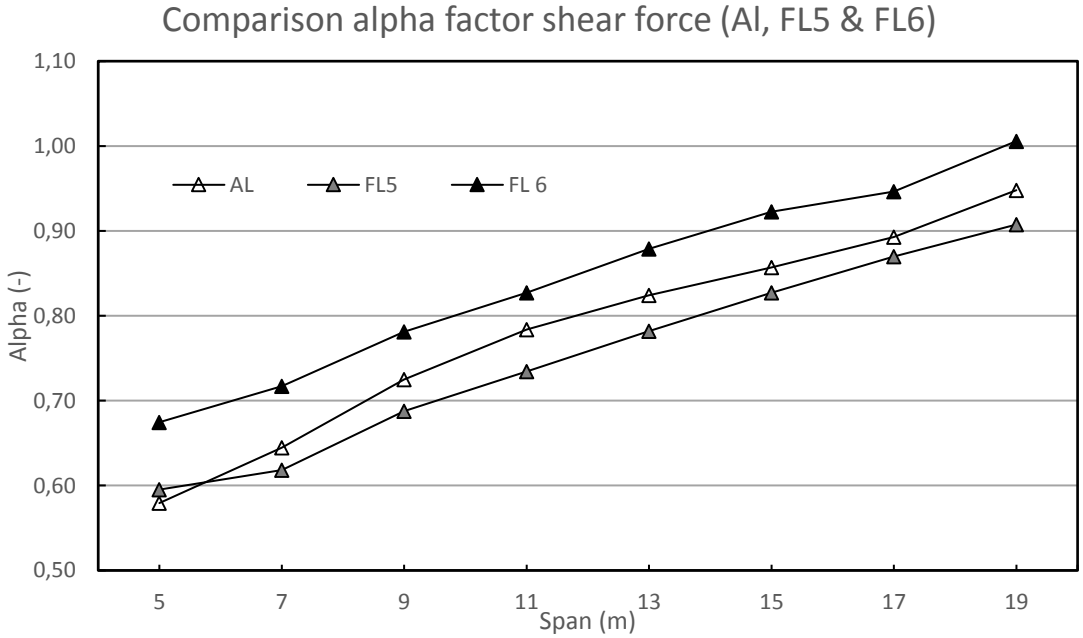

Figure 6-10 - α factors (Shear force) for the comparison of Load Model 1 and AL, FL5 and FL 6 different spans. Edge width = 2m

6.2 Conclusion

From the researches as described in the previous chapters, some conclusions can be drawn. The α factor was determined by the comparison of Load Model 1 with the asphalt lorry. Also, an α factor for overloading was determined by the comparison with Fatigue Lorry 6. For location specific loading (such as a bridge near a concrete or asphalt producer) the comparison with two Asphalt Lorries on two lanes was made. Also the distinction between the assessment for flexural moment and shear force was made. This is demonstrated in Appendix Figure 9-6 and Appendix Figure 9-14.

In Figure 6-11 the α factor from Figure 6-7, Figure 6-8 and *Appendix Figure 9-12* is summarized with α = 0,8 as lower boundary. For flexural moment the graphs are illustrated in Appendix Figure 9-7 and Appendix Figure 9-8.

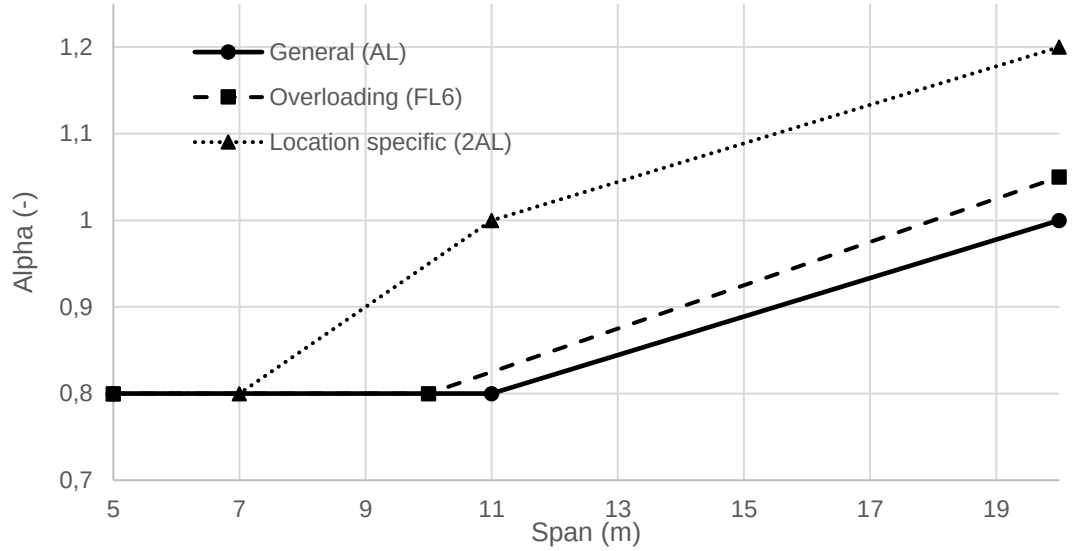

Figure 6-11 - A factor for general municipal bridges, overloaded bridges and bridges with location specific loading

The lower boundary of 0,8 was chosen due to the recommendation in the Eurocode. When this recommendation is not followed the α factor decreases more than 0,8. The line form Figure 6-7 can represent the α factor for spans smaller than 11m. For span from 5 to 11m, the α factor is 0,6 to 0,8.

Load class 60 from previous codes is similar to LM1 from the Eurocode for bridges with a span of 20m. This was as expected, because LM1 is calibrated on bridges with a span of at least 20m. For smaller spans, LC60 results in lower shear forces than LM1. Compared to reality (the asphalt lorry) LC60 represents real loads on small span bridges more accurate than LM1. Compared to the asphalt lorry, LC60 is still conservative. LC45 represents a real occurring lorry more accurately.

7 Force transmission in concrete slabs

7.1 Introduction

In this chapter, FEM research is used in order to explain the force transmission in concrete slabs. The difference between cracked and uncracked slabs is investigated. Also, the influence of the self-weight and the variable loads on the occurring shear force is addressed separately. Distinction was made between slabs cast in-situ and prefab slabs, since this influences the force transmission by self-weight. As described before, municipal bridges often have a sidewalk or bicycle lane separated by a kerb. This means the governing load model cannot be applied near the edge of the slab. For bridges without a certain edge distance (for example bridges on highways) the edge of the slab is typically governing for shear assessment. For municipal bridges with large edge distances this might not be the case, since somewhere near the middle of the support higher shear forces could occur. This can be further explained by looking at Figure 7-1 and Figure 7-2. For a large edge distance the loads have to be placed further away from the support and diagonally in order to generate the higher shear forces near the edge of the support. Placing axle loads further away means a decrease of the shear force since the forces can spread over a greater length of support. At a certain edge distance the axle loads have to be placed at such a distance to generate high shear forces at the edge that the load case where the loads are placed close to the support is governing (Figure 7-1). The goal is to find the critical edge distance for certain bridge dimensions. In this way the governing place for shear assessment can be found (near the middle of the support or near the edge of the support) by just looking at the bridge dimensions. This goal can be reached by investigating the force transmission in concrete slabs. The research is a comparison of different finite element models. The resulting shear force is compared.

7.2 Description of the research

With this research, the force transmission in solid concrete slab bridges was investigated. Different variable parameters that might be of influence were investigated. The resulting shear force has been compared. In this chapter the different parameters are described.

Different spans were investigated from 5m to 20m with an interval of 2m. Loads according to Load Model 1 from the Eurocode [2] were used. In every different configuration of loads and dimensions 2 traffic lanes were used. This situation is mostly present on municipal roads. Also, a possible third lane has little influence on the difference on the maximum occurring shear force. In many cases a footpath or bicycle lane is present next to the 2 traffic lanes. Different edge distances were investigated: 0 to 6m with an interval of 1,0m. Where 0-1m represents no footpath or bicycle lane, 2-4m represents one footpath or bicycle lane and 5-6m represents a footpath and a bicycle lane. This categorization is not used further and is purely meant for interpretation of certain edge distances.

In principal, the same FE model as for the determination of the α factor has been used (Chapter 6) Again, parametric modelling has been used to switch between dimension more easily. Also, the module RF-MOVE-surface has been used to generate the governing positions of the load models. A difference is that the transverse stiffness of the slab has great influence on the force transmission. In this chapter, also a difference between cracked and uncracked slabs has been made.

The parameters (variables) used in the FE model is summed up in short:

- The span (L) varies from 5 to 20m with an interval of 2m;

- The edge distance (b_{edge}) varies from 0 to 6m with an interval of 1,0m;
- The thickness (h) is a function of the span: $h = L/20$ with a minimum of 400mm ;
- The place of the axle loads from Load Model 1 on the bridge varies for generating the highest shear force near the edge of the support and near the middle of the support;
- The spring stiffness of the support is a function of the thickness according to the rule of thumb which states that the support displaces 1mm vertically under its self-weight. (*see Appendix G – Deflection due to self-*) $C = (\rho_c * h) * (\rho_a * t) \frac{L}{2}$;
- Since the transverse stiffness has great influence on the transverse force transmission, both cracked and uncracked slabs were tested.

The critical edge distance was determined by comparing the occurring shear stresses near the middle and the edge of the slab for different spans and edge widths. For different spans the edge distance at which the shear stress near the middle of the slab is the same as the shear stress near the edge of the slab was noted. This was done for cracked and uncracked slabs.

A difference in load configuration is presented below.

- Finding the governing load model in order to generate the highest shear stresses near the middle of the support (Example Figure 7-2);
- Finding the governing load model in order to generate the highest shear stresses near the edge of the support (Example Figure 7-1).

In the following chapters the 2 different researches (middle governing and edge governing) are elaborated.

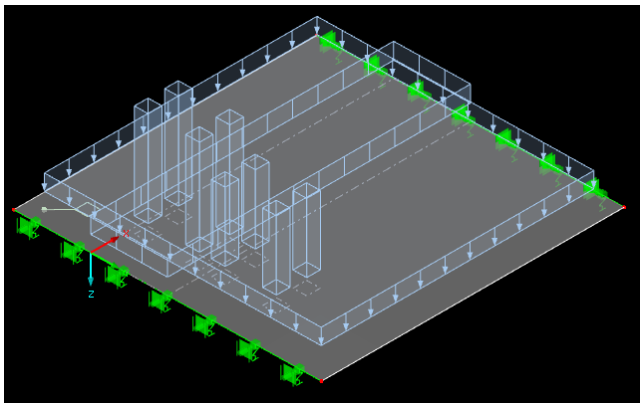

Figure 7-2 - Example determining maximum shear stress near middle support. b_{edge} = 3m, Span = 12m

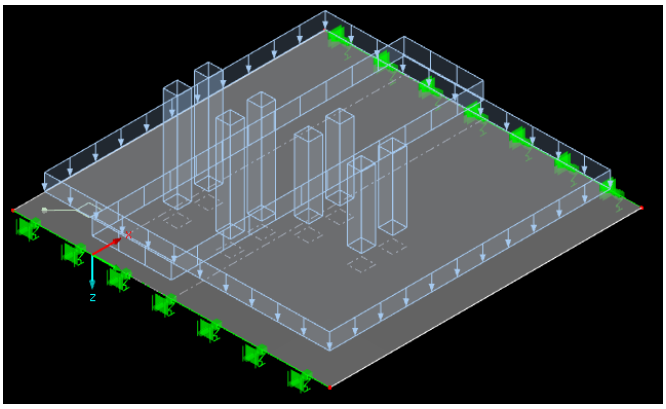

Figure 7-1 - Example determining maximum shear stress near edge support. b_{edge} = 3m, Span = 12m

In order to understand force transmission in concrete slabs in a better way the loads from Load Model 1 were separated. The occurring shear force due the axles separately and the permanent loads were investigated. This was done for cracked and uncracked slabs. Also distinction between shear forces near the middle and near the edge of the slab was made. An overview the different models to be compared is displayed in Figure 7-3.

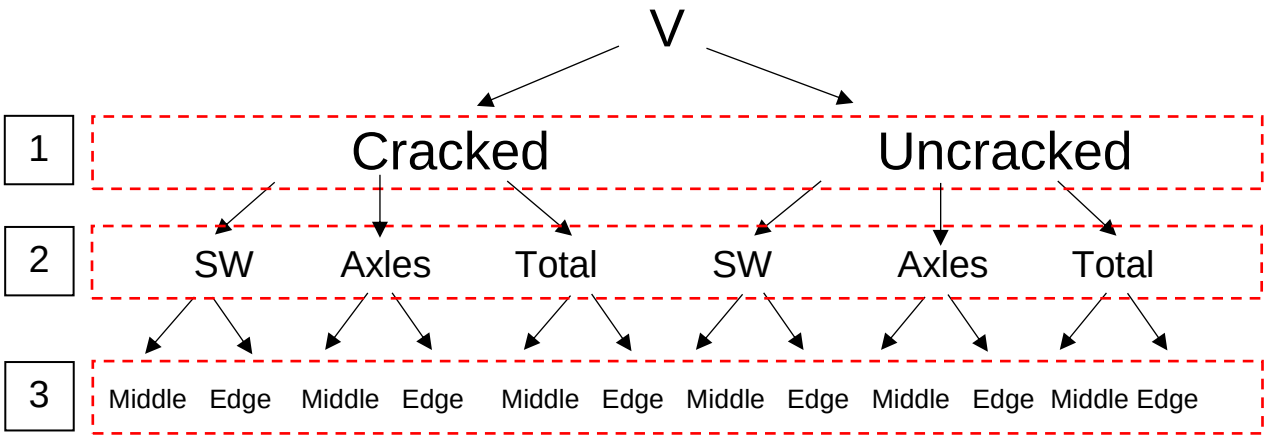

Figure 7-3 Overview research FE model

For all of these models, there was varied with the span and the edge distance. In the following chapters the different levels as illustrated in Figure 7-3 are investigated. First row 1 is assessed in chapter 7.3 Then row 2 is assessed in chapter 7.4. Finally row 3 is described in chapter 7.5. In this chapter the critical edge distance is determined.

The result of the comparison research is a factor which comes from the division of two shear forces. For these two shear forces one parameter is variable, for example transverse stiffness or the shear force near the edge/ middle of the support.

7.3 Difference cracked and uncracked slabs

The difference between cracked and uncracked slabs has been explained in chapter 5.2.3. For all tests that were done the distinction between cracked and uncracked slabs was made, which means a difference in transverse stiffness. This comparison was made for axles loads only, self-weight only, and the total loads according to Load Model 1.

7.3.1 Comparison axle loads

The resulting shear force on the support due to axle loads was compared for cracked and uncracked concrete. The results can be found in Appendix Figure 10-4 and Appendix Figure 10-5.

As expected, the shear force near the middle of the support is higher for a cracked slab. This is because the axle loads transfer to a smaller support length than for uncracked slabs. This results in a higher force per meter width on the support. This is also demonstrated in *Appendix F – Tests cracked/uncracked slabs*. For small edge distances this is not the case since the edge of the slab is then governing. The factor $V_{cracked}$ / $V_{uncracked}$ reaches 1,08 to 1,19 for large edge distances. So, a reduced transverse stiffness (which is the result from cracking) leads to higher shear forces at the middle of the support. The factor $V_{cracked}$ / $V_{uncracked}$ for the resulting shear force near the edge of the support decreases for increasing edge distances (from 1,0 to 0,4). This makes sense since in cracked state, the spread of the axles loads is much less than for a slab in uncracked state.

7.3.2 Comparison self-weight

The resulting shear force on the support due to self-weight has been compared for cracked and uncracked concrete. This is only done for prefab slabs, since cracking has no or little influence on the force transmission of self-weight in in-situ slabs. The results can be found in Appendix Figure 10-2 and Appendix Figure 10-3. The shape of the graphs is more or less the same as the comparison for the axle loads in chapter 7.3.1. The same conclusions as described in that chapter apply. For small spans the value are more scattered. The reason for this is that average values have been used with no decimals. For small spans a difference of 1 kN/m on a value of 30 or 40 kN/m already means a relatively high factor. The factor $V_{cracked}$ / $V_{uncracked}$ is lower compared to the comparison of the shear force due to axle loads. This is because a distributed load is applied instead of concentrated loads.

In reality, existing bridge can either be cracked or uncracked. However, when ULS is reached, the bridges is always fully cracked. Both situations have been investigated. If the differences are neglectable, a slab can be regarded as uncracked. The force transmission in uncracked slabs is generally more clear. Previous tests reveal that the difference is quite significant with a maximum difference of a factor 1,2 for the middle of the support and a maximum difference of a factor 0,4 for the edge of the support. Therefore, for the comparison of the total shear force due to load model 1 which determines the critical edge width, both situation (cracked and uncracked) were used.

7.3.3 Comparison total loads

In Appendix Figure 10-6 and Appendix Figure 10-7 the comparison between cracked and uncracked state for the total loads was made. For the shear force near the middle of the support a clear correlation can be found. This is also illustrated in Figure 7-4. The overall difference is a factor of $V_{cracked}/V_{uncracked}$ of around 1,07. This only counts for spans higher than 9m and edge distances higher than 2m. For small spans and small edge distances the factor is around 1,0.

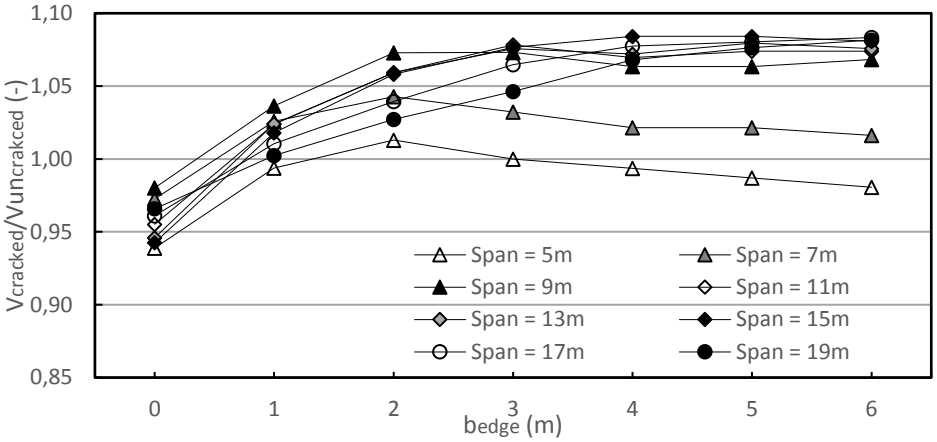

Figure 7-4 - Comparison of shear force due total loads near the middle of the support (cracked divided by uncracked)

7.3.4 Conclusion

First of all, there can be concluded that it is useful to differentiate between a cracked and an uncracked slab. Differences in maximum shear force are from 0,75 for the edge of the support up to a factor of 1,08 for the middle of the support. Differences for the dead loads are not significantly large, because a difference in transverse stiffness, and therefore in transverse force transmission, does not affect the force transmission of an uniformly distributed load substantially. The force transmission of axle loads however, is affected by the transverse stiffness. Especially for large spans (which leads to a larger distance of the axle loads to the support due to $a_v = 2{,}5*d$) and significant edge distances the transverse stiffness has influence, since the axle loads can spread to the support. For these dimensions the shear force near the middle of the support is higher for cracked slabs and shear forces near the edge are higher for uncracked slabs.

7.4 Shear force due to dead load and variable load separately

In order to understand the force transmission in a concrete slab, the resulting shear force of the dead load and the axle loads (variable loads) were investigated separately. The difference between cracked and uncracked state has been explained in chapter 7.3. The type of execution has influence on the force transmission of the self-weight as explained in chapter 3.3.6.

7.4.1 Shear force due to self-weight

Several tests for the shear force due to self-weight have been done, for example with the tests for Mindlin and Kirchhoff (5.2.2). In every case a slight increase of shear force was observed near the edge of the support due to torsional forces. This torsional forces due to self-weight are caused by the shape of the slab. The theoretical background was explained in chapter 5.2.

For an increasing span, also the thickness of the slab increases. This means that the maximum shear force due to self-weight increases quadratically of an increasing span. The values for the

occurring shear stress due to self-weight near the edge and the middle of the support are illustrated in *Appendix J – Comparing shear forces, chapter 10.1.* In the following chapter the comparison between the edge and the middle of the slab for self-weight is made.

7.4.1.1 Comparison middle / edge

For the self-weight including the asphalt layer the comparison between shear forces near the edge and the middle of the support has been made in *Appendix J – Comparing shear forces, chapter 10.4, comparison 1 and 2*. This has been done for cracked and uncracked concrete. For an uncracked slab this is illustrated in Figure 5-7. The shear force near the edge of the support has been divided by the shear force near the middle of the slab.

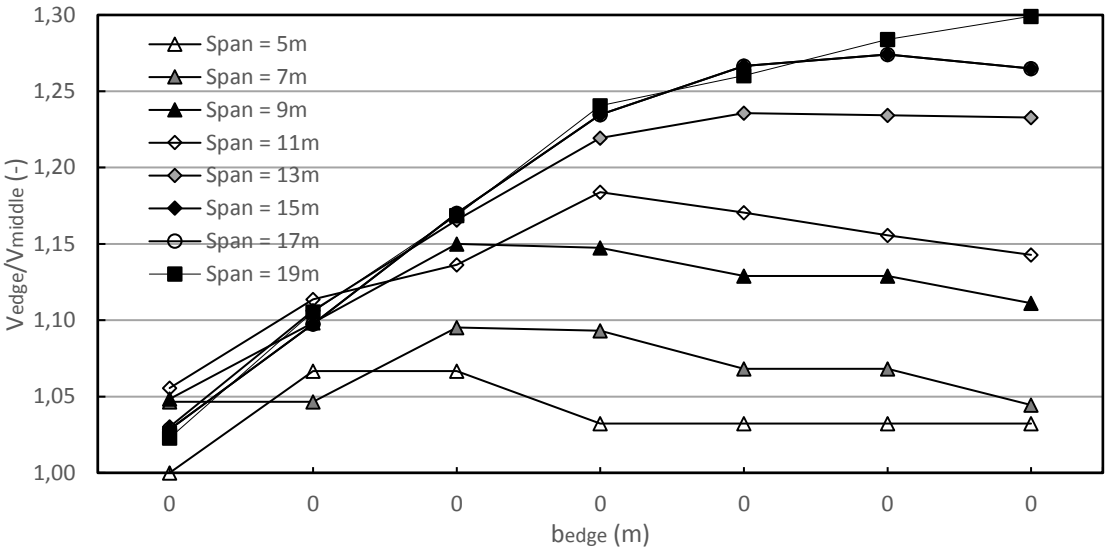

Figure 7-5 – Shear force near the edge of the support over the shear force near the middle of the slab due to permanent loads for different spans and edge distances (uncracked slab)

For uncracked slabs some tests have been done. The shape compared to the graph of the cracked slab is quite similar, especially for small edge distances. For large edge distances and large spans the factor V_{edge} / V_{middle} is higher for the uncracked slab than for the cracked slab. In general the factor is higher for every bridge dimension, which means that the shear force peak near the edge of the slab is higher than near the middle. The difference between of shear force the edge and the middle of the slab is up to 30% (factor 1,3).

The shear peak at the edge due to self-weight has a great influence on the critical edge width. In order to look at the influence of the bridge dimensions on the force transfer of the axle loads of Load Model 1 the shear forces due to the axle loads only are examined.

7.4.1.2 Difference cast in-situ and prefab

For slabs cast in-situ, the shear force on the support due to self-weight is assumed to be constant. Direct force transmission to the slab was taken into account as illustrated in Figure 7-6.

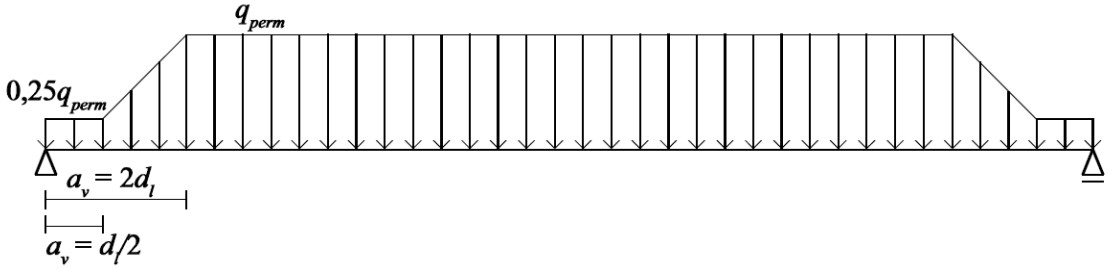

Figure 7-6 - Resulting distributed load for permanent loads when β(x) is taken into account [33]

As for the FE modelling, a permanent load factor of 1,1 was taken into account. In the FE model, the shear forces due to self-weight including the asphalt layer were taken. For the in-situ slabs

this was also done, although this asphalt layer may lead to small shear peak forces near the edge of the support. The asphalt layer is applied on the bridge after the concrete is hardened. These peaks are small and assumed to be neglectable. The results are demonstrated in Table 7-1.

Table 7-1 - Shear forces due to self-weight for a cast in-situ slab

Span (m)	5	7	9	11	13	15	17	19
Thickness (m)	0,4	0,4	0,45	0,55	0,65	0,75	0,85	0,95
Shear force on support (kN/m)	29	43	62	89	122	160	202	250

Compared to shear forces due to self-weight in prefab slab the shear forces for the middle of the support on average are similar. The average is an edge distance of 2 meters. This was as expected since peak forces near the edge of the support have little influence on the shear forces near the middle of the support.

Differences between the shear forces near the edge of the support for a prefab slab (cracked and uncracked) and a cast in-situ slab are illustrated in Figure 7-7. Results from *Appendix J – Comparing shear forces* were used for the comparison.

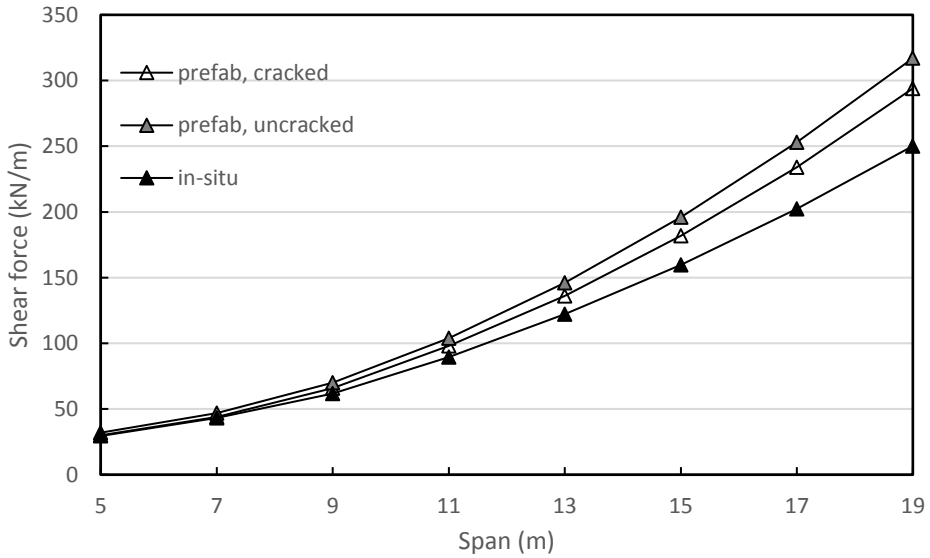

Figure 7-7 – Shear forces due to self-weight for prefab (cracked and uncracked) and in-situ cast slabs for the edge of the support (b_{edge} = 6m)

Since she shear forces near the middle of the support are approximately the same for prefab and cast in-situ slabs, the difference for the edge of the slab is approximately the same as illustrated in Figure 7-5. Results for the total loads of slabs cast in-situ are demonstrated in *Appendix J – Comparing shear forces, chapter 10.2*. These total loads are the sum of the variable loads from RFEM and the permanent loads from Table 7-1.

7.4.2 Shear force due to axles loads of Load Model 1

The shear force due to load model 1 has been determined. Distinction has been made between shear force near the edge and near the middle of the support. The values of the shear forces can be found in *Appendix J – Comparing shear forces, chapter 10.1.* These values are also illustrated in Figure 7-8 and Figure 7-9.

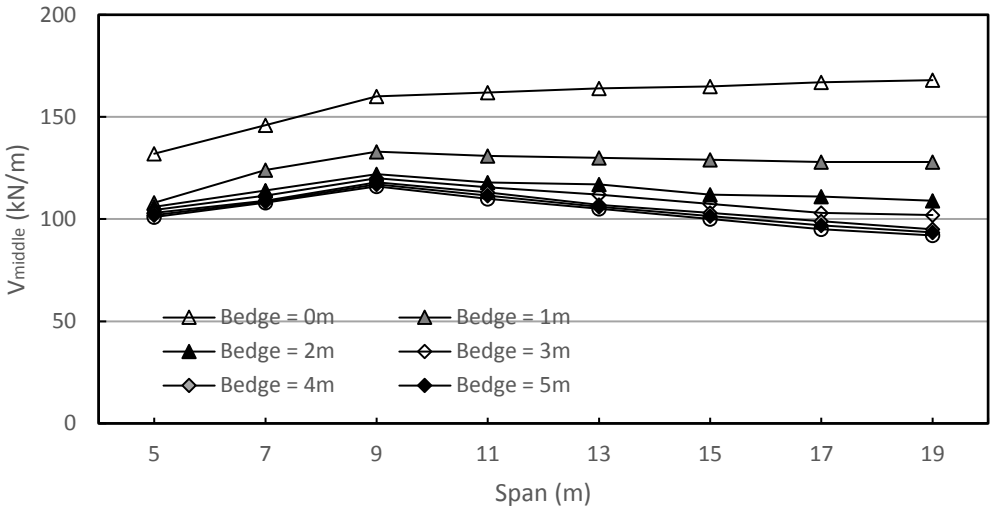

Figure 7-8 – Shear force near the middle of the slab for an uncracked slab.

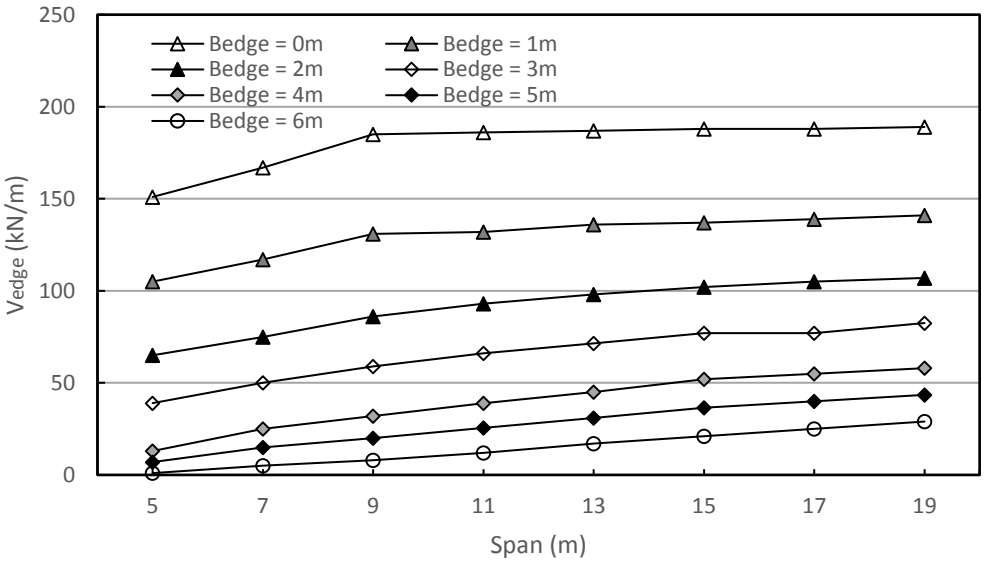

Figure 7-9 – Shear force near the edge of the slab for an uncracked slab.

Note that in these figures the x-axis represents the span (instead of the edge width in previous graphs). This was done because now the graphs can be compared better since the shape of the graphs is more clear.

Figure 7-9 illustrates that the edge distance has a great influence on shear force near the edge of the slab. The axle loads cannot spread to the edge entirely if the edge distance is too great. For cracked slabs the difference is even larger, since axles loads spread less due to reduced transverse stiffness.

Figure 7-8 illustrates the shear force near the middle of the slab for axle loads. The shape of the graphs is a result of two issues:

- For increasing span the shear force increases, because less force is transmitted to the opposite support.
- For an increasing span, the thickness of the slab increases and therefore also a_v (because a_v = 2,5*h and h = L/20). If a_v increases the maximum shear force becomes less, because the effective width is larger.

These two issues cancel each other out partly. For small spans (up to 8m) the second issue does not apply. This is because a minimum thickness of 400 mm is typically assumed. So, the thickness is constant for spans of 5-8m. This results in no reduction for small spans and therefore an increasing graph for spans up to 8m in Figure 7-8.

7.4.2.1 Comparison middle/ edge

The resulting shear forces near the edge and the middle of the slab for the axle loads of LM1 have been compared. The results can be found in *Appendix J – Comparing shear forces, chapter 10.4, comparison 3 and 4*. For uncracked slabs, the comparison is illustrated in Figure 7-10.

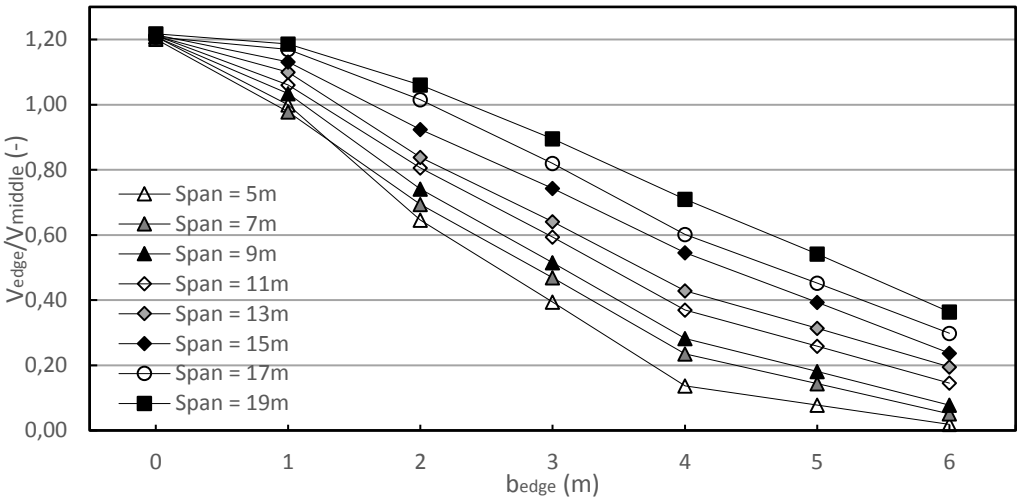

Figure 7-10 - Shear force near the edge of the support over the shear force near the middle of the slab due to axle loads for different spans and edge distances (uncracked slab)

This figure illustrates the division of Figure 7-9 and Figure 7-8. For an edge width of 0m the shear forces near the edge is 20% higher than near the middle (factor 1,20). For larger edge distances the factor decreases for every span.

7.5 Critical edge distance

For determining the critical edge distance the maximum shear force near the middle of the support are determined for every combination of bridge dimensions. The governing combination of the tandem system for both the edge and the middle are determined. For the middle of the support the governing location of the tandem system is as close as possible to the support (as described in chapter 7.5.1.1) For the edge of the support the governing location of the tandem system is close to the support for small edge distances and under an angle of 45° for larger edge distances as described in chapter 7.5.2.1.

7.5.1 Middle of the support governing

The maximum shear force near the middle of the support is typically a result the load configuration where the axles are as close as possible to the support. For an axle distance smaller than 2,5*d a reduction factor β has to be taken into account for direct force transmission to the support. The governing distance from the first axle to the support a_v is investigated.

7.5.1.1 Governing distance of the axle loads to the support

In order to know the governing distance to the support, different load distances to the support were investigated. The occurring shear force is compared. For loads very close to the support (≤ 2,5*d) a β factor has to be used. This β factor is a factor which takes into account the direct load distribution to the support for load very close to the support. The formula for this factor is $\beta_{new} = a_v/2{,}5d_l$ (see also chapter 4.3.1).

3 different load configurations were investigated (Table 7-2):

1. Distance to support = a_v;
2. Distance to support = $a_v - \frac{b_{wheel}}{2}$;
3. Distance to support = $a_v - b_{wheel}$.

Table 7-2 – Three different load configurations for loads near the support

1 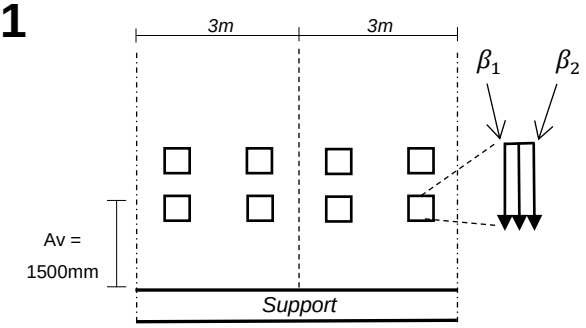 	**Span = 5m** h = 0,4m; d = 0,36; a_v = 0,563; β_1 = 1,0; β_2 = 1,0
	Span = 10m h = 0,50m; d = 0,450; a_v = 1,125; β_1 = 1,0; β_2 = 1,0
	Span = 15m h = 0,75m; d = 0,675; a_v = 1,688; β_1 = 1,0; β_2 = 1,0
	Span = 20m h = 1,00 m; d = 0,900; a_v = 2,250; β_1 = 1,0; β_2 = 1,0
2 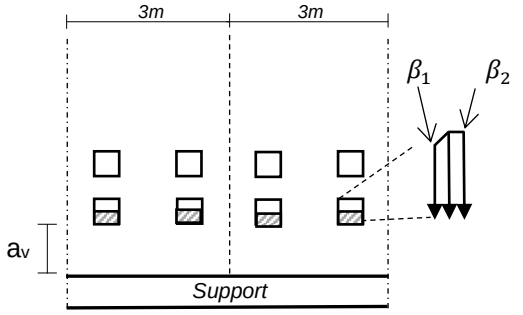 	**Span = 5m** h = 0,4m; d = 0,36; a_v = 0,293; β_1 = 0,52 β_2 = 1,0
	Span = 10m h = 0,50m; d = 0,450; a_v = 0,855; β_1 = 0,76 β_2 = 1,0
	Span = 15m h = 0,75m; d = 0,675; a_v = 1,418; β_1 = 0,84; β_2 = 1,0
	Span = 20m h = 1,00 m; d = 0,900; a_v = 1,980; β_1 = 0,88; β_2 = 1,0
3 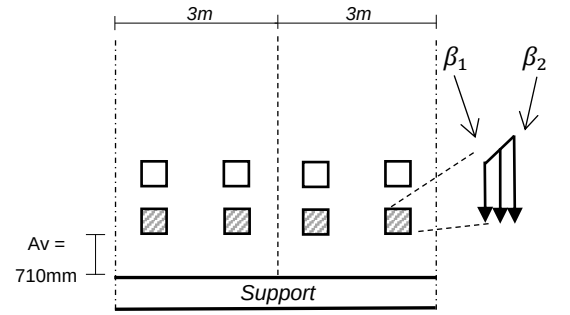 	**Span = 5m** h = 0,4m; d = 0,36; a_v = 0,023; β_1 = 0,04; β_2 = 1,0
	Span = 10m h = 0,50m; d = 0,450; a_v = 0,585; β_1 = 0,52; β_2 = 1,0
	Span = 15m h = 0,75m; d = 0,675; a_v = 1,148; β_1 = 0,68; β_2 = 1,0
	Span = 20m h = 1,00 m; d = 0,900; a_v = 1,710; β_1 = 0,76; β_2 = 1,0

These load configurations are tested with different values for the span and b_{edge}. The α values (for every load configuration) are: α_{Qi}=1,0; α_{q1}=1,0; α_{q2}=1,0; α_{qr}=1,0.

The hypothesis is that load configuration 1 is governing for every combination of span and b_{edge}, because there is no load reduction due to the β reduction factor. However, load configurations 2 and 3 could still be governing since the (reduced) loads stand closer to the support and could there generate higher shear forces due to a reduced effective width. This hypothesis was tested by comparing the maximum shear forces for the different load configurations. The results for the comparison of load configuration 1 and 2 are illustrated in Figure 7-11. Values for the shear force can be found in Appendix *K – Tests with axles at different distances from the support*.

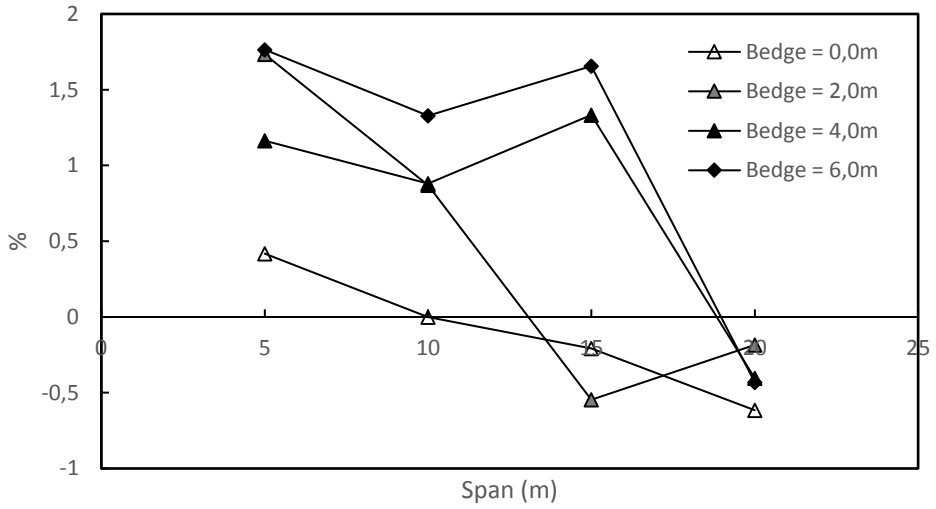

Figure 7-11 - Difference of the occurring shear force by load configuration 1 (set at 0%) and 2

Analyzing the results, it was found that load configuration 2 ($a_v - \frac{b_{wheel}}{2}$) is governing in most cases. Only for large spans load configuration 1 is governing. As can be seen in the Appendix, load configuration 3 is not governing for any combination of span and b_{edge}. In general, the differences are very small (<2%) as can be seen in Figure 7-11. In general, the real load configuration does not matter much. This means the reduction due to beta is about even match to the increase in shear force due to the fact that axle loads are closer to the support. For the sake of simplicity load configuration 1 can be assumed, so a distance of a_v = 2,5*d.

7.5.1.2 Results

For every combination of edge distance and span, the maximum shear force near the middle of the slab has been noted. According to the RBK, an average of the shear stress of 4*d over the support length has to be taken into account [5]. An overview of these shear forces for an uncracked slab is illustrated in Figure 7-12. The exact values (also for cracked slabs) can be found in *Appendix J – Comparing shear forces.*

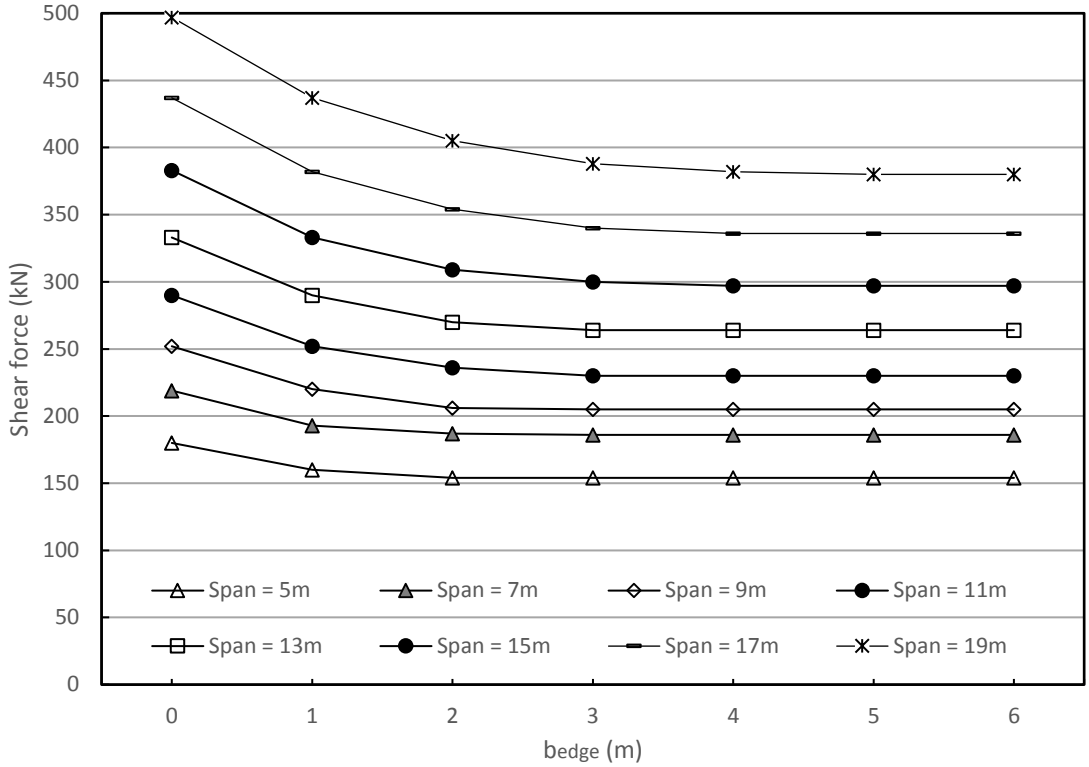

Figure 7-12 - Shear force near the middle of the support for different spans and edge distances (uncracked)

7.5.2 Edge support governing

Determining the governing load configuration in order to achieve the maximum shear stress near the edge is not as clear as for the middle of the support. This is because there has to be dealt with 2 times 4 wheel print which all distribute their loads individually to the support. The α values (for every load configuration) are again: $\alpha_{Qi}=1{,}0$; $\alpha_{q1}=1{,}0$; $\alpha_{q2}=1{,}0$; $\alpha_{qr}=1{,}0$. For determining the maximum shear stress near the edge of the support, the same dimensions as for the middle of the support were investigated.

7.5.2.1 a_v for different dimensions

According to the theory, the first axle should be at an angle of 45° to the edge of the support to generate the highest shear forces near the edge of the support. This has been explained in Figure 4-8. Note that this is only true for uncracked slabs. For cracked slabs, the transverse stiffness has reduced and therefore the transverse force transmission changes. The governing places of the tandem systems were determined by trial and error in RFEM. Together with the maximum shear force, also the distance from the axles to the support has been noted. The values for a_v on lane 1 and lane 2 are revealed in *Appendix L – values for av for the governing axle configuration.* In the graphs for a_v (Figure 7-13 and Appendix Figure 12-2) clearly two different parts can be distinguished. The horizontal part in the graphs stand for the governing situation where the tandem system stands as close to the support as possible (without reduction due to the β factor). Loads near the support generate the highest shear forces. For small edge distances the loads close to the support can spread to the edges and generates peak forces near the edge. For small edge distances this load configuration is governing.

For larger edge distances the loads near the support cannot spread to the edge. For these bridge dimensions the tandem system has to be placed further from the support in order to generate the highest shear stress near the support. This represents the diagonal part in Figure 7-13 and Appendix Figure 12-2. For larger edge distances, a general trend of around 45° can be observed. This is as expected, because the force distribution was assumed to be 45° according to [31] as described in chapter 4.3. The reason why the lines in the diagonal part are not straight is because

different tandem configurations can lead to the same shear force near the edge of the support. Also, only values for a_v with an interval of 0,5m were investigated. The tandem system on lane seemed to be (by far) most important for the maximum shear force near the edge. In some cases the same maximum shear force was found for the combination of a certain a_{v1} with 4 different values for a_{v2}. The loads from the tandem system on lane 2 have lower values. Also the distance to the support is higher in some cases (a_{v2}). This means the forces spreads more and have less influence on the magnitude of the shear force near the edge of the support. Therefore the exact location of the tandem system on lane 2 is not very important.

For cracked slabs the values for a_v have not been noted. This is because there were only a small number of combinations of bridge dimensions where a diagonal placed tandem system lead to an increase of the shear force. In almost every case the governing shear force was found by 2 tandem systems as close as possible to the support. This is because of the reduction of the transverse stiffness for cracked slabs. Due to this reduction, the 2 wheel loads close to the edge are most important for the shear force near the edge of the support.

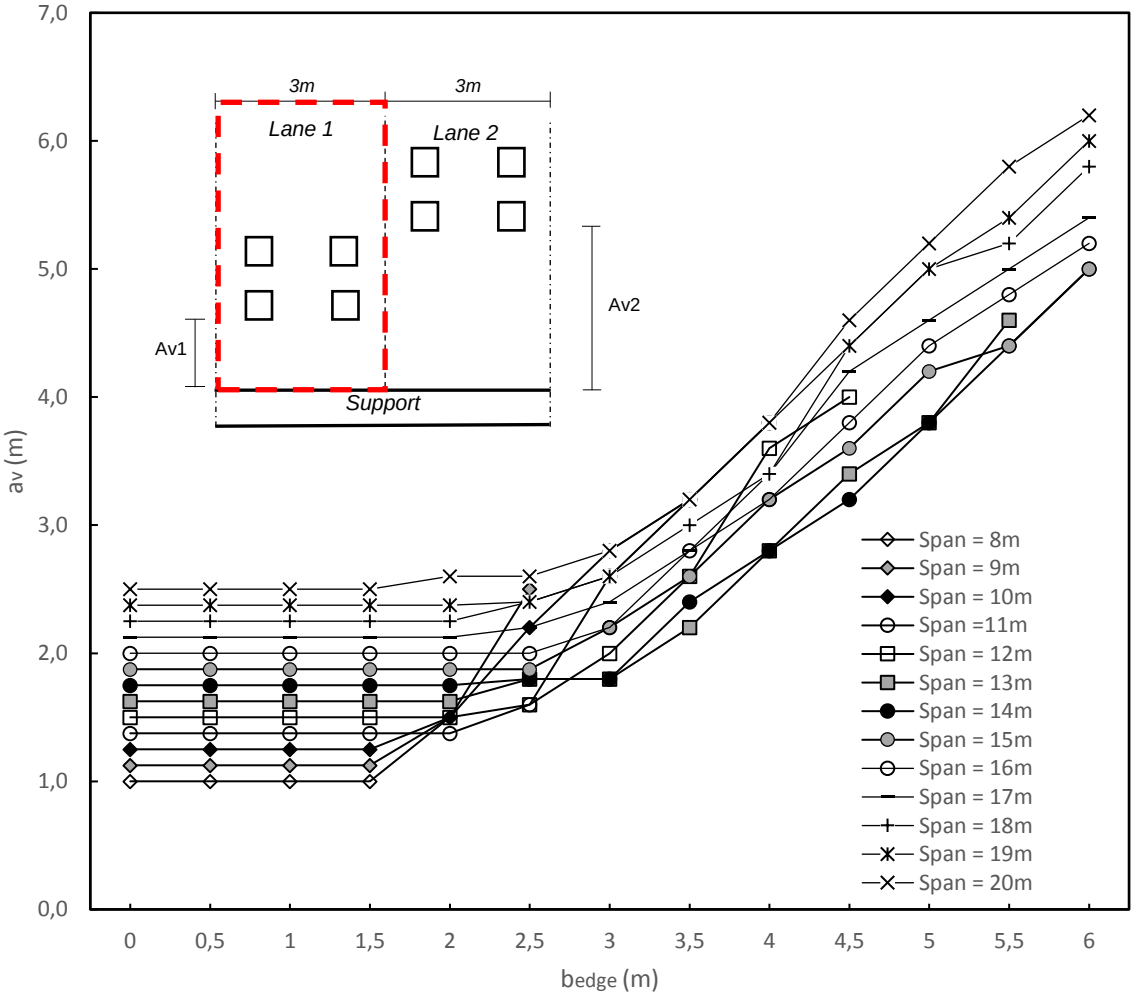

Figure 7-13 - a_v lane 1 for different spans and edge distances

7.5.2.2 Results

The occurring shear stress near the edge of the support for different spans and edge distances for a slab in uncracked state is illustrated in Figure 7-14. The exact values can be found in *Appendix J – Comparing shear forces*. These values are compared with the values of the shear force near the middle of the support in order to determine whether the edge or the middle of the support is governing for a certain combination of edge distance and span (chapter 7.5.3). This leads to the critical edge distance for different spans where the middle of the support becomes governing above the edge.

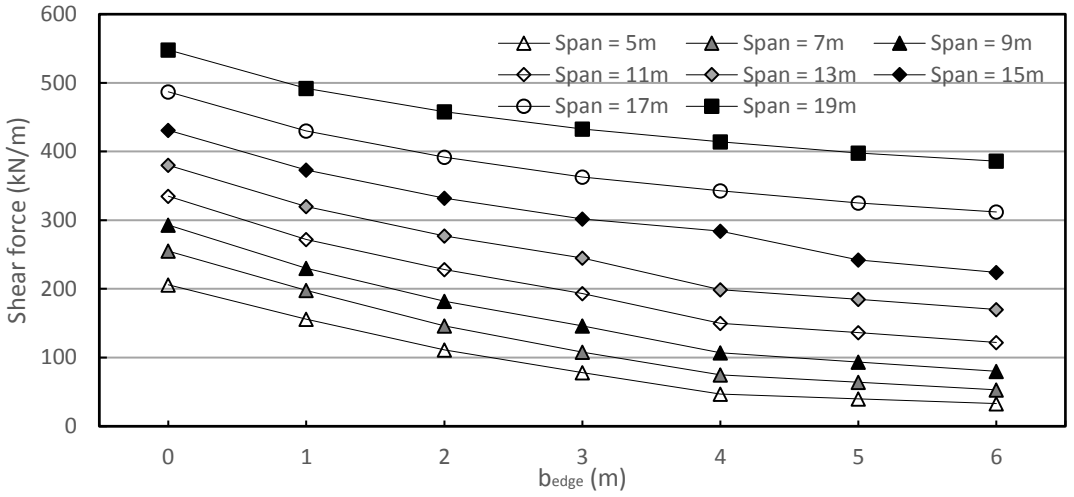

Figure 7-14 – Shear force near the edge of the support for different spans and edge distances (uncracked)

7.5.3 Comparing results

The results of Figure 7-12 and Figure 7-14 (uncracked slabs) were compared in order to determine the critical edge distance. Also, the results for cracked slabs were compared. These are results for prefab slabs, since a peak force due to self-weight near the edge of the support exists. In addition, results for in-situ slabs are compared. The combination of edge distance and span when the shear stress near the middle is the same as the shear stress near the edge of the support was found. This eventually gave a set of combinations which gave a boundary line. Below this boundary the edge is governing in shear and above this boundary the middle of the support is governing. This boundary line can be found by calculating the intersection of the different graphs.

7.5.3.1 Results uncracked prefab slabs

The effective width of the axle loads for uncracked slab is higher than for cracked slabs. Therefore it is expected that the edge is governing for more bridge dimensions than for cracked slabs. The comparison of the shear forces for all different spans has been done in the following way. Excel has been used to determine the formula of the graphs of Figure 7-12 and Figure 7-14. Maple 18 has been used to calculate the intersections of these formulas (*Appendix M – Determination critical edge width)*. The results are demonstrated in Table 7-3 and these points have been transformed into a graph (Figure 7-15).

Table 7-3 - The critical span for the intersection of the curves from Appendix M – Determination critical edge width, chapter 13.1

Span (m)	Edge distance (m)
5	0,8
7	1,1
9	1,3
11	1,7
13	2,3
15	3,2
17	4,4
19	6,5

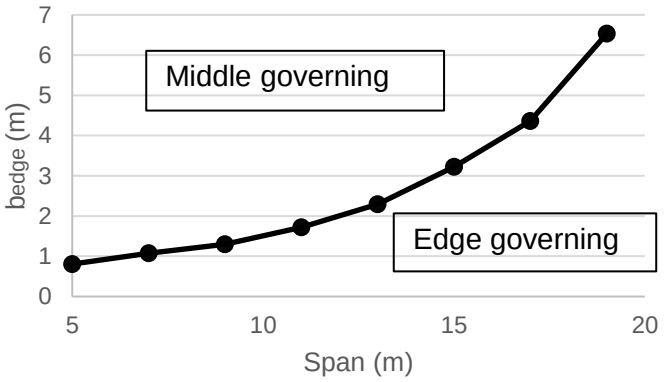

Figure 7-15 - Graph for the determination of the governing part of the support (uncracked prefab slab)

Figure 7-15 looks like an exponential graph. This has to do with self-weight for an increasing span. An increasing span means an increasing thickness of the slab. This leads to more self-weight which increases the shear force peaks at the edge of the slab. This goes together with a decrease of the shear force peak at the middle of the support due to the axle loads that are placed further from the support for an increasing thickness (av = 2,5*d). For edge distances smaller than 0,8m the edge of the support is governing in shear. The formula that fits best is equation 7.1 (values in [m]). The edge is governing if:

$$b_{edge} \leq 0{,}0027L^3 - 0{,}06L^2 + 0{,}6L - 1{,}0 \qquad \textit{(7.1)}$$

7.5.3.2 Results cracked prefab slabs

Appendix M – Determination critical edge width reveals values for determining the critical edge width of cracked slabs. This has been done by calculation the intersections of the different maximum shear force graphs.

Table 7-4 The critical span for the intersection of the curves from Appendix M – Determination critical edge width, chapter 13.2

Span (m)	Edge distance (m)
5	0,5
7	0,6
9	0,8
11	1,0
13	1,3
15	1,5
17	2,1
19	2,7

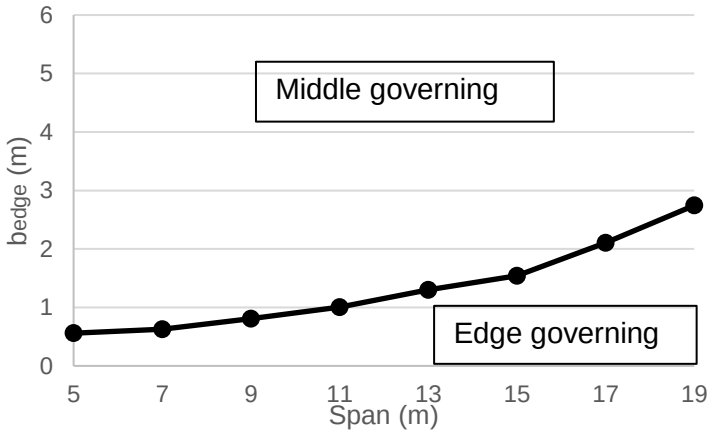

Figure 7-16 - Graph for the determination of the governing part of the support (cracked prefab slab)

For cracked slabs the middle of the support is governing for large edge widths. For an increasing span the self-weight becomes slightly more significant and the peak at the middle of the slab decreases. This leads small increase in the graph of Figure 7-16 at large spans. For edge distances smaller than 0,5m the edge of the support is governing in shear. The formula that fits best is equation 7.2 (values in [m]). The edge is governing if:

$$b_{edge} \leq 0{,}01L^2 - 0{,}11L + 0{,}87 \qquad \textit{(7.2)}$$

7.5.3.3 Results uncracked in-situ slabs

For in-situ slabs the middle of the slab is governing for more combinations of edge width and span than for prefab slabs. This is because the self-weight does not lead to an increase in shear force near the edge due to the lack of torsional moments near the edge. Therefore only the variable loads have influence on the critical edge distance. The critical edge distance is illustrated in Table 7-5 and Figure 7-17. The formula for this graph can be approximated by the a linear equation. The edge is governing if:

$$\boldsymbol{b_{edge} \leq 0{,}1L + 0{,}24} \qquad \textit{(7.3)}$$

Table 7-5 - Critical combination of span and edge width for the middle or the edge of the support governing in shear

Span (m)	Edge distance (m)
5	0,9
7	1
9	1,1
11	1,3
13	1,4
15	1,6
17	2
19	2,4

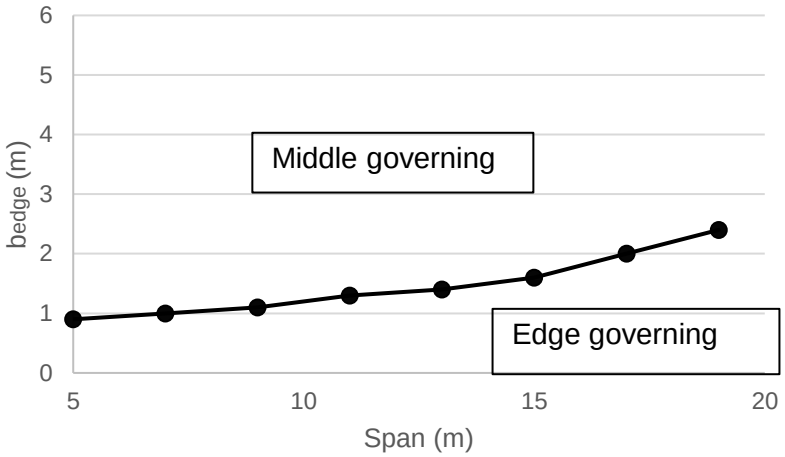

Figure 7-17 - Graph for the determination of the governing part of the support (uncracked in-situ slab)

7.5.3.4 Results cracked in-situ slabs

For cracked slabs the middle is governing more often due to the fact that axle loads spread less in a cracked slab. The critical edge distance is illustrated in Table 7-6 and Figure 7-18. The formula for this graph can be approximated by the a linear equation. The edge is governing if:

$$b_{edge} \leq 0,07L + 0,24 \qquad (7.4)$$

Table 7-6 - Critical combination of span and edge width for the middle or the edge of the support governing in shear

Span (m)	Edge distance (m)
5	0,6
7	0,7
9	0,8
11	1
13	1,1
15	1,2
17	1,4
19	1,5

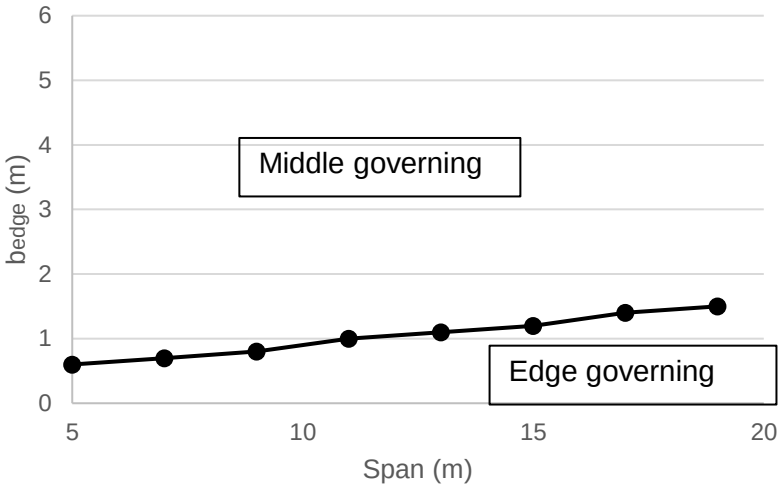

Figure 7-18 - Graph for the determination of the governing part of the support (cracked in-situ slab)

7.6 Conclusion

In order to gain insight in the force transmission in concrete slabs, the permanent and variable loads were investigated separately. This was done with FEM research using theories from literature for assumptions. The variable parameter were span and edge distance. Distinction was made between cracked and uncracked slabs and shear forces near the middle and near the edge of the support. Also, the axle loads end permanent loads were investigated separately. In addition, distinction was made between prefab slabs and slabs cast in-situ, which results in a constant sheaf force on the support due to self-weight for in-situ cast slabs.

Due to cracking of the slab the longitudinal and especially the transverse stiffness decrease. This leads to less spread of wheel loads which leads to a smaller effective width. Therefore, for cracked slabs the middle of the support is mostly governing for municipal bridges with a significant edge distance. For uncracked slabs, the axle loads can spread further to the edge. Also, peak forces due to permanent loads near the edge are slightly higher for uncracked slabs. For uncracked slabs the edge is governing for large spans and small edge distances, and the middle is governing for small spans and large edge distances. This only count for prefab slabs.

The self-weight of in-situ slabs does not lead to peak forces near the edge of the support. This results to the middle of the support being governing in more cases. For cracked existing slab bridges cast in-situ, the middle of the support is governing for an edge distance larger than 1,5m. The edge is governing for and edge distance smaller than 0,7m and in between it depends on the span.

Section 3 –
Quick Scan model

8 Quick Scan model

8.1 Introduction

The final goal of this thesis is the development of a Quick Scan model for existing municipal concrete slab bridges. Findings from researches as described in this thesis are used to create the model. The Quick Scan has to give more conservative results than the results from finite element modelling. Therefore, the comparison with these results was made. This is described in chapter 7. On the other hand, the Quick Scan has to be fast and easy to use. For this reason it is a spreadsheet based Quick Scan, developed with Excel. Also, it has to be accurate, otherwise a large number of bridges would have to be strengthened or replaced unnecessarily. In the following chapter, the assumptions and scope of the model are explained.

8.2 Scope

This Quick Scan model is especially designed for the critical bridges. These are mostly the existing bridges from before 1980. Also, small reinforced slab bridges are most critical. Prestressed slabs will therefore not be assessed extensively. In general, bridges from before 1980 with a small span (smaller than 15m) are not prestressed. In municipalities, most concrete slab bridges are small span statically determined structures. With these assumptions, the Quick Scan can be less conservative and more precise, which leads to a more reliable outcome.

8.2.1 Background

The calculations as made by the Quick Scan are described in this thesis. Especially chapter 4 described assumptions used in the Quick Scan. In Chapter 3, the determination of the partial factors for existing municipal bridges is described, which are used in the Quick Scan. In Chapter 6,the recommended α factor for certain bridge dimensions is described. Finally, chapter 7 contains the results for FE modelling which lead to more insight in the force transmission in concrete slabs. The results are compared with results from the Quick Scan.

8.3 How to use

The Quick Scan model is an easy to use model that can be used when a relatively small number of parameters of a bridge are known. The model consist of an input/output tab and several additional (calculation) tabs. These tabs will be elaborated briefly.

8.3.1 Material properties tab

In this tab material properties as described in the RBK [5] are displayed. The user can choose the right material strength if this is known. If these parameters are unknown, the model can chose the least favourable property according to the building year. In this case the least favourable property according to the code that was uses in the building year of the bridge is chosen automatically. The material parameters of interest are concrete class and reinforcing steel type (and prestressing steel type).

8.3.2 Axle loads tab

In this tab the governing axle load configuration is calculated. This is divided in the axle load configuration for which the edge- and for which the middle of the support is governing for shear. Making use of several rules and assumptions the governing axle configuration for different dimensions is determined automatically. This is explained briefly in this chapter.

As minimum distance from the support a distance of 2,5*d has been assumed as described in chapter 4.3. Therefore, the load configuration for the middle of the support as governing location only depends on the thickness. For the tests in RFEM and the comparison with the Quick Scan

model, the thickness was assumed to be a function of the span (h = L/20). For the determination of the location of the axles, the width of the bridge is the y-axis and the length of the bridge is the x-axis. When the location of the first axle is known, the location of the other axles are known automatically. A top view for the governing load configuration for the middle of the support is illustrated in Figure 8-1.

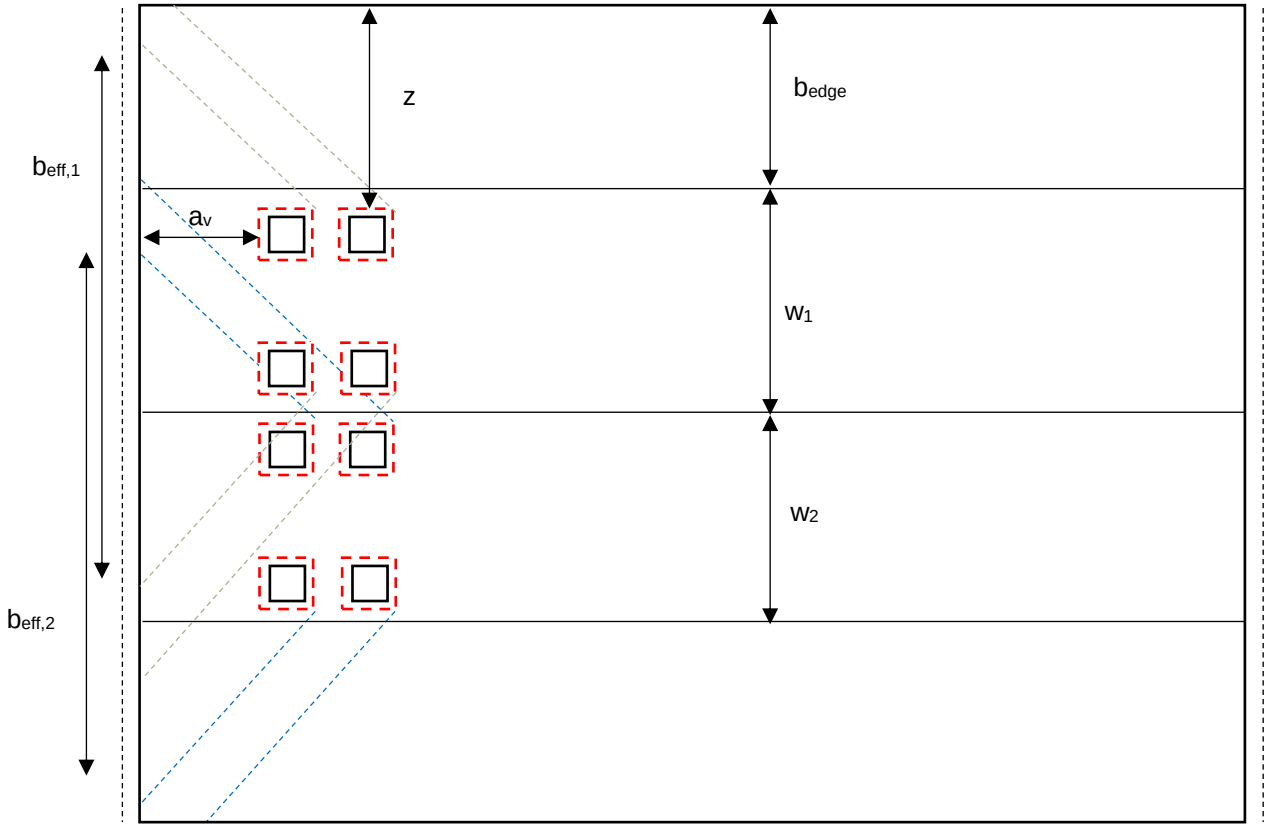

Figure 8-1 - Load configuration for the maximum shear force near the middle of the support

The governing load configuration for the situation where the edge of the support is governing is not the same. For this situation, findings from recent researches at the TU Delft are used as described in chapter 4.4. These researches conclude that a transverse force transmission under and angle of 45° can be assumed. The minimum distance of 2,5*d to the support does not apply for every dimension. For large edge distances the axles are placed further from the support to spread to the edge of the support. The tandem system on the first lane is placed at the maximum of the following values: 2,5*d and z – load width. The latter is due to the assumed force transmission under an angle of 45°. A top view for the governing load configuration for the edge of the support is illustrated in Figure 8-2.

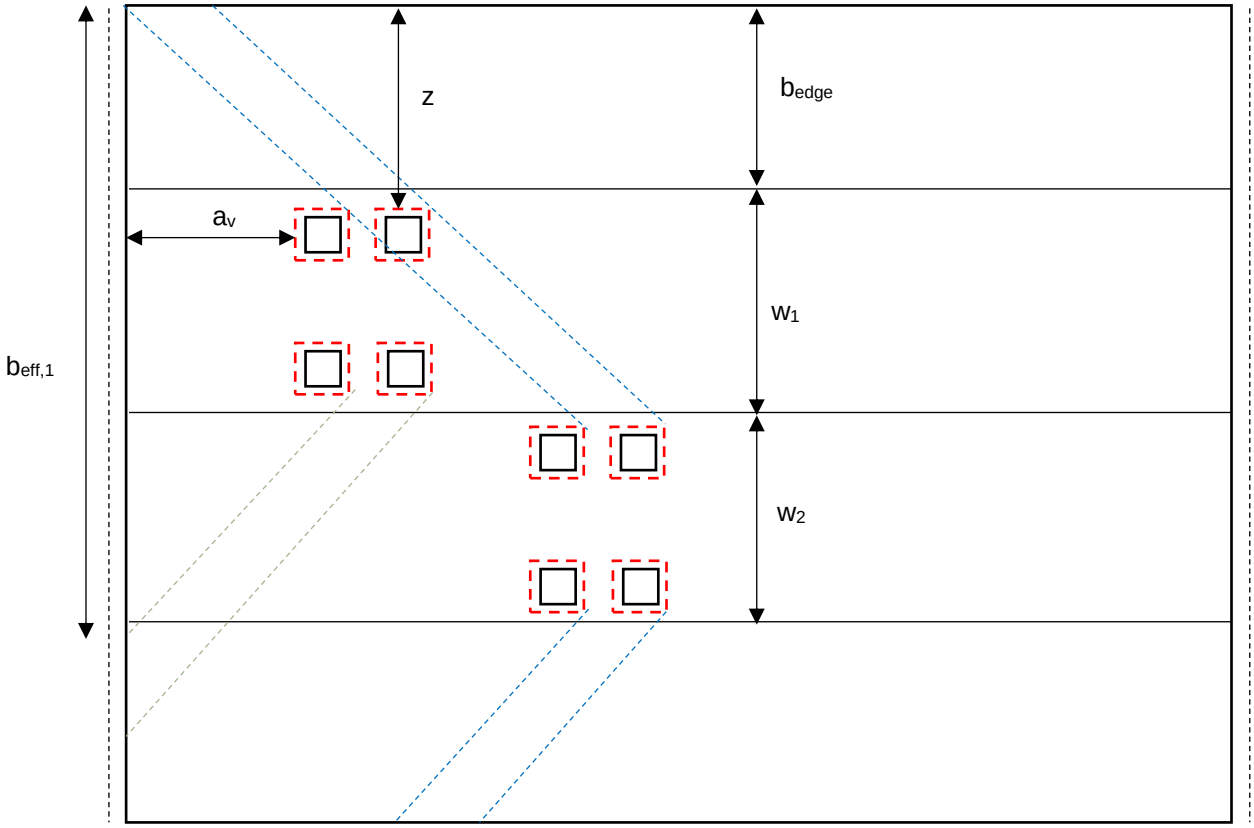

Figure 8-2 - Load configuration for the maximum shear force near the edge of the support

Constants and variables from Figure 8-2 and Figure 8-1 are explained below.

Constants:

Gauge =	2,0m
Axle distance =	1,2m
Wheel contact area =	400mm x 400mm
Wheel load area =	540mm x 540mm
Width notional lane 1 (w_1) =	3,0m
Width notional lane 2 (w_2) =	3,0m

Variables:

$a_v = 2{,}5*d$ for middle support governing

$a_v = z$ - load width for edge support governing

$$z = b_{edge} + \frac{w_1 \text{- gauge - load with}}{2}$$

$$b_{eff,1} = 2*(a_v + \text{load with}) + \text{gauge} + \text{load width}$$

From the calculated axle locations a top view of the governing tandem system configurations was made in Excel.

8.3.3 Calculation shear force tab

The tab ‘Calculation shear force’ is the ‘engine’ behind the model. In this tab different parameters are calculated which lead to the governing shear force.

8.3.3.1 Peak force due to permanent loads

In chapter 7.4.1, the shear force due to permanent loads was compared. To simulate the shear force in the right way, the peak forces near the edge of the support due to torsional forces need to be modelled. This is done according to results from the FEM research. The magnitude of the peak depends on the span and the edge width. The greatest peak occurs at a span of 20m and large edge widths. In this case the shear force near the edge is a factor 1,3 higher than near the middle. For every combination of span and edge distance the right factor is chosen by the model. In every case a conservative approach was chosen.

In this part of the tab, also two possible reductions are described. The first reduction is for an odd shape of the transverse cross-section. For example a reduced thickness near the edge of the slab. The second reduction for the direct load transfer of permanent loads close to the support. The reduction is performed as illustrated in Figure 8-3 [33].

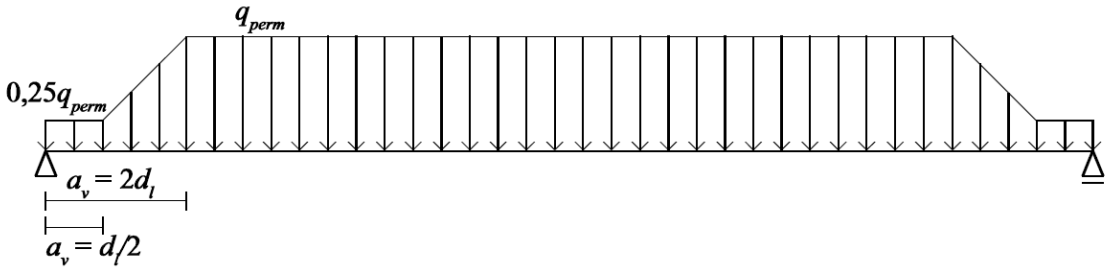

Figure 8-3 - Resulting distributed load for permanent loads when β(x) is taken into account [36]

Additional permanent loads can be present due to an edge beam or due to additional soil on the bridge.

8.3.3.2 Calculation UDL loads

The additional UDL load on lane 1 spreads to the support. As for the axle loads, a spreading angle of 45° was assumed. This leads to the maximum shear force on lane one. The shear force decreases toward the edge of the slab. For very small spans with large edge widths the additional loads on lane 1 cannot spread to the edge entirely.

For the ease of modelling, the calculation for the shear force due to the additional loads on lane 1 is divided into 4 parts as illustrated in Figure 8-4.

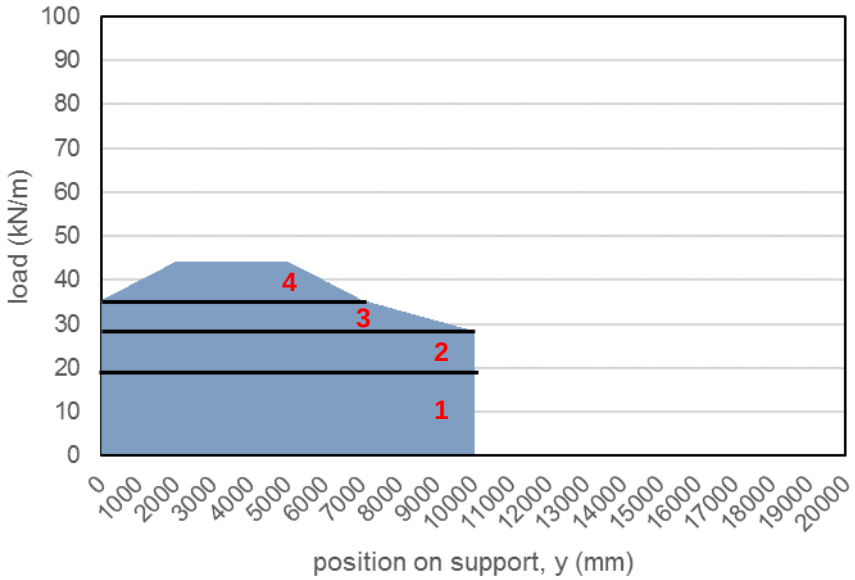

Figure 8-4 – Example of the calculation of the shear force due to UDL loads (Span = 15,0m, b_{edge} = 2,0m)

The different parts can be explained as follows:

Part 1. Shear force due to UDL load on the entire bridge;
Part 2. Constant part of the shear force due to the UDL on lane 1
Part 3. Shear force due to the UDL on lane 1, constant part at the left edge as upper boundary;
Part 4. Remaining part of the shear force due to UDL on lane 1, which increases till the location of lane 1 (width = 3,0m).

8.3.3.3 Correction factors cracked slabs

The Quick Scan model is calibrated on uncracked slabs. Most experimental researches were done on uncracked slabs. Also, force transmission in cracked slabs is a complex phenomenon as described in chapter 5.2.3. In order to make the Quick Scan model applicable for cracked slabs, results from the FEM research were used. The used results are illustrated in Appendix Figure 10-6 and Appendix Figure 10-7. The formulas of the graphs shown in these figures are used to calculate the reduction or amplification factor for shear force of cracked slabs. Since only the factor for a limited number of combinations is known (steps of 2m for span and steps of 1m for the edge width), in every case the most conservative value was chosen.

8.3.3.4 Shear force due to axle loads

Shear force due to permanent loads and UDL loads in both the RFEM model and the Quick Scan Model were approximately the same. On the contrary, the force transmission of the axles loads to the support is a complex phenomenon which depends on a lot of factors. There is lack of knowledge of the exact load transmission to 'translate' this phenomenon to the Excel model. In order to verify this, the occurring maximum shear stresses in the RFEM model and Excel model were compared. This was done for the maximum shear force near the middle and near the edge of the support. For the middle of the support, two different load transfer mechanisms were investigated (Figure 8-5).

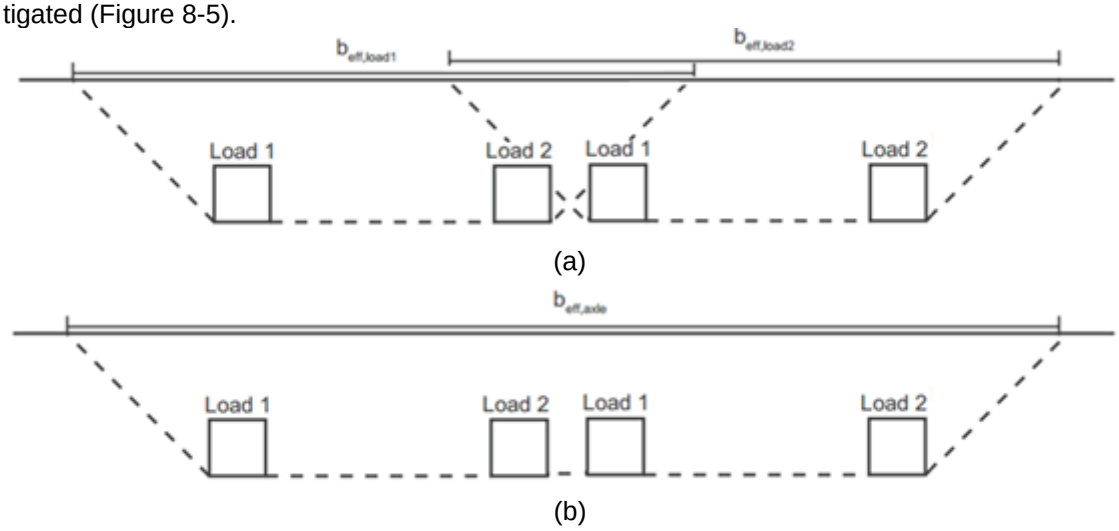

Figure 8-5 – Effective width of two axles separately (a) and two axles together (b)

Regarding the force spreading ability of a slab, mechanism (a) is expected to be too conservative, since the peak shear force in the middle might be too high. Mechanism (b) is expected to give too low shear forces. In this mechanism the forces from the 4 axles spread over the entire effective with. Although the slab has the ability to spread the axle forces over the support, an slight increase of the shear force near the middle is expected, because the two axles stand relatively close to each other. In reality, the occurring shear forces near the middle of the support are expected to lie between the resulting shear stress of mechanism (a) and (b).

Results of the two load transfer mechanisms in Excel were compared with the shear forces due to axle loads in RFEM. Results from RFEM were already known and demonstrated in *Appendix J – Comparing shear forces, chapter 10.1.* The values from the tables with the "shear force due to **axle loads** near the **middle** of the slab, (**uncracked)**" were used. In Excel, the axle loads were

determined by using a 'Macro'. This 'Macro' automatically varies the edge width and the span and notes the occurring shear stresses near the edge and near the middle of the support. The results are demonstrated in *Appendix N – Comparison RFEM – Excel.* As expected, mechanism (a) gives too high maximum shear forces and mechanism (b) gives too low maximum shear forces. In principal, the highest shear forces must be chosen in order to be on the safe side. This would imply that mechanism (a) must be chosen. However, for some configurations this mechanism gives shear forces that are twice as high as the RFEM results. Therefore, mechanism (b) is chosen with an additional amplification factor for the peak due to two axles close to each other. This amplification factor is based on the difference between RFEM and Excel. This difference for different spans and edge widths is illustrated in Figure 8-6. The amplification factor is chosen as 1,05 to 1,25 for an edge distance of 0,0m to 2,0. For larger edge distances the amplification factor is 1,25. This still gives a higher boundary for every span and is therefore legitimate.

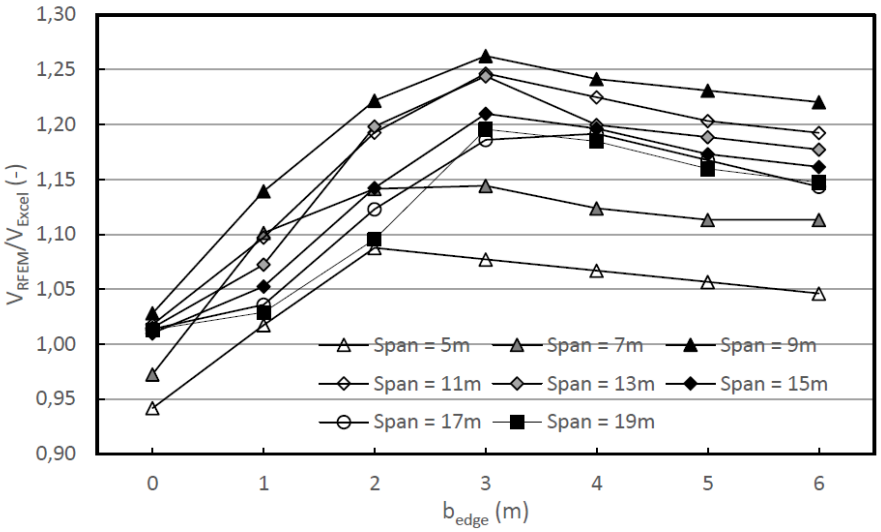

Figure 8-6 - Difference between the occurring shear force near the middle of the slab according to RFEM divided by Excel (load transfer mechanism (b))

The formula for the amplification factor is $\mathrm{AF} = 1{,}05 + 0{,}1{*}\mathrm{b_{edge}} \leq 1{,}25$, with b_{edge} in [m].

8.3.4 Input and Output tab

This tab is meant for the user of the Quick Scan model. It is divided in an input and an output part. Also, an additional part with capacity calculations is added. In this chapter, every parameter that is needed for the input is described briefly. Thereafter, the output part and the capacity part is explained briefly.

8.3.4.1 Input

The input parameters are summed up and described briefly from the top to the bottom of the tab. In the Quick Scan model a remark was made for most parameters. This remark appears when the cell is clicked. On the right hand side of the parameter, the chapter with more information is mentioned.

General

- Consequence class: This class is directly linked to the risk classes and the reliability index. The different classes stand for the consequence of failing of the structure regarding human life. Governmental bridges commonly fall in CC3. Municipal bridges often fall in CC2, and sometimes in CC1. When the consequence class is unknown, CC2 is recommended.
- Assessment level: Is the level on which the structures has to be regarded. Different reliability requirements for existing structures exist. Rebuild level, rejection level and new built level can be chosen. The assessment level is directly related to the reliability index and therefore to the partial factors.

- A factor: This factor is meant for the reduction of the LM1 loads. The reduction can be based on expected traffic loads, age of the structure and the span of the bridge. On the right hand side of this factor the recommended value is given, based on a comparative FEM research.
- Building year: If the building year is known and the material properties are not, the minimum material properties used in the year of construction are used.

Material Properties

- Concrete class: The concrete class (compressive strength) is used to determine the minimum shear capacity of the bridge. For existing governmental bridges a minimum concrete class C35/C45 is allowed to be assumed. For municipal bridges this has to be discussed with the owner of the bridge. Otherwise the minimum value has to be based on the year of construction;
- Reinforcing steel type: The steel type (yield strength) is also used to determine the minimum shear capacity of the bridge. Note that a higher yield strength means a reduction of the minimum shear capacity. For old bridges (in any case bridges built before 1964) mostly the steel type QR240 was used. Older bridges used higher quality steel. For municipal bridges the steel type has to be discussed with the owner of the bridge. Otherwise the maximum (!) value has to be based on the year of construction;
- Prestressing steel: In principle, the Quick Scan model is not meant for prestressed bridges. Only if the working prestressing stress of the tendons are known, prestressing force can be taken into account. However, there was assumed that prestressed bridges are not critical for shear (yet).

Bridge dimensions

- General: Bridge dimensions are required for the Quick Scan model. All dimensions need to be in [mm] with the significance of 10mm. The span is the distance from support to support (front side of the support). The edge distance is the distance from the carriageway to the edge of the slab. If the cross-section has a variable thickness, the thickness in the middle of the slab has to be noted;
- Transverse cross-section: If the cross-section has a non-rectangular shape the force transmission becomes complex and the assumed effective width does not apply. In the case of a non-rectangular cross-sections the shear force at the angle is checked together with the shear force near the middle of the support. In most cases the middle of the support is governing;
- Longitudinal cross-section: Some bridges have a longitudinal cross-section with a varying thickness. In this case the force transmission becomes complex. The quick scan checks 2 places: the shear force at the increased thickness at the support and the shear force at the angle. This is calculated by assuming a reduced span until the slab is rectangular. This is illustrated in Figure 8-7. The calculation is performed by a macro.

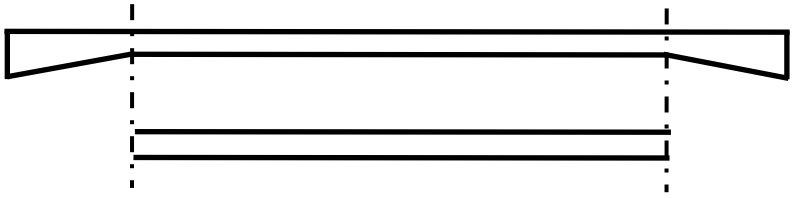

Figure 8-7 - Illustration of the assessment of a varying longitudinal cross-section

Since the lack of additional research to varying longitudinal cross-sections, a bridge with a tapered longitudinal cross-section should be regarded as informative only.

Additional information

- Longitudinal edge beam: The edge beam is assumed to give extra permanent loads on the support. In practice, an edge beam could lead to higher shear capacity near the edge of the slab. However, in most cases some dilatation joints are applied. This leads to uncertainty in the additional shear capacity. Therefore the edge beam is assumed to lead to additional permanent load only;

- Additional soil on bridge: An additional layer of soil can be applied. Only the thickness and the density have to be known. The layer is assumed to cover the entire bridge. For varying thickness of the layer an average can be assumed. In practice, an additional layer between the asphalt and the concrete slab leads to greater spread of the axle loads. However, since the force spread through this layer is unknown and depends on various variables, the conservative assumptions was made that the additional layer does not affect the force spreading.

8.3.4.2 Output

The output tab is divided into a part 'middle governing' and a part 'edge governing'. In the first figure the top view of the bridge with the governing places for the tandem system is illustrated. These governing places are calculated automatically making use of the input. This was done in the 'Axle Loads' tab. The second two figures are the occurring shear stresses on the support according to the Quick Scan model. This was calculated in the 'calculation shear force' tab. Below these figures the maximum occurring shear force near the middle and the edge of the support are demonstrated. This is divided into cracked and uncracked slabs. Also, some special cases for varying longitudinal or transverse cross-section are treated. Below this part the governing place together with the maximum occurring shear force is shown. From the 'Shear Capacity' part the Unity Check is calculated. The used formula for the shear capacity depends on the input. If the longitudinal reinforcement is unknown, the formula of unreinforced concrete according to the RBK is used (v_{min}).

8.3.5 Macro tab

The Macro tab contains a macro which calculates user specified loads. For example axle loads or permanent loads. The macro performs a total of 112 calculations. These calculations are the maximum loads near the edge and near the middle of the support for different values of the span and the edge distance. In this way a quick overview of certain loads for different dimension is given. The Macro tab is programmed on calculating the maximum loads. Cell L17 and L29 can be adapted to the desired loads. The loads are calculated by clicking 'RUN macro'. The maximum shear force is automatically noted together with the place on the support (edge or middle).

8.4 Parametric analysis

For some important parameter a parametric analysis is performed. The possible values for the parameters are compared. The parameters span end edge width have been considered extensively in chapter 7. Other parameters that are expected to be of influence are the thickness, concrete compressive strength and yield strength of the reinforcing steel.

8.4.1 Concrete class

The concrete compressive strength and therefore the concrete class is important for the shear capacity. Since the actual compressive strength of an existing structure is not known accurately, material tests can be beneficial for knowledge of the capacity. In Figure 8-8 the influence of the compressive strength is demonstrated. Since the square root of the compressive strength is in the formula for v_{min}, v_{min} increases as the square root of the compressive strength.

8.4.2 Steel type

Some experiments show a higher capacity for reinforced concrete with plain bars. Less shear cracks were observed which leads to a less reduced concrete compressive zone. For the determination of v_{min} this was not taken into account. Figure 8-8 shows the influence of the yield strength on the shear capacity. the concrete compressive strength is divided by the square root of the yield strength. This means v_{min} decreases as the square root of the yield strength.

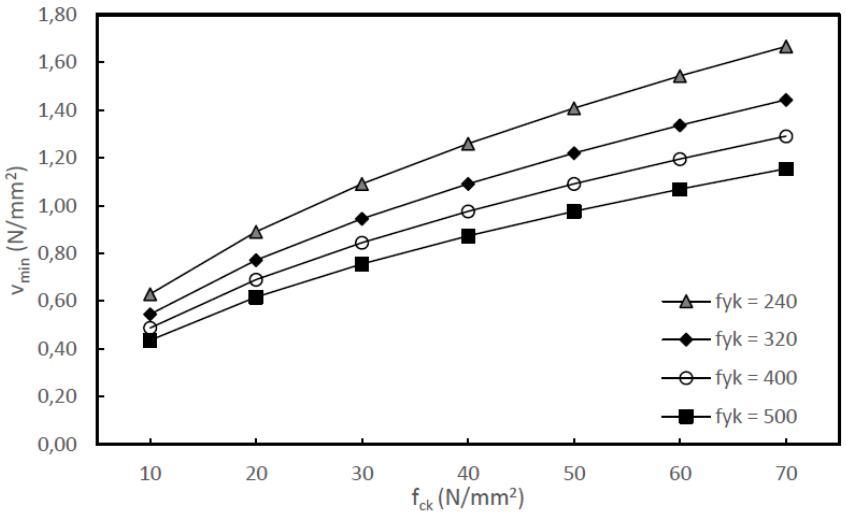

Figure 8-8 - v_{min} for different values of f_{yk} and f_{ck}

If the steel quality is unknown, rules from the RBK should apply. The RBK [5] states: 'Without tests to the steel quality, the lowest possible steel type from the corresponding standard has to be applied'. This is questionable since a low steel type leads to high shear capacities. This rule should only be followed if there is a reason to believe this is true. Assuming the highest possible steel type is mostly too conservative, especially in combination with the lowest possible concrete strength. This would mean that a bridge from 1970 with unknown material characteristics has to be calculated with f_{ck} = 9 N/mm^2 and f_{yk} = 500 N/mm^2. This is a combination that does not exist in practice.

The following proposal is made. If material properties are unknown this Quick Scan cannot function as determination of the structural safety of a structure. In this situation, the Quick Scan can be used as estimation of the structural safety, and as categorization for a range of different bridges. In this case rules for existing bridges according to the RBK are used (normally used for governmental bridges). For slab bridges with a building year before 1976 a concrete class of C35/45 is assumed. Bridges that were built after 1976 the concrete compressive strength should be determined by material testing. For the Quick Scan model, the compressive strength of these bridges can also be assumed as C35/45. The steel type is chosen according to the building year. If the building year is unknown, an estimation can be made. QR24 is used for bridges before 1962 and QR40 is used for bridges before 1980. FeB 500 should be used as steel type for bridges after 1980. If the material properties are known, this model can be used as verification for the structural safety of existing concrete slab bridges.

8.4.3 Thickness slabs

The thickness of the slab has influence on different parameters. An increase of the thickness means an increase of the self-weight which leads to higher shear forces. However, with this increase also the capacity of the slab increases for an increasing thickness. When regarding direct load transfer for axle loads nearby the support, the thickness has influence on the distance of the axles to the support. Consequently, this has influence on the effective width of the axle loads and the force transmission to the opposite support. The thickness of the slab also has influence on the k factor for the capacity of the slab. For the determination of the occurring shear stresses in RFEM the thickness was a function of the span (h=L/20). It is therefore interesting to vary the span as well.

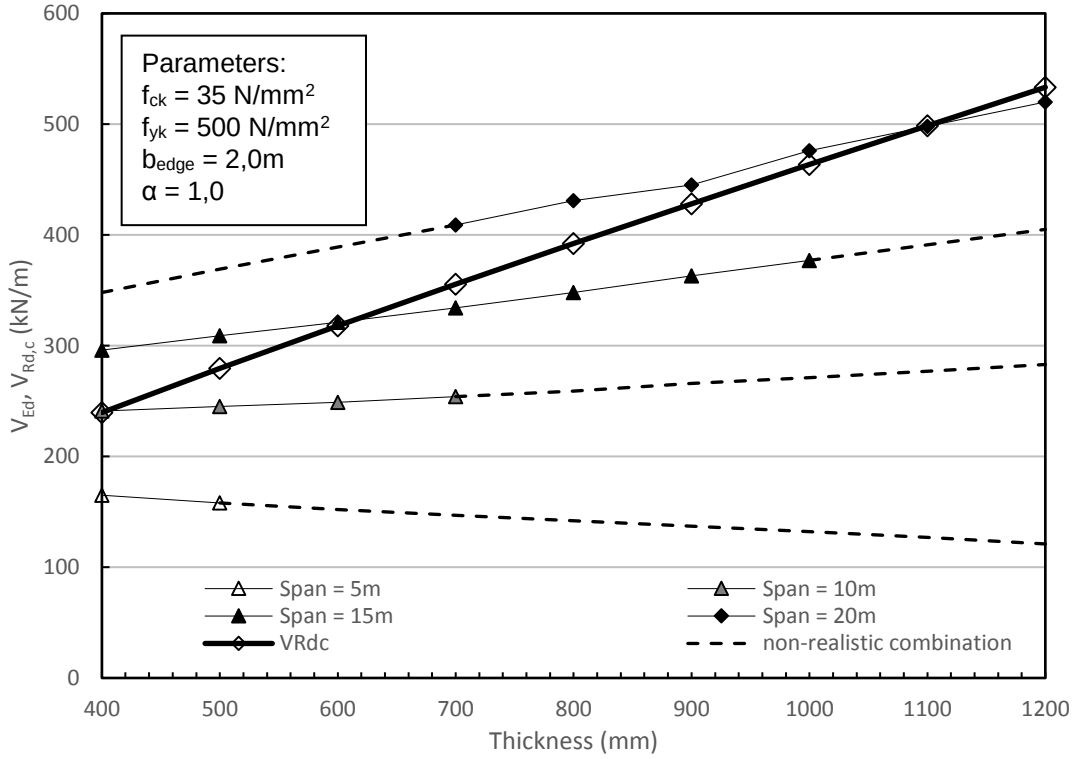

Figure 8-9 - Shear force and shear capacity for varying thickness

Since the thickness has influence on both the capacity and the loads, the unity check has to be compared for the parameter analysis. The results for the shear force and shear capacity for varying slab thickness is illustrated in Figure 8-9. Parameters that are less of interest for showing the influence of the slab thickness, such as edge width, concrete compressive strength, yield strength of the reinforcing steel partial factors, are kept constant and given in the figure. Dashes lines indicate results for a combination of span and thickness that not occur in practice.

As illustrated, the capacity does not depend on the span. For small spans the loads decrease for an increasing slab thickness. This comes due a larger distance to the support for thicker slabs. This leads to larger effective widths. For very small spans this outweighs the increase of self-weight. For larger spans the increase of the self-weight becomes more significant and the shear force increases for an increasing span. The shear force and shear capacity are divided to the Unity Check as illustrated in Figure 8-10. Some combinations of span and thickness do not exist in practice, such as a large span and a small thickness. These combinations are indicated as dashed lines.

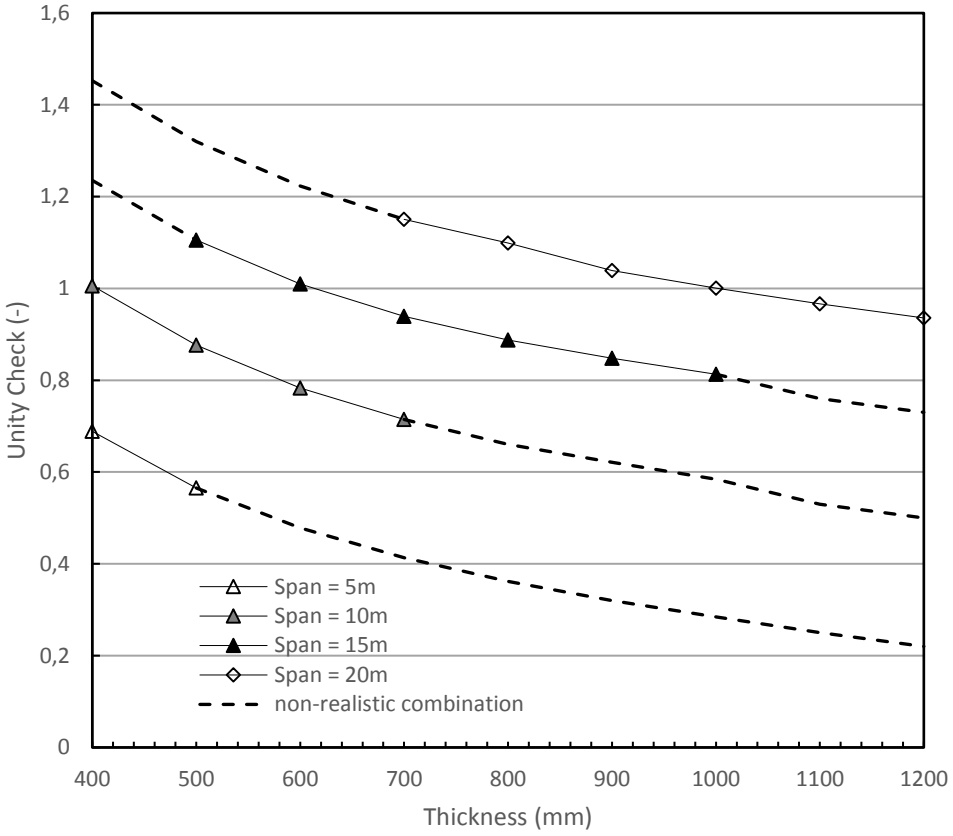

Figure 8-10 - Unity check for shear force for varying thickness

8.4.4 Comparison RFEM and the Quick Scan Model

The Quick Scan model was tested with the results from finite element modelling. For this comparison, a macro was created to reduce time for data gathering (See chapter 8.3.5). The Quick Scan was originally created using the theoretical rules for load transfer. However, this did not result in the correct resulting shear forces for every combination of dimensions. Some adaptions were made to approach reality in a better way. Besides, the Quick Scan model should give the same or a more conservative results than the finite element modelling results. With the adaptions as described in chapter 8.3, the results of the Quick Scan model and FEM results were compared. This check was done by dividing the shear force from RFEM with the shear force form the Quick Scan model. For every dimension, the resulting factor should be below 1,0. The resulting shear force from RFEM is shown in *Appendix J – Comparing shear forces, chapter 10.1.* The resulting shear force from the Quick Scan with the comparison is shown in *Appendix N – Comparison RFEM – Excel, chapter 14.2.* In total 4 comparisons were made. Shear forces near the middle and the edge of the support, for cracked and uncracked slabs. An example of the comparison between RFEM and Excel for the edge and the middle of the support (uncracked slabs) is illustrated in Figure 8-11 and Figure 8-12. In principle, the factor V_{RFEM}/V_{Excel} should be lower than 1,0 in every case. For some combinations (edge width of 0,0m, and a span of 5m in combination with large edge distance) this is not true. However, this is still acceptable, since an edge distances of 0m does not exist in practice. If the edge distance increases slightly, the factor reaches 1,0. For the combination of small span and large edge distance the middle of the slab is typically governing.

For the other comparisons described in the appendix the factor is 1,0 or lower for all realistic and governing cases. Some higher factors can be observed shear forces near the edge of a bridge with a small span and large edge distance. For this combination of span and edge distance, the middle of the support is typically governing. Therefore these higher factors are not used.

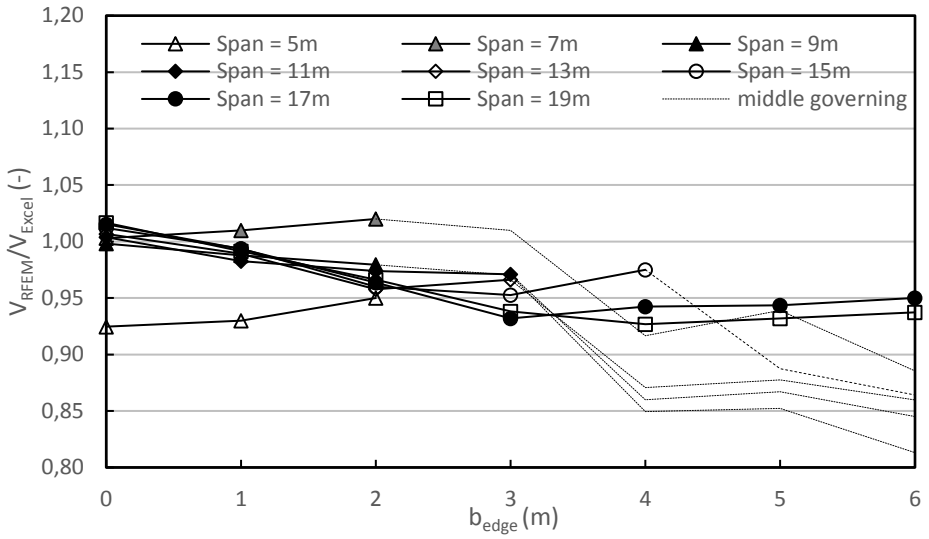

Figure 8-11 – Comparison shear force RFEM and Excel near the edge of the support for uncracked slabs

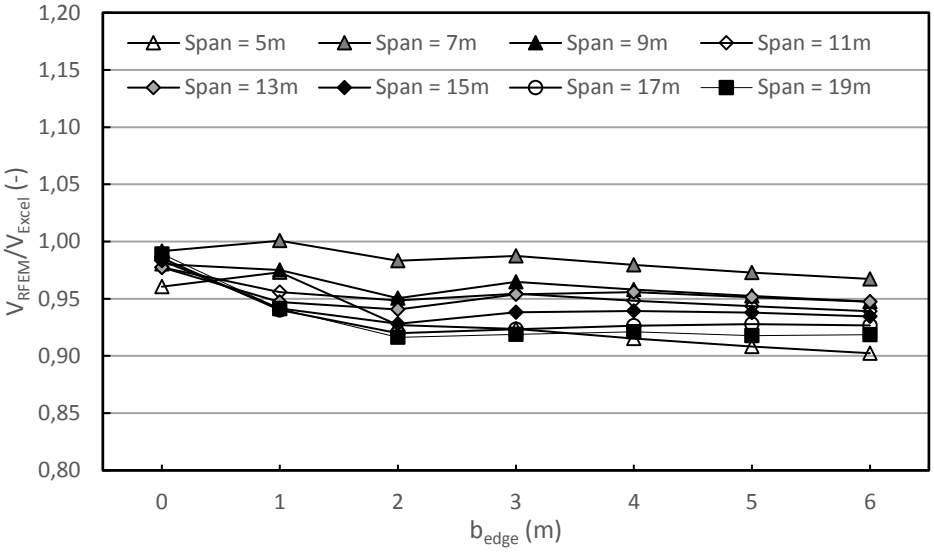

Figure 8-12 - Comparison shear force RFEM and Excel near the middle of the support for uncracked slabs

For every combination of span and edge distance the lower bound of the factor V_{RFEM}/V_{Excel} is 0,8. This means that occurring shear forces of the Quick Scan model have a maximum error of 20%. However, some combinations of span and edge distance do not have to be taken into account. These combinations are visualized as a dashed line. For these combinations, shear forces near the edge are never governing (this is typical for large edge distances). If the dashed lines are not taken into account the error is only 10%. This error is a result of multiple factors. Firstly, occurring shear forces in RFEM show deviations in the expected values. This is the result of the complexity of the load transfer of the 8 wheel loads individually. The deviations increase for increasing edge distance. Secondarily, the averaging of the shear force over 4d and the relatively large mesh size contribute to these deviations. Thirdly, the adaptions of the Quick Scan to approach reality in a better way were typically conservative. For some dimensions more conservative than for other, which lead to larger deviations. In general, differences between RFEM and the Quick Scan model are larger for assessment of the edge of the slab, cracked slabs and larger edge distances.

Regarding Figure 8-11, Figure 8-12, Appendix Figure 14-1, and Appendix Figure 14-2 a general average trend for the edge and the middle of the support can be observed. For the comparison near the edge this is 1,0 for b_{edge} = 0,0 and 0,88 for b_{edge} = 6,0 (on average). For the comparison near the middle this is 1,0 for b_{edge} = 0,0 and 0,93 for b_{edge} = 6,0 (on average). This count for cracked and uncracked slabs. This means that for large edge distances a final Untiy Check form the Quick Scan model just higher than 1,0 does not directly lead to disapproval. The errors of the translation from RFEM to the Quick Scan together other possible errors is quantified in the next chapter.

The critical edge distance was determined with the FEM results. This is the transition point where a combination of span and edge distance changes from edge governing to middle governing. The FEM results for the critical edge distance was compared to the Quick Scan result. Quick scan result were gathered using a macro as explained in chapter 8.3.5.

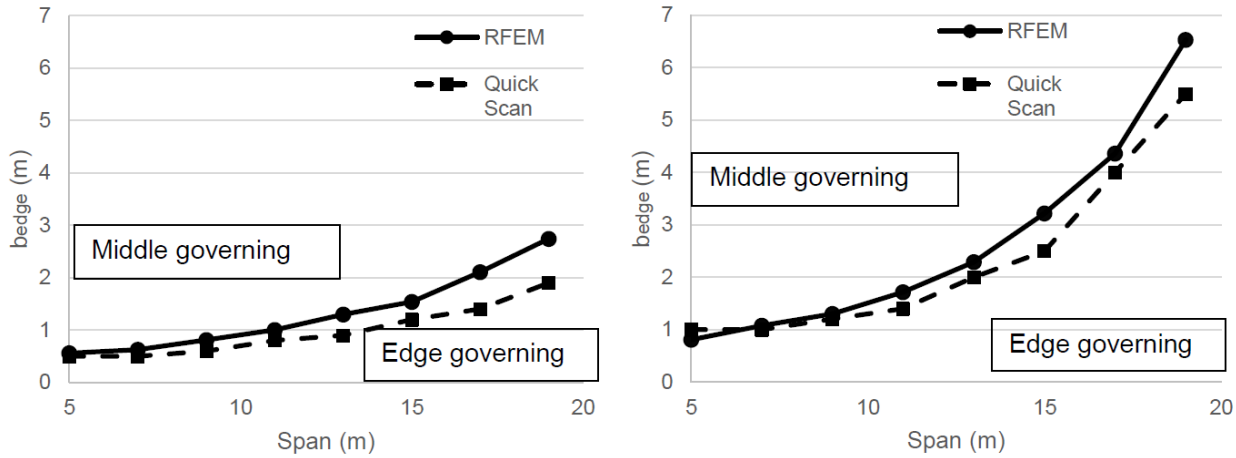

Figure 8-13 - Graph for the determination of the governing part of the support. RFEM results compared to Excel results. Left: cracked slab. Right: uncracked slab

Figure 8-13 illustrates the difference between the critical edge distance for different combinations of spans and edge distances. The shape of the different graphs are the same. Other differences are caused by small errors in the translation from FEM results to the Quick Scan model as described in this chapter. These differences are neglectable.

8.4.5 Critical consideration reliability Quick Scan

Assumptions as proposed in this thesis have influence on the reliability and precision of the output. This should be taken into account when using the Quick Scan model. The reliability and precisions of the output also depend on the given input. In this chapter uncertainties, conservative assumptions and possible irregularities are described. This leads to an error in the output, which is quantified in this chapter.

8.4.5.1 General assumptions

For existing bridges, the β factor for bridge repair was chosen instead of bridge disapproval. This was β = 3,2 instead of β = 2,5. This leads to an increase of the partial factor for variable loads from 1,1 to 1,2. If the disapproval level is chosen, this reduction can be applied.

Static indeterminacy was investigated in [33] for certain combinations of spans. α factors were proposed for the different variable loads. Too little research was done to formulate uniform factors for every dimensions. Therefore a conservative assumption for the α value was chosen. This is α = 1,1 for axle loads and α = 1,3 for UDL loads. These α values should be multiplied with the values found as result of the FEM research. More research is desired to desired for the right assessment of static indeterminacy. Therefore a statically indeterminate slab leads to more uncertainties in the shear assessment.

8.4.5.2 Loads

In the Quick Scan model, the calculation methods are based on literature and adapted according to the FEM results to approach reality in a better way. Since force transmission in slabs due to different permanent and variable loads is a complex phenomenon, no standard rules could be developed. Some empirical formulas based on findings with FE modelling were de developed. Due to relatively large steps in the different variables (2m for span and 1m for edge distance) the formulas are not entirely accurate. This has led to the differences in RFEM and the Quick Scan results as described in chapter 8.4.4. For the check of the edge of the support the maximum error is 23%. For the check of the middle of the support the maximum error is 11%. If only the combination of span and edge distance that are governing (edge or middle of the support) are regarded the maximum error decreases. The maximum error for the edge and the middle of the support is then 6% and 11% respectively. This is illustrated in Figure 8-15 and Figure 8-16. For cracked slabs this error for edge and the middle of the support is 5% and 18% respectively.

Assumptions for the FE modelling process can affect the FEM results compared to reality. The governing vehicle was based on WIM measurements in Rotterdam. The measured maximum axle loads were higher compared to WIM measurement on a governmental highway. This raises questions about the correctness of these loads. Therefore more WIM measurements on different roads in municipalities are desired. In this thesis, the WIM measurements from Rotterdam are used, and since no additional data are available, it was assumed that all values are conservative, as stated in [26] and [27]. To investigate the difference between the current used data and data which are expected to be more typical for municipal bridges, the WIM data are regarded again. Figure 3-19 shows the distribution in ‘normal traffic’ and ‘heavy traffic’. For municipal bridges, ‘normal traffic’ is expected. However, since no since no research was done to traffic in smaller municipalities, this is only an assumption and cannot be used as solid conclusion. Nevertheless, it can be interesting to look at the reduction of loads if ‘normal traffic’ can be assumed. The distinction between ‘normal traffic’ and ‘heavy traffic’ was made for the axle loads as shown in Figure 8-14. The ‘heavy traffic’ path was shown in Figure 3-17.

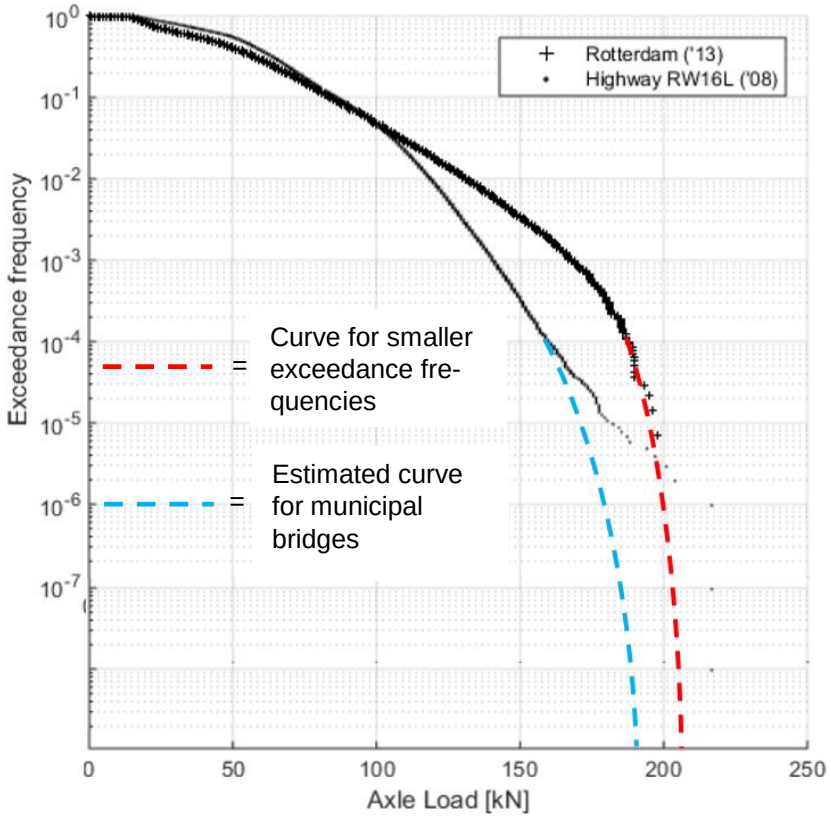

Figure 8-14 - Hypothetical path of the graph for axle loads of 'normal traffic' [4]

[4] This figure is an assumption and should be investigated further

Figure 8-14 shows a decrease of the maximum axle load of 15 kN (from 205kN to 190 kN). The estimated curve for municipal bridges (blue dashes line) ignores the highest axle loads, since these loads are assumed to not be present on municipal roads and bridges. This indicates that an additional research and WIM measurements to the axle loads in municipalities can be beneficial for knowledge about the real occurring axle loads. Next to the axle loads also the axle distance is very important. Further research should improve the Quick Scan by calculating with more realistic axle loads.

8.4.5.3 Shear capacity

The Quick Scan assumes a lower boundary (v_{min}) if the amount of longitudinal reinforcement (or the reinforcement ratio) is unknown. This may lead to an underestimation of the shear capacity. The difference between the two shear force checks is investigated in this chapter. Research was done to the influence of the longitudinal reinforcement ratio. Then, the question can be answered whether it may be beneficial to do extensive investigation of the amount of reinforcement in existing slab bridges.

Tests were performed with the minimum and maximum reinforcement ratio. When the minimum reinforcement ratio is used, the lower boundary for unreinforced concrete (v_{min}) is always governing. When the maximum reinforcement ratio is used, the lower boundary is never governing.

Table 8-1 Minimum and maximum reinforcement ratios for different concrete classes

Concrete class	$\rho_{l,min}$	$\rho_{l,max}$
C25	0,13	1,29
C35	0,17	1,80
C45	0,20	2,32

To give more insight in the influence of the reinforcement ratio, the two different shear checks were compared. The concrete compressive strength was kept constant (f_{ck} = 35 N/mm²) and the thickness, steel quality and reinforcement ratio were used as variable parameters. The values $v_{Rd,c}$ and v_{min} are demonstrated in Table 8-2 and Table 8-2.

Table 8-2 – $v_{Rd,c}$ for concrete elements without shear reinforcement (f_{ck} = 35 N/mm²)

$$v_{Rd,c} = C_{Rd,c} k_{cap} k (100 \rho_l f_{ck})^{\frac{1}{3}}$$

d (mm)	200	400	600	800	1000
k (-)	2,00	1,71	1,58	1,50	1,45
$100\rho_l$					
0,4	0,69	0,59	0,55	0,52	0,50
0,8	0,87	0,75	0,69	0,66	0,63
1,2	1,00	0,85	0,79	0,75	0,72
1,6	1,10	0,94	0,87	0,83	0,80
2,0	1,19	1,01	0,94	0,89	0,86

Table 8-3 - $v_{Rd,c}$ for unreinforced concrete elements (f_{ck} = 35 N/mm²)

$$v_{min} = 0{,}83 * k_{cap}^{\frac{3}{2}} * k^{\frac{3}{2}} * \frac{\sqrt{f_{ck}}}{\sqrt{f_{yk}}}$$

d (mm)	200	400	600	800	1000
k (-)	2,00	1,71	1,58	1,50	1,45
f_{yk}					
240	1,18	0,93	0,83	0,77	0,73
300	1,05	0,83	0,74	0,68	0,65
400	0,91	0,72	0,64	0,59	0,56
500	0,82	0,64	0,57	0,53	0,50

$V_{Rd,c}$ and V_{min} or different parameter combinations are determined. These values are calculated as $V_{Rd,c} = v_{Rd,c}*d*b$ and $V_{min} = v_{min}*d*b$. The shear force per meter is used: b = 1000mm. For f_{yk} = 500 N/mm^2 and f_{yk} =240 N/mm^2 the maximum values of $V_{Rd,c}$ or V_{min} is illustrated in Figure 8-15 and Figure 8-16. The horizontal part of the graph means that V_{min} is governing, since V_{min} does not depend on the reinforcement ratio. The arched graphs are the same in both figures, since $V_{Rd,c}$ does not depend on the steel strength.

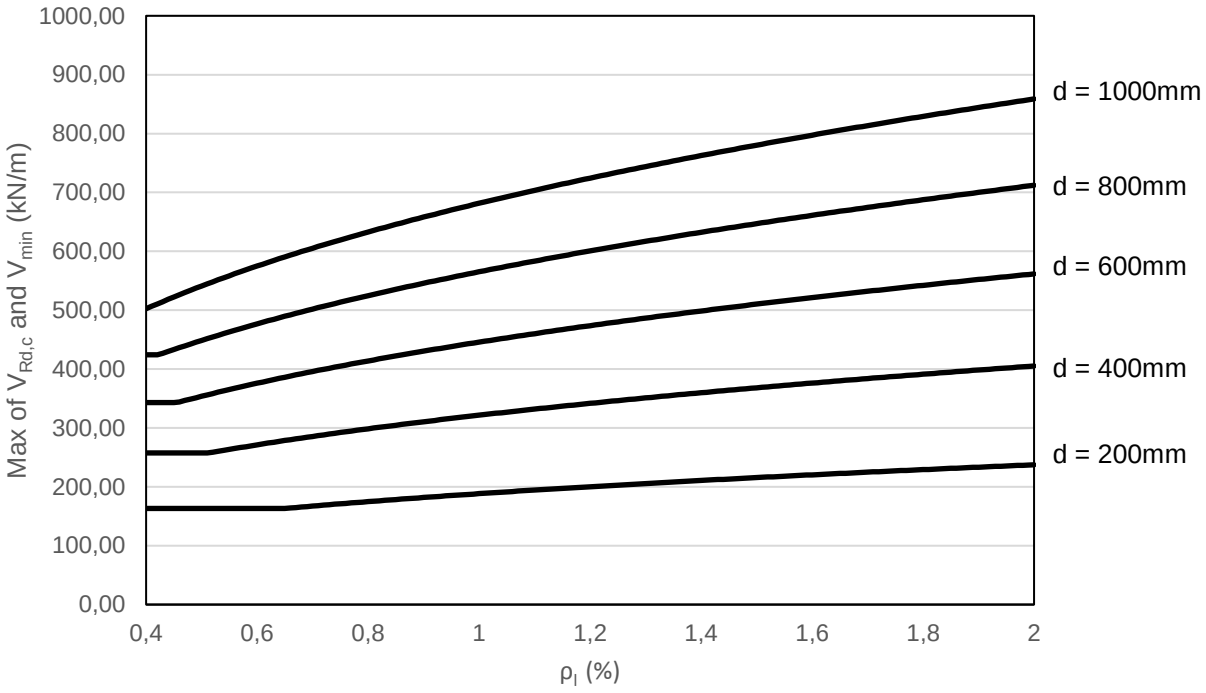

Figure 8-15 – The maximum value of $V_{Rd,c}$ or V_{min} for different effective depths and reinforcement ratios (f_{yk} = 500 N/mm^2)

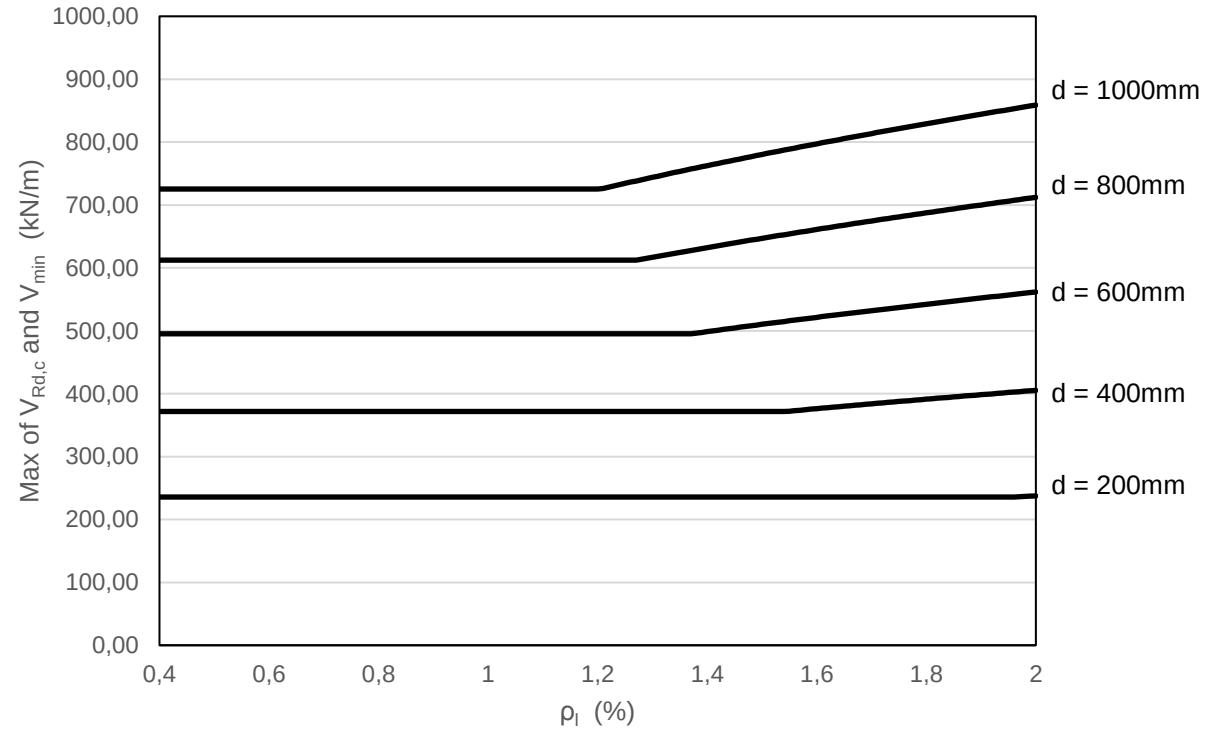

Figure 8-16 - The maximum value of $V_{Rd,c}$ or V_{min} for different effective depths and reinforcement ratios (f_{yk} = 240 N/mm^2)

Regarding these figures some conclusions can be drawn.

- An increase in slab thickness results in an increase for the shear stress capacity. The k factor decreases if the thickness increases. This influences V_{min} more strongly due to the power 3/2.
- The steel yield stress is an important parameter. For f_{yk} = 500 N/mm^2 $v_{Rd,c}$ is practically always governing. In this case it can be beneficial to know the actual reinforcement ratio, since it could lead to an increase of the shear capacity of 70% (860/500 for d = 100mm). For f_{yk} = 240 N/mm^2 (which is the other extreme) V_{min} governing in more cases. Now, knowing the real reinforcement ratio is less beneficial, since the maximum increase of the shear capacity is only 18% (860/730 for d = 1000mm).
- The concrete compressive strength influences both $V_{Rd,c}$ and V_{min}. Since v_{min} is influenced to the power ½ and $v_{Rd,c}$ to the power 1/3, an increase in the compressive strength leads to a higher v_{min} compared to $v_{Rd,c}$.
- Knowing the real reinforcement ratio is most beneficial for bridges with a high steel yield strength and low concrete compressive strength. However, a low concrete compressive strength also leads to a lower maximum longitudinal reinforcement ratio. Therefore a higher concrete class leads to a higher possible increase of the shear capacity as demonstrated in Table 8-4.

Table 8-4 – The maximum increase of the shear capacity if the longitudinal reinforcement ratio is known (d =1000mm)

Concrete class	$\rho_{l,max}$ [55]	Maximum increase of the shear capacity if ρ_l is known for f_{yk} = 500 N/mm^2 (at $\rho_{l,max}$)	Maximum increase of the shear capacity if ρ_l is known for f_{yk} = 240 N/mm^2 (at $\rho_{l,max}$)
C12/15	0,62	54%	6%
C20/25	1,03	67%	16%
C25/30	1,29	74%	20%
C30/37	1,55	79%	24%
C35/45	1,80	83%	27%
C40/50	2,06	88%	30%
C50/60	2,58	95%	35%

The percentile increases as demonstrated in this table are based on the maximum reinforcement ratio. This ratio is not likely to be present in existing bridges. As example for a more realistic bridge, a bridge with C35/45 and a reinforcement ratio of 1% is examined. In this case still an increase of 51% is observed.

Further research to the capacity of existing concrete slab bridges is desired. As done for governmental bridges it is beneficial to develop a standard lower boundary value for the concrete strength of existing municipal bridges. This can be done by comparing the results of material tests performed by different inspection companies.

The consequence of cracking of the slab on the shear capacity should be investigated further. The shear capacity of locally failed slabs was tested (severely cracked) and resulted in shear capacities with an average of 80% of the original shear capacity. More research is needed to the residual shear capacity of cracked (not locally failed) slabs.

8.4.5.4 Conclusion

The Quick Scan model leads to reliable output if the material properties are known. When assumptions were made with some uncertainties, always the conservative value was chosen. These conservative assumptions lead to uncertainties in the interpretation of the Unity Check. A bridge with a Unity check higher than 1 does not directly mean that repair or rebuilt is necessary. The freedom of interpretation of the Unity Check is quantified in this chapter. Conclusions for CC2 (repair level) bridges are mentioned:

- The translation from RFEM values to the Quick lead to a maximum error of 7% for cracked slabs and 10% for uncracked slabs;

- The assumption of the β factor for repair instead of rejection leads to an increase of the variable loads of 9% due to the variation in partial factor (1,1 to 1,2).
- The assumption of the lower boundary v_{min} for the shear capacity may give conservative results, especially for bridges with high reinforcement steel yield strength (f_{yk} = 500 N/mm^2). The maximum increase of the shear capacity if ρ_l is known is 74% for f_{yk} = 500 N/mm^2 (C25/30) and 20% for f_{yk} = 240 N/mm^2 (C25/30). This indicates that detailed analysis and material testing is especially valuable for bridges with an (expected) high steel yield strength.
- If axle loads and vehicle loads for 'normal traffic' instead of 'heavy traffic' can be assumed for municipal bridges, the axles loads of the governing loads can be decreased. This leads to a lower α factor. However too little data is available to draw substantiated conclusions.

8.5 Reliability model

In this thesis, assumptions were made that affect the reliability of the output of the Quick Scan model. In this chapter, all assumptions and parameters are summed up with the importance and the reliability. The Quick Scan model gives most reliable for the following types of bridges:

- No skew angle;
- Single span;
- Statically determined;
- Rectangular slab (no variation in transverse or longitudinal construction depth);
- Concrete compressive strength and steel yield strength known;
- No edge beam;
- Not prestressed;

For the type of bridge that is best applicable to the Quick Scan model all parameters and assumptions are noted. The relative importance and uncertainty are illustrated by a number (1 – 3) and a color (green – yellow – green – red). For the bridge parameters distinction was made between the situation where the material properties are known, and the situation where the material properties are unknown. (Table 8-5)

Table 8-6 contains the assumptions that were made with the FE modelling, α – factor research and the Quick Scan model. In this way distinction can be made between uncertainties in the finite element model, the α factor research and the Quick Scan model. Uncertainties in the Quick scan model are the combination of all parameters, since the Quick Scan model uses adaptions from the finite element model and the α factor.

Uncertainties:

Red	= Rough assumption, not substantiated
Orange	= Substantiated assumption, reason for doubt/ large uncertainty
Yellow	= Substantiated assumption, small uncertainty
Green	= Substantiated assumption, no uncertainty

Importance:

1 (high)	= Very important for the shear force assessment
2 (medium)	= important for the shear force assessment
3 (small)	= less important for the shear force assessment

Table 8-5 General parameter that apply to the bridge with their importance and uncertainty

Parameter	Importance	Uncertainty	
		Properties known	Properties unknown
Bridge			
Dimensions	1		
Asphalt thickness	3		
Material properties	1		
Reinforcement ratio	2		
Bridge support	3		
Current state of slab (severity cracking)	2		
Consequence Class	2		
Assessment level	2		

Table 8-6 - Parameters used in researches and modelling that apply to the loads with their importance and uncertainty

Parameter	Importance	Uncertainty
FEM assumptions		
Support stiffness	3	
Slab stiffness rule of thumb	2	
Slab thickness rule of thumb	1	
Self-weight assessment	2	
α – Factor		
Governing axle load (WIM)	1	
Governing load model (AL)	1	
Dynamic factor	2	
Normal lorry 2nd lane	1	
Quick Scan		
Errors in the Quick Scan	2	

The chosen importance and uncertainty of the parameters is explained briefly.

8.5.1 General parameters

- Dimensions

Dimensions are very easily and precisely measurable. Therefore the uncertainty is nil. The asphalt thickness can be hard to determine, but the influence is not significant.

- Material properties

Material properties are very important for the shear assessment. When material properties are known by material testing, no uncertainty can be assumed. When the material properties are known by original drawings or calculations the uncertainty is slightly more, especially for the concrete. Concrete strength can develop over time. Using the original concrete strength is however a safe assumption.

- Reinforcement ratio

The reinforcement ratio is not crucial for the shear assessment. If the reinforcement ratio is unknown the shear capacity is determined by the minimum shear capacity v_{min}. If the Unity Check becomes too high further research to the reinforcement details may be beneficial.

- Bridge support

The type of support can mostly be determined by visual inspection. Sometimes it is not entirely clear. The importance is low due to small influences on the shear assessment

- Current state of slab

The exact state of the slab is never exactly known (severity of cracking). For existing bridges always a cracked slab can be assumed. The exact stiffness and poisson ratio is typically not known. This has influence on the force transmission, but since only ULS calculations were done the importance is not very high.

- Consequence class / assessment level

When little information is known about a bridge also the consequence class and assessment level might be uncertain. This influences the partial factors. However, these parameters can be estimated since they are typically for certain types of bridges.

The capacity is the result of the parameter material properties and dimensions and therefore only known when material properties are known.

8.5.2 Parameters used in researches and modelling

- Support stiffness

The actual stiffness is commonly not known. The rule of thumb that was used gives a good approximation, but there are small uncertainties. Importance is low, since the difference in occurring shear force will not be significant.

- Slab stiffness

If the current state of the slab is known (severity of cracking), still the stiffness is not known. The difference between the longitudinal and transverse stiffness is especially important, since it determines the transverse force distribution. The assumption of the transverse stiffness being 1/3 of the longitudinal stiffness is likely to be an overestimation. Therefore the uncertainty is relatively large.

- Slab thickness

In the finite element model a rule of thumb for the slab thickness was used: h = L / 20. In reality this is always different. For example, bridges with a thickness of L / 15 also exist. Since the FEM model is calibrated on the rule of thumb, small variation for the shear force for real bridges may occur.

- Self-weight assessment

The self-weight of the concrete slab was regarded differently for slabs cast in-situ and prefab slabs. No peak in the shear force near the edge was assumed for in-situ casted slabs. For prefab slabs the peak force was determined by RFEM using the ‘Kirchhoff’ method. These assumptions lead to some uncertainties. These uncertainties are also related to the assumptions of the slab stiffness

- α – factor

The assumptions made for the comparison between Load Model 1 and the Asphalt Lorry lead to some uncertainties. The load from the governing load model were based on 2 months of WIM measurements from 1 municipal road. Therefore the axle loads and the governing load model (Asphalt Lorry) are slightly uncertain. The axle loads were increased by a dynamic factor of 1,25 according to the dynamic factor for fatigue lorries. This is marked as a large uncertainty.

- Errors Quick Scan

The shear forces from FEM modelling were compared to the shear forces from the Quick Scan model. Due to the large variation in span and edge distance the Quick Scan was not calibrated entirely accurate. Differences up to 10% were found. The uncertainty is low, since the differences were found rather precise.

8.5.3 Critical unity check

The Quick Scan model was developed in a way that a unity check lower than 1,0 always leads to fulfilment of the requirements. A unity check lower than 1,0 means that the structure is safe according to the shear assessment. Due to conservative assumptions, uncertainties and errors in the Quick Scan model, a unity check higher than 1,0 does not directly lead to disapproval of the structure. Regarding all uncertainties and assumptions, a unity check value is determined above which the structure does not fulfils the shear requirements. This is the result of a combination of uncertainties along the modelling process.

Regarding the uncertainties a range of the unity check can be specified between which the structure may fulfil if detailed assessment of a bridge is done.

- Lowering the assessment level to disapproval leads to an increase of the variable loads of 9%. The part of the variable loads compared to the total loads is different for different spans. As average, it is assumed that 50% of the total loads are caused by variable loads;
- For the uncertainties in the assessment of the severity of slab cracking (longitudinal or transverse cracks) an additional range of 5% is assumed. The assumption has influence on the force transmission, but the influence on the maximum shear force is not very high (**Fout! Verwijzingsbron niet gevonden.**);
- For uncertainties regarding the FEM model as described in Table 8-6 (transverse stiffness is equal to 1/3 of the longitudinal stiffness, support stiffness, slab thickness and self-weight assessment) a range of 5 % is assumed;
- For uncertainties regarding the α factor an additional range of 10% is chosen. This is especially due to uncertainties of the WIM measurements and dynamic factor;
- For possible errors in the Quick Scan model an additional range of 10% is assumed according to Figure 8-11 and Figure 8-12.

From these points, the maximum Unity Check is 1,045*1,05*1,05*1,1*1,1 ≈ 1,4. When material properties are known (included the reinforcement ratio) and the bridge satisfies the requirements for applicability of the Quick Scan model, the maximum Unity Check at which additional assessment and recalculation may be beneficial is 1,4. If the Unity Check is closer to 1,0 it is more likely that the structure will fulfil the shear requirements after a recalculation.

8.6 Conclusion

The Quick Scan model should only be used by engineers with sufficient knowledge of structural engineering. If the material properties are unknown, RBK states that the lowest applied material properties from the building year should be used. However, in this case the structure will not fulfil the requirements in most cases. Therefore, the Quick Scan model should be used as categorization model when the material properties are unknown. This means that a range of different bridges owned by a municipality can be arranged by how critical they are. Most critical bridges according to the arrangement should be assessed and invested first. The Quick Scan model can be used to determine what concrete class and steel type is needed for the bridge to fulfil the requirements.

Additional material research to the reinforcement details (longitudinal reinforcement ratio) is only desired if V_{min} is not governing. This is mostly the case for bridges with a high reinforcing steel yield strength.

Results found with finite element modeling were compared with results found by the Quick Scan model. The maximum error was found to be 10% for uncracked slabs and 7% for uncracked slabs for the governing location of the shear check (edge or middle). Bridges in the assessment level 'repair' can be assessed on the 'disapproval' level if the bridge has an Unity Check just higher than 1,0. The total shear force reduction is at most 5%. The maximum Unity Check at which a chance of fulfilment of the requirements is present is 1,4. A block diagram of the interpretation of the Unity Check is shown in Figure 8-17. This diagram is for bridges in CC2 with the assessment level 'repair'. The switch to the assessment level 'disapproval' should only be made if the Unity Check is higher than 1,0 with the assessment level 'repair'.

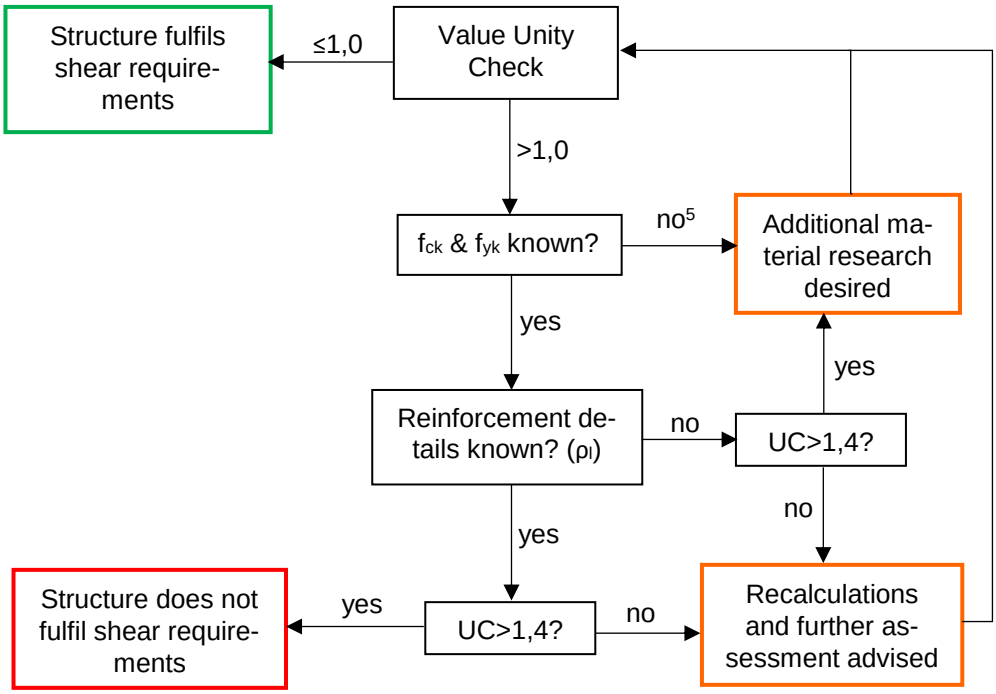

Figure 8-17 – Block diagram for the interpretation of the Unity Check

[5] The Quick Scan model can be used as categorization of a series of bridges

8.7 Discussion

The Quick Scan model was intended to use only theoretical rules based on experimental results. For some dimensions this resulted in conservative values. For other dimensions this resulted in values which are too low compared to reality. Therefore correction factors were calculated calibrated on the FEM results. These correction factors have no theoretical background and are determined empirically.

The maximum increase of the shear capacity if the reinforcement details are known are based on the maximum reinforcement ratio. In practice this ratio is not likely to occur in bridges. Therefore, the increase of shear capacity will be lower. However, calculations with a practical and economical reinforcement ratio of 1% for C25/30, C30/37 an C35/45 still show an increase of 59%, 55% and 51%, respectively (for f_{yk} = 500 N/mm^2). Additional research to the reinforcement ratio may be beneficial.

8.8 Limitations

The Quick Scan model can be further expanded to make it applicable to a greater scope of bridges. Also, after more research to the capacity of existing concrete slab bridges, the Quick Scan model can be adapted with new rules which leads to less conservative results.

In some cases or situations, the Quick Scan model should not be used:

- Extremely cracked slabs, which indicates local failure of the slab;
- Severely damaged slabs due to deterioration or damage;
- Slabs that are not solid concrete;
- Prestressed slabs can only be used when the prestressing force is known, but the model in principle is not meant for prestressed slabs;
- A skew angle smaller than 70˚ or higher than 110˚

If the material properties are unknown, the Quick Scan model can only be used as categorization of a range of different bridges. Research to the material properties of existing municipal bridges is desired. As for governmental bridges, a minimum value for the concrete compressive strength can be found based on building year.

9 Case Study

The Quick Scan model was tested on different case studies. The shear force and shear capacity results from the Quick Scan and the original calculations are compared.

9.1 Underpass N23 Westfrisiaweg

Figure 9-1 – Overview underpass

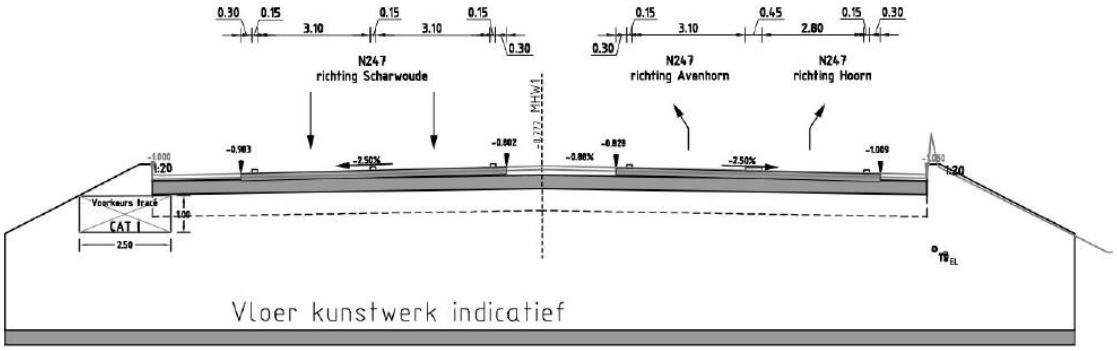

Figure 9-2 - Transverse cross-section at mid-span

The concrete compressive strength was determined by material testing and found as f_{ck} = 53,4 N/mm^2. The steel type was FeB400. The shear capacity was determined by v_{min} according to the RBK.

Parameter			
Span	L	5	m
Edge distance	b_{edge}	0,5	m
Total width	b_{tot}	20,1	m
Thickness slab	t	370	m
Concrete strength	f_{ck}	53,4	N/mm^2
Steel strength	f_{yk}	400	N/mm^2
α factor	α	1	-

Consequence Class	CC	2	-

Calculation according to Quick Scan:
Shear force = 186 kN/m
Minimum shear capacity = 312 kN/m
Unity check = 0,60

According to recalculation:

$V_{E,z,afschuin+d}$	=	184 [kN]	
Aanpassing v_{min} conform RBK H2.4 NEN-EN1992-1-1 art 6.2.2 (1):			
v_{min}	=	0,83 * 1,2^3/2*1,78^3/2 *52,4^1/2 *400^-1/2 =	0,94 [N/mm^2]
k_p	=		1,2 [-]
$V_{rd,c}$	=		309 [kN]
U.C.	=	0,60	

This underpass is statically undetermined and therefore the output is somewhat uncertain. Nevertheless, the unity check is the same as the recalculation. Although this bridge in a municipal bridge, an α factor of 1,0 was used for the comparison with the real recalculation.

9.2 Viaduct Bakkersloot

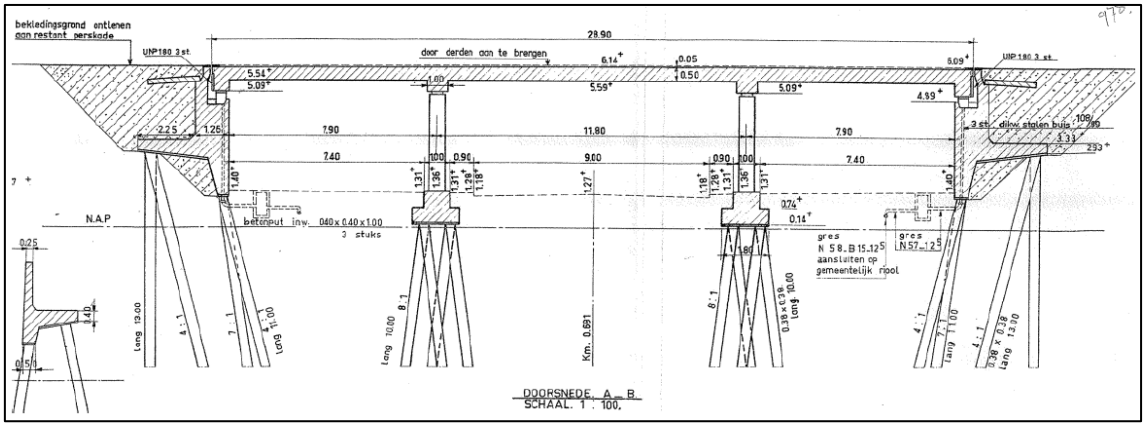

Figure 9-3 - Longitudinal cross-section

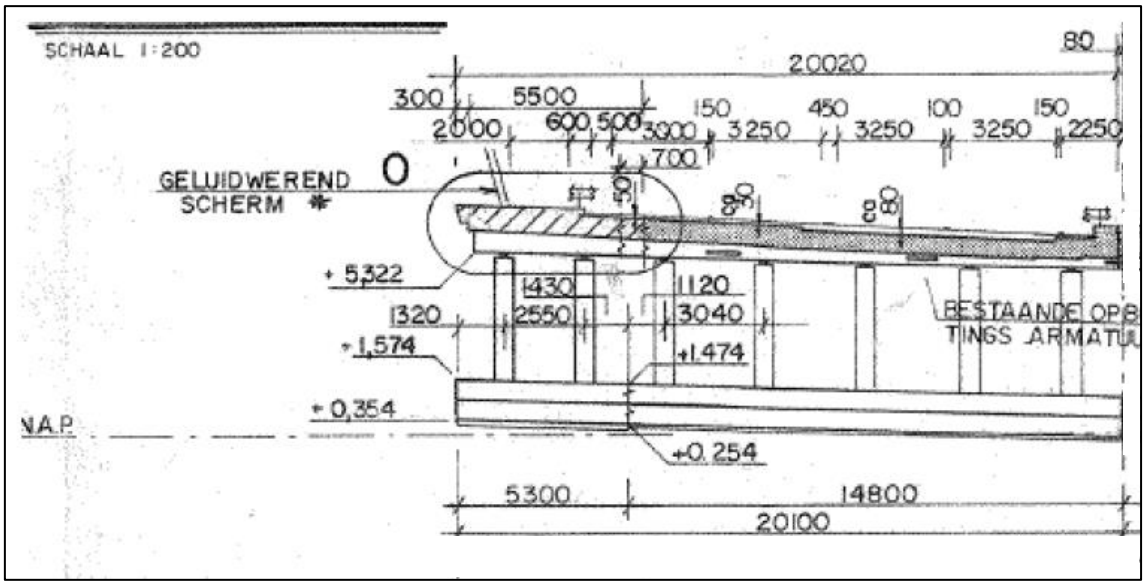

Figure 9-4 - Transverse cross-section

Table 9-1 - Important parameters

Parameter			
Span	L	11,8	m
Edge distance	b_{edge}	4,3	m
Total width	b_{tot}	20,1	m
Thickness slab	t	0,5	m
Concrete strength	f_{ck}	35	N/mm^2
Steel strength	f_{yk}	240	N/mm^2
A factor	α	1	-
Consequence Class	CC	3	-

Calculation according to Quick Scan:
Shear force = 315 kN/m
Shear capacity = 385 kN/m
Unity check = 0,77

According to recalculation:
Shear force = 298 kN/m
Shear capacity:

v_{min}	=	0,035 * k^3/2 * 35^1/2 +0,15*0=	0,45 [N/mm^2]	niet mg
$v_{min,RBK}$	=	0,83*1,2^3/2*1,67^3/2*(35^1/2/240^1/2)=	0,90	

U.C.	=	0,74

This viaduct consist of a part from 1966 and an additional part from 1991 (circled in Figure 9-4). Only the old part is checked with the Quick Scan (right part in Figure 9-4). In this re-calculation also rules from the RBK are used. Therefore, the shear capacity is the same. Also the occurring shear force is similar. In the re-calculation, the finite element program SCIA Engineer was used. This lead to a occurring shear force which is similar to the shear force from the Quick Scan (Since this is also based on a finite element calculation)

9.3 Conclusion

The two case studies described above give (almost) the same Unity Check for the recalculation as for the Quick Scan model. This indicates that the Quick Scan model is a good alternative for a recalculation. However, the validation is not complete, because only two case studies were done. For a complete validation a number of municipal bridges should be recalculation and compared to the Quick Scan result. This falls outside the scope of this thesis.

9.4 Discussion and recommendation

Sweco has done little recalculations to municipal concrete slab bridges. Therefore the case studies show some uncertainties in the output. This leads to the facts that the Quick Scan is not fully tested. Ideally, the Quick Scan has to be tested on a municipal bridges where the recalculation leads to a Unity Check of 1,0 or just over 1,0. Then the Unity Check according to the Quick Scan can be found and compared. After that, the reduced α factor can be applied.

Because the performed case studies are not typically suited for the Quick Scan (statically indeterminate, more than two driving lanes), no solid conclusions can be drawn for the validation of the model. Also, the shear forces in the case studies were found by a finite element program form which the exact input is unknown. The Quick Scan model should be tested to a significant number of relevant case studies before the validation is complete.

10 Conclusions and Recommendations

10.1 Conclusions

Conclusions can be drawn from the different researches to existing municipal concrete slab bridges as described in the literature review. The main focus of the thesis is the determination of the load reduction factor α, and to gain insight in the force transmission for typical municipal concrete slab bridges, both substantiated by Finite Element Modelling (FEM). Using results from these FEM researches, a Quick Scan model for existing municipal concrete slab bridge was developed. In order to carry out these FEM researches and develop the Quick Scan model, conclusions have been drawn according to literature research.

10.1.1 Difference municipal and governmental bridges

In general, loads from the Eurocode (LM1) are too high for municipal bridges, which leads to a conservative assessment. This is the result of differences between municipal bridges and governmental bridges:

- Size: Municipal bridges are typically smaller. Load Model 1 is calibrated on bridges with a span of at least 20m. For shorter span bridges, the importance of axle distance of a lorry becomes significant;
- Loads: Municipal bridges are typically exposed to less heavy and a smaller number of lorries;
- Lay-out**:** Municipal bridges may have a significant edge distance due to a separated footpath or bicycle lane (>1,2m for more than 50% of the municipal traffic bridges). This affects the load transmission of wheel loads to the support. Due to these differences municipal bridges are recalculated with loads that are unrealistic.

10.1.2 Difference existing and new bridges

Besides the difference between municipal bridges and governmental bridges, the assessment of existing bridges differs from new bridges.

- The minimum reference period for an existing bridge is assumed to be 15 years. This leads to less chance of occurrence of the governing loads;
- A reliability index of β = 3,1 is chosen, which corresponds to the 'repair' level at Consequence Class 2. This leads to a partial factor of 1,1 for permanent loads and 1,2 for variable loads;
- The theoretical α factor for existing municipal bridges was calculated as 0,92. For this calculation the reduced span and increased edge distances were not taken into account. The actual α value is investigated by Finite Element Modelling (FEM) and described in the following chapter.

10.1.3 Research questions

1. **How much can the loads from Load Model 1 be reduced for existing municipal concrete slab bridges?**

Axle loads from Load Model 1 can be reduced by a factor α if the expected traffic is demonstrably less than heavy industrial traffic. A general α factor for existing municipal bridges was investigated with FEM research. This factor can be used for recalculation of these bridges, and for bridge assessment using a Quick Scan model. The α factor is determined by comparing occurring

stresses due to Load Model 1 with occurring stresses due to other load models. These load models represent real occurring loads on a municipal bridge. The loads from the new developed load models are calibrated by Weight-In-Motion (WIM) at a municipal bridge in Rotterdam. The governing vehicle was the 'Asphalt Lorry' with 5 axles close to each other. The axle loads were 150kN and 125kN (dynamic factor included). The α factor is based on the comparison of the occurring shear stress and flexural moment stress due to the Asphalt Lorry and Load Model 1. For this comparison the edge distance from the carriageway to the edge of the slab (b_{edge}) and the span (L) were variable. Results were found for a normal load situation on municipal bridges, a situation of overloading, and a situation of location specific loads (bridges near a concrete or asphalt producer). In a normal situation, the lower boundary (as stated in the Eurocode) of α =0,8 can be used for spans up to 11m. This α factor goes linearly to 1,0 for a span of 20m. When the recommendation of the Eurocode for a minimum α factor of 0,8 is not followed, the alfa factor lowers to a value of 0,6 for a 5m span bridge.

An existing bridge is assumed to be cracked, since the cracking moment was reached during its lifetime. For uncracked slabs the forces can spread to the edge more, which leads to higher stresses near the edge. In cracked slabs, an increase of the shear forces of 20% were found at the middle of the support compared to uncracked slabs. Shear stresses near the edge of the support are around 15% lower for cracked slabs (with a large edge width) compared with uncracked slabs.

2. How can the occurring shear forces due to loads from Load Model 1 in a concrete slab be explained?

Additional FEM research was done to the shear force transmission in solid slabs. The permanent loads and variable loads were assessed separately. Also, the influence of cracking of the slab on the force transmission was investigated. In order to gain insight in the force transmission in slab bridges, different situations were modeled in a Finite Element program and variable parameters were used:

- State of the slab: cracked and uncracked slabs were investigated;
- Execution type: slabs cast in-situ and prefab slabs were investigated;
- The shear force due to variable and permanent loads were investigated separately.
- The span and the edge distance were variable parameters;

Cracking of the slab influences on the longitudinal and transverse stiffness, which has influence on the force transmission. The transverse stiffness of a cracked slab was found between 1/3 and 2/3 of the longitudinal stiffness, depending on the severity of cracking. Variation in transverse stiffness especially influences the force transmission of the axle loads. Cracking leads to a smaller effective width of the axle loads. In the Finite Element model, a transverse stiffness of 1/3 of the longitudinal stiffness was used for cracked slabs.

The FEM model shows peak forces near the edge of the support due to self-weight. This is the result of transverse contraction in slabs. However, when a slab bridge was cast in-situ (which is mostly the case for old bridges) these peak forces will not be present in reality due to the redistribution of loads due to self-weight during the hardening process.

It was found that the tandem system on the second lane has little influence on the shear force near the edge. This is because the tandem system has to be placed far away from the support to spread the axle loads to the edge. Therefore the effective width becomes very large and the force transmission to the opposite support becomes significant.

3. What is the critical edge distance of a concrete slab bridge?

For governmental bridges, the edge of the slab near the support was assumed to be governing. Since municipal bridge often have a significant edge distance, the governing place for maximum shear force on the support is unclear (middle or edge). The critical edge distance is the distance

from the carriageway to the edge of the slab for which the middle of the slabs becomes governing instead of the edge of the slab (regarding shear forces). The critical edge distance was found for different combinations of spans and edge distances. For the type of slab that occurs the most (cracked slab cast in-situ) the critical edge distance is 1,5m, independent of the span. In general, the edge of the slab is governing if:

$$b_{edge} \leq 0{,}07L + 0{,}24 \text{ [m]}$$

10.2 Quick Scan model

It was found that the Quick Scan model leads to reliable output if the material properties (f_{ck} and f_{yk}) are known. A bridge with a Unity Check ≤ 1 satisfies the requirements for shear and is not critical. Due to conservative assumptions made in the Quick Scan and uncertainties, a Unity Check between 1 and 1,4 could also fulfil the requirements. In this case further assessment of the bridge is necessary. A Unity Check > 1,4 does lead to disapproval, or further material research, depending on knowledge of the material properties and amount of longitudinal reinforcement. If the material properties are unknown, the Quick Scan can result in a categorization of a range of bridges. Material properties can be assumed according to the year of construction. The Quick Scan is best applicable to bridges that are: municipal concrete slab bridges with a constant height, simply supported, no edge beam and statical determined. If this is not the case the Quick Scan is still applicable, but an uncertainty is implemented.

10.3 Discussion and recommendations

This study has demonstrated that reduced loads can be used for recalculations of existing municipal bridges. However, there are particular issues that can be improved or where additional research can be beneficial.

10.3.1 Further experimental research

Experimental research based on one wheel load was used. Research to one or more axle loads can be beneficial. Tandem systems could be placed in a certain configuration for the maximum loads near the middle of the support and near the edge of the support. In this way the results from FEM research and experimental research with one wheel load can be verified for Load Model 1 loads.

More experimental research is needed for certain parameters and types of bridges:

- The influence of a skew angle on the force transmission;
- The influence of a varying thickness of the transverse or longitudinal cross-section;
- The adaption factors for continues spans can be extended to a larger scope;
- The difference in longitudinal and transverse stiffness of cracked slabs;

10.3.2 α factor

For the determination of the α factor some uncertainties were faced. The axle loads from the developed load models are based on one WIM measurement of 2 months. This is questionable, because 2 months is relatively short. For less uncertainty, at least measurements of one year should be used. Also, WIM measurements of only 1 location are used as reference for every municipality. These measurements might not be representative for smaller, more remote municipalities. It can be useful to do more WIM measurements in municipalities in the Netherlands. Then, the assumed governing load model (Asphalt Lorry) can be verified and standards for municipal bridges can be made less conservative.

10.3.3 Capacity

This thesis mainly focusses on the loads on municipal bridges. Standards for the capacity of existing bridges (NEN 8702) are currently being developed. The capacity of existing municipal bridges is often unknown. Research to the residual capacity of existing concrete bridges is needed to make the Quick Scan less conservative. This can be established by material research and proof load testing. Proof loading is important to understand the bridges' behavior and refining assessment methods. For existing governmental bridges the RBK can be used. For municipal

bridges currently a new CUR recommendation is being developed. More research to the minimum material properties and capacity of municipal bridges can improve these recommendations.

10.3.4 Slab cracking

For slab cracking only 2 situations have been investigated: Cracked slabs (Transverse stiffness is 1/3 * Longitudinal stiffness) and uncracked slabs (Transverse stiffness = Longitudinal stiffness). These are rough assumptions and can be investigated further. Cracking is a complex phenomenon, but very important for the force transmission in slabs. Also, it can be beneficial to investigate the real state and stiffness of existing bridges. To what extent are the bridges fully cracked and what is the real influence on the force transmission? According to researches the force transmission under an angle of 45˚can be assumed. This was determined by looking at the maximum loads at failure. The FEM model indicates a smaller force transmission angle for cracked slabs. This indicates that the assumption of 1/3 * longitudinal stiffness may be incorrect. The real transverse stiffness in a cracked slab needs further research.

10.3.5 The Finite Element Model

In this thesis, only linear elastic modeling was used. It might be beneficial to use non-linear elastic modelling, or use solids to predict the force transmission in slabs more realistically. Also, odd shaped bridges with a varying transverse or longitudinal cross-section can be investigated. For the support type, a line support was assumed. In reality some bridges have other types of supports. The consequence of this assumption may need further investigation.

With additional research, the knowledge about the force transmission in concrete slabs can be improved, and the Quick Scan model can be applicable to more bridge types. Also, the results can become less conservative and lead to higher assessment quality.

10.3.6 Quick Scan

The Quick Scan needs to be verified for existing municipal slab bridges. The Quick Scan has been tested with three case studies. The Quick Scan model was not entirely applicable to the bridges in these case studies, because multiple span bridges (statically indeterminate) were tested. The Quick Scan model should be tested with simply supported small span concrete slab bridges

11 Bibliografie

[1] R. Mulder, „Onderzoek gemeentelijke bruggen," Bouwend Nederland, 2015.

[2] Europese Commissie voor Normalisatie, „CEN, Eurocode 1 - Actions on structures - part 2: Traffic loads on bridges, EN 1991-2," Brussel, 2011.

[3] Europese Commissie voor Normalisatie, „CEN, Eurocode 0 - Basis of structural design," Brussel, 2011.

[4] I. C. Brandsen, „Richtlijnen Ontwerpen Kunstwerken (ROK 1.3)," Rijkswaterstaat, 2015.

[5] Rijkswaterstaat, „Richtlijnen Beoordeling Kunstwerken (RBK 1.1)," Rijkswaterstaat, 2013.

[6] Dutch Institution for Normalization, „NEN 8700 - Assessment of existing structures in case of reconstruction and disapproval (Basic Rules)," NEN, Delft, 2011.

[7] Dutch Institution for Normalization, „NEN 8701 - Assessment nof existing structures in case of reconstruction and disaapproval - Actions," NEN, Delft, 2011.

[8] L. Sanpalaolesi en P. Croce, „Design of Bridges: Guide to basis of bridge design related to Eurocodes supplemented by practical examples," Pisa, 2005.

[9] J. Haug en F. Schuurman, „Voetpaden voor iedereen," Bouw Advies Toegankelijkheid, Utrecht, 2016.

[10] D. F. Wisniewski, „Safety Formats fot the Assesment of Concrete Bridges," University of Minho, Guimaraes, Portugal, 2007.

[11] „Concrete bridge development group," [Online]. Available: http://www.cbdg.org.uk/intro3.asp.

[12] i. F. Soons, B. v. Raaij en p. i. L. Wagemans, Quick Reference, edition 2011, Delft: TU Delft, 2011.

[13] R. Bowen, S. Gasbarro, P. Graham, W. R. Hauser, T. Hill, M. A. Naber en N. Schamu, „A context for common historic bridge types," National Cooperative Highway Research Program , Ohio, 2005.

[14] „kennisportaal technische gegevens brugoplossingen," Spanbeton, [Online]. Available: http://www.spanbeton.nl/nl/media/kennisportaal/. [Geopend 13 october 2016].

[15] A. Kar, V. Khatri, P. R. Maiti en P. K. Singh, „Study on Effect of Skew Angle in Skew Bridges," International Jounral of ENgineering Research and Development, Varanasi, 2012.

[16] B. Sindhu, K. Ashwin, J. Dattatreya en S. Dinesh, „Effect of skew angle on static behaviour of reinforced concrete slab bridge decks," International Journal of Research in Engineering and Technology, Tumkur, 2013.

[17] N. V. Deshmukh en U. P. Waghe, „Analysis and design of skew bridges," International journal of science and research (IJSR), Maharashtra, India, 2015.

[18] R. Vergoossen, M. Naaktgeboren, M. 'T Hart, A. De Boer en E. Van Vugt, „Quick Scan on Shear in Existing Slab Type Viaducts," Rotterdam, 2013.

[19] E. Duran, Design of Edge Beams, Stockholm, 2014.

[20] H. Baji en H. R. Ronagh, „Investigation of ductility of RC beams designed based on AS3600," The University of Queensland, St. Lucia, Australia, 2011.

[21] i. D. Weertman en i. W. de Rijke, „Richtlijnen Beoordelen Bestaande Kunstwerken," Ministerie van verkeer en waterstaat, 2004.

[22] A. Vrouwenvelder, N. Scholten en R. Steenbergen, „Veiligheidsbeoordeling bestaande bouw. Achtgergrondrapport bij NEN 8700”.

[23] R. Steenbergen en A. Vrouwenvelder, „Safety philosophy for existing structures and partial factors for traffic loads on bridges,” TU Delft, Delft, 2010.

[24] R. Steenbergen, A. d. Boer en C. v. d. Veen, „Calibration of partial factors in the safety assessment of existing concrete slab bridges for shea failure,” TU Delft, Delft, 2012.

[25] J. Schneider, Introduction to safety and reliability of structures, Zurich, Switzerland: IABSE, 2006.

[26] L. Hellebrandt, „Structural Reliability of Existing City Bridges,” TU Delft, Delft, 2014.

[27] E. Huibregste, L. Abspoel en R. Steenbergen, „TNO 2014 R105128 Verwerking WIM metingen 2013 Gemeente Rotterdam,” 2014.

[28] R. Steenbergen, O. Morales Napoles en A. Vrouwenvelder, „ALgemene veiligheidsbeschouwing en modellering van wegverkeerbelasting voor brugconstructies,” TNO, Delft, 2012.

[29] L. Hellebrandt, C. Blom en R. Steenbergen, „Probabilistic traffic load model for short span city bridges,” HERON, Delft, 2014.

[30] E. O. Lantsoght, C. van der Veen, J. C. Walraven en A. De Boer, „Shear Assesment of Reinforced Concrete Slab Bridges,” TU Delft, Delft, 2012.

[31] E. Lantsoght, „Shear in Reinforced Concrete Slabs under Concentrated Loads close to Supports,” TU Delft, Delft, 2013.

[32] N. Bagge, C. Popescu en L. Elfgren, Failure tests on concrete bridges: Have we leart the lessons?, Lulea, Sweden, 2017.

[33] E. Lansoght, „Shear in Reinforced Concrete Slabs under Concentrated Loads close to Supports,” Delft, 2012.

[34] E. O. Lantsoght, C. van der Veen, J. C. Walraven en A. De Boer, „Effective shear width of concrete slab bridges,” Delft, 2015.

[35] E. O. Lantsoght, C. van der Veen en A. De Boer, „Shear and Moment Capacity of the Ruytenschildt Bridge,” 2016.

[36] E. O. Lantsoght, „Shear assessment of solid slab bridges,” Delft, 2012.

[37] E. O. Lantsoght, C. van der Veen en A. De Boer, „One-Way Slab Subjected to Combination of Loads Failing in Shear,” Delft, 2014.

[38] E. Lantsoght, „Voortgangsrapportage: Experimenten op platen in gewapend beton. Deel 2: Analyse van de resultaten,” TU Delft, Delft, 2012.

[39] Walraven, Prof. dr. ir, Dr.-Ing. hc. J.C., „Minimum afschuifdraagvermogen van platen uit gewapend beton zonder schuifwapening,” Rijkswaterstaat, 2013.

[40] G. Konig en J. Fischer, „Model uncertainties concerning Design Equations for the Shear Capacity of Concrete Members without Shear Reinforcement,” 1995.

[41] G. Kani, „The Riddle of Shear Failure and its Soluition,” Journal of the American Concrete Institute, Vol 61, 1996.

[42] P. Regan, „Ultimate limit state pinciples: basic design for moment, shear and torsion,” Textbook of structural concrete.

[43] D. Angelakos, E. C. Bentz en M. P. Collins, „Effect of concrete strength and minimum stirrups on shear resistance of large members,” ACI Structural Journal, 2001.

[44] p. d. i. J. Blaauwendraad, „Plate analysis, theory and application. Volume 1: Theory,” TU Delft, Delft, 2006.

[45] J. Blaauwendraad, „Plates and FEM, Surprises and Pitfalls,” Springer, 2010.

[46] i. F. Bockhoudt, i. C. v. d. V. van der Vliet, P. d. i. J. Blaauwendraad en i. J. Jongedijk, „Eindige elementenmethode voor in het vlak en loodracht op het vlak belaste plaatconstructies,” Betonvereniging / Bouwen met Staal, Gouda / Zoetermeer, 2005.

[47] J. Blaauwendraad, „Platen en programma's,” CEMENT, 2010.

[48] SCIA Engineer, „Training Finite Element Method,” SCIA Engineer, 2015.

[49] Dlubal Software GmbH, „RFEM 5 spatial models calculated according to Finite Element Method," Dlubal Software GmbH, 2013.

[50] A. Pipinato, Innovative Bridge Design Handbook. Chapter 28 - Bridge assessment retrofit and management, 2015.

[51] Europese Commissie voor Normalisatie, „NEN 6723 (VBB 1995)," Europese Commissie voor Normalisatie, 1995.

[52] Europese Commissie voor Normalisatie, „NEN 6702:1991, Technical principles for building structures - TGB 1990 - loadings and deformations," NEN, 1991.

[53] P. Dawe, „Traffic loading on highway bridges," Thomas Telford Publishing, London, 2003.

[54] A. Paeglitis en A. Paeglitis, „Traffic load models for short span road bridges in Latvia," Riga, Latvia.

[55] d. i. d. C. Braam en i. P. Lagendijk, Constructieleer Gewapend Beton, 2008.

[56] „Bridge Type Selection," [Online]. Available: http://www.dot.state.mn.us/stateaid/bridge/docs/4.pdf. [Geopend 5 September 2016].

[57] J. C. Walraven en C. R. Braam, Prestressed concrete, Delft: TU Delft, 2015.

1 Appendix A – Investigated municipalities

Abbreviations municipalities:

Dl = Delft
Dz = Delfzijl
Dv = Deventer
G = Gorinchem
H = Helmond
K = Krimpernerwaard
O-W = Olst - Wijhe
O-B = Oud – Beijerland
W = Woerden
Z = Zwolle

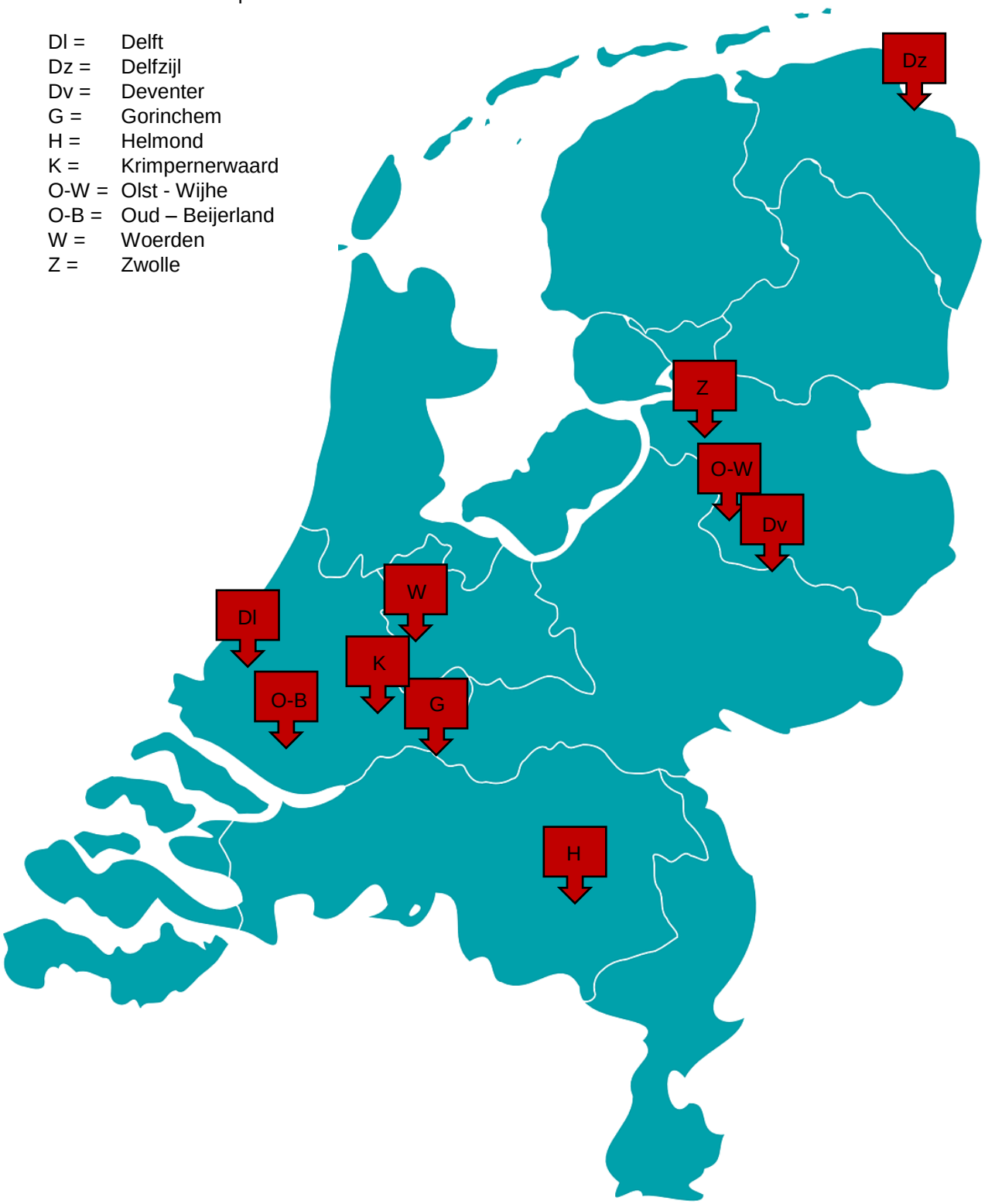

Appendix Figure 11-1 - Location of investigated municipalities in the Netherlands

2 Appendix B – Load reduction signs

2.1 Signs

NEN 8701-2011 [7] provides some standards for load reduction due to signage. This load reduction can be realized by:

- Reduction of the total mass of a vehicle (sign C21)
- Reduction of the maximum axle load of a vehicle (sign C20)
- A barrier for vehicles (sign C06)

2.1.1 Reduction total mass

If total mass reduction signs are used, a reduction factor α_{c21} can be applied to the axle loads and uniform distributed loads from Load Model 1. An overview of the reduction factors is illustrated in Appendix Table 2-1.

Appendix Table 2-1 - Reduction factor α_{c21} for characteristic loads for load signs C21 [23]

α_{C21}	bord C21 (ton)	bord C21 (kN)	BM1					
			Q_{1k} per as (kN)	q_{1k} (kN/m^2)	Q_{2k} per as (kN)	q_{2k} (kN/m^2)	Q_{3k} per as (kN)	$q_{ik,\ i\geq3}$ (kN/m^2)
1	60	600	300	9,00	200	2,5	100	2,5
0,83	***50***	***500***	250	7,50	167	2,5	83	2,5
0,75	***45***	***450***	225	6,75	150	2,5	75	2,5
0,67	***40***	***400***	200	6,00	133	2,5	67	2,5
0,58	***35***	***350***	175	5,25	117	2,5	58	2,5
0,50	***30***	***300***	150	4,50	100	2,5	50	2,5
0,42	***25***	***250***	125	3,75	83	2,5	42	2,5
0,33	***20***	***200***	100	3,00	67	2,5	33	2,5

2.1.2 Reduction total axle load

For the reduction sign of total axle load (C20), the following reduction factors can be applied (Appendix Table 2-2)

Appendix Table 2-2 - Reduction factor α_{c20} for the characteristic loads for load signs C20 [23]

α_{C20}	bord C20 (ton)	bord C20 (kN)	Q_{1b} per as (kN)	Q_{2b} per as (kN)
1,000	12	120	300	200
0,773	**10**	**100**	232	155
0,668	**9**	**90**	200	134
0,569	**8**	**80**	171	114
0,477	**7**	**70**	143	95
0,391	**6**	**60**	117	78
0,310	**5**	**50**	93	62
0,236	**4**	**40**	71	47
0,168	**3**	**30**	50	34

3 Appendix C – Other types of concrete bridges

3.1.1 T-beam bridge

A T-beam bridge is a bridge which consists of T-shaped sections. The ‘stem’ of the T functions as a beam for longitudinal support. The top section of the T is connected rigidly to the stem and functions as deck. The longitudinal T-shaped sections are sometimes connected by transverse girders. T-beam bridges can have longer spans than slab bridges. Also, double T-beam bridges can be made, which are two capital T’s placed side by side.

Nowadays T-beams are often applied prestressed and prefabricated. Also, reversed T-beams can be used. In this case, the horizontal part of the T is used as tension zone. In some cases it is also used as formwork for additional concrete. These are called SJP-bridges and are discussed later.

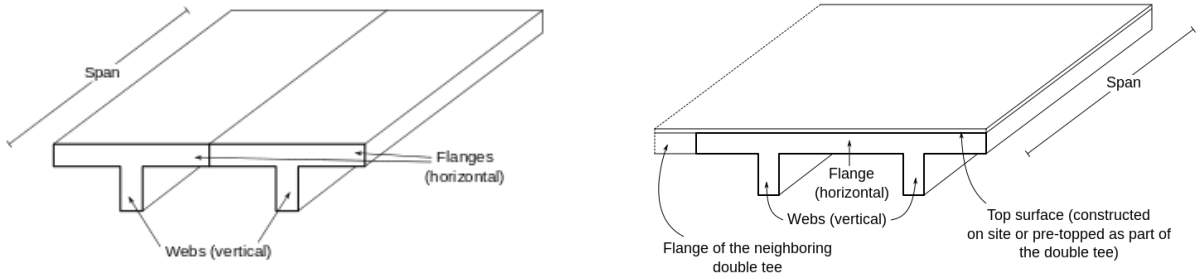

Figure 3-1 - Example of a T-beam (left) and a double T-beam (right) (source: https://en.wikipedia.org/wiki/T-beam)

3.1.2 Beam or girder bridge

Beam bridge is a more common type for medium span bridges. It consists of 2 or more longitudinal members which carry a slab as roadway or pavement. These longitudinal members create height to increase the moment of inertia and section modulus, and therefore the stiffness and strength. The slab on top can be integrated with the beams or not. Integrated beams are often known as ribs or T-beams. The top flange can act as compressive flange. The used beams can have many different shapes for structural or esthetical reasons. For example an I shaped beam to save material, or an arched shape beam for better force distribution to the support.

The name beam bridge or girder bridge is often used for the same type of bridge. Some say that the difference has to do with transverse members. A beam bridge does not have transverse members, and a girder bridge does. The difference with a T-beam bridge is that the longitudinal members are not connects rigidly in beam or girder bridges.

The maximum span for a beam bridge without prestressing steel is about 20 meters. With prestressing steel, the maximum length is about 35-45 meters. [11] [12] [56]

3.1.3 Concrete rigid frames

As with the T-Beam bridge, the vertical and horizontal components of the concrete rigid frame bridge are integral, forming one solid cast-in-place structure. The rigid frame bridge can be composed of either a single or multiple spans. The cross-sections of the beams or vertical sections are usually shaped like I-beams or boxes, but there can be great variety in shape. In older rigid frame bridges, the vertical beams are often located at the ends of the “slab” or deck component when viewed in cross section. Also in older bridges of this type, the horizontal

component is often haunched, and is thicker at the ends than in the middle, thus presenting the image of a shallow arch.
After the introduction of pre-stressing in the 1950s, the rigid frame span began to lose popularity in comparison to more economical types of reinforced concrete bridges. [13]

3.1.4 Box girder bridges

A box girder is a special type of beam construction. 2 parallel beams are connected at the top- and bottom side with a concrete flange. This provides flexural and torsional stability and is often used with large spans and large variable loads like trains or lorries. Besides, the bottom flange is esthetical attractive by its smooth and equal surface. Box girders are often not considered as small to medium spans. There are many different types of box gird bridges, such as mono box bridges, curved box beam bridges and U-shaped box-beams. A more common type for medium span bridges in the Netherlands is the SKK bridge. This is a beam-type bridge that consists of several prestressed box girders in a row. These box girders also have transverse prestressing steel. (Figure 3-2)

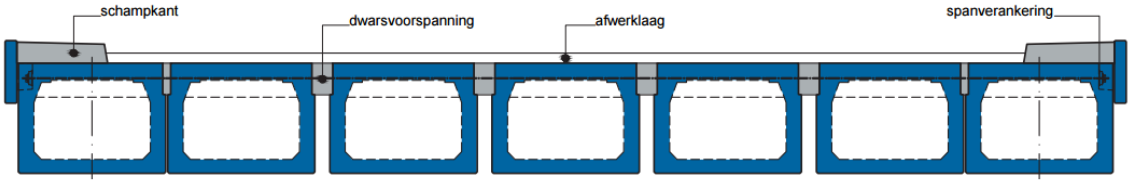

Figure 3-2 - cross-section SKK bridge [14]

In general, box girder bridges are not used much municipal bridges.

3.1.5 Prestressing

In the Netherlands, prestressing steel was first used in 1948. Nowadays, prestressing steel is indispensable in concrete structures. Concrete is relatively weak in tension. The use of prestressing steel is a way to compensate the tensile forces. Prestressing force can be applied in several ways. The important ones are:

- Pre-tensioning, where the tendons are tensions prior to the concrete being cast
- Post-tensioning, where tendons are tensioned after the surrounding concrete has been cast;
  - Bonded post-tensioning, where the tendons are permanently bonded to the surrounding concrete
  - Unbonded post-tensioning, where the tendons have freedom of longitudinal movement.

Prestressing steel can be used more effectively by applying it eccentric or with a curved tendon. When applied eccentric, the eccentricity of the compressive force generates an extra hogging bending moment (Figure 3-4). When a curved tendon is applied, this also generates an extra hogging bending moment. However, an advantage is that this way of prestressing does not generate tensile stresses at the top side of the beam near the support. This is because the anchorages are positioned in the kern area of the cross-section (Figure 3-3). In both cases, one has to make sure that no tensile stresses can occur in any load case during the whole lifetime. [57]

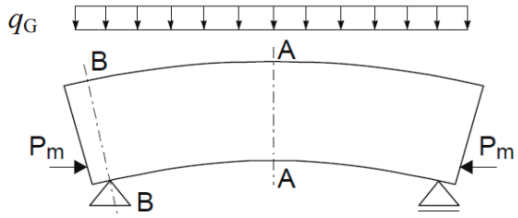

Figure 3-4 - Eccentric prestressing [57]

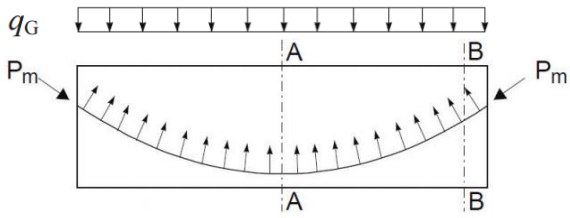

Figure 3-3 - Parabolic prestressing tendon profile [57]

By using prestressing steel, larger spans can be obtained. Nowadays, prestressing steel is used many concrete bridges. Often, prestressed concrete beams are combined with normal reinforced concrete as compression layer.

As example, prestressed I-shaped beams are used much in medium-to-long span bridges nowadays (Figure 3-5). See also chapter 3.2.2. This type can be used simply supported as well as continuous bridges. For long span beams, often transporting the beams could raise problems.

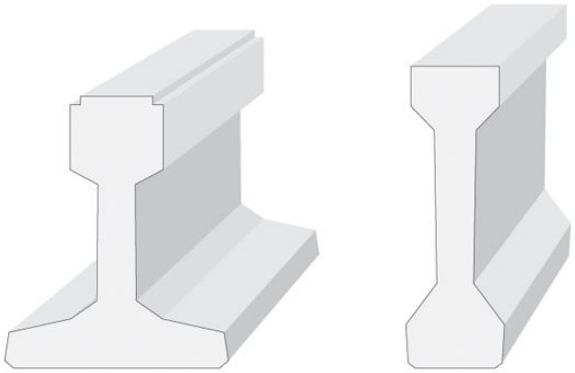

Figure 3-5 - Example of an M-beam[6] (I-beam with wide bottom flange) and an I-beam (source: http://www.scib.com.my/prestressed_beam.html)

[6] Also called 'Rail beam'

4 Appendix D – Former codes

4.1 GBV 1950

In former standards (GVB 1950), concrete was not specifically distinguished in concrete qualities. It was divided in the need of application of construction control, with associated cubic compressive strength. The RBBK translated this to recent characteristic compressive strength. Details can be found in the RBBK report. [21]
Steel types QR 22 and QR 24 were most applied. The number after QR stands for the minimum yield strength. The design value for the tensile strength is determined by dividing the yield strength with the material factor ($\gamma_m = 1{,}15$). QRn means that the steel had been treated (heat-treatment). Most steel bars were not ribbed. If not mentioned, smooth steel can be assumed.
Allowed shear force was calculated using the diagonal tensile stress. The following formula was used:

$$\sigma_b = \rho = \frac{T}{b*z} \qquad (4.1)$$

Where:
$\sigma_b = \rho$ is the diagonal tensile stress in the concrete
z is the lever arm
b is the width
T is the occurring shear force

In practice this means that shear force can lead to problems. Especially with concrete slab bridges. Generally the construction depth was chosen just thick enough to prevent the need of shear reinforcement [21].

Appendix Table 4-1 - Concrete compressive strength former standards [21]

	Concrete quality	f'_{ck} (N/mm^2)
GBV 1950	K150	10
	K200	13
	K250	16,5
GBV 1962	K160	11
	K225	16
	K300	22
	K400	33
	K450	37
R.V.B. 1962/1967	K500	42
(addition)	K600	50
VB74 / VB74-84	B12,5	12,5
	B17,5	17,5
	B22,5	22,5
	B30	30
	B37,5	37,5
	B45	45
	B52,5	52,5
	B60	60

Appendix Table 4-2 - Material properties reinforcing and prestressing steel in former standards [22]

	Steel quality	f_s (N/mm^2)
GBV 1950/	QR 22	191
GVB 1962	QR 24	209
	QR 30	240
	QR 36	270
	QR 42	300
	QRn 36	270
	QRn 42	300
	QRn 48	330
	QRn 54	360
R.V.B. 1962/1967	QP 90	883
(Prestressing steel)	QP 105	1030
	QP 130	1275
	QP 140	1374
	QP 150	1470
	QP 160	1570
	QP 170	1670
	QP 180	1770
	QP 190	1864
	QP 200	1962

4.2 GBV 1962

The GBV 1962 is in many ways different from GVB 1950. For example the notation of many parameters. Also, the units have changed. Higher concrete quality was developed and described in this standard.
It is estimated that around 1967 FeB400 was used more. QR22 and QR24 were reduced to one low quality steel type: FeB220.

4.3 RVB 1962/1967

Since RVB 1962, there were separate standard for prestressed concrete. More information about minimum prestressing forces and types in RVBB 1962 and RVB 1967 is provided in appendix 3 and 4 from [21].
The minimum concrete quality for prestressed concrete structures is K300.

4.4 VB 74 and VB 74/84

Since VB 74, the prescriptions for reinforced and prestressed concrete were combined in one document. Also, lightweight concrete was introduced. Since 1978, FeB500 was introduced and possibly also used. In 1985 only FeB500 was applied in concrete structures.
Since the introduction of the ROBK (Richtlijnen voor het Ontwerpen van Betonnen Kunstwerken) in 1988 and the ROBK 2 in 1991 some minimum strength were adapted.
Since 1988:

- Prestressed concrete: minimum of B37,5
- Reinforced concrete: prefab and in-situ a minimum of B30
- Under water concrete: minimum of B12,5

Since 1991:

- Prestressed concrete: minimum of B45
- Reinforced concrete: prefab and in-situ a minimum of B35
- Under water concrete: minimum of B25

The following recommendations are presented:

- IN VB 74, the maximum allowable shear force is assumed to be $0{,}5 * f_b$

- In many existing concrete structures (before 1974) reinforcement that is bent upward is used. Increased shear capacity by these reinforcement bars can only be assumed if the reinforcement satisfies the statements in VBC article 9.11.4.3. [21]
- Information that has been found in the former standard can be used to estimate material parameters if these are unknown. By knowing the building year of a structure, we can estimate which standard is used for the design of the structure. In this way we can determine a lower boundary of material parameters. A disadvantage is that the estimation is often too conservative.

5 Appendix E - Tests Mindlin/Kirchhoff

Appendix Table 5-1 - Shear force per m' (kN/m) under self-weight at the support for a different slab thickness (h) and support stiffness (C) for Mindlin and Kichhoff approach. Span = 20m, slab width = 12m

		Mindlin	Kirchhoff
C = 50N/mm²	h = 200mm	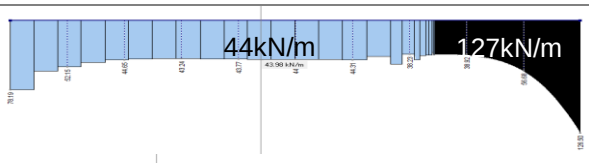	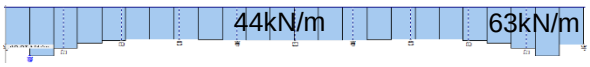
	h = 1000mm	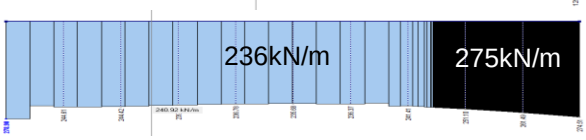	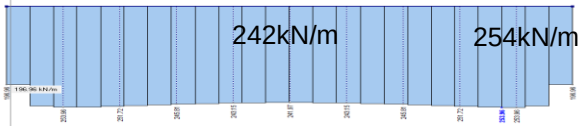
	h = 2000mm	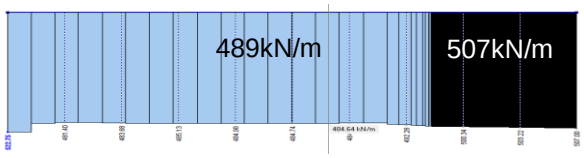	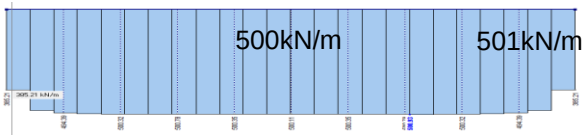
C = 250N/mm²	h = 200mm	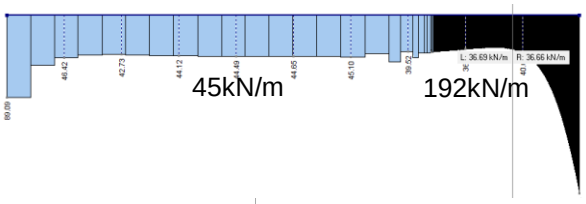	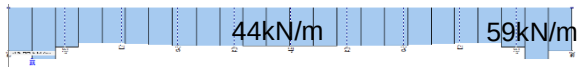
	h = 1000mm	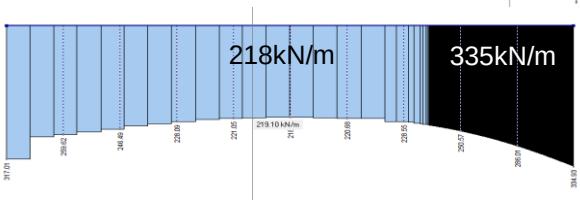	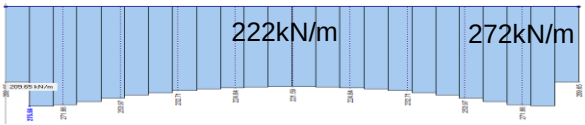
	h = 2000mm	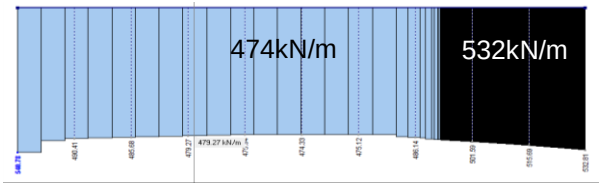	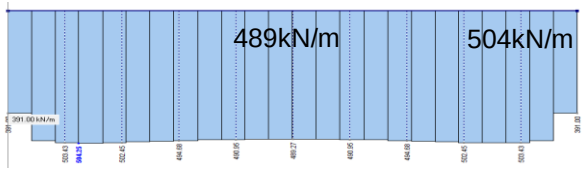
C = 500N/mm²	h = 200mm	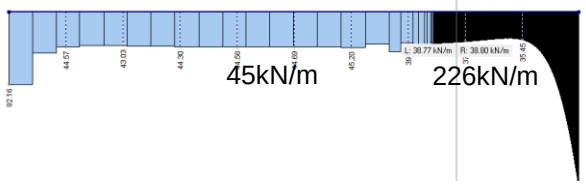	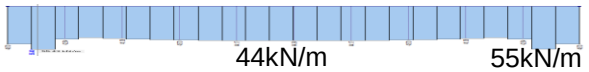

h = 1000mm

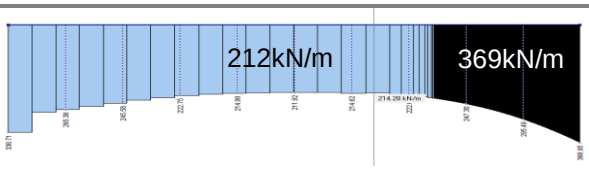

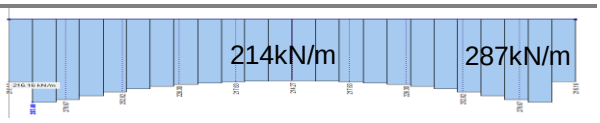

h = 2000mm

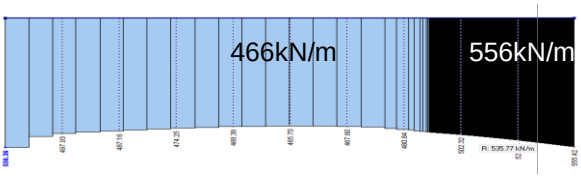

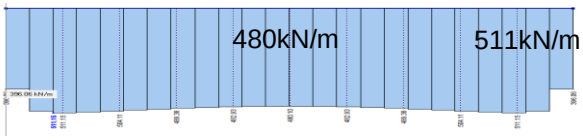

6 Appendix F – Tests cracked/uncracked slabs

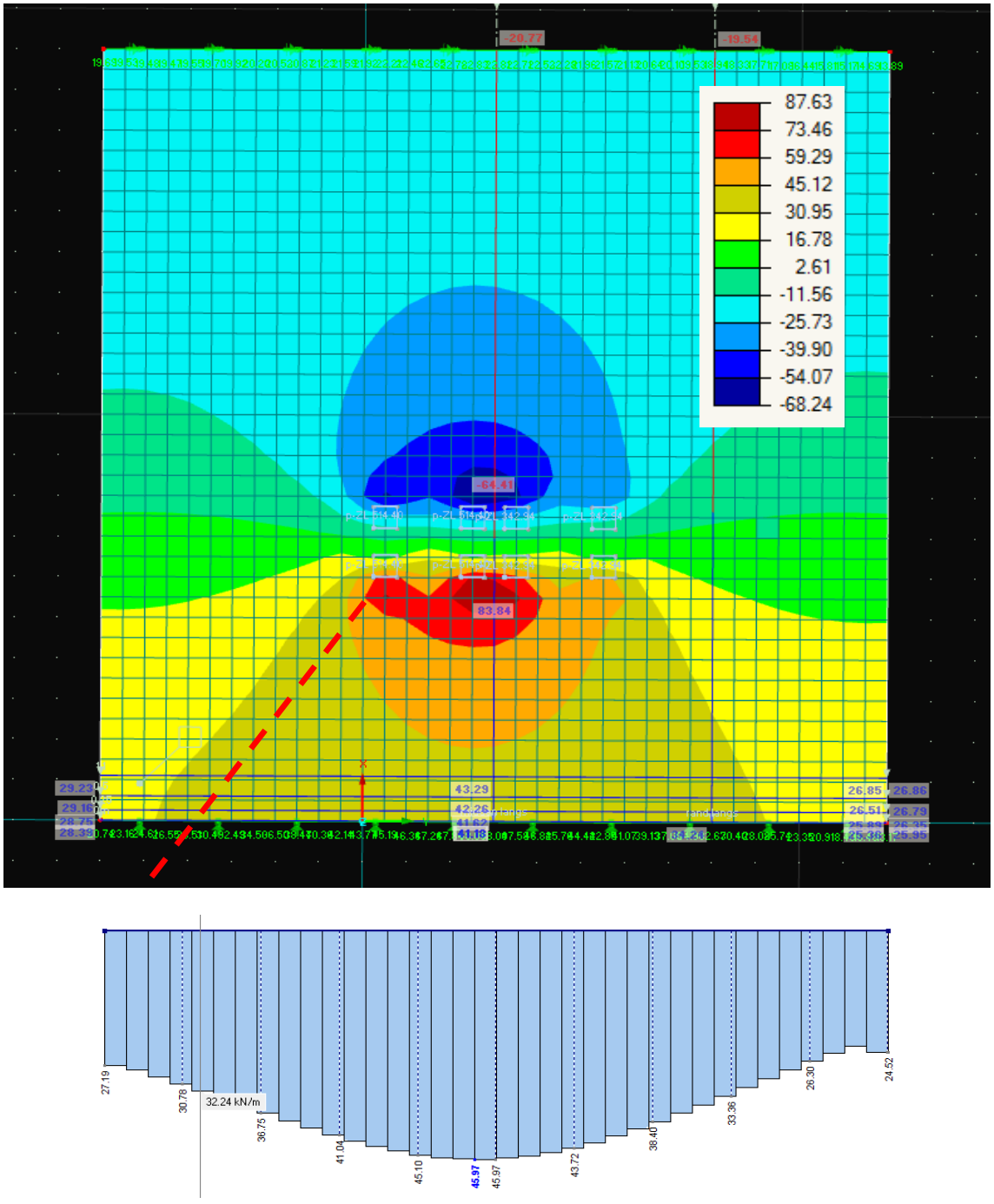

Appendix Figure 6-1 – Shear force due to LM1 axles. (span: 19m, b_{edge} = 6m, E_y = 33 GPa, h = 950 mm

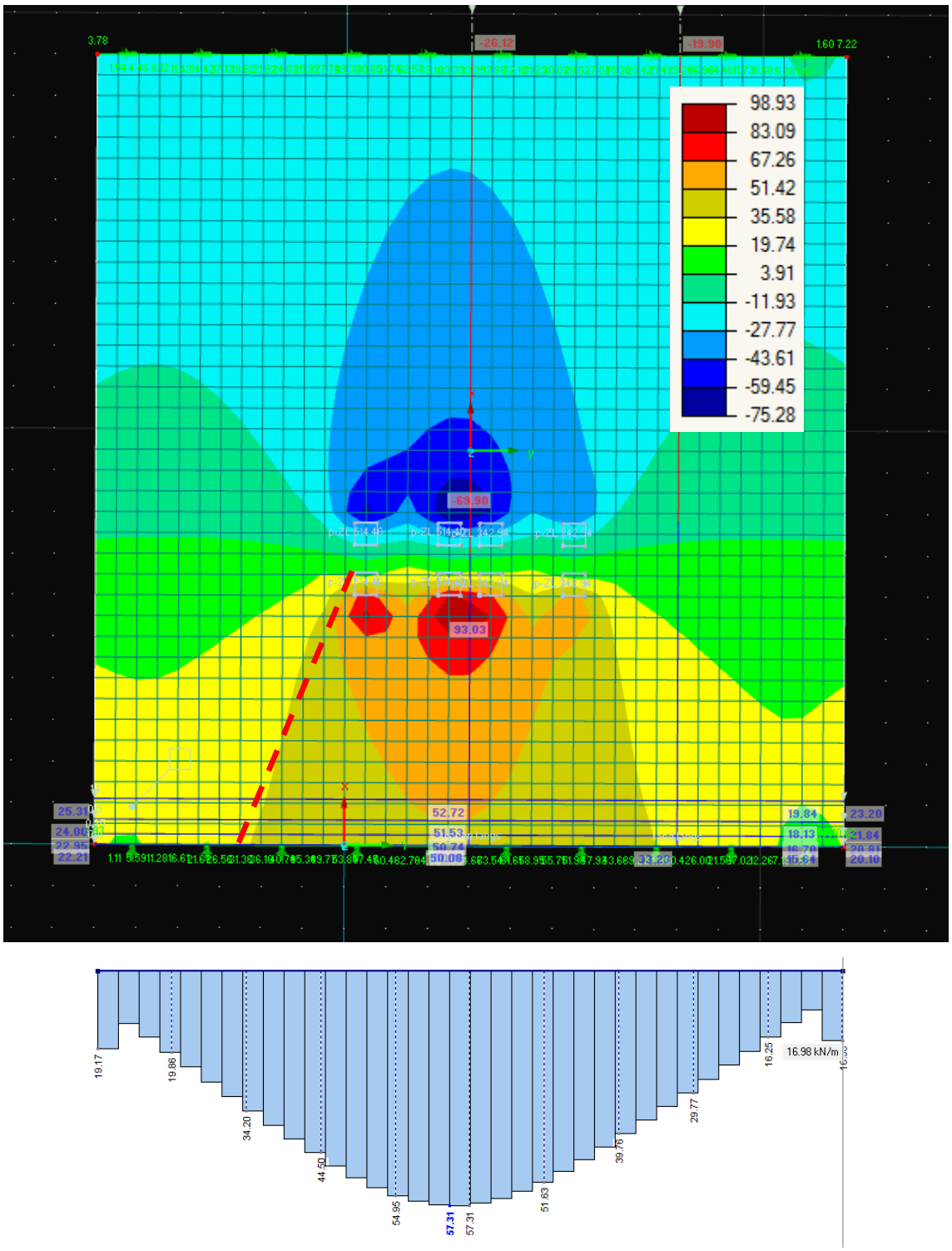

Appendix Figure 6-2 Shear force due to LM1 axles. (span: 19m, bedge = 6m, Ey = 11 GPa, h = 950 mm

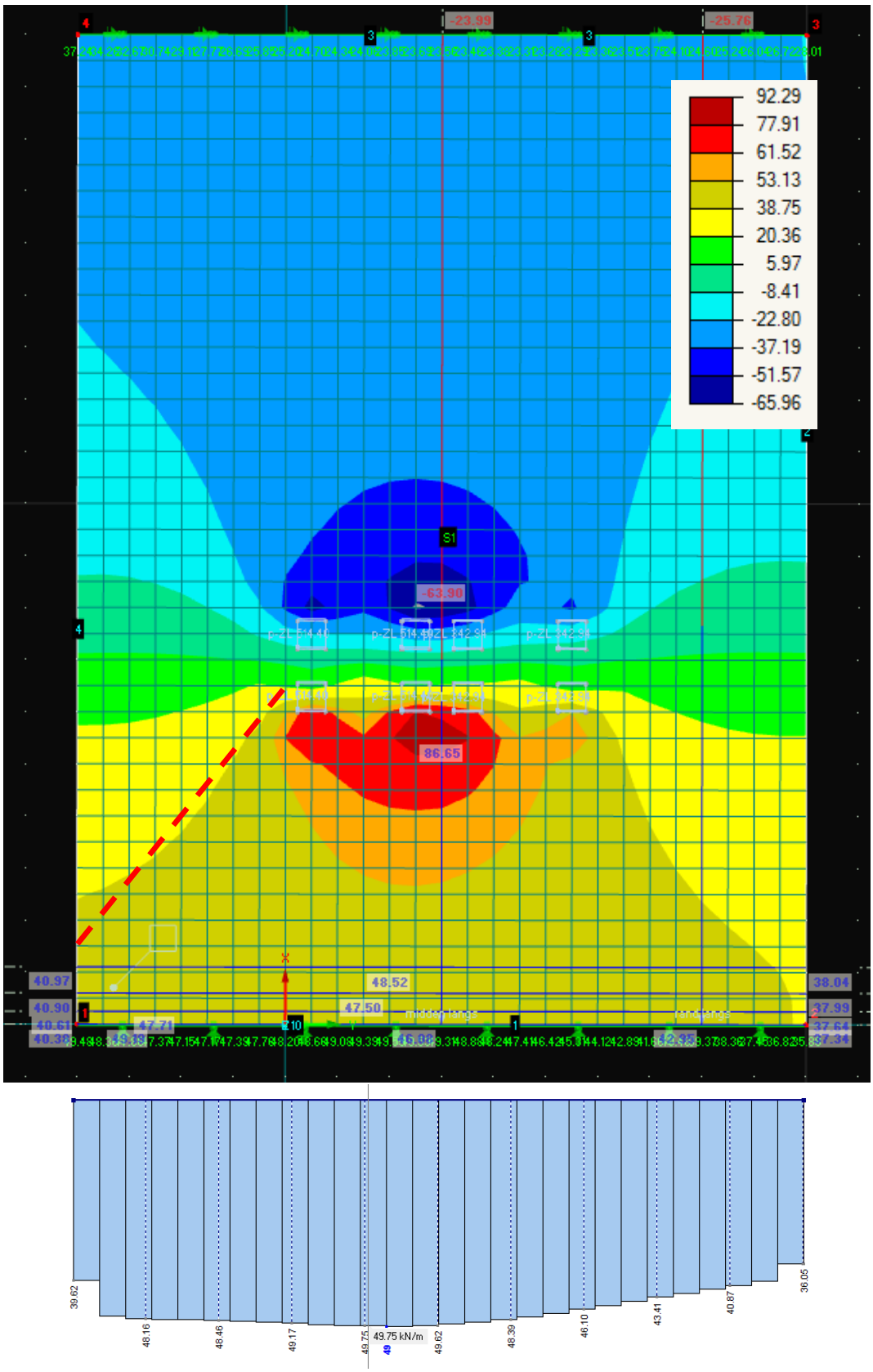

Appendix Figure 6-3 - Shear force due to LM1 axles. (span: 19m, b_{edge} = 4m, E_y = 33 GPa, h = 950 mm

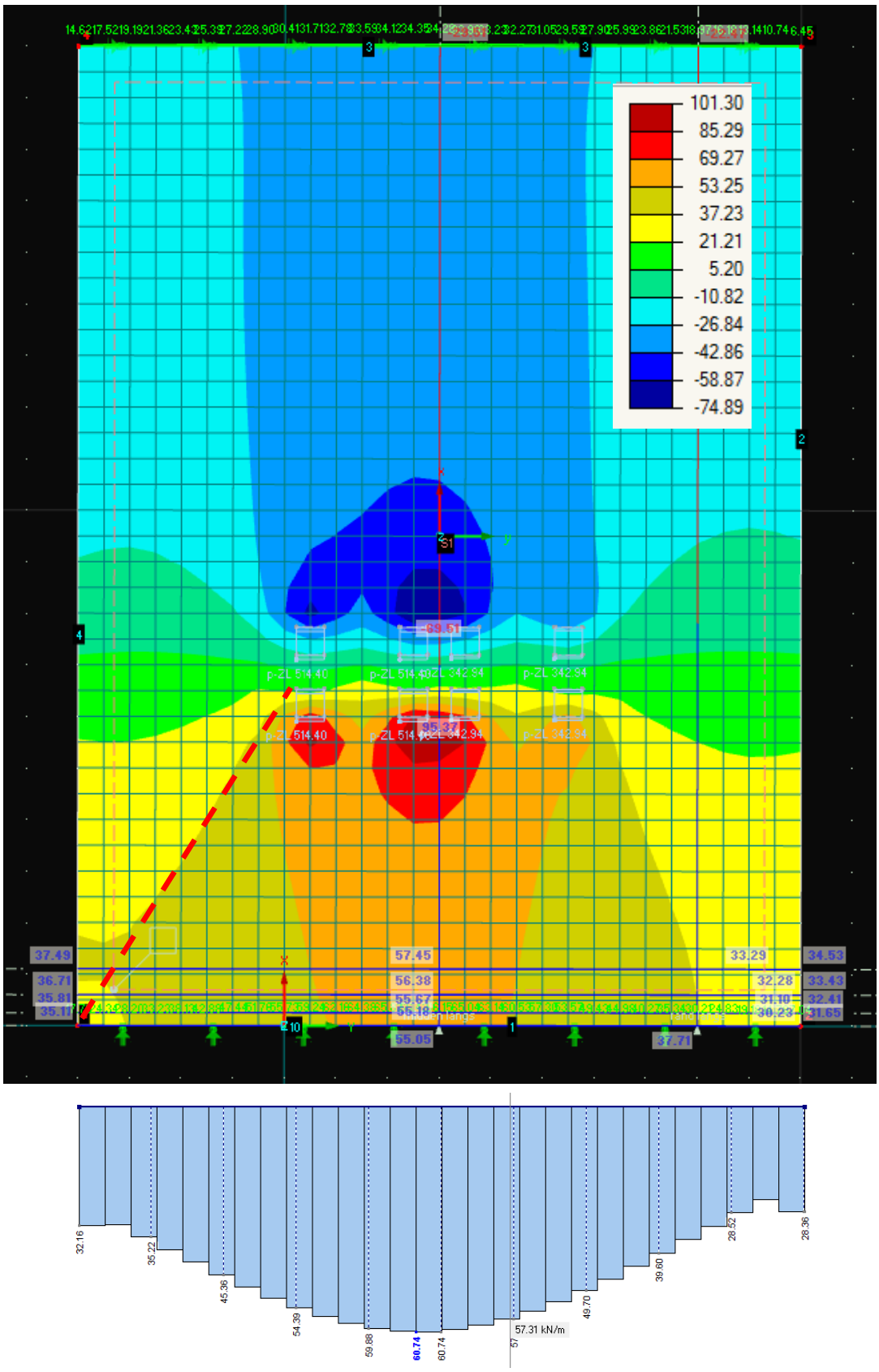

Appendix Figure 6-4 Shear force due to LM1 axles. (span: 19m, bedge = 4m, Ey = 11 GPa, h = 950 mm

7 Appendix G – Deflection due to self-weight

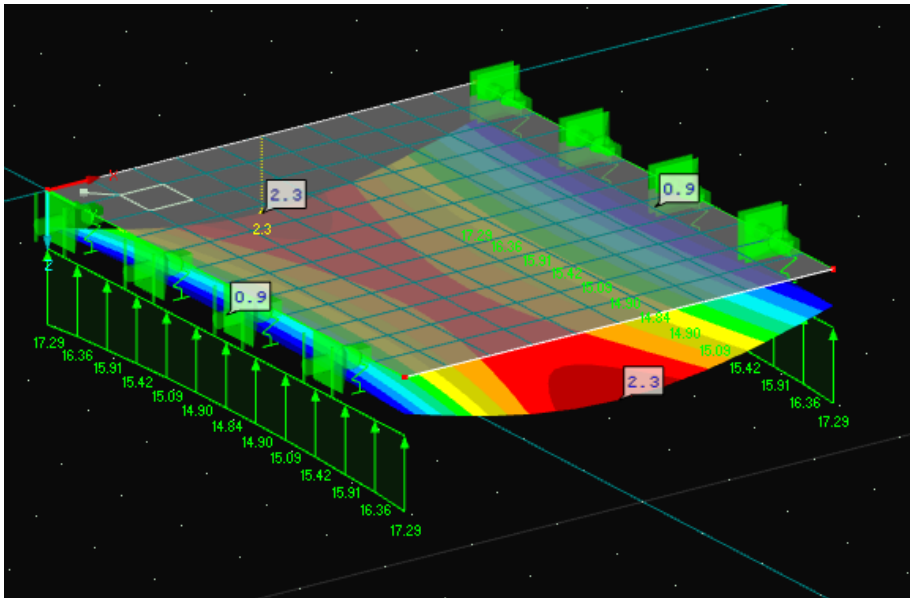

Appendix Figure 7-1 – Deflection by self-weight, 0,9mm at support, span: 5m

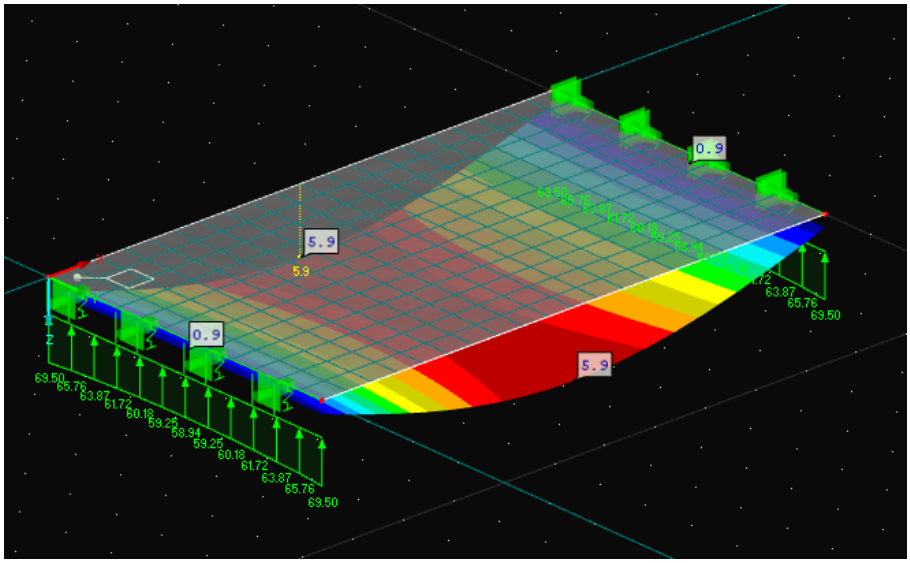

Appendix Figure 7-2 - Deflection by self-weight, 0,9mm at support, span: 10m

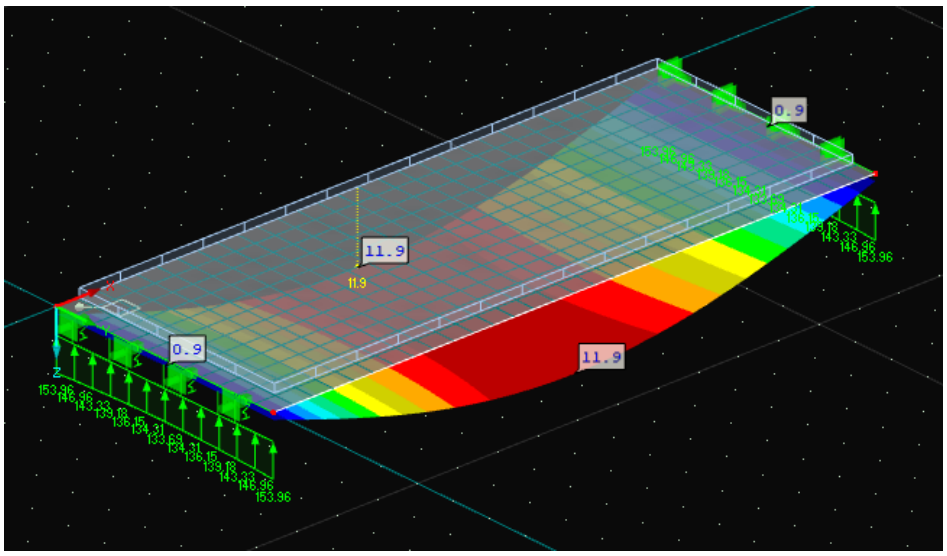

Appendix Figure 7-3 - Deflection by self-weight, 0,9mm at support, span: 15m

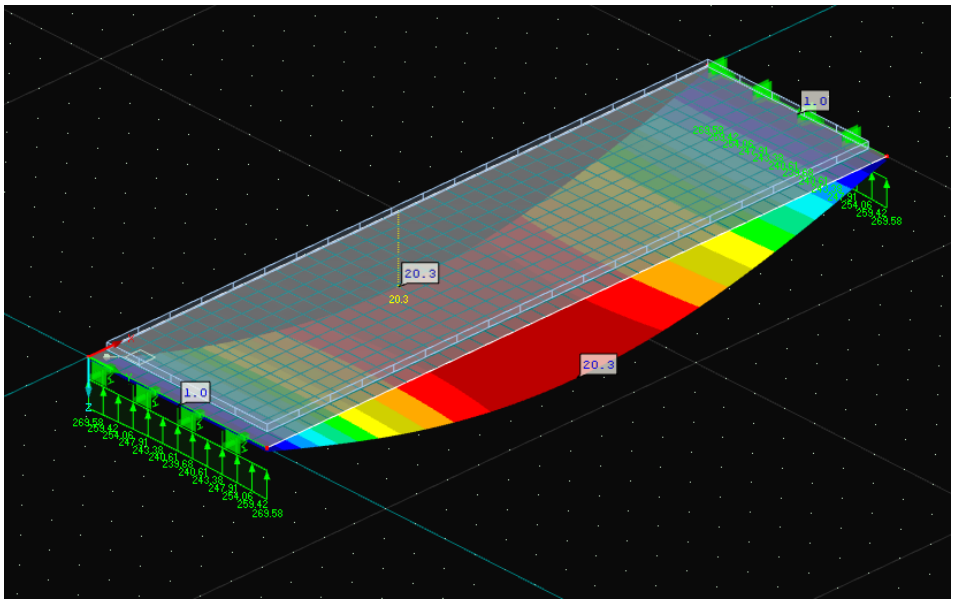

Appendix Figure 7-4 - Deflection by self-weight, 1,0 mm at support, span: 20m

8 Appendix H - Comparative FEM test results for different fatigue load models

8.1 Flexural moment

b_{edge} = 0m

Span	Lorry 1	Lorry 2	Lorry 3	Lorry 4	Lorry 5	Asphalt lorry
5	89,05	104,59	91,66	95,25	114,98	105,5
10	225,05	268,41	236,27	247,68	302,2	340,58
15	401,23	478,95	466,06	462,93	553,87	655,08
20	597,81	707,5	787,52	766,5	886,48	1041,62

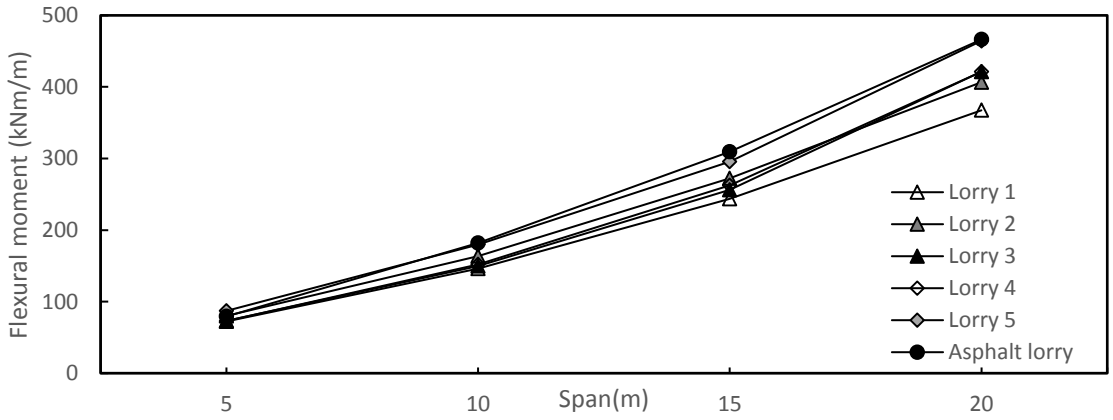

Appendix Figure 8-1 - Flexural moment for an edge distance of 0m for different fatigue load models

b_{edge} = 3,0m

Span	Lorry 1	Lorry 2	Lorry 3	Lorry 4	Lorry 5	Asphalt lorry
5	72,8	80,95	73,79	73,67	88,07	80,14
10	157,78	179,14	162,82	166,19	198,04	206,08
15	275,46	313,77	300,59	303,57	348,66	380,81
20	419,74	474,86	508,76	502,27	563,17	593,91

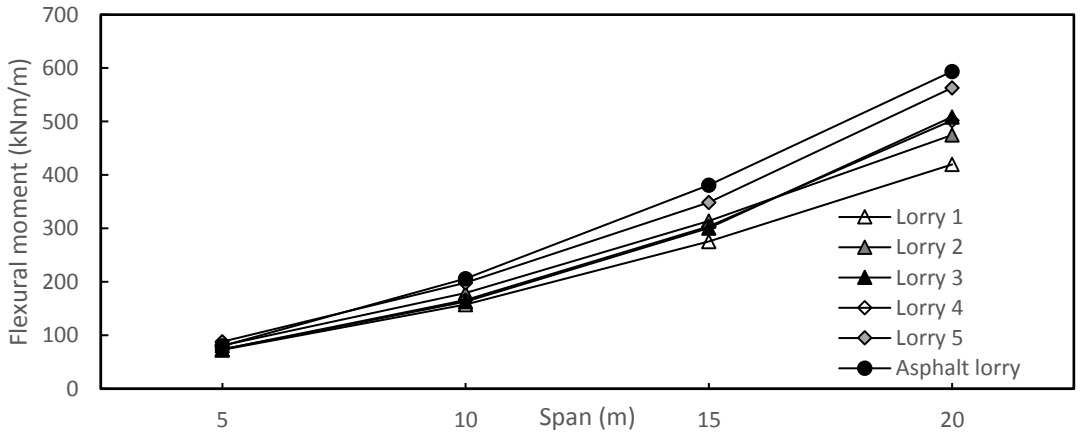

Appendix Figure 8-2 - Flexural moment for an edge distance of 3m for different fatigue load models

b_{edge} = 6,0m

Span	Lorry 1	Lorry 2	Lorry 3	Lorry 4	Lorry 5	Asphalt lorry
5	72,28	80,1	73,18	72,9	87,05	79,27
10	146,18	163,47	149,87	151,85	179,49	182,03
15	243,83	272,26	256,31	262,44	295,33	309,31
20	367,35	406,64	421,36	421,26	464,39	466,28

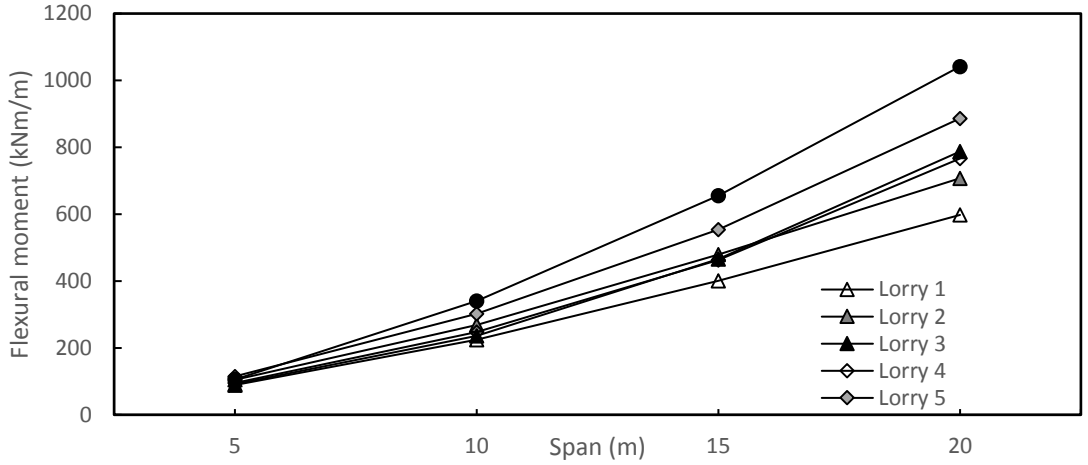

Appendix Figure 8-3 - Flexural moment for an edge distance of 6m for different fatigue load models

8.2 Shear force

b_{edge} = 0m

Span	Lorry 1	Lorry 2	Lorry 3	Lorry 4	Lorry 5	Asphalt lorry
5	71,34	93,33	79,8	83,18	86,59	85,35
10	129,64	155,55	139,76	153,13	168,01	202,14
15	162,72	194,97	209,15	219,96	248,48	275,07
20	188,41	223,85	272,06	273,53	304,87	317,00

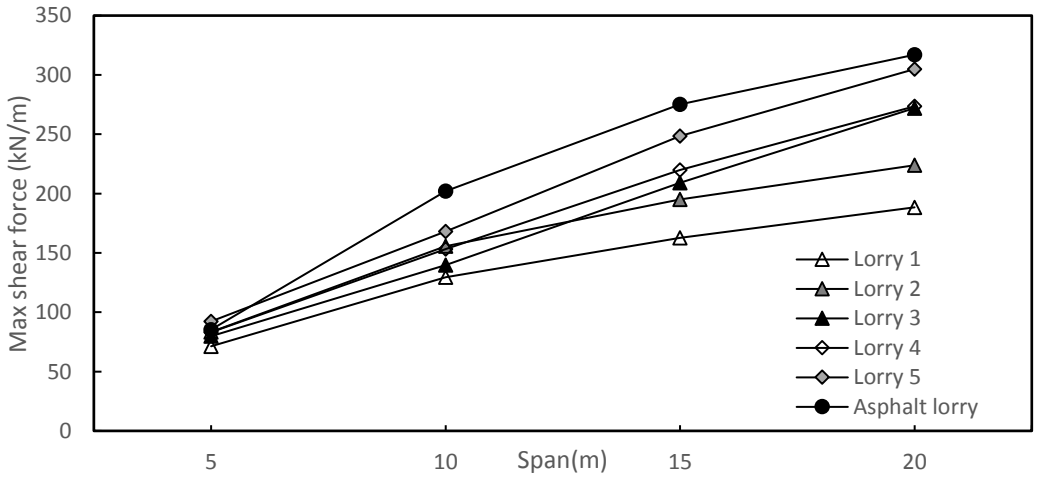

Appendix Figure 8-4 – Shear force for an edge distance of 0m for different fatigue load models

b_{edge} = 3,0m

Span	Lorry 1	Lorry 2	Lorry 3	Lorry 4	Lorry 5	Asphalt lorry
5	49,8	63,21	56,7	54,34	55,09	56,33
10	68,7	87,02	79,8	78,2	85,66	107,82
15	91,25	101,37	95,86	101,95	110,62	122,41
20	126,88	140,47	158,24	147,46	170,8	154,28

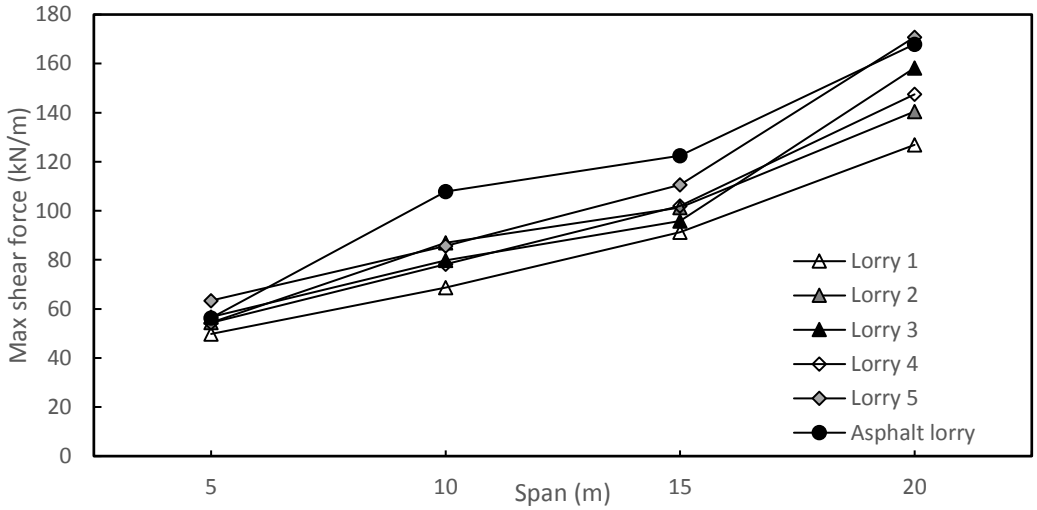

Appendix Figure 8-5 - Shear force for an edge distance of 3m for different fatigue load models

b_{edge} = 6,0m

Span	Lorry 1	Lorry 2	Lorry 3	Lorry 4	Lorry 5	Asphalt lorry
5	48,9	63,01	55,65	54,14	54,91	60,9
10	69,78	85,19	79,8	76,76	83,58	100,44
15	89,57	98,67	98,89	97,83	105,88	117,54
20	99,79	109,44	108	112,79	121,54	127,89

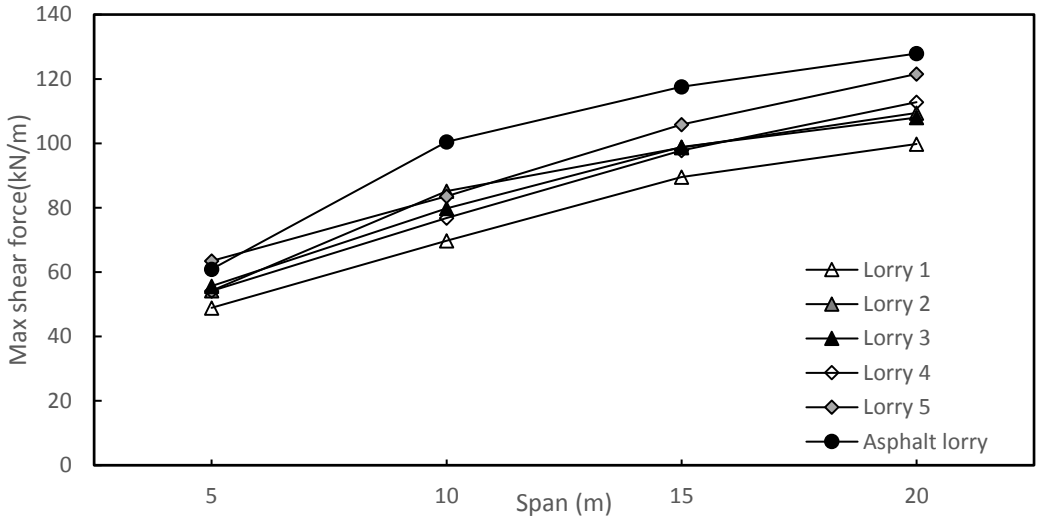

Appendix Figure 8-6 - Shear force for an edge distance of 6m for different fatigue load models

9 Appendix I – FEM results: calculation of the α factor

9.1 Flexural moment

Flexural moment due to LM1 existing structures(kNm/m)

b_{edge} → Span↓	0	1	2	3	4	5	6
5	286	225	212	208	205	204	203
7	453	360	331	317	311	307	305
9	651	526	481	456	442	435	430
11	902	747	682	646	624	611	602
13	1208	1020	937	888	858	838	825
15	1578	1357	1255	1193	1154	1127	1109
17	2020	1766	1643	1567	1517	1485	1462
19	2537	2251	2108	2019	1860	1820	1891

Flexural moment due to LM1 new structures, CC2 (kNm/m)

b_{edge} → Span↓	0	1	2	3	4	5	6
5	317	249	235	230	227	226	225
7	501	398	366	350	344	339	337
9	720	581	531	503	487	480	474
11	996	824	751	711	687	672	662
13	1332	1123	1031	976	943	921	906
15	1738	1492	1379	1310	1266	1236	1216
17	2222	1939	1803	1718	1663	1627	1602
19	2788	2470	2311	2212	2146	2102	2069

Flexural moment due to LM1 new structures, CC3 (kNm/m)

b_{edge} → Span↓	0	1	2	3	4	5	6
5	353	276	260	255	251	250	249
7	557	441	404	387	379	374	372
9	797	640	584	553	535	526	520
11	1097	903	822	777	749	733	722
13	1461	1226	1122	1061	1023	998	982
15	1898	1622	1494	1416	1368	1334	1311
17	2418	2101	1947	1851	1789	1749	1720
19	3024	2666	2487	2376	2302	2251	2215

Flexural moment due to Load Class 60 (kNm/m)

b_{edge} → Span↓	0	1	2	3	4	5	6
5	239,8	205,3	193,6	189,4	187,7	186,9	186,5
7	398,3	339,4	312,8	300,5	294,6	291,7	290,3
9	624,3	534,5	489,3	464,7	451,1	443,5	439,3
11	925,1	800,0	734,4	695,4	671,7	657,1	648,2
13	1287,1	1127,4	1042,3	989,3	955,2	932,7	917,8
15	1738,8	1542,3	1435,8	1367,7	1321,7	1289,8	1267,2
17	2281,0	2049,0	1920,9	1838,6	1781,8	1741,2	1711,6
19	2928,6	2661,9	2511,6	2415,0	2347,5	2298,3	2261,6

Flexural moment due to Load Class 45 (kNm/m)

b_{edge} → Span↓	0	1	2	3	4	5	6
5	216	191	182	179	178	177	176
7	353	310	292	283	279	277	276
9	528	469	441	425	416	412	409
11	805	720	675	650	636	627	622
13	1149	1040	982	946	924	909	900
15	1575	1440	1367	1323	1294	1275	1262
17	2092	1933	1845	1790	1754	1733	1717
19	2709	2526	2424	2361	2319	2291	2271

Flexural moment due to the Asphalt Lorry (kNm/m)

b_{edge} → Span↓	0	1	2	3	4	5	6
5	165	141	136	134	133	133	132
7	297	251	238	231	229	226	225
9	482	415	387	373	365	361	358
11	731	641	596	574	560	551	545
13	1036	922	861	829	809	796	787
15	1405	1273	1191	1150	1121	1101	1089
17	1847	1681	1596	1542	1507	1485	1468
19	2366	2181	2074	2010	1869	1842	1922

Flexural moment due to Fatigue Lorry 5 (kNm/m)

b_{edge} → Span↓	0	1	2	3	4	5	6
5	179	149	143	141	140	140	140
7	294	249	237	231	228	226	225
9	455	393	372	360	353	350	348
11	680	600	567	549	538	530	526
13	970	869	822	796	780	769	763
15	1330	1207	1147	1113	1090	1074	1065
17	1768	1626	1551	1506	1477	1457	1444
19	2297	2128	2036	1981	1845	1820	1902

Flexural moment due to Fatigue Lorry 6 (kNm/m)

b_{edge} → Span↓	0	1	2	3	4	5	6
5	178	165	157	154	153	152	152
7	333	276	258	250	246	244	243
9	504	429	399	385	377	374	369
11	737	642	599	578	564	556	551
13	1035	917	859	829	810	797	789
15	1404	1263	1190	1150	1124	1106	1095
17	1854	1692	1601	1548	1514	1493	1477
19	2397	2203	2094	2028	1887	1859	1938

Flexural moment due to the 2 Asphalt Lorries (location specific loading) (kNm/m)

b_{edge} → Span↓	0	1	2	3	4	5	6
5	179	162	150	148	146	145	145
7	332	300	269	262	255	253	252
9	555	496	437	421	405	400	395
11	860	762	678	645	626	618	603
13	1199	1082	964	924	884	867	850
15	1620	1470	1326	1262	1227	1192	1170
17	2106	1930	1753	1688	1622	1592	1561
19	2672	2466	2260	2166	2104	2059	2028

9.1.1 A factor flexural moment

The formula for α is:

$$\alpha = \frac{(M_{SW1} + M_1 - M_{SW,LM1})}{M_{LM1}}$$

Where:

M_{SW1} = The flexural moment due to self-weight by LC45, LC60 or AL (kNm/m)
M_1 = The flexural moment due to variable loads LC45, LC60 or AL (kNm/m)
$M_{SW,LM1}$ = The flexural moment due to self-weight by a Load Model 1 (kNm/m)
M_{LM1} = The flexural moment due to variable loads by Load Model 1 (kNm/m)

In order to determine the α factor the flexural moment due to self-weight is needed. This is demonstarted in the tables below.

Maximum flexural moment due to self-weight with a permanent load factor of 1,1

b_{edge} → Span↓	0	1	2	3	4	5	6
5	42	42	42	42	42	42	42
7	83	83	83	83	83	83	83
9	151	151	152	152	152	152	152
11	267	268	269	270	270	270	270
13	432	433	434	435	436	436	437
15	653	654	656	658	659	659	660
17	939	941	943	944	945	947	948
19	1296	1299	1302	1304	1306	1308	1309

Values for the self-weight with other load factors can easily be determined by multiplying the values above with a certain factor (for example by 1,2/1,1 for a load factor of 1,2)

A values for the comparison with Load Class 60 and LM1 CC3

b_{edge} → Span↓	0	1	2	3	4	5	6
5	0,73	0,82	0,83	0,83	0,84	0,84	0,84
7	0,73	0,81	0,83	0,84	0,84	0,85	0,85
9	0,75	0,82	0,84	0,86	0,87	0,87	0,88
11	0,82	0,89	0,92	0,93	0,95	0,96	0,96
13	0,87	0,95	0,98	1,01	1,02	1,04	1,04
15	0,92	1,00	1,04	1,08	1,10	1,12	1,13
17	0,96	1,05	1,10	1,14	1,17	1,20	1,22
19	1,00	1,10	1,15	1,20	1,25	1,28	1,30

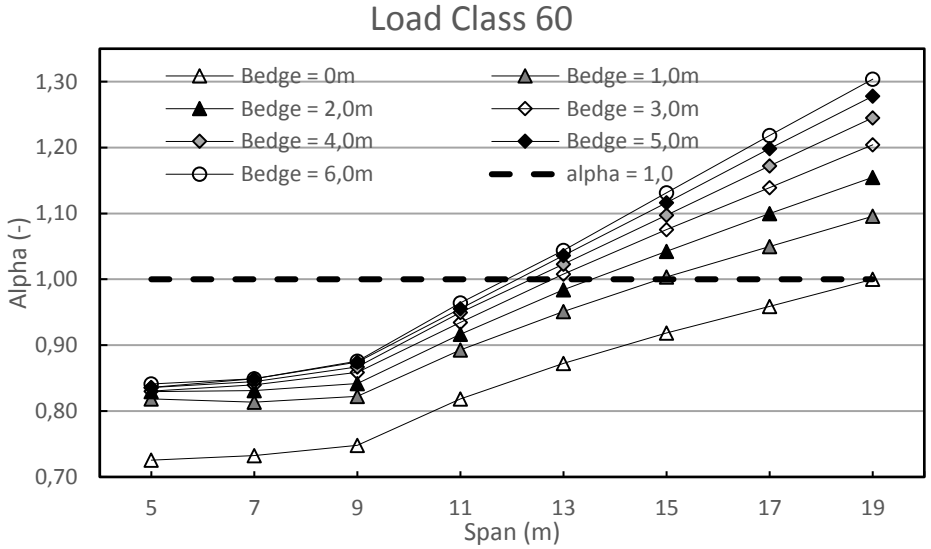

Appendix Figure 9-1 - A factor (flexural moment) for the comparison of Load Model 1 (CC3) and Load Class 60 for different spans and edge widths

A values for the comparison with Load Class 45 and LM1 CC2

b_{edge} → Span↓	0	1	2	3	4	5	6
5	0,63	0,71	0,72	0,72	0,73	0,73	0,73
7	0,64	0,71	0,73	0,74	0,75	0,75	0,75
9	0,65	0,73	0,75	0,77	0,78	0,78	0,79
11	0,73	0,81	0,83	0,85	0,87	0,88	0,89
13	0,79	0,87	0,91	0,94	0,96	0,97	0,99
15	0,84	0,93	0,98	1,02	1,05	1,07	1,09
17	0,89	0,99	1,05	1,10	1,14	1,18	1,20
19	0,94	1,05	1,13	1,19	1,39	1,44	1,31

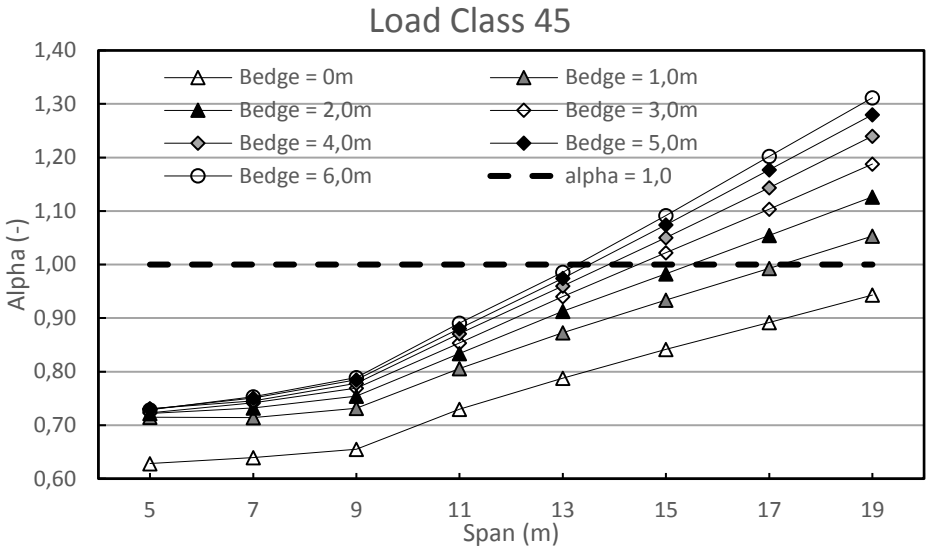

Appendix Figure 9-2 - A factor (flexural moment) for the comparison of Load Model 1 (CC2) and Load Class 45 for different spans and edge widths

A values for the comparison with the Asphalt Lorry

b_{edge} → Span↓	0	1	2	3	4	5	6
5	0,50	0,54	0,55	0,55	0,56	0,56	0,56
7	0,58	0,61	0,63	0,63	0,64	0,64	0,64
9	0,66	0,70	0,71	0,73	0,73	0,74	0,74
11	0,73	0,78	0,79	0,81	0,82	0,82	0,83
13	0,78	0,83	0,85	0,87	0,88	0,90	0,90
15	0,81	0,88	0,89	0,92	0,93	0,94	0,96
17	0,84	0,90	0,93	0,96	0,98	1,00	1,01
19	0,86	0,93	0,96	0,99	1,01	1,04	1,05

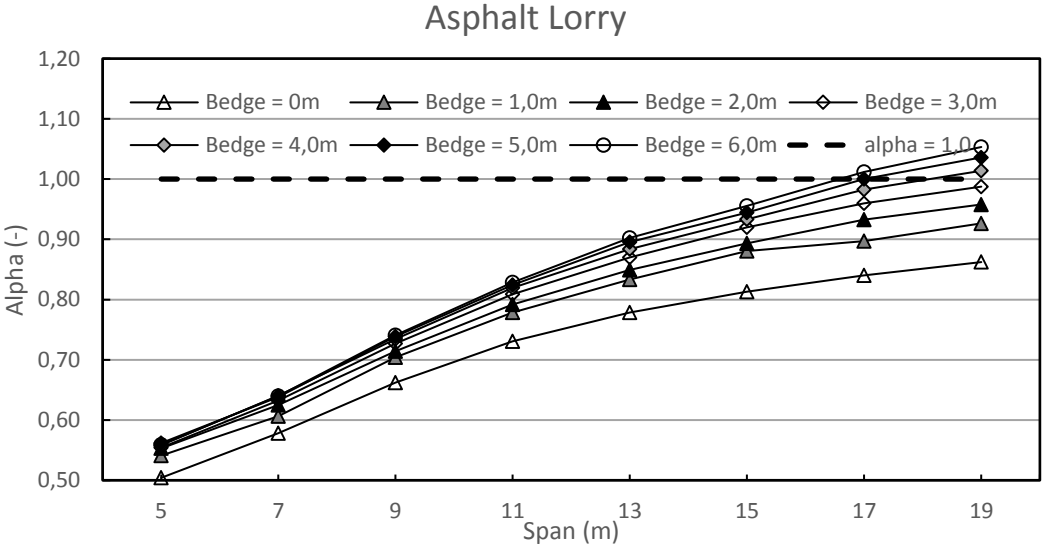

Appendix Figure 9-3- A factor (flexural moment) for the comparison of Load Model 1 and the Asphalt Lorry for different spans and edge widths

A values for the comparison with Fatigue Lorry 5

b_{edge} → Span↓	0	1	2	3	4	5	6
5	0,56	0,58	0,59	0,60	0,60	0,60	0,61
7	0,57	0,60	0,62	0,63	0,64	0,64	0,64
9	0,61	0,65	0,67	0,68	0,69	0,70	0,71
11	0,65	0,69	0,72	0,74	0,76	0,76	0,77
13	0,69	0,74	0,77	0,80	0,82	0,83	0,84
15	0,73	0,79	0,82	0,85	0,87	0,89	0,90
17	0,77	0,83	0,87	0,90	0,93	0,95	0,96
19	0,81	0,87	0,91	0,95	0,98	1,00	1,02

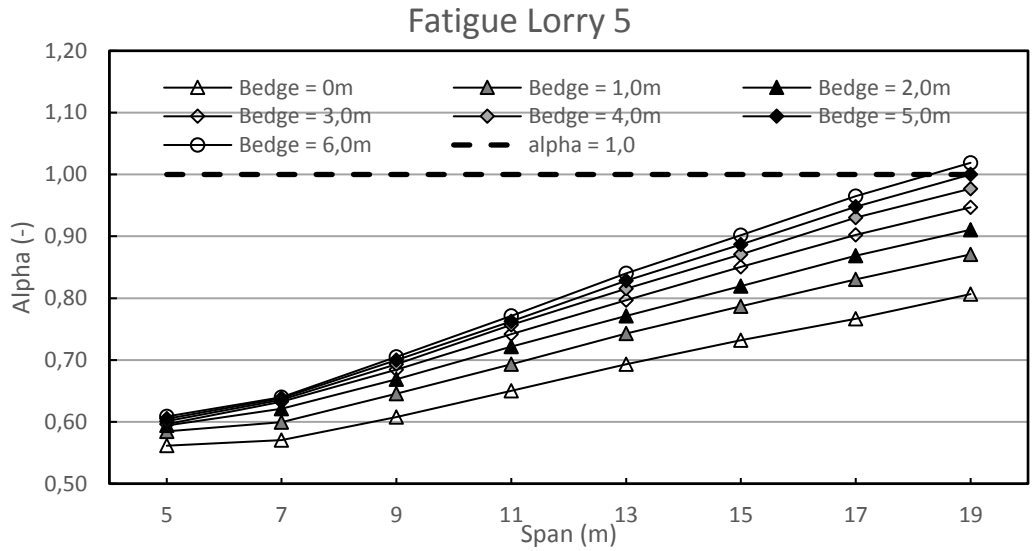

Appendix Figure 9-4 - A factor (flexural moment) for the comparison of Load Model 1 and fatigue load model 5 for different spans and edge widths

A values for the comparison with the Fatigue Lorry 6

b_{edge} → Span↓	0	1	2	3	4	5	6
5	0,56	0,67	0,68	0,67	0,68	0,68	0,68
7	0,68	0,70	0,71	0,71	0,71	0,72	0,72
9	0,71	0,74	0,75	0,77	0,78	0,78	0,78
11	0,74	0,78	0,80	0,82	0,83	0,84	0,85
13	0,78	0,82	0,84	0,87	0,89	0,90	0,91
15	0,81	0,87	0,89	0,92	0,94	0,96	0,97
17	0,85	0,91	0,94	0,97	0,99	1,01	1,03
19	0,89	0,95	0,98	1,01	1,04	1,06	1,08

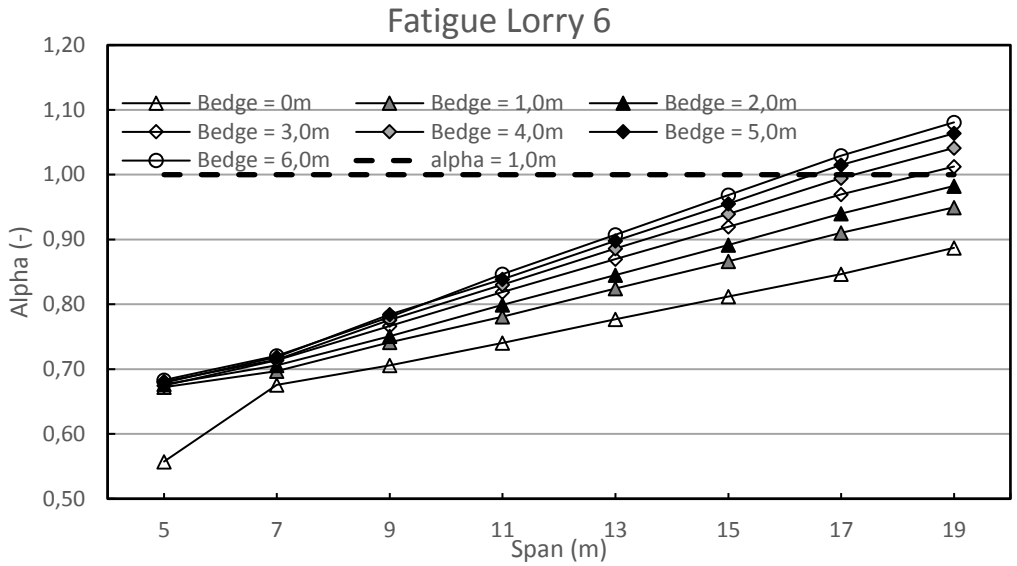

Appendix Figure 9-5 - A factor (flexural moment) for the comparison of Load Model 1 and fatigue load model 6 for different spans and edge widths

A values for the comparison with the 2 Asphalt Lorries (Location specific loading)

b_{edge} → Span↓	0	1	2	3	4	5	6
5	0,55	0,72	0,71	0,72	0,72	0,71	0,72
7	0,65	0,84	0,80	0,81	0,82	0,81	0,82
9	0,76	0,98	0,91	0,91	0,91	0,90	0,89
11	0,83	1,08	0,99	0,99	1,00	0,99	0,99
13	0,88	1,06	1,02	1,02	1,03	1,01	1,02
15	0,90	1,02	1,04	1,05	1,06	1,06	1,06
17	0,92	1,03	1,14	1,13	1,11	1,11	1,11
19	0,94	1,04	1,25	1,19	1,16	1,14	1,13

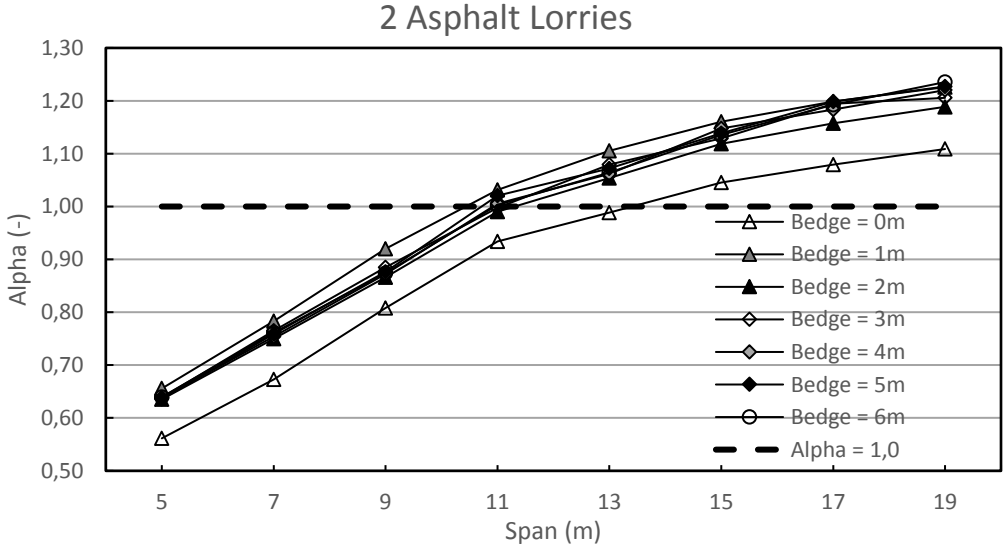

Appendix Figure 9-6 - A factor (flexural moment) for the comparison of Load Model 1 and two Asphalt Lorries (location specific) for different spans and edge widths

9.1.2 Summary α factors flexural moment

For flexural moment distinction between small and large edge widths has been made.
This had been done according to Appendix Figure 9-3, Appendix Figure 9-5 and Appendix Figure 9-6 with α = 0,8 as lower boundary.

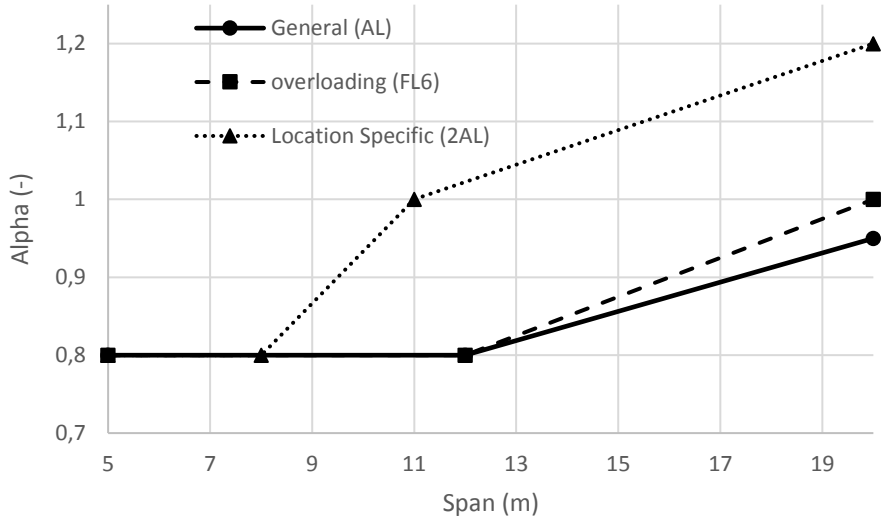

Appendix Figure 9-7 - General α factor for flexural moment, small edge widths

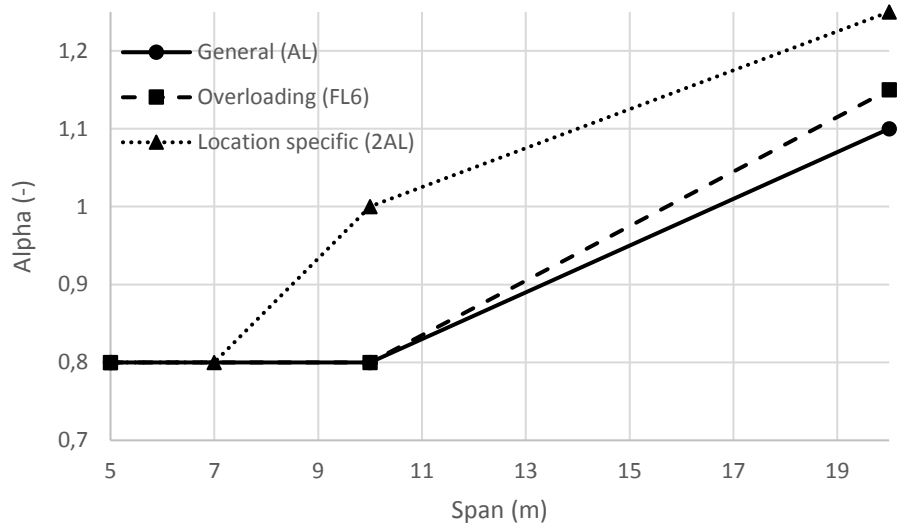

Appendix Figure 9-8 - General α factor for flexural moment, large edge widths

9.2 Shear force

The maximum occurring shear force due to Load Model 1, Load Class 60, Load Class 45, and the fatigue lorries are demonstrated in the tables below.

Shear force due to LM1 existing structures(kN/m)

b_{edge} → Span↓	0	1	2	3	4	5	6
5	205	159	156	154	153	152	151
7	256	198	195	192	190	190	189
9	293	228	221	220	218	218	219
11	225	258	250	248	246	247	247
13	381	310	286	284	283	285	284
15	432	359	327	323	322	322	321
17	488	420	368	362	362	363	364
19	551	482	419	406	408	409	411

Shear force due to LM1, CC2 (kN/m)

b_{edge} → Span↓	0	1	2	3	4	5	6
5	227	176	173	170	169	168	167
7	283	219	216	212	210	210	209
9	324	252	244	243	241	241	242
11	370	285	276	273	271	272	272
13	420	341	315	313	311	314	313
15	476	395	359	355	354	354	353
17	537	461	404	397	397	398	399
19	606	529	460	445	447	448	451

Shear force due to LM1, CC3 (kN/m)

b_{edge} → Span↓	0	1	2	3	4	5	6
5	253	195	192	189	188	187	185
7	315	243	239	235	233	233	231
9	359	278	269	268	265	265	267
11	408	313	303	300	297	298	298
13	462	373	344	341	340	342	341
15	521	429	391	386	384	384	383
17	585	500	437	430	430	431	431
19	658	571	496	480	482	483	485

Shear force due to Load Class 60(kN/m)

$b_{edge} \rightarrow$ Span↓	0	1	2	3	4	5	6
5	206	167	162	160	159	158	157
7	268	217	214	212	211	210	209
9	319	258	253	252	249	248	248
11	372	302	294	293	291	292	291
13	430	360	344	341	340	341	341
15	494	430	396	392	391	394	394
17	565	505	455	451	449	450	449
19	638	587	552	507	508	511	515

Shear force due to Load Class 45(kN/m)

$b_{edge} \rightarrow$ Span↓	0	1	2	3	4	5	6
5	165	135	131	130	129	128	127
7	213	177	175	173	172	171	171
9	261	214	210	209	206	207	207
11	311	256	251	250	248	249	249
13	367	315	299	297	296	297	298
15	429	382	351	348	347	350	351
17	496	453	427	407	405	406	406
19	570	535	511	462	464	468	473

Shear force due to Asphalt Lorry(kN/m)

$b_{edge} \rightarrow$ Span↓	0	1	2	3	4	5	6
5	129	104	103	101	100	100	101
7	180	142	141	139	138	138	138
9	230	183	177	178	177	176	176
11	283	238	215	214	214	213	214
13	336	290	257	255	256	256	257
15	392	346	322	300	301	302	303
17	451	409	378	350	347	347	348
19	514	472	450	448	400	402	404

Shear force due to Fatigue Lorry 5 (kN/m)

$b_{edge} \rightarrow$ Span↓	0	1	2	3	4	5	6
5	132	110	105	104	103	102	101
7	168	139	137	136	136	136	135
9	212	173	171	171	170	170	170
11	263	221	207	207	206	207	207
13	321	277	250	249	250	252	251
15	378	336	298	295	296	297	297
17	439	399	363	342	342	343	343
19	504	465	443	422	396	397	399

Shear force due to fatigue Lorry 6 (kN/m)

$b_{edge} \rightarrow$ Span↓	0	1	2	3	4	5	6
5	154	120	115	114	114	114	114
7	194	154	153	152	151	151	150
9	239	191	190	189	188	188	188
11	292	235	231	230	228	228	226
13	352	298	279	279	277	276	275
15	410	358	333	333	330	330	329
17	472	423	387	396	388	386	383
19	538	489	460	434	452	452	452

Shear force due to 2 Asphalt Lorries (location specific loading) (kN/m)

$b_{edge} \rightarrow$ Span↓	0	1	2	3	4	5	6
5	126	123	120	119	118	117	117
7	182	173	165	164	163	162	162
9	237	220	207	205	204	203	202
11	294	264	249	247	246	245	245
13	350	320	290	288	287	287	287
15	407	372	334	332	332	332	331
17	467	436	391	384	379	380	381
19	533	498	463	436	433	431	431

9.2.1 A factor shear force

The formula for α is:

$$\alpha = \frac{(V_{SW1} + V_1 - V_{SW,LM1})}{V_{LM1}}$$

Where:

V_{SW1} = The shear force due to self-weight by LC45, LC60 or AL (kN/m)
V_1 = The shear force due to variable loads LC45, LC60 or AL (kN/m)
$V_{SW,LM1}$ = The shear force due to self-weight by a Load Model 1 (kN/m)
V_{LM1} = The shear force due to variable loads by Load Model 1 (kN/m)

In order to determine the α factor the shear force due to self-weight is needed. This is demonstrated in the tables below. Distinction has been made between shear force near the edge of the support and near the middle of the support.

Maximum shear force due to self-weight with a load factor of 1,1 near the middle of the support

$b_{edge} \rightarrow$ Span↓	0	1	2	3	4	5	6
5	30	30	30	30	30	30	30
7	43	43	43	43	43	43	43
9	61	61	61	62	62	62	63
11	88	88	88	89	90	91	92
13	122	121	121	121	123	125	126
15	160	159	159	158	161	163	164
17	204	202	200	198	201	204	207
19	253	249	246	244	247	250	254

Maximum shear force due to self-weight with a load factor of 1,1 near the edge of the support

b_{edge} → Span↓	0	1	2	3	4	5	6
5	30	30	30	30	30	30	30
7	44	44	44	44	44	44	44
9	64	64	65	66	66	66	66
11	94	96	97	98	98	98	98
13	129	131	134	136	136	136	136
15	170	173	178	181	181	182	182
17	216	222	228	233	233	234	234
19	268	275	286	291	292	293	294

Values for the self-weight with other load factors can easily be determined by multiplying the values above with a certain factor (for example by 1,2/1,1 for a load factor of 1,2)

A values for the comparison with Load Class 60

b_{edge} → Span↓	0	1	2	3	4	5	6
5	0,79	0,82	0,81	0,81	0,81	0,81	0,81
7	0,82	0,87	0,87	0,88	0,88	0,88	0,88
9	0,86	0,90	0,92	0,92	0,92	0,91	0,90
11	0,88	0,95	0,96	0,97	0,97	0,97	0,96
13	0,90	0,94	1,00	1,00	1,00	0,99	1,00
15	0,92	1,00	1,03	1,03	1,03	1,05	1,06
17	0,94	1,02	1,08	1,10	1,10	1,10	1,09
19	0,94	1,06	1,17	1,13	1,13	1,14	1,15

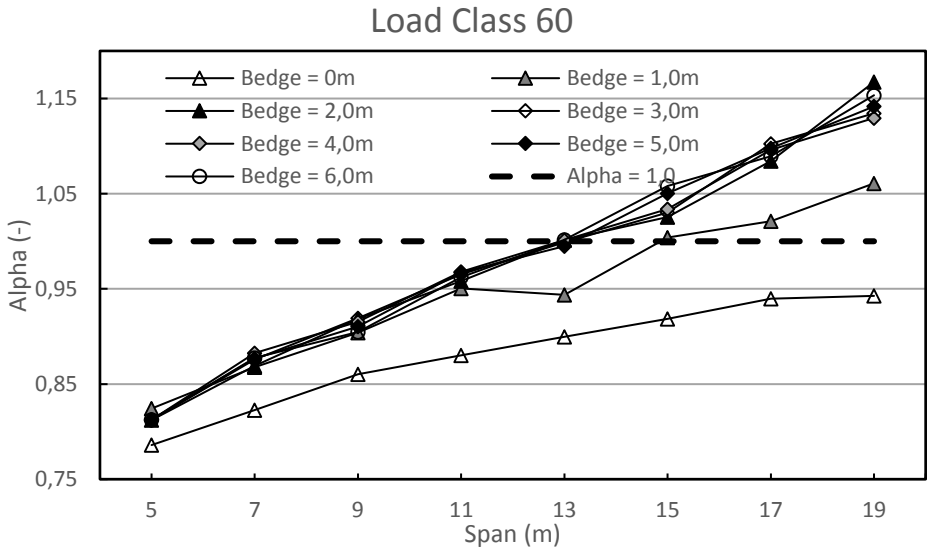

Appendix Figure 9-9 - A factor (Shear force) for the comparison of Load Model 1 and Load Class 60 for different spans and edge widths

A values for the comparison with Load Class 45

b_{edge} → Span↓	0	1	2	3	4	5	6
5	0,68	0,71	0,70	0,71	0,71	0,70	0,70
7	0,70	0,76	0,76	0,76	0,77	0,76	0,77
9	0,75	0,80	0,81	0,81	0,80	0,81	0,80
11	0,78	0,85	0,86	0,87	0,87	0,87	0,87
13	0,81	0,87	0,91	0,91	0,91	0,91	0,92
15	0,84	0,94	0,95	0,96	0,96	0,98	0,99
17	0,86	0,96	1,03	1,05	1,04	1,04	1,04
19	0,89	1,03	1,08	1,09	1,09	1,11	1,13

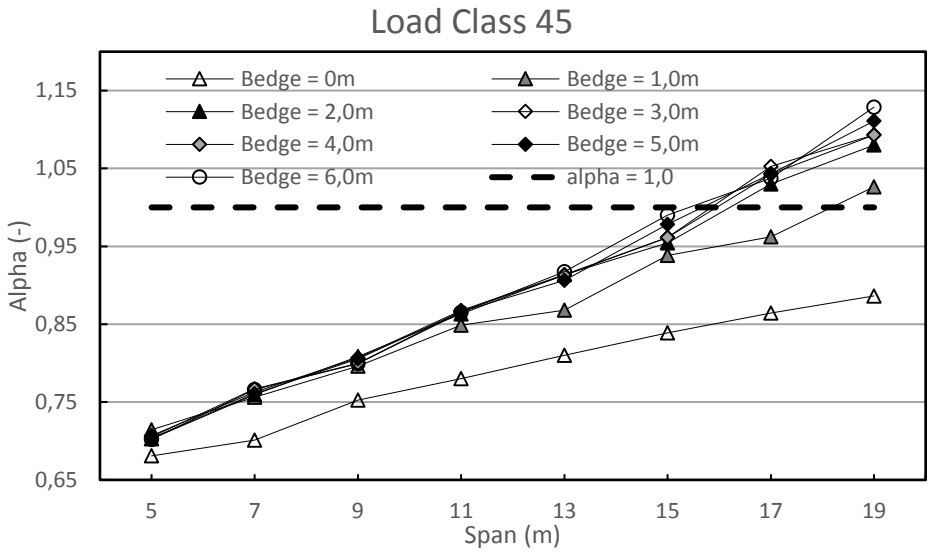

Appendix Figure 9-10 - A factor (Shear force) for the comparison of Load Model 1 and Load Class 45 for different spans and edge widths

A values for the comparison with Asphalt Lorry

b_{edge} → Span↓	0	1	2	3	4	5	6
5	0,57	0,57	0,58	0,57	0,57	0,57	0,59
7	0,64	0,64	0,64	0,64	0,65	0,65	0,65
9	0,72	0,73	0,73	0,73	0,74	0,73	0,72
11	0,78	0,84	0,78	0,79	0,79	0,78	0,79
13	0,82	0,89	0,82	0,82	0,83	0,82	0,83
15	0,85	0,93	0,86	0,86	0,87	0,87	0,89
17	0,86	0,94	0,89	0,93	0,91	0,90	0,90
19	0,87	0,95	0,95	0,97	0,95	0,96	0,96

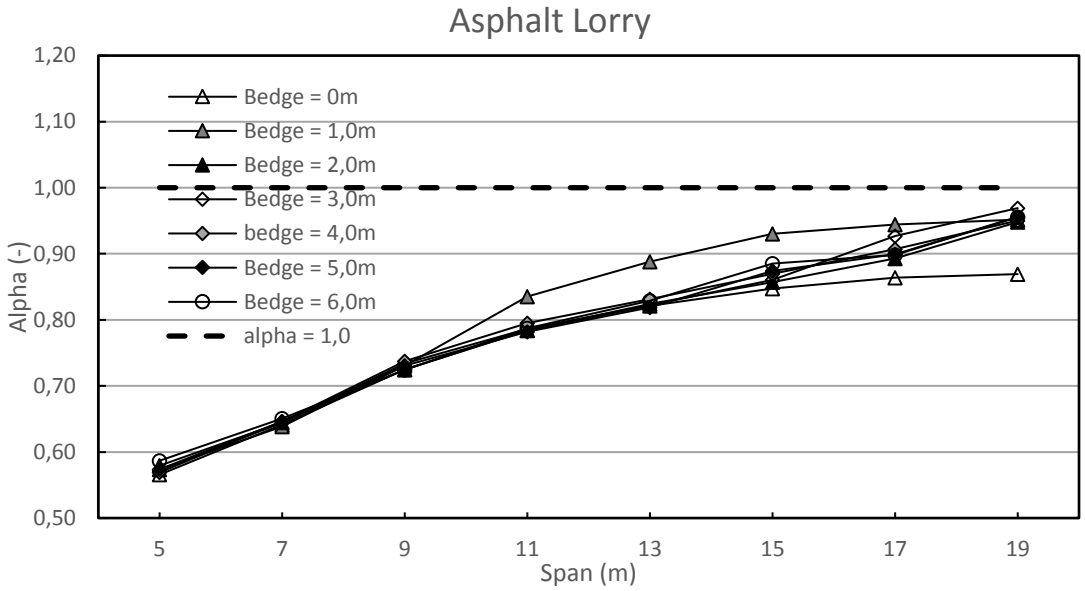

Appendix Figure 9-11 - A factor (Shear force) for the comparison of Load Model 1 and the Asphalt Lorry for different spans and edge widths

A values for the comparison with Fatigue Lorry 5

b_{edge} → Span↓	0	1	2	3	4	5	6
5	0,58	0,62	0,60	0,60	0,59	0,59	0,59
7	0,58	0,62	0,62	0,62	0,63	0,63	0,63
9	0,65	0,67	0,69	0,69	0,69	0,69	0,69
11	0,70	0,74	0,73	0,74	0,74	0,74	0,74
13	0,76	0,82	0,78	0,79	0,79	0,79	0,79
15	0,79	0,88	0,83	0,83	0,84	0,84	0,85
17	0,82	0,89	0,87	0,88	0,88	0,87	0,87
19	0,83	0,92	0,91	0,92	0,93	0,92	0,92

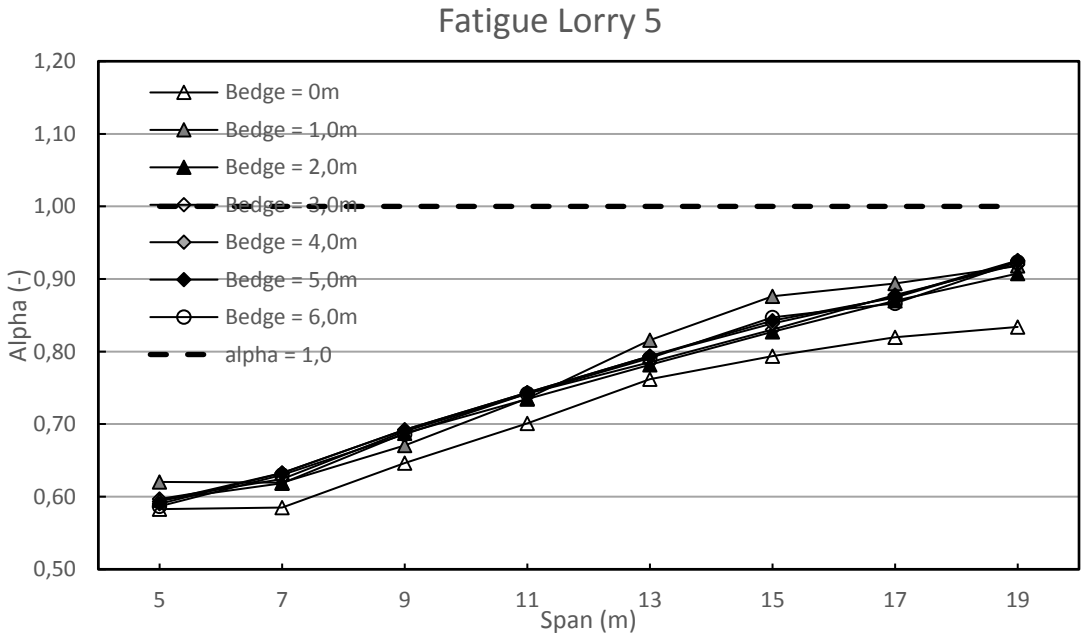

Appendix Figure 9-12 - A factor (Shear force) for the comparison of Load Model 1 and the Fatigue Lorry 5 for different spans and edge widths

A values for the comparison with Fatigue Lorry 6

b_{edge} → Span↓	0	1	2	3	4	5	6
5	0,71	0,70	0,67	0,68	0,68	0,69	0,69
7	0,71	0,71	0,72	0,72	0,73	0,73	0,73
9	0,76	0,76	0,78	0,78	0,78	0,78	0,78
11	0,82	0,82	0,83	0,83	0,83	0,83	0,83
13	0,88	0,93	0,88	0,88	0,88	0,88	0,88
15	0,92	0,99	0,92	0,92	0,93	0,93	0,94
17	0,94	1,02	0,95	0,99	0,96	0,96	0,95
19	0,95	1,03	1,01	1,00	0,99	1,00	1,01

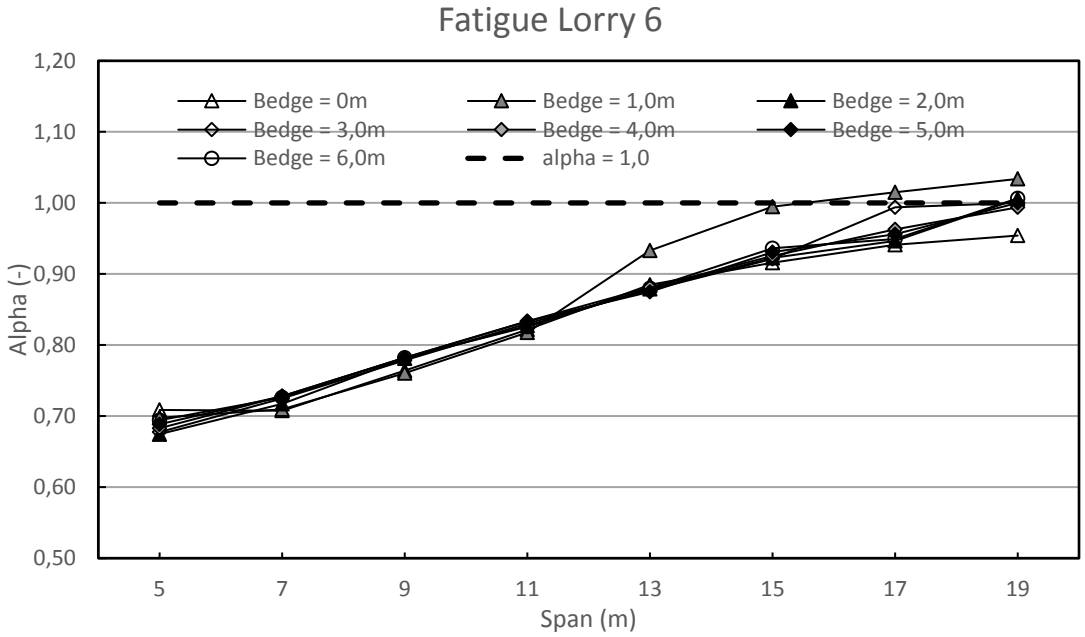

Appendix Figure 9-13 - A factor (Shear force) for the comparison of Load Model 1 and the Fatigue Lorry 6 for different spans and edge widths

A values for the comparison with 2 Asphalt Lorries

b_{edge} → Span↓	0	1	2	3	4	5	6
5	0,55	0,72	0,71	0,72	0,72	0,71	0,72
7	0,65	0,84	0,80	0,81	0,82	0,81	0,82
9	0,76	0,95	0,91	0,91	0,91	0,90	0,89
11	0,83	1,04	0,99	0,99	1,00	0,99	0,99
13	0,88	1,06	1,02	1,02	1,03	1,01	1,02
15	0,90	1,07	1,04	1,05	1,06	1,06	1,06
17	0,92	1,08	1,14	1,13	1,11	1,11	1,11
19	0,94	1,08	1,25	1,19	1,16	1,14	1,13

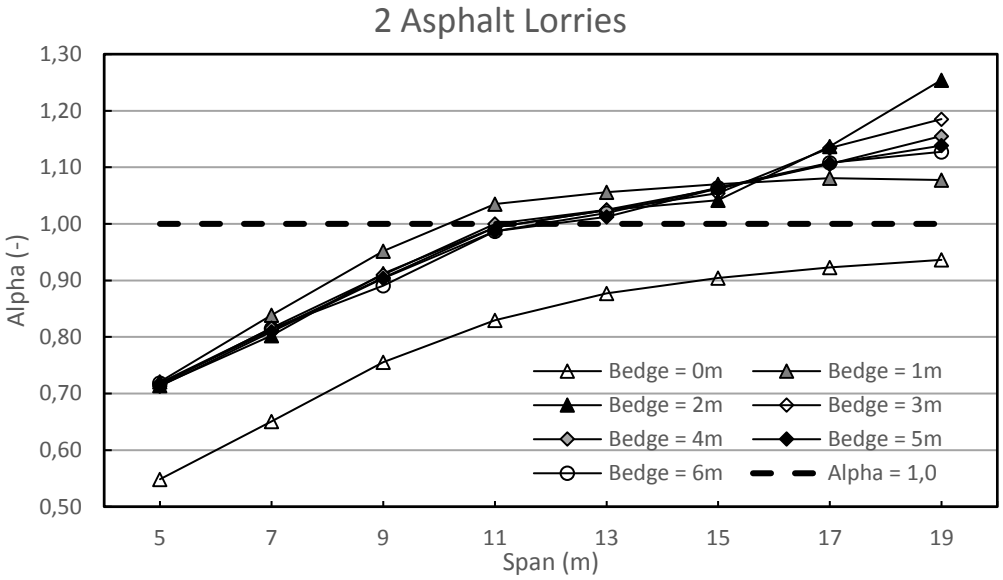

Appendix Figure 9-14 - A factor (Shear force) for the comparison of Load Model 1 and two asphalt lorries for different spans and edge widths

9.2.2 Summary α factors flexural moment

For shear force the edge distance has little influence on the α factor. The general graphs for the α factor have been made according to Appendix Figure 9-11, Appendix Figure 9-13 and Appendix Figure 9-14 with α = 0,8 as lower boundary.

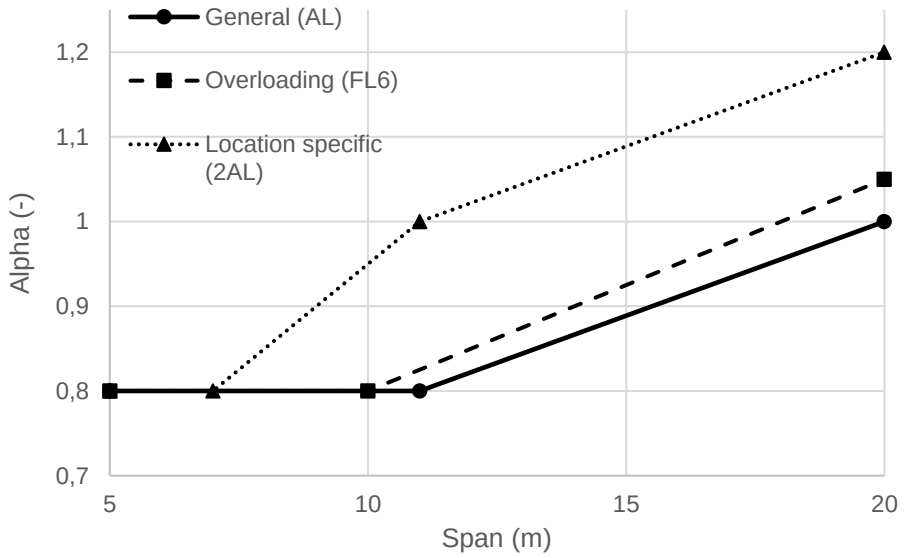

Appendix Figure 9-15 - General α factor for shear force

10 Appendix J – Comparing shear forces

10.1 Occurring shear forces

In this appendix, all occurring shear stresses in level 3 of Appendix Figure 10-1 are demonstrated in the tables below (from left to right).

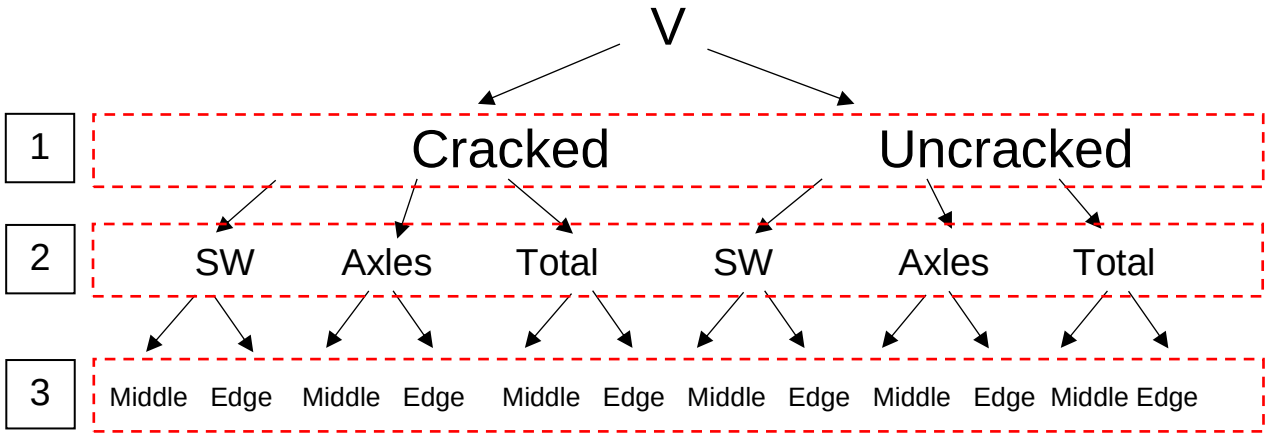

Appendix Figure 10-1 - Overview research FE model

Shear force due to **self-weight** near the **middle** of the slab (partial factor 1,1), **cracked slab**

b_{edge} → Span↓	0	1	2	3	4	5	6
5	30	30	30	30	30	30	30
7	43	43	43	43	43	43	43
9	61	61	61	62	62	62	63
11	88	88	88	89	90	91	92
13	122	121	121	121	123	125	126
15	160	159	159	158	161	163	164
17	204	202	200	198	201	204	207
19	253	249	246	244	247	250	254

Shear force due to **self-weight** near the **edge** of the slab (partial factor 1,1), **cracked slab**

b_{edge} → Span↓	0	1	2	3	4	5	6
5	30	30	30	30	30	30	30
7	44	44	44	44	44	44	44
9	64	64	65	66	66	66	66
11	94	96	97	98	98	98	98
13	129	131	134	136	136	136	136
15	170	173	178	181	181	182	182
17	216	222	228	233	233	234	234
19	268	275	286	291	292	293	294

Shear force due to **axle loads** near the **middle** of the slab, **cracked**

$b_{edge} \rightarrow$ Span↓	0	1	2	3	4	5	6
5	130	118	115	113	111	110	110
7	151	138	132	130	128	126	125
9	157	140	134	132	130	129	129
11	159	136	132	131	131	130	130
13	160	136	126	125	124	123	123
15	162	135	124	121	118	116	114
17	163	133	121	117	114	112	110
19	163	131	118	114	110	108	106

Shear force due to **axle loads** near the **edge** of the slab (**cracked**)

$b_{edge} \rightarrow$ Span↓	0	1	2	3	4	5	6
5	152	104	50	31	12	6	0
7	166	120	66	41	16	9	2
9	172	128	74	47	20	12	4
11	187	130	80	55	31	18	6
13	188	132	85	59	33	20	8
15	189	134	90	62	35	22	10
17	190	135	93	65	38	25	12
19	190	136	96	69	42	28	15

Shear force due to the **total loads** near the **middle** of the slab (**cracked**)

$b_{edge} \rightarrow$ Span↓	0	1	2	3	4	5	6
5	169	159	156	154	153	152	151
7	213	198	195	192	190	190	189
9	247	228	221	220	218	218	219
11	277	258	250	248	246	247	247
13	315	297	286	284	283	285	284
15	361	339	327	323	322	322	321
17	420	386	368	362	362	363	364
19	480	438	416	406	408	409	411

Shear force due to the **total loads** near the **edge** of the slab (**cracked**)

$b_{edge} \rightarrow$ Span↓	0	1	2	3	4	5	6
5	205	134	84	63,5	43	36,5	30
7	256	179	119	90,5	62	54	46
9	293	219	159	120,5	90	80	70
11	335	257	206	163,5	134	119,5	105
13	381	310	255	209	176	160,5	145
15	432	359	310	275	225	210	194
17	488	420	371	336	283	267,5	251
19	551	482	440	403	349	332	315

Shear force due to **self-weight** near the **middle** of the slab (partial factor 1,1), **uncracked slab**

$b_{edge} \rightarrow$ Span↓	0	1	2	3	4	5	6
5	31	30	30	31	31	31	31
7	43	43	42	43	44	44	45
9	62	61	60	61	62	62	63
11	90	88	88	87	88	90	91
13	125	122	119	119	120	121	123
15	166	160	157	155	157	158	159
17	211	205	200	196	195	197	200
19	263	256	249	241	242	243	244

Shear force due to **self-weight** near the **edge** of the slab (partial factor 1,1), **uncracked slab**

$b_{edge} \rightarrow$ Span↓	0	1	2	3	4	5	6
5	31	32	32	32	32	32	32
7	45	45	46	47	47	47	47
9	65	67	69	70	70	70	70
11	95	98	100	103	103	104	104
13	130	135	140	143	145	146	146
15	171	177	183	189	194	195	196
17	217	225	234	242	247	251	253
19	269	283	291	299	305	312	317

Shear force due to **axle loads** near the **middle** of the slab, (**uncracked)**

$b_{edge} \rightarrow$ Span↓	0	1	2	3	4	5	6
5	132	108	106	104	103	102	101
7	146	124	114	111	109	108	108
9	160	133	122	120	118	117	116
11	162	131	118	115	113	111	110
13	164	130	117	112	107	106	105
15	165	129	112	107	103	101	100
17	167	128	111	103	99	97	95
19	168	128	109	102	95	93	92

Shear force due to **axle loads** near the **edge** of the slab (**uncracked)**

$b_{edge} \rightarrow$ Span↓	0	1	2	3	4	5	6
5	151	105	65	39	13	7	1
7	167	117	75	50	25	15	5
9	185	131	86	59	32	20	8
11	186	132	93	66	39	25	12
13	187	136	98	71	45	31	17
15	188	137	102	77	52	36	21
17	188	139	105	77	55	40	25
19	189	141	107	82	58	43	29

Shear force due to the total **loads near** the **middle** of the slab (**uncracked**)

$b_{edge} \rightarrow$ Span↓	0	1	2	3	4	5	6
5	180	160	154	154	154	154	154
7	219	193	187	186	186	186	186
9	252	220	206	205	205	205	205
11	290	252	236	230	230	230	230
13	333	290	270	264	264	264	264
15	383	333	309	300	297	297	297
17	437	382	354	340	336	336	336
19	497	437	405	388	382	380	380

Shear force due to the **total loads** near the **edge** of the slab (**uncracked**)

$b_{edge} \rightarrow$ Span↓	0	1	2	3	4	5	6
5	206	156	111	78	47	40	33
7	255	198	146	108	75	64	53
9	293	230	182	146	107	93	80
11	335	272	228	193	150	136	122
13	380	320	277	245	199	185	170
15	431	373	332	302	284	242	224
17	487	430	392	363	343	325	312
19	548	492	458	433	414	398	386

10.2 Total shear forces in-situ slabs

In the tables below the total shear forces for in-situ slabs are demonstrated. This is the result of variable loads determined by RFEM and permanent loads determined by a hand calculation. The permanent loads are assumed to results in a constant shear force on the support.

Shear force due to the total **loads near** the **middle** of the slab (**cracked**)

$b_{edge} \rightarrow$ Span↓	0	1	2	3	4	5	6
5	180	160	154	154	154	154	154
7	219	193	187	186	186	186	186
9	252	220	206	205	205	205	205
11	290	252	236	230	230	230	230
13	333	290	270	264	264	264	264
15	383	333	309	300	297	297	297
17	437	382	354	340	336	336	336
19	497	437	405	388	382	380	380

Shear force due to the **total loads** near the **edge** of the slab (**cracked**)

b_{edge} → Span↓	0	1	2	3	4	5	6
5	198	143	83	63	42	36	29
7	233	178	118	90	61	53	45
9	264	209	147	116	86	76	66
11	314	243	184	155	125	111	96
13	354	283	228	195	162	147	131
15	400	328	273	238	204	188	172
17	450	376	322	287	252	236	219
19	504	430	376	342	307	289	271

Shear force due to the total **loads near** the **middle** of the slab (**uncracked**)

b_{edge} → Span↓	0	1	2	3	4	5	6
5	168	145	142	141	139	138	137
7	202	178	167	165	162	162	161
9	240	209	197	195	193	192	191
11	273	237	223	220	216	215	213
13	312	272	258	253	248	246	245
15	356	312	292	286	281	279	278
17	404	355	334	324	320	318	316
19	457	406	382	375	367	364	360

Shear force due to the **total loads** near the **edge** of the slab (**uncracked**)

b_{edge} → Span↓	0	1	2	3	4	5	6
5	197	145	102	73	44	37	30
7	234	175	129	100	71	60	49
9	277	214	162	130	99	85	72
11	312	246	197	167	136	122	107
13	352	287	236	206	176	161	146
15	398	332	282	254	226	207	188
17	446	381	336	301	273	255	236
19	502	435	390	362	333	312	290

10.3 Comparison cracked/uncracked

For the comparison of cracked and uncracked slabs, only the transverse stiffness needs to be adapted. So, the left side of the figure below divided by the right side. The different comparisons are numbered as illustrated below. As example the comparison for the shear force due to self-weight near the middle of the support is circled red in the figure below.

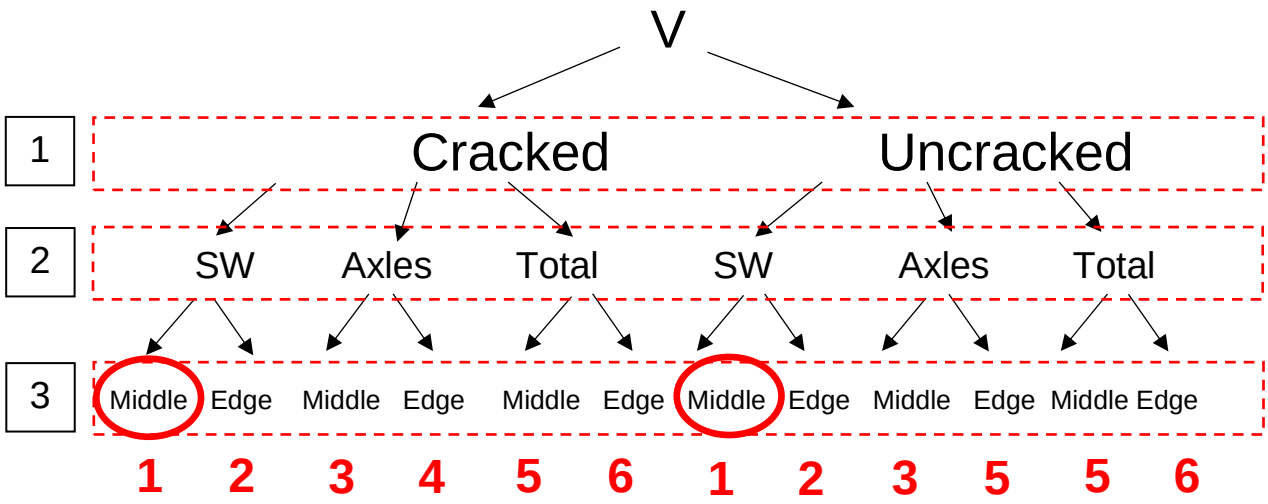

$V_{cracked}$ / $V_{uncracked}$ Middle of the support, self-weight (circled red)

b_{edge} → Span↓	0	1	2	3	4	5	6
5	0,97	1,00	1,00	0,97	0,97	0,97	0,97
7	1,00	1,00	1,02	1,00	0,98	0,98	0,96
9	0,98	1,00	1,02	1,02	1,00	1,00	1,00
11	0,98	1,00	1,00	1,02	1,02	1,01	1,01
13	0,98	0,99	1,02	1,02	1,03	1,03	1,02
15	0,96	0,99	1,01	1,02	1,03	1,03	1,03
17	0,97	0,99	1,00	1,01	1,03	1,04	1,04
19	0,96	0,97	0,99	1,01	1,02	1,03	1,04

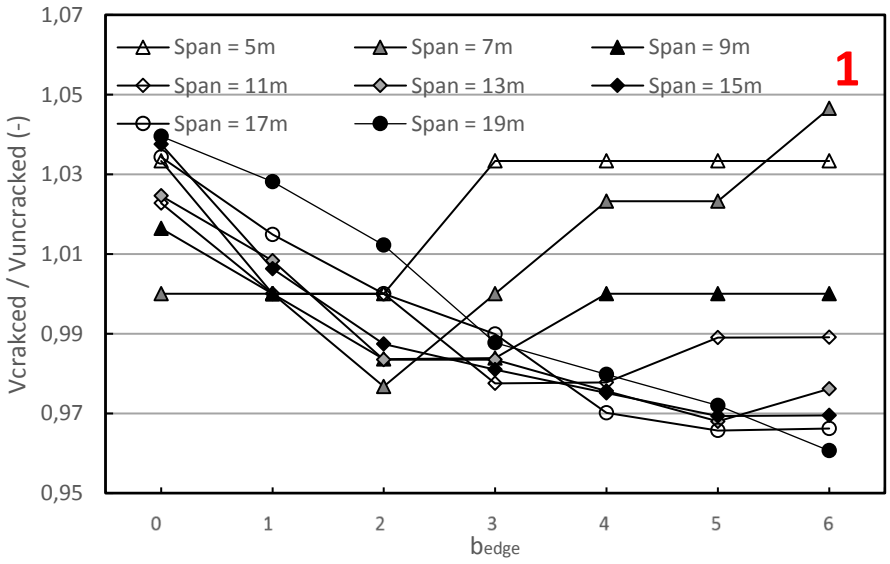

Appendix Figure 10-2 - Comparison of shear force due to self-weight near the middle of the support (cracked divided by uncracked)

$V_{cracked}$ / $V_{uncracked}$ Edge of the support, self-weight

b_{edge} → Span↓	0	1	2	3	4	5	6
5	0,97	0,94	0,94	0,94	0,94	0,94	0,94
7	0,98	0,98	0,96	0,94	0,94	0,94	0,94
9	0,98	0,96	0,94	0,94	0,94	0,94	0,94
11	0,99	0,98	0,97	0,95	0,95	0,94	0,94
13	0,99	0,97	0,96	0,95	0,94	0,93	0,93
15	0,99	0,98	0,97	0,96	0,93	0,93	0,93
17	1,00	0,99	0,97	0,96	0,94	0,93	0,92
19	1,00	0,97	0,98	0,97	0,96	0,94	0,93

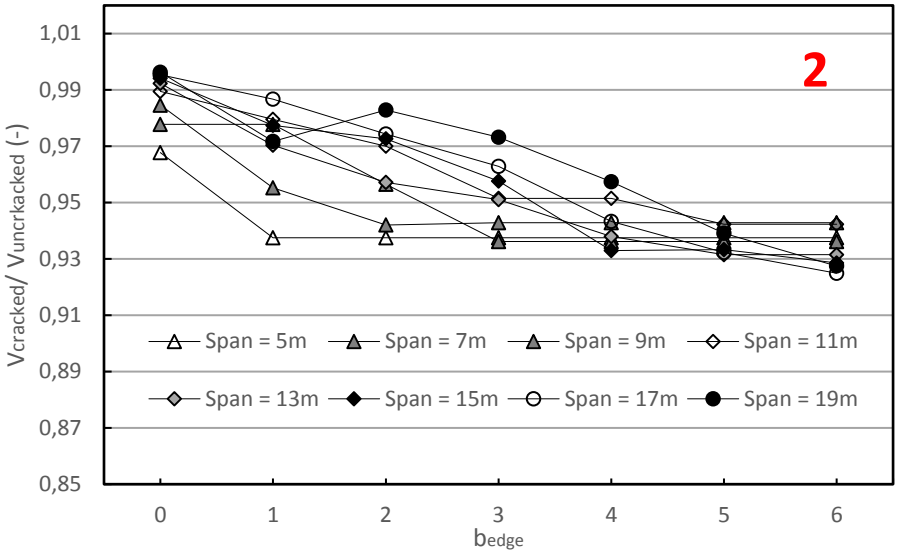

Appendix Figure 10-3 - Comparison of shear force due to self-weight near the edge of the support (cracked divided by uncracked)

$V_{cracked}$ / $V_{uncracked}$ Middle of the support, axle loads

b_{edge} → Span↓	0	1	2	3	4	5	6
5	1,01	1,09	1,09	1,09	1,08	1,08	1,08
7	1,03	1,11	1,15	1,16	1,18	1,16	1,15
9	0,98	1,05	1,10	1,10	1,10	1,10	1,11
11	0,98	1,04	1,12	1,15	1,17	1,18	1,19
13	0,97	1,05	1,06	1,10	1,13	1,14	1,15
15	0,98	1,04	1,11	1,13	1,15	1,14	1,14
17	0,98	1,04	1,11	1,13	1,15	1,16	1,16
19	0,97	1,04	1,08	1,11	1,14	1,16	1,18

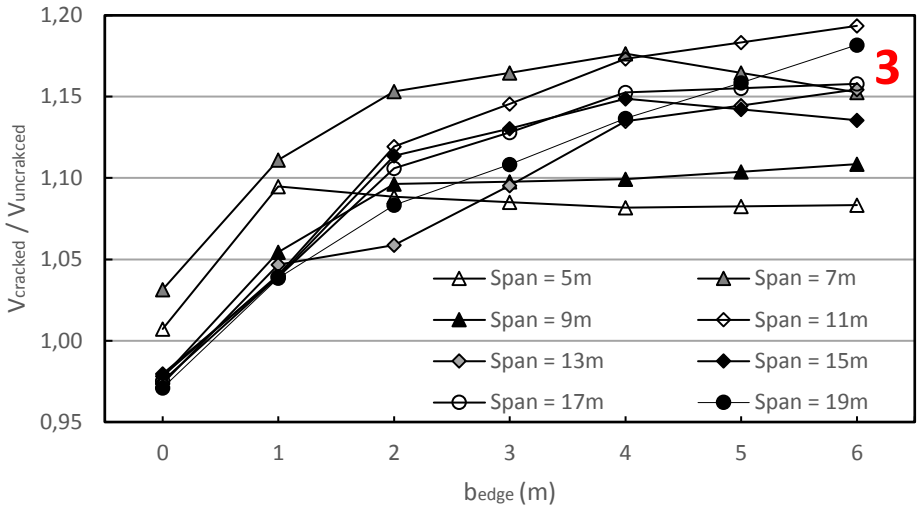

Appendix Figure 10-4 - Comparison of shear force due to axle loads near the middle of the support (cracked divided by uncracked)

$V_{cracked}$ / $V_{uncrakced}$ Edge of the support, axle loads

b_{edge} → Span↓	0	1	2	3	4	5	6
5	1,01	0,98	0,74	0,76	0,87	0,82	0,50
7	0,99	1,02	0,87	0,82	0,64	0,59	0,33
9	0,94	0,97	0,85	0,80	0,65	0,60	0,40
11	1,01	0,98	0,88	0,85	0,77	0,66	0,39
13	1,01	0,98	0,93	0,87	0,74	0,63	0,38
15	1,01	0,98	0,93	0,84	0,67	0,60	0,43
17	1,02	0,97	0,90	0,83	0,70	0,64	0,50
19	1,01	0,97	0,90	0,82	0,69	0,63	0,53

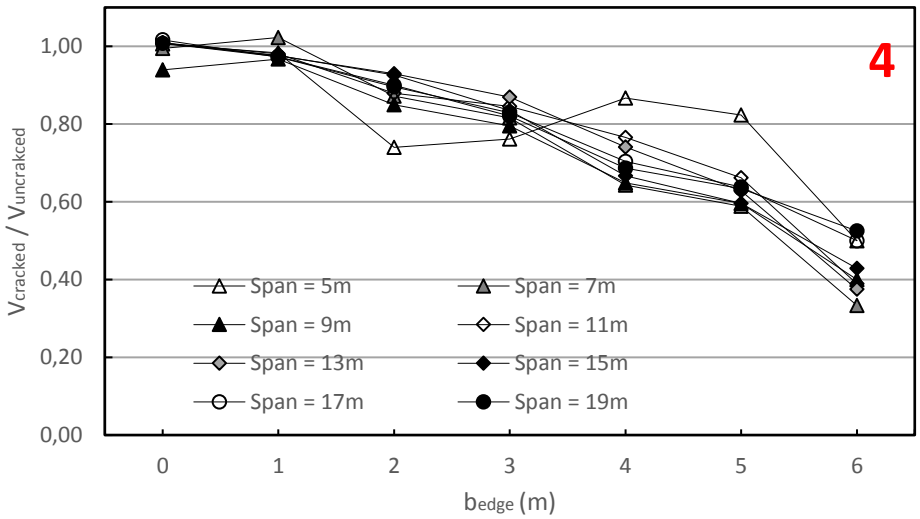

Appendix Figure 10-5 - Comparison of shear force due to axle loads near the edge of the support (cracked divided by uncracked)

$V_{cracked}$ / $V_{uncracked}$ Middle of the support, total loads

b_{edge} → Span↓	0	1	2	3	4	5	6
5	1,01	1,09	1,09	1,09	1,08	1,08	1,08
7	1,03	1,11	1,15	1,16	1,18	1,16	1,15
9	0,98	1,05	1,10	1,10	1,10	1,10	1,11
11	0,98	1,04	1,12	1,15	1,17	1,18	1,19
13	0,97	1,05	1,06	1,10	1,13	1,14	1,15
15	0,98	1,04	1,11	1,13	1,15	1,14	1,14
17	0,98	1,04	1,11	1,13	1,15	1,16	1,16
19	0,97	1,04	1,08	1,11	1,14	1,16	1,18

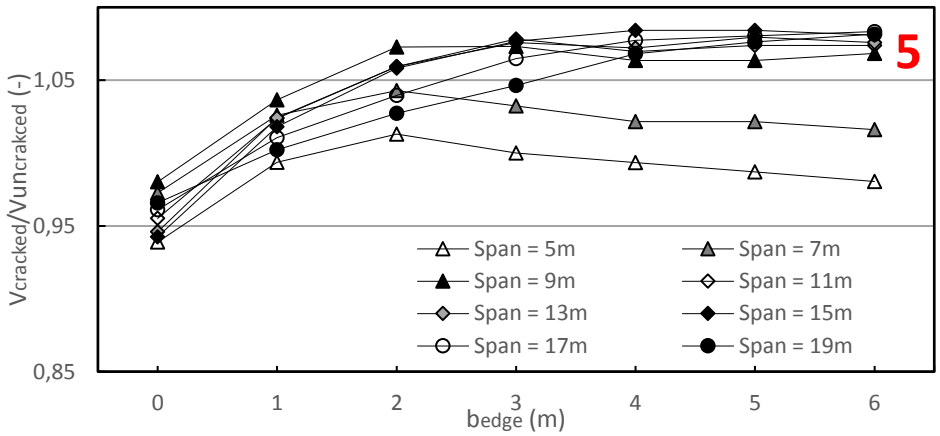

Appendix Figure 10-6 - Comparison of shear force due total loads near the middle of the support (cracked divided by uncracked)

$V_{cracked}$ / $V_{uncracked}$ Edge of the support, total loads

b_{edge} → Span↓	0	1	2	3	4	5	6
5	1,00	0,86	0,76	0,81	0,91	0,91	0,91
7	1,00	0,90	0,82	0,84	0,83	0,84	0,87
9	1,00	0,95	0,87	0,83	0,84	0,86	0,88
11	1,00	0,94	0,90	0,85	0,89	0,88	0,86
13	1,00	0,97	0,92	0,85	0,88	0,87	0,85
15	1,00	0,96	0,93	0,91	0,79	0,87	0,87
17	1,00	0,98	0,95	0,93	0,83	0,82	0,80
19	1,01	0,98	0,96	0,93	0,84	0,83	0,82

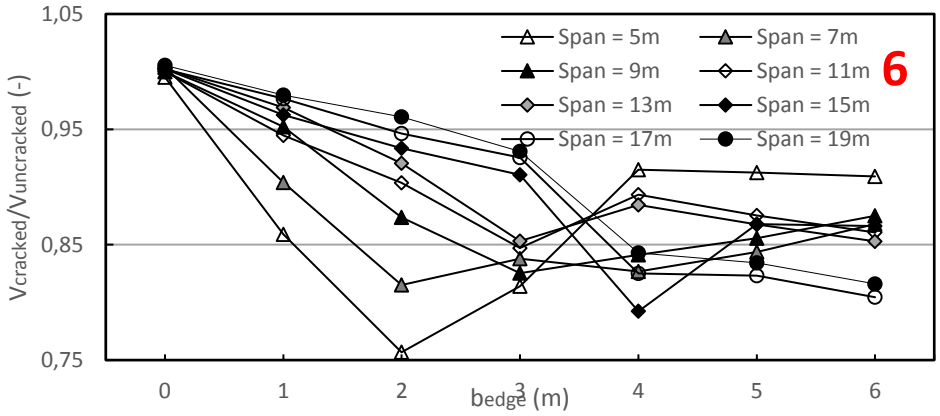

Appendix Figure 10-7 - Comparison of shear force due to total loads near the edge of the support (cracked divided by uncracked)

10.4 Comparison shear force edge/middle support

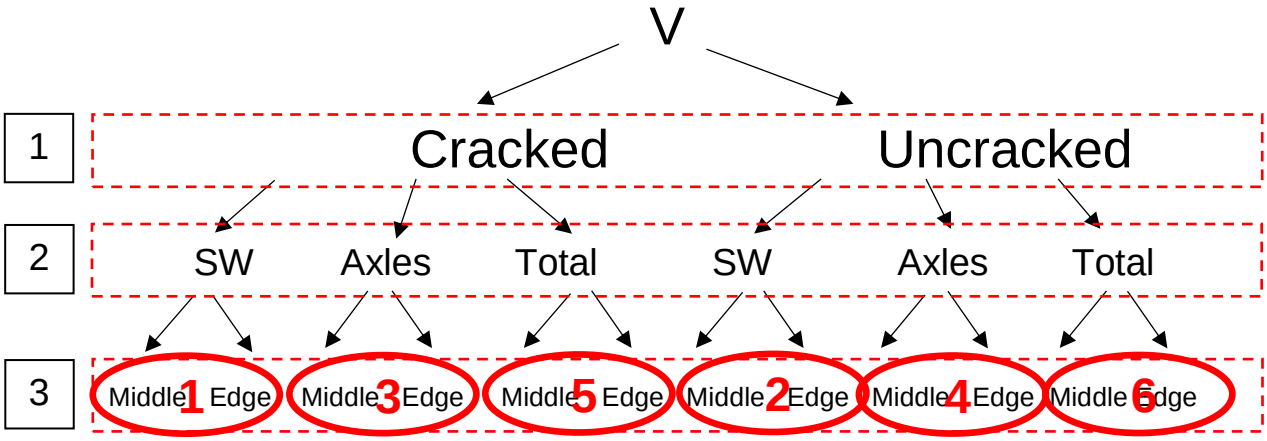

V_{edge} / V_{middle} cracked, self-weight

b_{edge} → Span↓	0	1	2	3	4	5	6
5	1,01	1,01	1,01	1,01	1,01	1,01	1,01
7	1,04	1,04	1,04	1,04	1,04	1,04	1,04
9	1,06	1,05	1,07	1,07	1,07	1,06	1,05
11	1,07	1,08	1,09	1,10	1,09	1,07	1,06
13	1,06	1,08	1,11	1,12	1,11	1,09	1,08
15	1,06	1,09	1,12	1,15	1,13	1,12	1,11
17	1,06	1,09	1,13	1,17	1,15	1,14	1,13
19	1,06	1,11	1,16	1,19	1,18	1,17	1,16

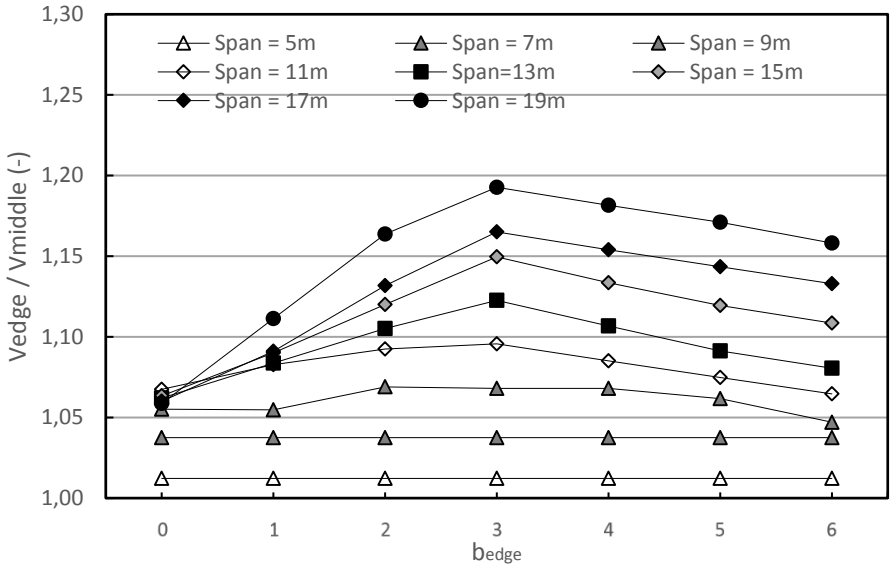

Appendix Figure 10-8 - Comparison of shear force near the edge divided by the shear force near the middle of the support due to self-weight (cracked slab)

V_{edge} / V_{middle} Uncracked, self-weight

b_{edge} → Span↓	0	1	2	3	4	5	6
5	1,00	1,07	1,07	1,03	1,03	1,03	1,03
7	1,05	1,05	1,10	1,09	1,07	1,07	1,04
9	1,05	1,10	1,15	1,15	1,13	1,13	1,11
11	1,06	1,11	1,14	1,18	1,17	1,16	1,14
13	1,04	1,11	1,18	1,20	1,21	1,21	1,19
15	1,03	1,11	1,17	1,22	1,24	1,23	1,23
17	1,03	1,10	1,17	1,23	1,27	1,27	1,27
19	1,02	1,11	1,17	1,24	1,26	1,28	1,30

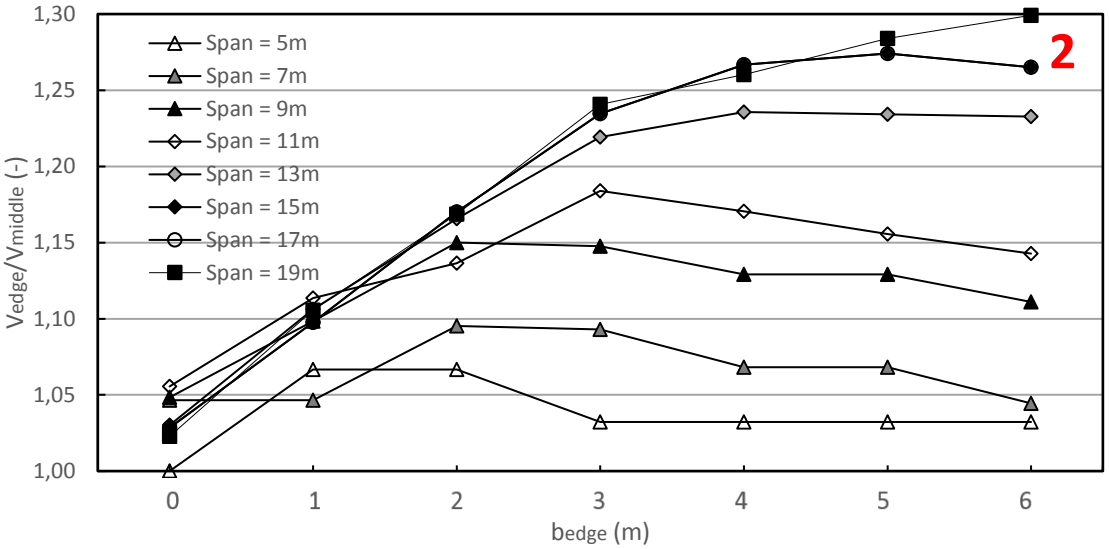

Appendix Figure 10-9 - Comparison of shear force near the edge divided by the shear force near the middle of the support due to self-weight (uncracked slab)

V_{edge} / V_{middle} cracked, axle loads

b_{edge} → Span↓	0	1	2	3	4	5	6
5	1,21	0,90	0,44	0,28	0,11	0,06	0,01
7	1,16	0,90	0,52	0,33	0,13	0,07	0,01
9	1,16	0,95	0,57	0,37	0,17	0,10	0,03
11	1,25	1,00	0,63	0,44	0,24	0,14	0,05
13	1,25	1,03	0,74	0,51	0,28	0,17	0,06
15	1,25	1,06	0,77	0,55	0,32	0,21	0,09
17	1,26	1,09	0,82	0,60	0,37	0,25	0,13
19	1,26	1,11	0,88	0,66	0,43	0,30	0,16

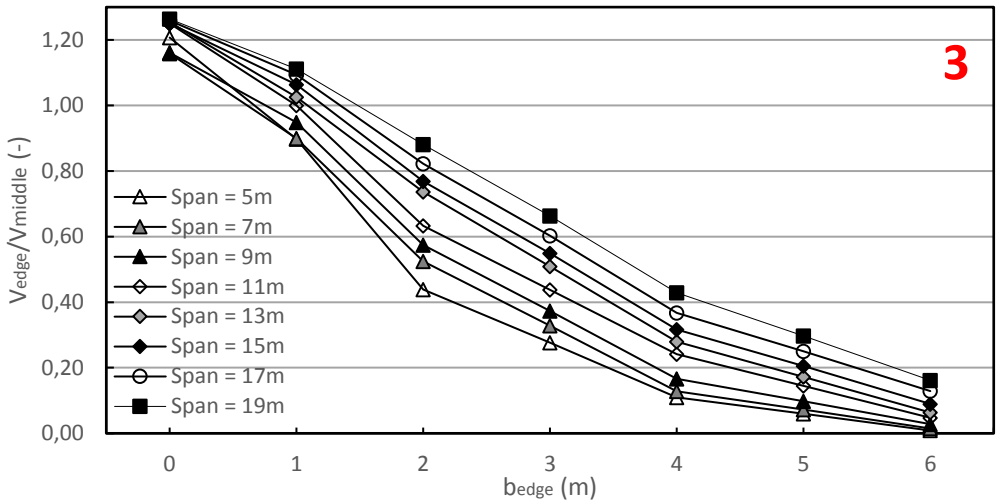

Appendix Figure 10-10 - Comparison of shear force near the edge divided by the shear force near the middle of the support due to axle loads (cracked slab)

V_{edge} / V_{middle} uncracked, axle loads

b_{edge} → Span↓	0	1	2	3	4	5	6
5	1,21	1,00	0,65	0,39	0,14	0,08	0,02
7	1,20	0,98	0,69	0,47	0,24	0,14	0,05
9	1,21	1,03	0,74	0,52	0,28	0,18	0,08
11	1,21	1,06	0,81	0,59	0,37	0,26	0,15
13	1,21	1,10	0,84	0,64	0,43	0,31	0,20
15	1,21	1,13	0,92	0,74	0,55	0,39	0,24
17	1,21	1,17	1,02	0,82	0,60	0,45	0,30
19	1,22	1,19	1,06	0,90	0,71	0,54	0,36

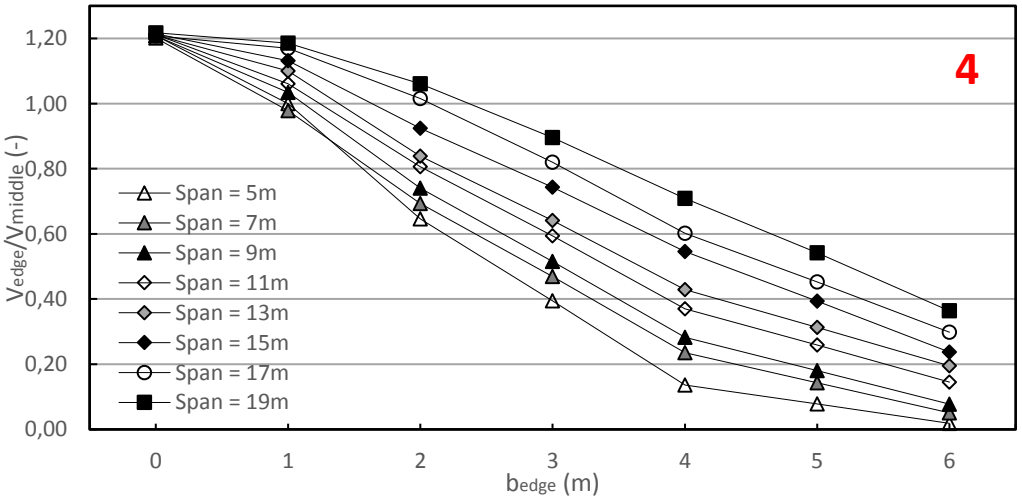

Appendix Figure 10-11 - Comparison of shear force near the edge divided by the shear force near the middle of the support due to axle loads (uncracked slab)

V_{edge} / V_{middle} cracked, total loads

b_{edge} → Span↓	0	1	2	3	4	5	6
5	1,21	0,90	0,44	0,28	0,11	0,06	0,01
7	1,16	0,90	0,52	0,33	0,13	0,07	0,01
9	1,16	0,95	0,57	0,37	0,17	0,10	0,03
11	1,25	1,00	0,63	0,44	0,24	0,14	0,05
13	1,25	1,03	0,74	0,51	0,28	0,17	0,06
15	1,25	1,06	0,77	0,55	0,32	0,21	0,09
17	1,26	1,09	0,82	0,60	0,37	0,25	0,13
19	1,26	1,11	0,88	0,66	0,43	0,30	0,16

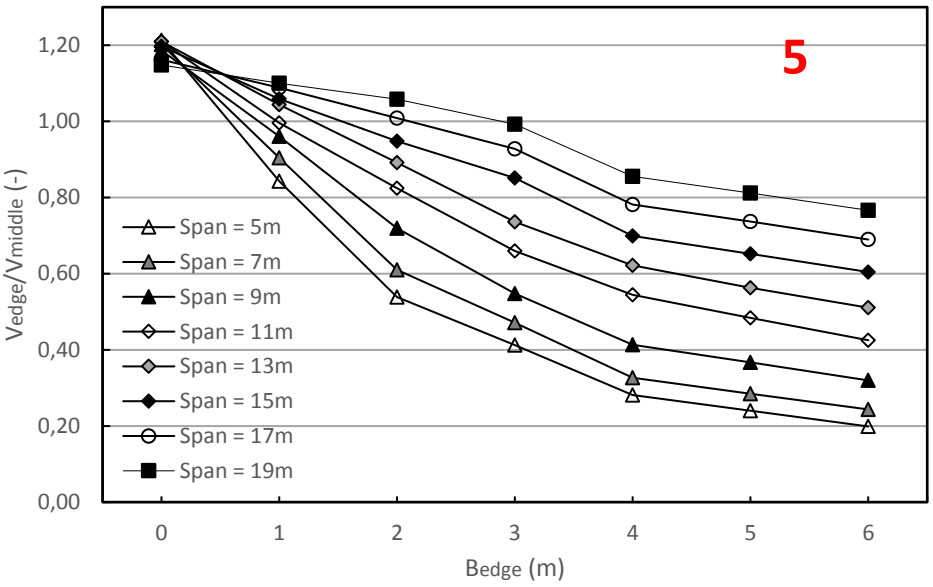

Appendix Figure 10-12 - Comparison of shear force near the edge divided by the shear force near the middle of the support due to total loads (cracked slab)

V_{edge} / V_{middle} uncracked, total loads

b_{edge} → Span↓	0	1	2	3	4	5	6
5	1,21	1,00	0,65	0,39	0,14	0,08	0,02
7	1,20	0,98	0,69	0,47	0,24	0,14	0,05
9	1,21	1,03	0,74	0,52	0,28	0,18	0,08
11	1,21	1,06	0,81	0,59	0,37	0,26	0,15
13	1,21	1,10	0,84	0,64	0,43	0,31	0,20
15	1,21	1,13	0,92	0,74	0,55	0,39	0,24
17	1,21	1,17	1,02	0,82	0,60	0,45	0,30
19	1,22	1,19	1,06	0,90	0,71	0,54	0,36

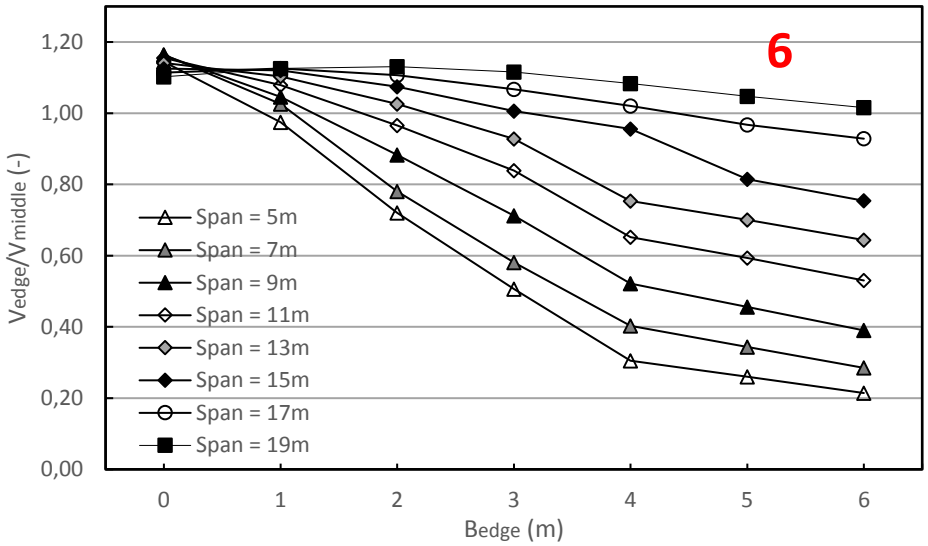

Appendix Figure 10-13 - Comparison of shear force near the edge divided by the shear force near the middle of the support due to total loads (uncracked slab)

11 Appendix K – Tests with axles at different distances from the support

b_{edge} = 0,0m

Span	LC1	LC2	LC3
5	239,8	240	213
10	343,5	350	337
15	482,6	481	475
20	653,3	646	643

% relative to LC1

Span	LC1	LC2	LC3
5	0	0,42	0,89
10	0	0	0,96
15	0	-0,21	0,99
20	0	-0,62	0,99

b_{edge} = 2,0m

Span	LC1	LC2	LC3
5	173,8	176	159
10	223,1	232	226
15	356,6	364	358
20	531,7	540	537

% relative to LC1

Span	LC1	LC2	LC3
5	0	0,42	0,89
10	0	0	0,96
15	0	-0,21	0,99
20	0	-0,62	0,99

b_{edge} = 4,0m

Span	LC1	LC2	LC3
5	171,7	174	156
10	220,1	229	223
15	297,7	304	303
20	486,5	493	489

% relative to LC1

Span	LC1	LC2	LC3
5	0	0,42	0,89
10	0	0	0,96
15	0	-0,21	0,99
20	0	-0,62	0,99

b_{edge} = 6,0m

Span	LC1	LC2	LC3
5	170,74	173	155
10	222,8	229	224
15	301,81	307	305
20	455,7	462	460

% relative to LC1

Span	LC1	LC2	LC3
5	0	0,42	0,89
10	0	0	0,96
15	0	-0,21	0,99
20	0	-0,62	0,99

12 Appendix L – values for a_v for the governing axle configuration

Values for a_v for the first lane

b_{edge} → Span↓	0	0,5	1	1,5	2	2,5	3	3,5	4	4,5	5	5,5	6
5	1,0	1,0	1,0										
6	1,0	1,0	1,0										
7	1,0	1,0	1,0										
8	1,0	1,0	1,0	1,0	1,5								
9	1,1	1,1	1,1	1,1	1,5	2,5							
10	1,3	1,3	1,3	1,3	1,5	2,2	2,8	3,2					
11	1,4	1,4	1,4	1,4	1,4	1,6	2,6	3,2	3,8				
12	1,5	1,5	1,5	1,5	1,5	1,6	2,0	2,6	3,6	4,0			
13	1,6	1,6	1,6	1,6	1,6	1,8	1,8	2,2	2,8	3,4	3,8	4,6	
14	1,8	1,8	1,8	1,8	1,8	1,8	1,8	2,4	2,8	3,2	3,8	4,4	5,0
15	1,9	1,9	1,9	1,9	1,9	1,9	2,2	2,6	3,2	3,6	4,2	4,4	5,0
16	2,0	2,0	2,0	2,0	2,0	2,0	2,2	2,8	3,2	3,8	4,4	4,8	5,2
17	2,1	2,1	2,1	2,1	2,1	2,2	2,4	2,8	3,4	4,2	4,6	5,0	5,4
18	2,3	2,3	2,3	2,3	2,3	2,4	2,6	3,0	3,4	4,4	5,0	5,2	5,8
19	2,4	2,4	2,4	2,4	2,4	2,4	2,6	3,2	3,8	4,4	5,0	5,4	6,0
20	2,5	2,5	2,5	2,5	2,6	2,6	2,8	3,2	3,8	4,6	5,2	5,8	6,2

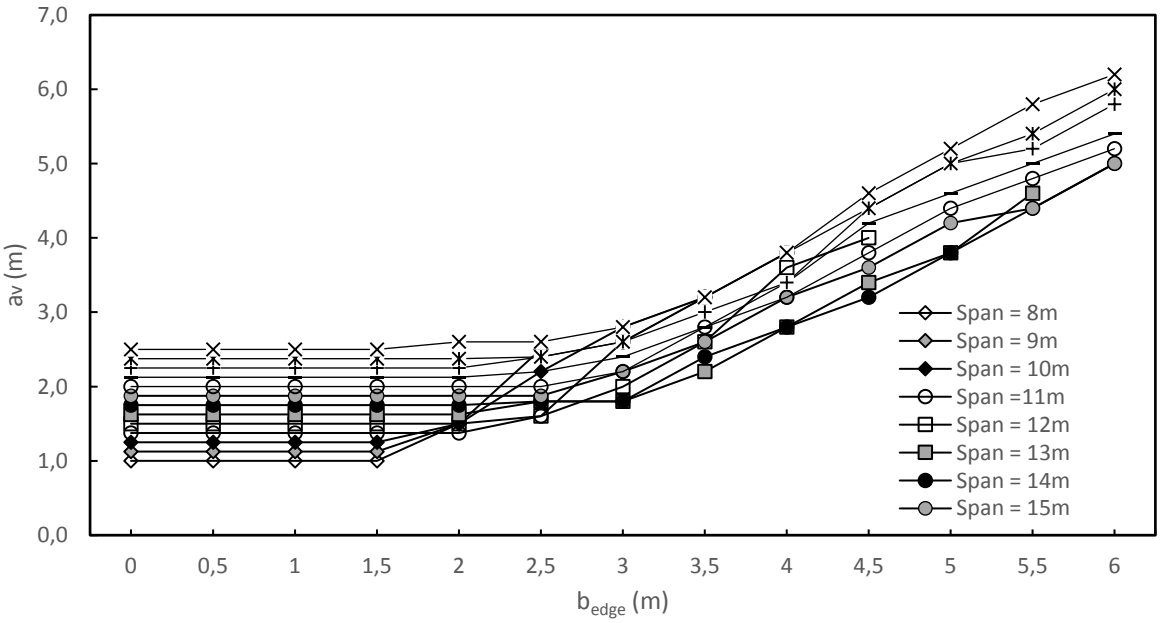

Appendix Figure 12-1 – a_v values for lane 1 for different spans and edge widths

Values for a_v for the second lane

b_{edge} → Span↓	0	0,5	1	1,5	2	2,5	3	3,5	4	4,5	5	5,5	6
5	1,0	1,0	1,0										
6	1,0	1,0	1,0										
7	1,0	1,0	1,0										
8	1,0	1,0	1,0	1,0	3,0								
9	1,1	1,1	1,1	1,1	4,0	5,0							
10	1,3	1,3	1,3	1,3	3,2	5,2	4,8	6,4					
11	1,5	1,5	1,5	1,5	1,5	4,2	5,4	6,6	7,2				
12	1,5	1,5	1,5	1,5	1,5	4,4	4,6	6,4	7,2	7,6			
13	1,6	1,6	1,6	1,6	1,6	4,4	4,2	4,8	5,8	7,2	7,2	8,2	
14	1,8	1,8	1,8	1,8	1,8	4,4	4,4	5,2	5,8	6,6	7,2	7,6	8,6
15	1,9	1,9	1,9	1,9	1,9	1,9	4,4	5,4	6,6	7,2	7,6	7,6	8,6
16	2,0	2,0	2,0	2,0	2,0	2,0	4,6	5,8	6,6	7,6	7,8	8,6	8,8
17	2,1	2,1	2,1	2,1	2,1	4,4	5,2	5,8	7,2	7,8	8,4	8,6	9,2
18	2,3	2,3	2,3	2,3	2,3	5,4	5,4	6,0	7,2	7,8	8,6	8,8	9,6
19	2,4	2,4	2,4	2,4	2,4	5,4	5,4	6,6	7,2	7,8	8,6	9,2	9,8
20	2,5	2,5	2,5	2,5	4,4	5,4	5,8	6,6	7,8	8,4	8,8	9,4	10,2

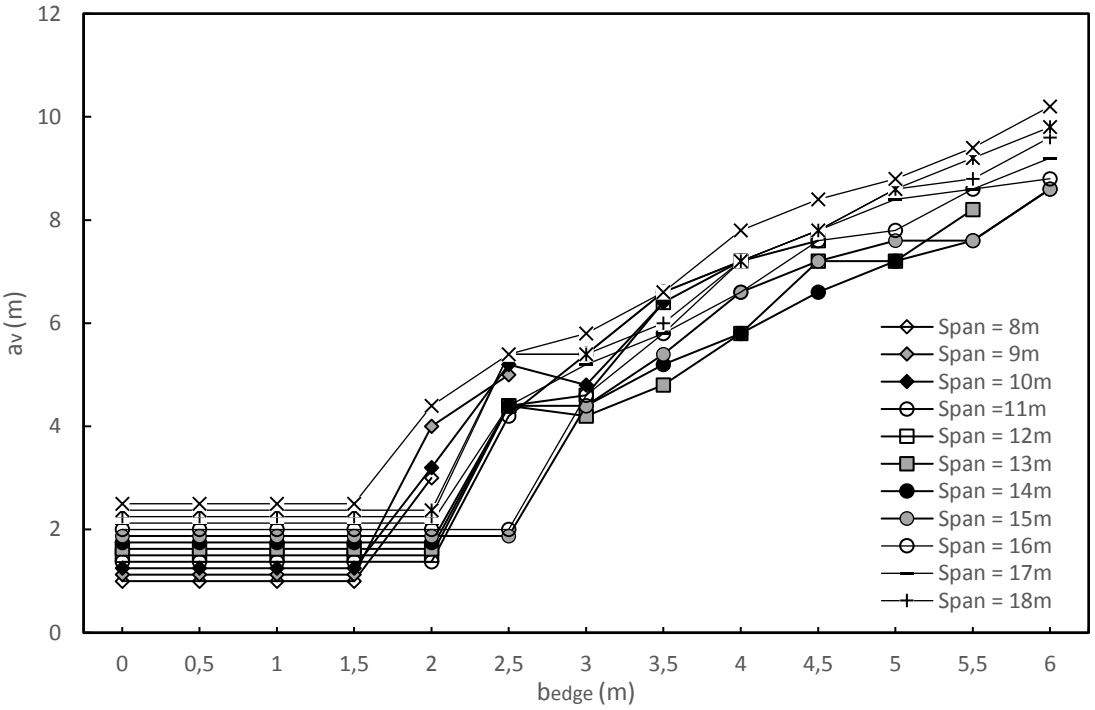

Appendix Figure 12-2 - a_v values for lane 2 for different spans and edge widths

13 Appendix M – Determination critical edge width

Excel determined the formulas for the graphs of the total shear force. These formulas are shown in Appendix Figure 13.1 and 13.2. These formulas are determined by drawing a trend line through the measured points. The right type of graph is chosen by curve fitting. In most cases 3rd or 4th order polynomial fitted best.

13.1 Uncracked slab

Middle governing:

$$B1 := -0.5556*x^3 + 8.2143*x^2 - 38.373*x + 210;$$
$$B2 := 0.1932*x^4 - 3.7854*x^3 + 26.958*x^2 - 82.635*x + 278.14;$$
$$B3 := 0.1402*x^4 - 3.1035*x^3 + 25.208*x^2 - 88.691*x + 318.57;$$
$$B4 := -0.8889*x^3 + 14.024*x^2 - 71.516*x + 347.71;$$
$$B5 := -1.0278*x^3 + 16.226*x^2 - 82.746*x + 400;$$
$$B6 := -1.0556*x^3 + 17.214*x^2 - 91.873*x + 458;$$
$$B7 := -1.0278*x^3 + 17.512*x^2 - 98.317*x + 518.29;$$
$$B8 := -1.0278*x^3 + 17.952*x^2 - 104.52*x + 584;$$

Edge governing:

$$C1 := 4.25*x^2 - 64.15*x + 266.25;$$
$$C2 := 4.75*x^2 - 73.05*x + 323.75;$$
$$C3 := -0.5*x^3 + 10.5*x^2 - 91*x + 374;$$
$$C4 := -1.6667*x^3 + 19.5*x^2 - 109.83*x + 427;$$
$$C5 := -1*x^3 + 14.5*x^2 - 96.5*x + 463;$$
$$C6 := -0.4167*x^3 + 10.25*x^2 - 85.333*x + 506.4;$$
$$C7 := -0.5833*x^3 + 11.024*x^2 - 84.107*x + 560.14;$$
$$C8 := -0.6667*x^3 + 11.833*x^2 - 83.643*x + 619.57;$$

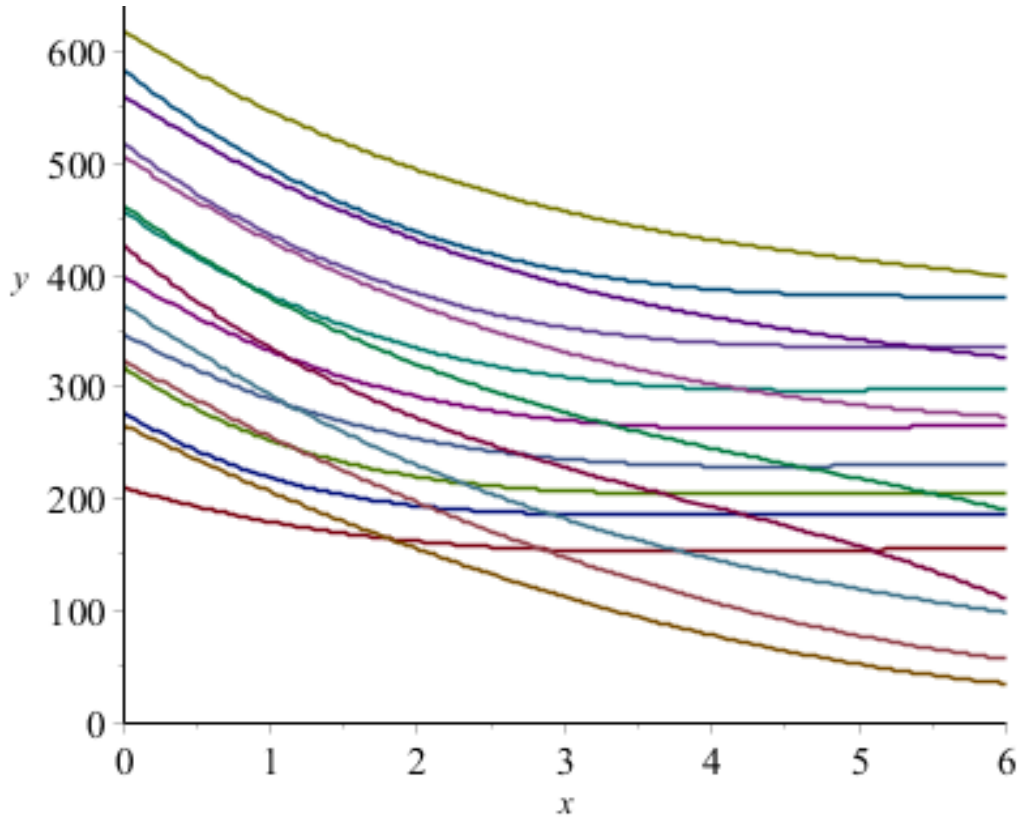

Appendix Figure 13-1 – Calculation of the intersection of graphs for shear force near the middle and near the edge of the slab (uncracked slab)

13.2 Cracked slab

Middle governing:

$B1 := -0.2222*x^3 + 3.3452*x^2 - 17.075*x + 182.57;$

$B2 := -0.3056*x^3 + 4.7024*x^2 - 24.135*x + 232;$

$B3 := 0.1326*x^4 - 2.5379*x^3 + 18.042*x^2 - 57.359*x + 288.71;$

$B4 := -0.4167*x^3 + 6.6667*x^2 - 34.56*x + 304.86;$

$B5 := -0.4444*x^3 + 7.1429*x^2 - 36.984*x + 345.43;$

$B6 := -0.5*x^3 + 8.0357*x^2 - 42.464*x + 395.86;$

$B7 := -0.75*x^3 + 12.357*x^2 - 65.464*x + 473.71;$

$B8 := -0.8889*x^3 + 14.94*x^2 - 80.385*x + 546.29;$

Edge governing:

$C1 := 1.4167 \cdot x^3 + 2 \cdot x^2 - 86.917 \cdot x + 288.5;$

$C2 := -0.7778*x^3 + 16.536*x^2 - 122.97*x + 363.5;$

$C3 := -0.4167*x^3 + 11.976*x^2 - 109.18*x + 391.21;$

$C4 := -0.5694*x^3 + 13.095*x^2 - 110.48*x + 432.36;$

$C5 := -0.1155*x^4 + 1.6402*x^3 - 1.5208*x^2 - 74.312*x + 454.93;$

$C6 := 0.303*x^4 - 4.9596*x^3 + 32.583*x^2 - 138.58*x + 542.14;$

$C7 := 0.2822*x^4 - 4.4179*x^3 + 27.854*x^2 - 123.12*x + 586.93;$

$C8 := 0.4053*x^4 - 6.346*x^3 + 37.542*x^2 - 139.71*x + 658.29;$

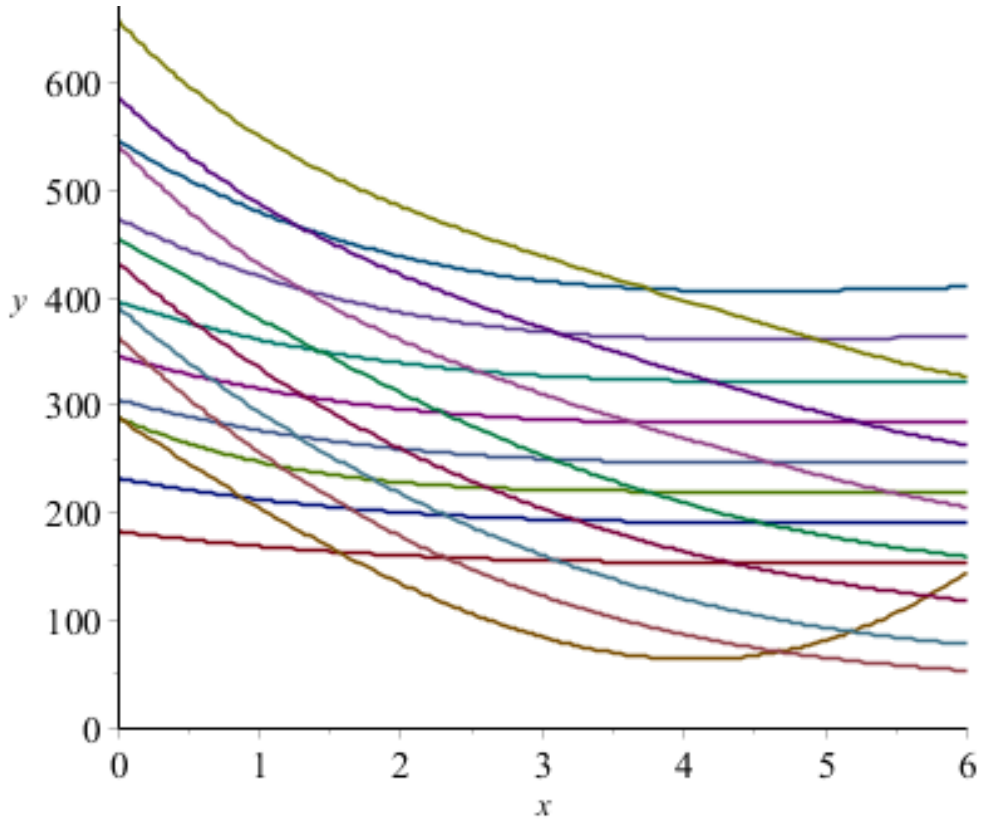

Appendix Figure 13-2 - Calculation of the intersection of graphs for shear force near the middle and near the edge of the slab (cracked slab)

The intersection of these formulas has been calculated by Maple 18.
With making use of the command fsolve(B_i=C_i), where i =1 to 10, Maple can calculate the intersections. Since x=1 for an edge distance of 0m, the found x values at the intersections need to be subtracted by 1.

14 Appendix N – Comparison RFEM – Excel

14.1 Comparison axle loads

V_{Excel} edge, uncracked, axle loads

b_{edge} → Span↓	0	1	2	3	4	5	6
5	146,7	118,5	72,6	36,9	11,7	0,4	0,0
7	185,9	156,4	106,9	66,8	39,4	20,7	6,7
9	200,9	172,5	127,9	90,2	61,9	40,2	24,4
11	202,8	176,7	138,3	103,4	77,0	56,4	39,9
13	202,3	178,1	144,1	111,4	86,7	67,2	51,6
15	200,6	177,9	145,7	116,5	93,0	74,6	59,7
17	198,2	176,9	145,7	119,7	97,3	79,7	65,4
19	195,5	175,4	145,1	121,6	100,3	83,4	69,7

V_{RFEM} / V_{Excel} edge, uncracked, axle loads

b_{edge} → Span↓	0	1	2	3	4	5	6
5	1,03	0,89	0,89	1,06	1,11	1,13	1,23
7	0,90	0,75	0,70	0,75	0,63	0,73	0,74
9	0,92	0,76	0,67	0,65	0,52	0,50	0,33
11	0,92	0,75	0,67	0,64	0,51	0,44	0,30
13	0,92	0,76	0,68	0,64	0,52	0,46	0,33
15	0,94	0,77	0,70	0,66	0,56	0,48	0,35
17	0,95	0,79	0,72	0,64	0,57	0,50	0,38
19	0,97	0,80	0,74	0,67	0,58	0,52	0,42

V_{Excel} middle, uncracked, axle loads, mechanism (a)

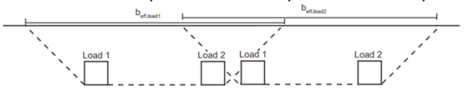

b_{edge} → Span↓	0	1	2	3	4	5	6
5	248,1	205,2	186,7	181,6	181,6	181,6	181,6
7	248,1	205,2	186,7	181,6	181,6	181,6	181,6
9	241,7	200,8	180,8	174,8	174,8	174,8	174,8
11	230,0	192,7	170,3	162,6	162,6	162,6	162,6
13	221,5	185,2	161,1	153,0	152,1	152,1	152,1
15	215,7	178,3	155,1	145,3	142,8	142,8	142,8
17	210,4	171,8	150,2	138,5	134,7	134,7	134,7
19	205,5	165,8	145,6	132,4	127,4	127,4	127,4

V_{RFEM} / V_{Excel} middle, uncracked, axle loads mechanism (a)

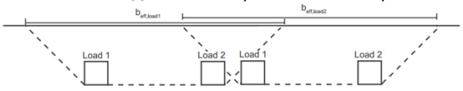

b_{edge} → Span↓	0	1	2	3	4	5	6
5	0,53	0,53	0,57	0,57	0,57	0,56	0,56
7	0,59	0,60	0,61	0,61	0,60	0,59	0,59
9	0,66	0,66	0,67	0,69	0,68	0,67	0,66
11	0,70	0,68	0,69	0,71	0,69	0,68	0,68
13	0,74	0,70	0,73	0,73	0,70	0,70	0,69
15	0,76	0,72	0,72	0,74	0,72	0,71	0,70
17	0,79	0,74	0,74	0,74	0,74	0,72	0,71
19	0,82	0,77	0,75	0,77	0,75	0,73	0,72

V_{Excel} middle, uncracked, axle loads, mechanism (b)

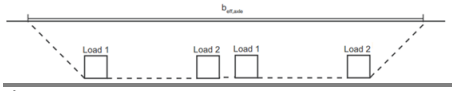

b_{edge} → Span↓	0	1	2	3	4	5	6
5	125,2	93,9	82,3	79,5	79,5	79,5	79,5
7	146,5	109,9	95,8	92,2	92,2	92,2	92,2
9	155,6	116,8	99,9	95,0	95,0	95,0	95,0
11	159,2	119,4	98,9	92,3	92,3	92,3	92,3
13	161,6	121,2	97,6	90,0	89,2	89,2	89,2
15	163,4	122,6	98,0	88,4	86,1	86,1	86,1
17	164,7	123,6	98,9	86,8	83,1	83,1	83,1
19	165,8	124,4	99,5	85,3	80,2	80,2	80,2

V_{RFEM} / V_{Excel} middle, uncracked, axle loads mechanism (b)

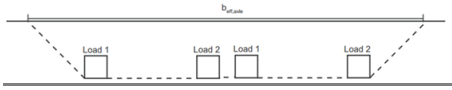

b_{edge} → Span↓	0	1	2	3	4	5	6
5	1,05	1,15	1,29	1,30	1,30	1,28	1,27
7	1,00	1,13	1,19	1,20	1,18	1,17	1,17
9	1,03	1,14	1,22	1,26	1,24	1,23	1,22
11	1,02	1,10	1,19	1,25	1,22	1,20	1,19
13	1,01	1,07	1,20	1,24	1,20	1,19	1,18
15	1,01	1,05	1,14	1,21	1,20	1,17	1,16
17	1,01	1,04	1,12	1,19	1,19	1,17	1,14
19	1,01	1,03	1,10	1,20	1,18	1,16	1,15

14.2 Comparison total loads

V_{Excel} edge, uncracked, total loads

b_{edge} → Span↓	0	1	2	3	4	5	6
5	222,8	167,7	109,0	72,2	46,6	34,9	33,9
7	254,2	192,8	140,7	104,4	81,8	68,2	59,9
9	293,5	232,9	185,8	150,5	125,9	109,1	98,4
11	333,7	276,8	234,1	198,8	174,4	156,9	144,4
13	377,4	323,5	289,2	253,6	228,6	210,8	197,7
15	425,9	375,4	345,9	317,0	291,3	272,7	259,2
17	479,7	432,9	406,8	389,5	363,9	344,4	330,0
19	539,1	496,3	473,9	461,6	446,7	427,1	411,8

V_{RFEM} / V_{Excel} edge, uncracked, total loads

b_{edge} → Span↓	0	1	2	3	4	5	6
5	0,92	0,93	1,02	1,08	1,01	1,15	0,97
7	1,00	1,01	1,02	1,00	0,92	0,94	0,89
9	1,00	0,99	0,98	0,97	0,85	0,86	0,81
11	1,00	0,98	0,97	0,97	0,86	0,87	0,85
13	1,01	0,99	0,96	0,97	0,87	0,88	0,86
15	1,01	0,99	0,96	0,95	0,97	0,89	0,86
17	1,02	0,99	0,96	0,93	0,94	0,94	0,95
19	1,02	0,99	0,97	0,94	0,93	0,93	0,94

V_{Excel} middle, uncracked, total loads

b_{edge} → Span↓	0	1	2	3	4	5	6
5	187,4	167,1	171,0	171,6	173,1	174,4	175,5
7	220,8	195,7	195,2	193,2	194,7	196,0	197,1
9	257,1	228,6	221,7	217,2	218,7	220,0	221,1
11	296,7	266,6	253,7	245,6	247,1	248,4	249,5
13	340,7	309,2	291,9	281,3	280,7	282,0	283,1
15	389,5	356,8	337,8	324,2	320,5	321,0	322,1
17	443,4	409,4	389,8	372,6	366,8	366,3	366,7
19	502,5	467,3	447,0	426,6	418,8	418,1	417,7

V_{RFEM} / V_{Excel} middle, uncracked, total loads

b_{edge} → Span↓	0	1	2	3	4	5	6
5	0,96	0,96	0,90	0,90	0,89	0,88	0,88
7	0,99	0,99	0,96	0,96	0,96	0,95	0,94
9	0,98	0,96	0,93	0,94	0,94	0,93	0,93
11	0,98	0,95	0,93	0,94	0,93	0,93	0,92
13	0,98	0,94	0,92	0,94	0,94	0,94	0,93
15	0,98	0,93	0,91	0,93	0,93	0,93	0,92
17	0,99	0,93	0,91	0,91	0,92	0,92	0,92
19	0,99	0,94	0,91	0,91	0,91	0,91	0,91

V_{Excel} edge, cracked, total loads

b_{edge} → Span↓	0	1	2	3	4	5	6
5	222,8	152,6	89,4	52,7	29,8	19,2	15,6
7	254,2	175,5	115,4	76,2	52,4	37,5	27,5
9	293,5	216,6	159,8	118,9	90,7	70,9	57,1
11	333,7	265,7	215,4	174,9	146,5	125,5	109,7
13	377,4	310,6	266,1	223,2	192,0	168,7	150,3
15	425,9	367,9	332,0	298,0	268,0	245,4	228,1
17	479,6	424,2	390,5	366,1	334,8	310,0	290,4
19	539,0	491,3	464,5	447,8	428,8	405,8	387,1

V_{RFEM} / V_{Excel} edge, cracked, total loads

b_{edge} → Span↓	0	1	2	3	4	5	6
5	0,92	0,88	0,94	1,20	1,44	1,90	1,92
7	1,01	1,02	1,03	1,19	1,18	1,44	1,67
9	1,00	1,01	0,99	1,01	0,99	1,13	1,23
11	1,00	0,97	0,96	0,93	0,91	0,95	0,96
13	1,01	1,00	0,96	0,94	0,92	0,95	0,96
15	1,01	0,98	0,93	0,92	0,84	0,86	0,85
17	1,02	0,99	0,95	0,92	0,85	0,86	0,86
19	1,02	0,98	0,95	0,90	0,81	0,82	0,81

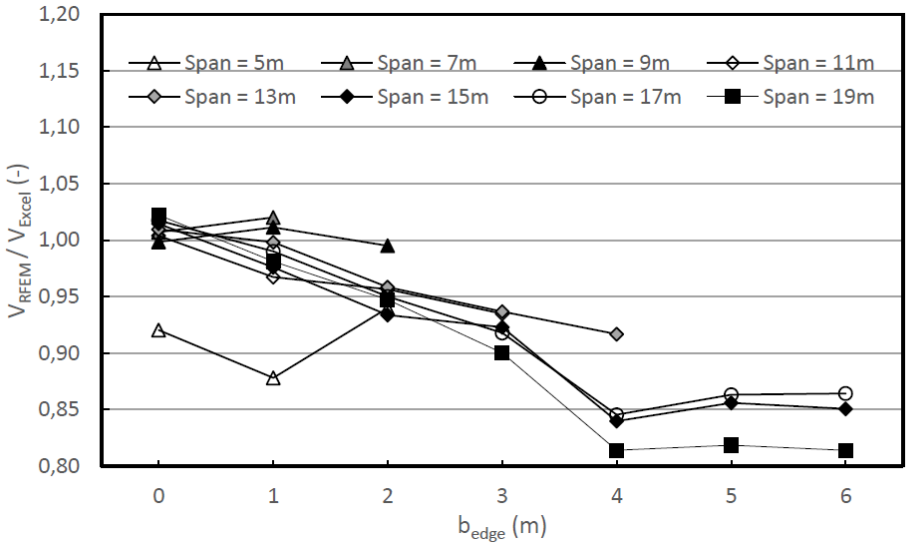

Appendix Figure 14-1 - Comparison shear force RFEM and Excel near the edge of the support for cracked slabs

Note that the unrealistic values (>> 1) are not displayed in this figure, the edge of the support is not governing for this combination of span and edge distance.

V_{Excel} middle, cracked, total loads

b_{edge} → Span↓	0	1	2	3	4	5	6
5	194,9	171,0	172,8	173,4	175,0	176,3	177,5
7	229,7	200,6	197,8	195,9	197,5	198,8	200,0
9	272,5	239,2	229,7	225,2	226,8	228,2	229,4
11	290,5	274,4	265,9	259,1	259,7	260,6	264,7
13	333,5	318,7	306,8	297,5	295,8	296,6	301,2
15	369,0	361,1	352,8	343,5	339,6	338,8	340,5
17	420,0	414,8	407,8	395,6	389,5	387,4	388,5
19	474,1	471,8	468,2	456,2	450,9	450,3	450,6

V_{RFEM} / V_{Excel} middle, cracked, total loads

b_{edge} → Span↓	0	1	2	3	4	5	6
5	0,87	0,92	0,88	0,86	0,85	0,84	0,83
7	0,93	0,97	0,96	0,96	0,94	0,93	0,92
9	0,91	0,94	0,94	0,96	0,94	0,93	0,93
11	0,95	0,93	0,92	0,94	0,93	0,93	0,92
13	0,94	0,92	0,92	0,94	0,94	0,95	0,93
15	0,98	0,93	0,91	0,93	0,94	0,94	0,93
17	1,00	0,92	0,89	0,90	0,92	0,93	0,93
19	1,01	0,92	0,88	0,88	0,90	0,90	0,90

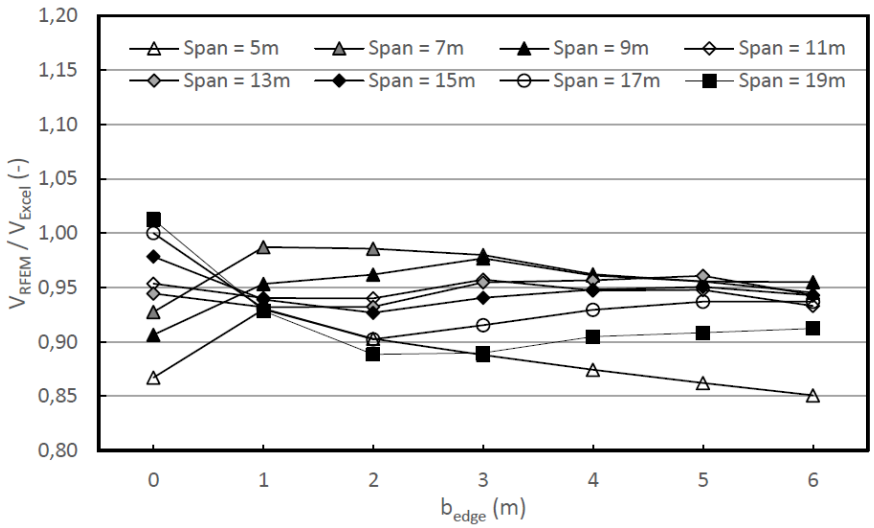

Appendix Figure 14-2 - Comparison shear force RFEM and Excel near the middle of the support for cracked slabs